

IGS

SPECIAL TOPICS

AND

NEW DIRECTIONS

**WORKSHOP PROCEEDINGS
POTSDAM, MAY 15 - 18, 1995**

GeoForschungsZentrum Potsdam
Potsdam, Germany

Edited by
G. Gendt and G. Dick



International GPS Service for Geodynamics



Association Internationale de Géodésie

Union of Geodesists of Geophysical
International

International Association of Geodesy

International Union of Geodesy and
Geophysics

The research described in this publication was sponsored by many international agencies who actively participate in the International GPS Service for Geodynamics. The proceedings from this workshop were prepared and published by the GeoForschungsZentrum Potsdam, Germany.

FOREWORD

The IGS community met from 15th to 17th May, 1995 to conduct its 1995 Workshop. The meeting was held in Potsdam at the 'Jagdschloß Glienicke', a charming baroque castle belonging originally to the Prussian princes, and located in the picturesque Havel landscape at a site directly adjacent to the former iron curtain between East and West. Host for the meeting was the GeoForschungsZentrum Potsdam, a newly established large-scale research centre in re-unified Germany performing basic research work in the solid earth sciences.

Besides describing the state-of-the-art of the service following the first year of its existence, a main target of the meeting was to forge links to foreseeable non-geodetic applications of GPS technology. It is predicted that this area will soon cover such applications as the ground- and satellite-supported GPS measurement and monitoring of the condition of the lower atmosphere and ionosphere. The utilisation of GPS signal refraction, especially in the combination of ground- and satellite-supported measurements, will then undoubtedly have considerable influence on future weather and climate research. Such an application could then play a decisive role for daily weather forecasting and for generating real-time information on the condition of the ionosphere. The Workshop contributions gave an impressive picture of future possibilities for both science and routine practical applications resulting from this development.

New opportunities and standards bring about new demands on precision, the spatial distribution of data and products and their temporal availability. The IGS service - with each of its individual components - will be fundamentally influenced by these new requirements. The Workshop contributions and discussions were aimed far into the future and thus gave clear illustrations of developments to come.

The Workshop was a most productive and inspiring event for the IGS community. Valuable contributions from many scientists, including those presented in the Proceedings here, helped to make it the success that it was. At this point, I would like to express my deep gratitude to **all** of those who contributed.

Christoph Reigber
Potsdam, February 1996

TABLE OF CONTENTS

Foreword	III
Table of Contents	v
Agenda	VIII
List of participants	XII

Session 1: The IGS in 1994

Note: Reports to this session will be published in the "IGS Annual Report 1994"

Session 2: New Directions of IGS

Applications of the IGS in the Next Decade <i>W G Melbourne and R E Neilan</i>	1
GPS Meteorology and the International GPS Service <i>M Bevis and S Businger</i>	6
Ionospheric Research and Future Contributions of the IGS Network <i>N Jakowski</i>	17
Applications and Uses of IGS Information <i>G T Johnston</i>	30
The University NAVSTAR Consortium: Global Positioning for Geosciences Research <i>R H Ware</i>	40

Session 3: The IGS and the Earth's Atmosphere

Global Monitoring of Ionospheric Total Electron Content Using the IGS Network <i>A J Mannucci, B D Wilson, Dah-Ning Yuan, U J Lindqwister and T F Runge</i>	49
--	----

Monitoring Ionospheric Disturbances Using the IGS Network <i>L Wanninger</i>	57
Real-time Monitoring of the Ionosphere <i>E Engler, E Sardón, N Jakowski, A Jungstand and D Klähn</i>	67
Global and Regional Ionosphere Models Using the GPS Double Difference Phase Observable <i>S Schaer, G Beutler, L Mervart, M Rothacher and U Wild</i>	77
Application of IGS Data to GPS Sensing of the Atmosphere for Weather and Climate Research <i>C Rocken, F S Solheim, R H Ware, M Exner, D Martin and M Rothacher</i>	93
A Review of the NOAA Geosciences Lab's Automated Water Vapor Project <i>M S Schenewerk, G L Mader, T M vanDam and W E Carter</i>	104
Consistency in the Troposphere Estimations Using the IGS Network <i>G Gendt and G Beutler</i>	115
 Session 4: Orbits, Clocks, and Other Modeling Issues	
A new Model for GPS Yaw Attitude <i>Y E Bar-Sever</i>	128
Estimation of Precise GPS Clock Bias Values by the ESOC IGS Analysis Centre <i>T J Martín Mur</i>	141
The Perturbation of the Orbital Elements of GPS Satellites Through Direct Radiation Pressure and y-Bias <i>M Rothacher, G Beutler and L Mervart</i>	152
An Estimate of Ocean-Loading Effects on Baseline Repeatability from GPS Observations <i>M S Schenewerk, G L Mader and T M vanDam</i>	167
EMR Clock Estimation <i>P Tétreault, J Kouba, R Ferland and J Popelar</i>	177

Session 5: Technical Aspects of the Densification

ANALYSIS ISSUES

Type Two Associate Analysis at Newcastle-upon-Tyne 183
P Davies and G Blewitt

ITRF and IGS Regional Densifications 199
C Boucher

Determination of Antenna Phase Center Variations Using GPS Data 205
M Rothacher, S Schaer, L Mervart and G Beutler

Australian, Antarctica, Pacific, and Indian Plate Velocities
Using the IGS Network 221
K M Larson and J T Freymueller

NETWORK AND COMMUNICATION ISSUES

The Finnish Permanent GPS Array FinnNet: Current Status 230
*J Kakkuri, H Koivula, M Ollikainen, M Paunonen, M Poutanen
and M Vermeer*

The Central Europe Regional Geodynamic Project
and its Relation to IGS 235
P Pesec

Experience with Data Flow in the CORS Network 242
W Strange, N Weston and M Schenewerk

APPENDIX

Control GPS Networks for the Geophysical Applications (Russia and CIS) AI
S K Tatevian

AGENDA

1995 IGS Workshop

THE IGS: SPECIAL TOPICS AND NEW DIRECTIONS

GeoForschungsZentrum, Potsdam, Germany
May 15-17, 1995

Conveners : Ch. Reigber & R. Neilan
Program Committee : G. Gendt, G. Beutler, J. Kouba, J. Dow,
J. Zumberge, W. Gurtner
Local Org. Committee : G. Dick et al.

MONDAY May 15

12:00 Registration

13:00 Conveners Welcome and Greetings (Ch Reigber)
Greetings from the Chair of IGS (G Beutler)
Greetings from the IAG (I I Mueller)

Session 1 The IGS in 1994

CHAIR: Reigber

13:20 R Neilan:
Central Bureau Report

13:30 Analysis Center Reports (7 ACs)

14:40 Data Center Reports (CCDIS,IGN)

14:55 J Kouba:
Report of Analysis Center Coordinator

15:10 D McCarthy:
Report of USNO

15:30 Break

Session 2 New Directions of **IGS**

CHAIR: Neilan

16:00 W G Melbourne and R E **Neilan** (INVITED):
Applications of the IGS in the Next Decade.

16:20 M **Bevis** and S **Businger** (INVITED):
IGS Support of Global and Local Meteorology, Meteorological
Applications for Ground-based GPS Recovery of Water Vapor.

16:40 N Jakowski (INVITED):
Ionospheric Research and Future Contributions of the IGS Network.

17:00 G Johnston (INVITED):
Commercial Applications of the **IGS**: The Value and Use **IGS** Data and Products.

17:20 R Ware (INVITED):
Global Positioning for Geosciences Research

17:40 Contributions, Discussion

19:00 Visit to Einstein Science Park at the **Telegrafenberg** with tour of the
GeoForschungsZentrum, followed by an
informal grill-party in the garden (weather permitting) or in one of the
historical buildings

TUESDAY May 16

Session 3 The IGS and the Earth's Atmosphere

CHAIR: Gendt, Beutler

9:00 A J Mannucci, B D Wilson, **Dah-Ning Yuan**, U J **Linqwister**, T F Runge (INVITED):
Global Monitoring of Ionospheric Total Electron Content Using the **IGS** Network

9:25 L **Wanninger** (INVITED):
Monitoring Ionospheric Disturbances Using the **IGS** Network

9:50 A Jungstand, E **Engler**, E Sardon, N Jakowski (INVITED):
Real-time Monitoring of Ionosphere

10:15 St **Schaer**, L **Mervart**, U Wild, M **Rothacher**:
Regional and Global Ionospheric Parameters Using the GPS Phase Observable

10:30 Break

11:00 C Rocken, M Rothacher, R H Ware (INVITED):
GPS Sensing of Atmospheric Water Vapor for Weather and Climate Research

11:25 M S Schenewerk, G L Mader, T M vanDam, W E Carter:
A Review of the NOAA Geosciences Lab's Automated Water
Vapor Monitoring Project

11:40 G Gendt, G Beutler:
Consistency in the Troposphere Estimations Using the IGS Network

11:55 Contributions, Discussion

12:30 Lunch

Session 4 Orbits, Clocks, and other Modeling Issues CHAIR: Dow, Kouba

14:30 Y E Bar-Sever (INVITED):
New Yaw Attitude Model for GPS Satellites

15:00 T Martin-Mur (INVITED):
On the ESA Clock Estimation

15:30 M Rothacher, G Beutler (INVITED):
Towards a new Radiation Pressure Model Within the IGS Community

16:00 Break

16:30 M Schenewerk:
Evaluation of Ocean-Loading at IGS Sites in North America

16:45 J Zumberge:
Another Look at Formats for IGS Orbit and Clock Products

17:00 P Tetreault:
EMR Clock Estimation

17:15 Contributions, Discussion

19:00 RECEPTION

WEDNESDAY May 17

Session 5 Technical Aspects of the **Densification**

CHAIR: Zumberge

ANALYSIS ISSUES

9:00 G Blewitt, P B H Davies, P Manurung (INVITED):
IGS Associate Analysis Center Activities at Newcastle

9:20 C Boucher (INVITED):
ITRF and IGS Regional Densifications

9:40 P Fang and Y Bock (INVITED):
Rapid Orbit Service at S10

10:00 M Rothacher, S Schaer, W Schlueter (INVITED):
Antenna Phase Center Calibrations

10:15 K Larson, J Freymueller:
Australian, Antarctic, Pacific and Indian Plate Velocities
Using the IGS Network

10:30 Break

NETWORK AND COMMUNICATION ISSUES

11:00 J Kakkuri, H Koivula, M Ollikainen, M Paunonen,
M Poutanen, and M Vermeer (INVITED):
The Finnish Permanent GPS Array FinnNet: Current Status.

11:20 P Pesec (INVITED):
The Central Europe Regional Geodynamic Project
and its Relation to IGS

11:40 W Strange, N Weston and M Schenewerk (INVITED):
Current Status and Future Development of the CORS GPS Network

12:00 Contributions, Discussion

12:30 CLOSING

Afternoon: Internal Meetings/Splinter Sessions (Resolutions, etc.)

LIST OF PARTICIPANTS

Altamimi, Zuheir

Institut Geographique National, IGN, ENSG/LAREG, 2 Avenue Pasteur BP 68, F-94160
Saint-Mandé, France
Phone: ++33/1/4398-8209 Fax: ++33/1/4398-8488 E-mail: altamimi@ign.fr

Ambrosius, Boudewijn A.C.

Delft University of Technology, Faculty of Aerospace Eng., Kluyverweg 1, NL-2629 HS Delft,
The Netherlands
Phone: ++31/15/785-173 Fax: ++3 1/15/783444 E-mail: boudewijn.ambrosius@lr.tudelft.nl

Angermann, Detlef

GeoForschungsZentrum (GFZ), Department of Kinematics and Dynamics of the Earth,
Telegrafenberg Al 7, D-14473 Potsdam, Germany
Phone: ++49/33 1/288-1113 Fax: ++49/33 1/288-1111 E-mail: dang@gfz-potsdam.de

Bar-Sever, Yoaz

Jet Propulsion Laboratory (JPL), MS 238-600, 4800 Oak Grove Drive, Pasadena/California 91109,
USA
Phone: ++1/81 81354-2665, Fax: ++1/8 18/393-4965 E-Mail: yeb@cobra.jpl.nasa.gov

Baustert, Gerald

GeoForschungsZentrum (GFZ), Department of Kinematics and Dynamics of the Earth,
Telegrafenberg A 17, D-14473 Potsdam, Germany
Phone: ++49/33 1/288-1113 Fax: ++49/33/1/288-1111 E-mail: gbau@gfz-potsdam.de

Beutler, Gerhard

University of Berne, Astronomical Institute, Sidlerstr. 5, CH-3012 Berne, Switzerland
Phone: ++4 1/31/631-85-91 Fax: ++41/3 1/631-3869 E-mail: beutler@aiub.unibe.ch

Bevis, Michael

University of Hawaii, HIGP, 2525 Correa Road, Honolulu/HI 96822, USA
Phone: ++1/808/956-7864 Fax: ++ 1/808/956-3188 E-mail: bevis@soest.hawaii.edu

Blewitt, Geoffrey

University of Newcastle upon Tyne, Department of Surveying, Newcastle upon Tyne NE1 7RU,
United Kingdom
Phone: ++44/1 91/222-5040 Fax: ++44/191/222-8691 E-mail geoffrey.blewitt@ncl.ac.uk

Boucher, Claude

Institut Geographique National, IGN, ENSG/LAREG, 2 Avenue Pasteur BP 68, F-94160
Saint-Mandé, France
Phone: ++33/1/4398-8565 Fax: ++33/1/4398-8488 E-mail: boucher@ign.fr

Daniel, Loïc

Institut Geographique National, IGN, 2 Avenue Pasteur BP 68, F-94160 Saint-Mandé, France
Phone: ++33/1/4398-8338 Fax: ++33/1/4398-8488 E-mail: daniel@schubert.ign.fr

Davies, Philip H.B.

University of Newcastle upon Tyne, Department of Surveying, Newcastle upon Tyne NE I 7RU,
United Kingdom
Phone: ++44/191 /222-5040 Fax: ++44/191/222-8691 E-mail: geoffrey.blewitt@ncl.ac.uk

Dick, Galina

GeoForschungsZentrum (GFZ), Department of Kinematics and Dynamics of the Earth,
Telegrafenberg Al 7, D-14473 Potsdam, Germany
Phone: ++49/33 1/288-1185 Fax: ++49/33 1/288-1111 E-mail: dick@gfz-potsdam.de

Dietrich, Reinhard

Technische Universität Dresden, Institut für Planetare Geodäsie, Mommsenstr. 13, D-0162 Dresden,
Germany
Phone: ++49/35 1/463-4652 Fax: ++49/35 1/463-7063 E-mail: dietrich@kpgrs1.geo.tu-dresden.de

Dixon, Kevin
 RACAL Survey Limited, South Denes, Great Yarmouth, Norfolk NR30 3NU, United Kingdom
 Phone: ++44/1 493/857011 Fax: ++44/1 493/852420

Dodson, Alan H.
 University of Nottingham, IESSG, University Park, Nottingham NG7 2RD, United Kingdom
 Phone: ++44/1 15/951-3882 Fax: ++44/1 15/951-3881 E-mail: alan.dodson@nottingham.qc.uk

Dow, John M.
 ESA/ESOC, Orbit and Attitude Division, Robert-Bosch-Str. 5, D-64293 Darmstadt, Germany
 Phone: ++49/615 1/90-2272 Fax: ++49/615 1/904272 E-mail: jdow@esoc.esa.de

Drozyner, Andrzej
 Nicolaus Copernicus University, Inst. of Astronomy, Chopina 12/18, PL-87- 100 Torun,
 Poland
 Phone: ++48/56/26018 Fax: ++48/56/24602 E-mail: drozyner@astri.uni.torun.pl

Dube, Maurice
 NASA/GSFC, Hughes STX, Code 920.1, Greenbelt/Maryland 20771-0001, USA
 Phone: ++1/301/286-4835 Fax: ++ 1/301/286-0213 E-mail: dube@cddis.gsfc.nasa.gov

Engen, Bjorn
 Statens Kartverk, Geodetic Institute, Norwegian Mapping Authority, N-3500 Honefoss, Norway
 Phone: ++47/321/18150 Fax: ++47/321/18101 E-mail: bjorn.engen@gdiv.statkart.no

Fang, Peng
 University of California, San Diego, S10/ Institute of Geophysics and Planetary Physics, 9500
 Gilman Drive/IGPP 0225, La Jolla/California 92093-0225, USA
 Phone: ++1/619/534-2445, Fax: ++1/619/534-9873 E-mail: pfang@pgga.ucsd.edu

Fejes, István
 FÖMI, Satellite Geodetic Observatory, Cartography and Remote Sensing, P.O. Box 546, H-1373
 Budapest, Hungary
 Phone: ++36/27/310-980 Fax: ++36/27/310 982 E-mail: fejes@novell.sgo.fomi.hu

Fisher, Steven S.
 Jet Propulsion Laboratory, c/o UNAVCO/UCAR, 3340 Mitchell Lane, Boulder/Colorado 80301,
 USA
 Phone: ++1/303/497-8046 Fax: ++1/303/497-8028 E-mail: sfisher@ near.ucar.edu

Förste, Christoph
 GeoForschungsZentrum (GFZ), Department of Kinematics and Dynamics of the Earth,
 Telegrafenberg A 17, D-14474 Potsdam, Germany
 Phone: ++49/33 1/288-1116 Fax: ++49/331/288-1111 E-mail: foer@gfz-potsdam.de

Galas, Roman
 GeoForschungsZentrum (GFZ), Department of Kinematics and Dynamics of the Earth,
 Telegrafenberg A17, D-14473 Potsdam, Germany
 Phone: ++49/33 1/288-1 179 Fax: ++49/331/288-1111 E-mail: galas@gfz-potsdam.de

Gendt, Gerd
 GeoForschungsZentrum (GFZ), Department of Kinematics and Dynamics of the Earth,
 Telegrafenberg A 17, D-14473 Potsdam, Germany
 Phone: ++49/33 1/288-1114 Fax: ++49/33 1/288-1111 E-mail: gend@gfz-potsdam.de

Habrigh, Heinz
 Institut für Angewandte Geodäsie (IfAG), Richard-Strauss-Allee 11, D-60598 Frankfurt a. Main,
 Germany
 Phone: ++49/69/6333-267 Fax: ++49/69/6333-425 E-mail: habrich@igs.ifag.de

Heck, Bernhard
 Universität Karlsruhe, Geodätisches Institut, Englerstr. 7, D-76128 Karlsruhe, Germany
 Phone: ++49/721/608-3674 Fax: ++49/72 1/694552 E-mail: heck@gik.bau-verm.uni-karlsruhe.de

Hehl, Klaus
 GeoForschungsZentrum (GFZ), Department of Kinematics and Dynamics of the Earth,
 Telegrafenberg A 17, D-14473 Potsdam, Germany
 Phone: ++49/331/288-1 132 Fax: ++49/331/288-1111 E-mail: hehl@gfz-potsdam.de

Jakowski, Norbert
 DLR Neustrelitz, FE-Station, Kalkhorstweg 53, D-17235 Neustrelitz, Germany
 Phone: ++49/3981 /480- 151 Fax: ++49/3981 /480-299 E-mail: jakowski@nz.dlr.de

Johnston, Gordon T.
 RACAL Survey Limited, South Denes, Great Yarmouth, Norfolk NR30 3NU, United Kingdom
 Phone: ++44/1493/857011 Fax: ++44/1493/852420

Jungstand, Arne
 DLR Neustrelitz, FE-Station, Kalkhorstweg 53, D-17235 Neustrelitz, Germany
 Phone: ++49/398 1/480 150 Fax: ++49/398 1/480 299 E-mail: jungstan@nz.dlr.de

Kang, Zhigui
 GeoForschungsZentrum (GFZ), Department of Kinematics and Dynamics of the Earth,
 Telegrafenberg A 17, D-14473 Potsdam, Germany
 Phone: ++49/33 1/288-1139 Fax: ++49/33 1/288-1111 E-mail: kang@gfz-potsdam.de

Kaniuth, Klaus
 DGF, Marstallplatz 8, D-80539 München, Germany
 Phone: ++49/89/23031 -114 Fax: ++49/89/23032-240 E-mail: kaniuth@dgfi.badw-muenchen.de

Klotz, Jürgen
 GeoForschungsZentrum (GFZ), Department of Kinematics and Dynamics of the Earth,
 Telegrafenberg A 17, D-14473 Potsdam, Germany
 Phone: ++49/331/288-111 8 Fax: ++49/331/288-1111 E-mail: klotz@gfz-potsdam.de

Kolaczek, Barbara
 Polish Academy of Sciences, Space Research Centre, Department of Planetary Geodesy, Bartycka
 18A, PL-00-716 Warsaw, Poland
 Phone: ++48/22/403766 Fax: ++48/39-121273 E-mail: kolaczek@cbk.waw.pl

Kosek, Wieslaw
 Polish Academy of Sciences, Space Research Centre, Department of Planetary Geodesy, Bartycka
 18A, PL-00-716 Warsaw, Poland
 Phone: ++48/22/403766 Fax: ++48/39-121273 E-mail: kosek@cbk.waw.pl

Kouba, Jan
 Natural Resources Canada (NRCan), Geodetic Survey of Canada, Geomatics Canada, 615 Booth
 Street, Ottawa/Ontario K 1 A 0E9, Canada
 Phone: ++1/61 3/992-2678 Fax: ++1/613/995-3215 E-mail: kouba@geod.emr.ca

Kulhawczuk, Izabella
 Statens Kartverk, Geodetic Institute, Norwegian Mapping Authority, N-3500 Honefoss, Norway
 Phone: ++47/321 1/8474 Fax: ++47/321 1/8101 E-mail: izabella@gdiv.statkart.no

Kumkova, Irina
 Institute of Applied Astronomy, RAS, 8 Zhdanovskaya Str., St. Petersburg 197042, Russia
 Phone: ++7/8 12/235-3216 Fax: ++7/8 12/230-7413 E-mail: kumkova@ipa.rssi.ru

Larson, Kristine
 University of Colorado, Department of Aerospace Engineering, Campus Box 429,
 Boulder/Colorado 80309, USA
 Phone: ++1/303/492-6583 Fax: ++ 1/303/492 7881 E-mail: kristine.larson@colorado.edu

Liebsch, Gunter
 Technische Universität Dresden, Institut für Planetare Geodäsie, Mommsenstr. 13, D-OJ 62 Dresden,
 Germany
 Phone: ++49/35 1/463-3045 Fax: ++49/35 1/463-7063 E-mail: liebsch@kpgrs1.geo.tu-dresden.de

Madsen, Frede
National Survey and Cadastre, Geodetic Division, Rentemestervej 8, DK-2400 Copenhagen NV,
Denmark
Phone: ++45/35/875286 Fax: ++45/35/875052 E-mail: fm@kms.min.dk

Martin-Mur, Tomás
ESA/ESOC, Robert-Bosch-Str. 5, D-64293 Darmstadt, Germany
Phone: ++49/615 1/90-2376 Fax: ++49/615 1/90227 E-mail: tmur@esoc.bitnet

McCarthy, Dennis D.
U.S. Naval Observatory (UNSO), International Earth Rotation Service/Time Service Dept.,
3450 Massachusetts Avenue N.W., Washington/DC 20392-5420, USA
Phone: ++1/202/653-0066 Fax: ++1/202/653-0587 E-mail: dmc@maia.unso.navy.mil

Melbourne, William G.
Jet Propulsion Laboratory (JPL), MS 238-540, 4800 Oak Grove Drive, Pasadena/California 91109,
USA
Ph:++1/818/354-5071 Fax:++1/818/393-6686 E-mail: William. G. Melbourne@cc:mail.jpl.nasa.gov

Menge, Falko
Universität Hannover, Institut für Erdvermessung, Nienburger Str. 5, D-30167 Hannover, Germany
Phone: ++49/5 11/762-2475 Fax: ++49/5 11/762-4006 E-mail: menge@mbox.ife.uni-hannover.de

Montag, Horst
GeoForschungsZentrum (GFZ), Department of Kinematics and Dynamics of the Earth,
Telegrafenberg Al 7, D-14473 Potsdam, Germany
Phone: ++49/33 1/288-1112 Fax: ++49/33 1/288-1111 E-mail: montag@gfz-potsdam.de

Morgan, Peter
University of Canberra, Info Sci. & Engineering, P.O. Box 1, Belconnen A.C.T. 2616, Australia
Phone: ++61/6/201-2557 Fax: ++61/6/201-5041 E-mail: peterm@ise.canberra.edu.au

Mueller, Ivan I.
Ohio State University, Department of Geodetic Science and Surveying, 1958 Neil Avenue,
Columbus/Ohio 43210-1247, USA
Phone: ++1/614/292-2269 Fax: ++1/614/292-2957 E-mail: mueller@mps.ohio-state.edu

Nawrocki, Jerzy
Astronomical Latitude Observatory, Space Research Centre, Polish Academy of Sciences, 62-035
Kornik, Poland
Phone: ++48/61/170-187 Fax: ++48/61/170219 E-mail: aospl@pozn1.v.tup.edu.pl

Neilan, Ruth E.
Jet Propulsion Laboratory (JPL), MS 238-540, 4800 Oak Grove Drive, Pasadena/California 91109,
USA
Phone: ++1/8 18/354-8330 Fax: ++1/818/393-6686 E-mail: ren @logos.jpl.nasa.gov

Novák, Pavel
Research Institute of Geodesy, Topography and Cartography, Geodetic Observatory Pecny, CZ-251
65 Ondrejov 244, Czech Republic
Phone: ++42/204/85235 Fax: ++42/204/85236 E-mail: novak@asu.cas.cz

Paquet, Paul
Observatoire Royal de Belgique, Avenue Circulaire 3, B-1180 Bruxelles, Belgium
Phone: ++32/2/373-0249 Fax: ++32/2/374-9822 E-mail: paulpaq@astro.oma.be

Paunonen, Matti
Finnish Geodetic Institute, Metsähovi Observatory, Ilmalankatu 1A, SF-00240 Helsinki, Finland
Phone: ++358/0/264-994 Fax: ++358/0/264995 E-mail: geodeet@csc.fi

Pavlis, Erricos C.
NASA/GSFC, Space Geodesy Branch, Code 926, Greenbelt/Maryland 20771-0001, USA
Phone: ++1/301/286-4880 Fax: ++1/301/286-1760 E-mail: epavlis@ltpmail.gsfc.nasa.gov

Pesec, Peter
 Institut for Space Research Graz, Lustbühelstr. 46, A-8042 Graz, Austria
 Phone: ++43/316/472231 Fax: ++43/316/462678 E-mail: pesec@flubiw01.tu-graz.ac.at

Piraszewski, M.
 Warsaw University of Technology, Inst. of Geodesy and Geodetic Astronomy, Pl. Politechniki 1,
 PL-00-661 Warszawa, Poland
 Phone: ++48/2/622-8515 Fax: ++48/2/621 0052 E-mail: igga@gik.pw.edu.pl

Pujol, Enrique R.
 Instituto Geografico Nacional, (I. G.N.), General Ibañez de Ibero 3, 28003 Madrid, Spain
 Phone: ++34/1/5350525 Fax: ++34/1/5331158 E-mail: pujol@geo.ign.es

Ray, Jim
 NOAA/ N/OES 13/ SSMC-4, Geosciences Laboratory, 1305 East-West Highway St.8 110, Silver
 Spring/Maryland 20910-3281, USA
 Phone: ++1/301/713-2850 Fax: ++ 1/301/713-4475 E-mail: jimr@ray.grdl.noaa.gov

Reigber, Christoph
 GeoForschungsZentrum (GFZ), Department of Kinematics and Dynamics of the Earth,
 Telegrafenberg Al 7, D-14473 Potsdam, Germany
 Phone: ++49/33 1/288-1100 Fax: ++49/33 1/288-1111 E-mail: reigber@gfz-potsdam.de

Reinking, Jorg
 GeoForschungsZentrum (GFZ), Department of Kinematics and Dynamics of the Earth,
 Telegrafenberg A17, D-14473 Potsdam, Germany
 Phone: ++49/33 1/288-1118 Fax: ++49/33 1/288-1111 E-mail: klotz@gfz-potsdam.de

Rogowski, Jerzy
 Warsaw University of Technology, Inst. of Geodesy and Geodetic Astronomy, Pl. Politechniki 1,
 PL-00-661 Warszawa, Poland
 Phone: ++48121622-8515 Fax: ++48/2/6210052 E-mail: jbr@orion.gik.pw.edu.pl

Rothacher, Markus
 University of Berne, Astronomical Institute, Sidlerstrasse 5, CH-3012 Berne, Switzerland
 Phone: ++41/3 1/631-85-91 Fax: ++41/3 1/631-3869 E-mail: rothacher@aiub.unibe.ch

Sardón, Esther
 DLR Neustrelitz, FE-Station, Kalkhorstweg 53, D-17235 Neustrelitz, Germany
 Phone: ++49/398 1/480-143 Fax: ++49/398 1/480-299 E-mail: sardon@nz.dlr.de

Schaer, Stefan
 University of Berne, Astronomical Institute, Sidlerstrasse 5, CH-3012 Berne, Switzerland
 Phone: ++41 /31/63 1-85-91 Fax: ++41 /3 1/63 1-3869 E-mail: sschaer@aiub.unibe.ch

Schenewerk, Mark
 NOAA/ N/OES 13/ SSMC-4 Sta 8115, Geosciences Laboratory, 1305 East-West Highway, Silver
 Spring/Maryland 20910, USA
 Phone: ++ 1/301/713-2852 Fax: ++1/301/7 13-4475 E-mail: mark@tony.grdl.noaa.gov

Schlüter, Wolfgang
 Institut für Angewandte Geodäsie, Fundamentalstation Wettzell, D-93444 Koetzing, Germany
 Phone: ++49/9941/603-107 Fax: ++49/9941/603222 E-mail: schlueter@wettzell.ifag.de

Schwintzer, Peter
 GeoForschungsZentrum (GFZ), Department of Kinematics and Dynamics of the Earth,
 Telegrafenberg A17, D-14473 Potsdam, Germany
 Phone: ++49/33 1/288-1130 Fax: ++49/33 1/288-1111 E-mail: psch@gfz-potsdam.de

Seeber, Gunter
 Universität Hannover, Institut für Erdvermessung, Nienburger Str. 5, D-30167 Hannover, Germany
 Phone: ++49/5 11/762-2475 Fax: ++49/5 11/762-4006 E-mail: seeber@mbox.ife.uni-hannover.de

Slater, James
 Defense Mapping Agency, Headquarters OPG, 8613 Lee Highway, Fairfax/Virginia 22031-2137,
 USA
 Phone: ++1/703/285-9273 Fax: ++1/703/285-9383 E-mail: slaterj@dma.gov

Springer, Tim
 University of Berne, Astronomical Institute, Sidlerstrasse 5, CH-3012 Berne, Switzerland
 Phone: ++41/31/631-85-91 Fax: ++41/31/631-3869 E-mail: springer@aiub.unibe.ch

Stowell, James L.
 Ashtech Inc., 1170 Kifer Rd., Sunnyvale/California 94086, USA
 Phone: ++1/408/524-1689 Fax: ++1/408/524-1500 E-mail: stow@ashtech.com

Tatevian, Suriya
 Institute of Astronomy, INASAN, 48 Pjatnizkaya, 109017 Moscow, Russia
 Phone: ++7/095/23 12923 Fax: ++7/095/2302081 E-mail: statev@inasan.rssi.ru

Tétreault, Pierre
 Natural Resources Canada (NRCan), Geodetic Survey of Canada, Geomatics Canada, 615 Booth
 Street, Ottawa/Ontario K1A 0E9, Canada
 Phone: ++1/613/992-2218 Fax: ++1/613/995-3215 E-mail: pierre@geod.emr.ca

Van Loon, Danny L.F.
 Delft University of Technology, Kootwijk Observatory for Satellite Geodesy, P.O. Box 581,
 NL-7300 AN Apeldoorn, The Netherlands
 Phone: ++31/5769-8219 Fax: ++31/5769/1344 E-mail: vanloon@geo.tudelft.nl

Wanninger, Lambert
 Technische Universität Dresden, Geodätisches Institut, Mommsenstr. 13, D-01062 Dresden,
 Germany
 Phone: ++49/351/463-2852 Fax: ++49/351/463-7201 E-mail: wanning@rmhs2.urz.tu-dresden.de

Ware, Randolph
 UNAVCO/UCAR, P.O. Box 3000, Boulder/Colorado 80307-3000, USA
 Phone: ++1/303/497-8005 Fax: ++1/303/449-7857 E-mail: ware@unavco.ucar.edu

Wild, Urs
 Bundesamt f. Landestopographie, Seftigenstrasse 264, CH-3084 Wabern, Switzerland
 Phone: ++41/31/1963-2232 Fax: ++41/31/963-2459 E-mail: wild@aiub.unibe.ch

Wilson, Brian D.
 Jet Propulsion Laboratory (JPL), MS T1 129, 4800 Oak Grove Drive, Pasadena/California 91109,
 USA
 Phone: ++1/818/354-2790 Fax: ++1/818/393-6890 E-mail: bdw@logos.jpl.nasa.gov

Wilson, Peter
 GeoForschungsZentrum (GFZ), Department of Kinematics and Dynamics of the Earth,
 Telegrafenberg Al 7, D-14473 Potsdam, Germany
 Phone: ++49/331/288-1172 Fax: ++49/331/288-1111 E-mail: wilson@gfz-potsdam.de

Xu, Guochang
 GeoForschungsZentrum (GFZ), Department of Kinematics and Dynamics of the Earth,
 Telegrafenberg Al 7, D-14473 Potsdam, Germany
 Phone: ++49/331/288-1139 Fax: ++49/331/288-1111 E-mail: xu@gfz-potsdam.de

Zhu, Sheng Yuan
 GeoForschungsZentrum (GFZ), Department of Kinematics and Dynamics of the Earth,
 Telegrafenberg Al 7, D-14473 Potsdam, Germany
 Phone: ++49/331/288-1119 Fax: ++49/331/288-1111 E-mail: zhu@gfz-potsdam.de

Zumberge, James F.
 Jet Propulsion Laboratory (JPL), MS 238-600, 4800 Oak Grove Drive, Pasadena/California 91109,
 USA
 Phone: ++1/818/354-6734 Fax: ++1/818/393-3965 E-mail: jfz@cobra.jpl.nasa.gov

APPLICATIONS OF THE INTERNATIONAL GPS SERVICE FOR GEODYNAMICS IN THE NEXT DECADE

William G. Melbourne and Ruth E. Neilan
Jet Propulsion Laboratory, California Institute of Technology
Pasadena, CA 91109 USA

ABSTRACT

The International GPS Service for **Geodynamics** is facing new challenges and opportunities. The past seven years of development and the international collaboration for optimizing the use of the GPS Global Network have been more successful than anyone imagined, and so the question becomes -- Where do we go from here? In this paper we will discuss the potential expansion of the IGS to meet the GPS support requirements from other scientific applications. Also, we will touch on the probable commercial activities that could use IGS services and products, and the policy issues for IGS operations that might arise.

INTRODUCTION

There are a number of forces at work that are changing the utilization of GPS by many different sectors of society. The reduction of Cold War tensions is resulting in shifting priorities and increased focus on societal and economic priorities, Governments are becoming smaller, decentralized in many cases, and in many developed countries there is less government funding available for science and technology. With increasing population pressures worldwide, the interest in the environmental impact becomes a priority as we look to the future world of our children.

In Space a revolution is underway, fueled by technological and programmatic innovations that are resulting in much smaller space missions than advocated in the past, Small, automated, lower cost satellites that are launched in large numbers within a couple years instead of a decade or two, are providing a wealth of scientific information about our planet, as well as global communications and navigation services. In addition to its conventional roles in navigation, surveying and Space Geodesy, GPS will play a prominent role in ground and space applications in remote sensing of atmospheric and ionospheric processes.

Possible new directions for the IGS have been presented over the last year, We look at the possibility of new participants and sponsors for this activity, evaluate the IGS structure and try to determine how the IGS should interface with other government agencies and institutions, both private and public. The IGS has a very flexible, yet strong and robust infrastructure in place and receives a great deal of support from the scientific community,

As we become more involved in responding to the multi-disciplinary applications of GPS, the question arises -- are the auspices of the International Association of Geodesy (**IAG**) sufficiently broad? If IGS services and products are used increasingly for atmospheric and ionospheric applications, should the IGS consider expanding its sponsorship to include the International Association of **Geomagnetism and Aeronomy (IAGA)** and the International Association of Meteorology and Atmospheric Physics (**IAMAP**)? If sea level applications become prominent, should the International Association for the Physical Sciences of the Ocean (**IAPSO**) not also become a sponsor? Another direction to consider is the way in which the IGS relates to the commercial sector, which has been discussed since 1993. We are just beginning to assess the use and **value** of the GPS data and products for commercial companies,

The key areas for the use of GPS are: **i.e.**, seismic hazard monitoring and detection, tide gauge benchmark monitoring, ground based meteorology, space-based atmospheric sounding and ionospheric tomography applications, Other areas of primary civilian use are Differential GPS (**DGPS**) for real-time

navigation, Wide Area Augmentation System (WAAS) for real-time control of aviation, and GPS positioning as the registration points for all types of geographic information systems, mapping and charting.

BACKGROUND AND CURRENT STATUS

The development of the IGS is documented in a variety of publications (Zumberge, Liu, & Neilan, editors, 1995). A key to the success of the IGS through the last seven years has been the broad support from the international geodynamics and geodetic communities and their sponsoring organizations

IGS currently provides its users with GPS tracking data, precise IGS orbits, clocks, high resolution Earth rotation parameters (ERP's), and precise station coordinates and velocities. The IGS has a solid structure that provides support for science and engineering. The infrastructure for maintenance and control of the GPS global reference frame is nearing completion. The map in Figure 1 shows the operational stations of the IGS Network in July 1995; a number of future stations are still being planned to optimize the global distribution, particularly in the areas of Africa, Asia and the oceanic areas.

The direction that many scientists and agencies are heading is the implementation of dense or regional GPS arrays, often coupled with other instrumentation. The link between these arrays and the IGS is primarily in the hierarchy of reference frame and global data products. A pilot project for the Regional Densification of the IGS is underway and will provide a mechanism to extend the Terrestrial Reference Frame of the International Earth Rotation Service (the ITRF) to all GPS stations included in the project. (Zumberge & Liu, cd., 1995).

SEISMIC HAZARD MONITORING AND DETECTION

The use of GPS for monitoring strain accumulation and seismic displacements is increasing. The Japanese are implementing a system that involves a network of nearly 1000 receivers for seismic hazard detection in the Tokyo/Kanto region, with a larger array throughout Japan as a national reference network. These groups are using the data and products of the IGS for orbit and reference frame control.

The Southern California Integrated GPS Network (SCIGN) in Southern California is an initiative established by a group of U.S. agencies (NASA, USGS, UCLA, USC, SIO, etc.) to monitor the metropolitan area of Los Angeles in the aftermath of the Northridge 6.7 earthquake on January 17, 1994. To enhance real-time strain monitoring, rapid predicted orbits from the IGS for near to real-time analysis are essential. To accomplish this, the timely availability of IGS tracking data is required. Improvements for these real-time applications will demand rapid real-time communication links and real-time processing of the data. More of these arrays will unquestionably be implemented in the next decade.

LOCAL MONITORING OF TIDE BENCHMARKS FOR SEA LEVEL CHANGE

The IGS is in the process of a joint initiative with the Permanent Service for Mean Sea Level (PSMSL) to assess the current state of, and develop a technique for, precise monitoring of tide gauge benchmarks. This will help to understand long term sea level change and coastal processes (where altimeter missions are limited) when coupled with the long record tide gauges of the Global Sea Level Observing System (GLOSS) Network of the Intergovernmental Oceanographic Commission (IOC). This is a joint IAG-IAPSO activity.

GROUND-BASED MONITORING FOR WEATHER AND CLIMATE

Research results over the last two years promise that GPS can be used to greatly enhance our understanding of weather processes and in particular storm hazard warnings (Bevis et al., 1993). GPS signal sensitivity to atmospheric delays has generally been a nuisance for GPS analysis that can be nearly eliminated for high precision applications (orbits, etc.). However, by equipping stations with meteorological packages for determining the dry air component of atmospheric delay, the delay due to total precipitable water vapor may be obtained, By determining the vertical precipitable water vapor at the

temperature and pressure profiles, and TEC measurements of the ionosphere (Melbourne et al, 1994). Future missions such as *Ørsted*, *Sunsat*, *CHAMP*, *SAC-C* and *Hummingbird* will provide further demonstrations of atmospheric sounding using the radio occultation technique. Spaceborne GPS receivers will also be used to recover gravity information with unprecedented resolution down to the **mesoscale** level.

Within the next few years an operational constellation of small, dedicated and automated low Earth orbiters (LEO) probably will be deployed to continuously sound the atmosphere and ionosphere using the GPS radio occultation technique. A constellation of twenty LEOS would provide 5,000-10,000 occultations per day, with a mean geographical spacing of about 300 km. These data streams, when combined with atmospheric models and ground observation programs involving GPS, **radiosondes** and other instrumentation, promise significant improvements in medium-term weather forecasting; they would also contribute to global climate change studies. If **future** technological enhancements enable the GPS radio occultation technique to reliably recover refractivity profiles in the lower troposphere (which has been a difficult medium because of sharp vertical refractivity gradients), accurate (-5% in tropical oceanic regions) monitoring of global water vapor distributions could be achieved by combining the recovered refractivity profile with atmospheric models to account for the contribution of dry air. Water vapor is the principal medium for transport of thermal energy and its uncertainty is a major error source in state-of-the-art atmospheric models.

Another dramatic contribution of the LEO constellation operating in conjunction with globally distributed ground networks will be the mapping of the ionosphere **using** tomography. High tomographic resolution is achieved by probing the ionosphere with densely spaced sounding paths whose directions adequately span three-dimensional space. Ground-based TEC measurements of a common zone of the ionosphere tend to transect the medium along nearly parallel paths, resulting in **large** correlations between TEC measurements from neighboring ground stations and poor "vertical" resolution. On the other hand, TEC measurements from LEOS transect the ionosphere over widely varying directions and altitudes, which can result on average in much sharper 3-D tomographic resolution, particularly when combined with concurrent ground observations. Future monitoring of ionospheric variability may be revolutionized using **flight/ground** GPS observation programs such as that just described.

CIVILIAN SECTOR APPLICATIONS

Civilian applications are expanding rapidly from smart vehicle tracking with geographic information systems (**GIS**) to precision farming and autonomous route construction. One of the aspects most likely to mesh with the IGS is the need in many regions for control of GIS and mapping. Many GPS companies are now beginning to integrate GPS systems with the real-time collection and designation of assets for database development and mapping.

IGS has received requests for assistance for establishing national GPS reference networks in developing nations, and the question becomes how far to provide such advice or assistance. Perhaps the various national geodetic agencies participating in the IGS would be most suitable for such activities, such as IfAG, NGS etc. However, it is evident that the **IGS** is recognized as an organization with the expertise to advise and work with these groups for control networks. It is in this area that the **IGS** also has a long term goal of bringing **all** national networks into a common, precise reference frame.

The IGS may also have some input to the field of aviation by providing air **traffic** with the precise international Reference Frame and GPS orbits for precision navigation, approach and landing. Conceivably, a number of the IGS stations could be used in real-time mode for integrity monitoring and assurance and as an international augmentation to the Federal Aviation Administrations WAAS.

In selecting such active stations, we will have to carefully assess the reliability and liability issues. It could be that various contributing agencies of the **IGS** make these arrangements while continuing to support the primary charter of the IGS.

IGS: TO CHANGE OR NOT TO CHANGE

There are alternative views regarding appropriate **IGS** roles and functions in the next decade and consensus is needed to determine these directions and maintain the spirit of international cooperation that we have enjoyed for the last seven years. While there are other GPS service organizations, the **IGS** is the only one with such global scope and participation, and the most demanding scientific users in mind.

There is clearly a need for scientific and engineering services building on the current **IGS** charter as noted in the applications described above and discussed throughout these proceedings. The impacts on the **IGS** are mostly questions of organization. Should we co-opt additional Analysis Centers for specific application(s)? Should we add Coordinators for specific applications? Should we introduce Data Information Systems (**DIS**) Centers for specific applications? Should we introduce marketing functions within the **IGS** organization? Should we implement a financial management organization? Should we modify representation on **IGS** Governing Board to reflect expansion in these functions? Should we modify the **IGS** Central Bureau to cover expanded communications, management, and service requirements? All of these questions will come up over the next few years and will take careful thought and consideration,

Another thorny issue is the question of cost recovery and establishing a policy with regard to the commercial use of the services and products of the **IGS**. A number of national and international institutions providing scientific products and services have or are adopting a tiered policy with respect to users, depending on their classification, Scientific users or users from agencies providing significant support tend to have **free** access to the services and products, but commercial users and non-supporting agencies are charged a fee based on cost recovery considerations. The **IGS** during its development phase has been blessed by beneficent **sponsors**, but will this continue into the future? There are storm clouds on the horizon today that warn of changing spending priorities in several key nations. Our view is that the **IGS** Governing Board should promptly review these questions of scope and cost recovery and take appropriate action.

GENERAL RECOMMENDATIONS

In conclusion, it seems as though the **IGS** should build on our foundation to support these multi-disciplinary activities. A key point is to continue to establish the **IGS** as *the* network and reference system for GPS applications of the future. Where it makes sense, we should expand to meet user requirements. Of course, we must evaluate the need for **IGS** involvement in the different disciplines remaining thoughtful about the activities in which we become involved over the next decade.

Acknowledgments The preparation of this paper was carried out in part by the Jet Propulsion Laboratory, California Institute of Technology, under contract with the National Aeronautics and Space Administration. Information related to the **IGS** can be found by accessing the Central Bureau Information Service through the World Wide Web: <http://igscb.jpl.nasa.gov/>, or through Anonymous File Transfer Protocol (FTP): [igscb.jpl.nasa.gov](ftp://igscb.jpl.nasa.gov) (or 128.149.70.171) .

REFERENCES

- Bevis, M. S., S. Businger, T.A. Herring, R.A. Anthes, C. Rocken, R.H. Ware, S. Chiswell, 1993, "GPS Meteorology: Mapping Zenith Wet Delays onto Precipitable Water Vapor", *Journal of Applied Meteorology*, 33, p. 379-386.
- Gendt, G. and G. Beutler, ""Consistency in the Tropospheric Estimations Using the IGS Network", pp.1 15-127, this publication.
- Melbourne, W.G., E.S. Davis, C.B. Duncan, G.A. Hajj, K.R. Hardy, E.R. Kursinski, T.K. Meehan, L.E. Young, T.P. Yunck, 1995 "The Application of Spaceborne GPS to Atmospheric Limb Sounding and Global Change Monitoring". JPL Publication 94-18, NASA/California Institute of Technology.
- Zumberge, J., R. Liu, editors, 1995, "Proceedings of the IGS Workshop on the Densification of the ITRF through Regional GPS Networks, Nov. 30 -Dec. 2, 1994, IGS Central Bureau, JPL Publication 95-11, Pasadena, CA. 1995.

GPS METEOROLOGY AND THE INTERNATIONAL GPS SERVICE

Michael Bevis
Hawaii Institute of Geophysics and Planetology
2525 Correa Road
Honolulu, Hawaii 96822, USA

Steven Businger
Department of Meteorology
University of Hawaii
Honolulu, Hawaii 96822, USA

ABSTRACT

There is a rapidly growing awareness that GPS observations collected from continuously operating geodetic GPS receivers based on earth, or in low earth orbit satellites, will be of great benefit to the meteorological community. IGS support of these meteorological applications could bring major benefits to the geodetic community as well as provide a useful service to science and society. The major ways in which IGS can immediately promote this synergy are (i) making continuous meteorological observations at all IGS tracking stations and disseminating these data along with the GPS observations, and (ii) providing tracking station observations and precise orbit solutions in nearly-real-time.

INTRODUCTION

The term 'GPS meteorology' refers to remote sensing of the troposphere and the stratosphere by gauging the refraction (slowing and bending) of GPS signals that propagate through the atmosphere (Bevis et al., 1992). The fundamental physical basis for GPS meteorology is the pressure, temperature and humidity dependence of microwave refractivity in the neutral atmosphere. There are two main classes of GPS meteorology:

- o Ground-based GPS meteorology. Delays accumulated in the neutral atmosphere by signals propagating from GPS satellites to earth-bound networks of geodetic GPS receivers are estimated during standard geodetic analyses of network observations. These delays are strongly sensitive to the total quantity of water vapor integrated along the signal path. Emerging networks of continuously operating geodetic GPS receivers can be used to estimate vertically integrated water vapor (I WV) above each station with

a temporal resolution of 30 minutes or better, and, in addition, to estimate the lateral gradients in IWV. Nearly all existing GPS networks are so sparse that they can be used only to characterize IWV at each station. However, very dense arrays of GPS receivers (with interstation spacing of ≤ 1 km or less) could be used to characterize water vapor distribution in all three spatial dimensions as well as in time.

o **Space-based GPS meteorology.** GPS receivers aboard low earth orbit (LEO) satellites collect signals transmitted from GPS satellites during brief atmospheric occultation events. The bending and slowing of the GPS signal observed during the one minute or so that the sub-horizontal transmitter - receiver signal path sweeps vertically through the atmosphere ('active limb sounding') can be inverted to provide a vertical refractivity profile. Roughly speaking, these profiles constrain temperature distribution within the stratosphere and water vapor distribution within the troposphere.

The space- and ground-based approaches are complementary rather than competing in that (i) most ground-based measurements will involve vertical integration or averaging of atmospheric properties while the space-based approach involves significant lateral averaging. Ground-based networks will be able to estimate lateral gradients in integrated water vapor at each station while a single occultation event provides no significant information on lateral variability. (ii) Ground-based meteorology provides continuous measurements at a network of fixed points, while the space-based approach does not. Continuity in both space and time will be advantageous in contexts such as severe weather monitoring near major population centers and airports. (iii) Because of the sub-horizontal nature of its sampling geometry, space-based measurements are subject to obstruction by mountain ranges, and in adjacent low lying areas this may render much of the lower troposphere invisible. (iv) Ground-based meteorology will never achieve good coverage over the oceans, while the space-based approach is essentially global.

The ground-based approach is likely to mature more rapidly in that it can exploit the explosive growth in continuous GPS networks already underway, and can achieve its goals at little incremental cost. The space-based approach, in order to reach its full potential, requires the existence of tens of suitable GPS receivers in LEO satellites. Both the development and the maintenance costs of the space-based approach will exceed those associated with the ground-based approach.

GROUND-BASED GPS METEOROLOGY

The physical and technical basis for ground-based GPS meteorology is described in Bevis et al. (1992, 1994), Rocken et al. (1993, 1995) and Duan et al. (1995). The first major field test of GPS-based water vapor mapping took place in Oklahoma and Kansas during May 1993 in an experiment called GPS/STORM. Water vapor radiometers (WVRs) were collocated with four of the seven GPS receivers that were used to infer integrated water vapor histories within the study area. Rocken et al. (1995) processed the GPS observations

There are two major steps to mapping integrated water vapor with GPS. The first step is to use geodetic techniques to estimate the zenith wet delay history at each GPS receiver in the network. The critical requirement here is access to precise measurements of atmospheric pressure at each GPS receiver in order that the total delay due to the neutral atmosphere can be decomposed into its hydrostatic and wet components before, during or after the geodetic inversion. The second step is to **transform** the retrieved zenith wet delay into an estimate of **precipitable water (PW)**. This transformation can be tuned using surface temperature observations or numerical weather predictions of temperature throughout the troposphere. Nearly all of the uncertainty in a GPS-derived PW estimate derives from estimation of the ZWD and not from the subsequent transformation of this quantity into an estimate of PW.

For GPS networks with interstation spacing of less than several hundred kilometers, a significant problem is encountered in estimating total neutral or wet zenith delay histories from GPS observations. The zenith neutral delay (ZND) or zenith wet delay (ZWD) parameters inferred across the network contain unusually large but highly correlated errors (Rothacher, 1992; Rocken et al., 1993, 1995; Duan et al., 1995). The problem arises because receivers at each end of a short baseline observe satellites at almost identical elevation angles. As a result of this geometrical degeneracy the differential delay associated with two receivers and one satellite is sensitive only to the differential or relative zenith delay and not to the absolute values of the zenith delays at each receiver. Accordingly a GPS network of limited spatial extent can estimate the relative values of the ZWD and thus PW more accurately than it can estimate the absolute values of these quantities.

This problem is best resolved by using global tracking stations to augment a small regional network, thereby introducing large interstation spacing, and side-stepping the sensitivity problem associated with a limited aperture. By incorporating four global tracking stations into the geodetic analysis of the GPS/STORM network Duan et al. (1995) were able to resolve the absolute (not merely the relative) value of the ZWD and thus P W at each station. Since IGS tracking stations do not now make or disseminate accurate surface pressure measurements, it was not possible to decompose the hydrostatic and wet delays at these sites during the course of the geodetic analysis. Accordingly Duan et al. chose to model total neutral delay at both the regional and the global tracking stations during the geodetic analysis, and to decompose the neutral delay subsequently for the regional stations equipped with precise barometers. Modeling the neutral delay with a single mapping function rather than using separate mapping functions for the hydrostatic and wet delays is sub-optimum, and prevented Duan et al. from utilizing GPS observations acquired at elevation angles of less than 15 degrees. While this is not a serious problem if the analysis focuses only on recovery of the PW history at each station, it may prove disadvantageous if lateral gradients in PW are to be estimated in addition (using delay models and mapping functions that incorporate azimuthal anisotropy).

During the development of ground-based GPS meteorology the focus to date has been on mapping PW. For this purpose it was adequate to employ atmospheric delay models based

on the assumption of azimuthal symmetry. A key goal of future developmental efforts is the incorporation of delay models that incorporate azimuthal variability of the hydrostatic and wet delays (Herring et al., 1992; Rogers et al., 1993; Davis et al., 1993). The advantages of this will be twofold: First the estimate of the ZWD will be improved, and thus PW will be recovered more accurately. More importantly, estimates of the horizontal gradients in the wet delay can be transformed into estimates of PW gradients, which will constitute an additional product of meteorological significance.

Even greater insight into the space-time structure of atmospheric water vapor would be provided by dense arrays of geodetic GPS receivers with interstation spacing significantly smaller than the scale height of the troposphere. It would be possible to infer the time varying refractivity structure overlying the array using tomographic techniques, and by estimating the temperature distribution using numerical weather predictions, or independent measurements, to recover the water vapor distribution in four dimensions (Bevis et al., 1992). Water vapor tomography based on GPS observations has not yet been demonstrated.

SPACE-BASED GPS METEOROLOGY

The radio occultation technique was developed and refined in order to study the atmospheres of Mars, Venus, and several outer planets and their moons (Fjeldbo and Eshleman, 1968; Eshleman et al, 1977; Linda] et al, 1981). This well-established technique could now be applied much closer to home. Phase measurements of GPS signals as they are occluded by Earth's atmosphere could provide atmospheric refractivity soundings, and so yield information on global atmospheric temperature and humidity distributions (Yunck et al, 1988; Gurvich and Krasil'nikova, 1990; Hardy et al, 1992). In the stratosphere and arid regions of the troposphere refractivity can be inverted to recover atmospheric temperature with a resolution of order 1 Kelvin. Where significant tropospheric moisture is present, temperature can be measured by GPS occultation if humidity is modeled, or vice-versa. In cold and dry conditions such as those found during polar night, temperature soundings may be obtained down to altitudes of 1 km or so. In the tropics, operational models predict temperature distribution more reliably than humidity, and so the emphasis would be on humidity soundings.

The first proof-of-concept experiment for space-based GPS meteorology is now underway. The GPS/MET satellite was launched on March 18, 1995, and preliminary analyses, reported elsewhere in this volume, are very encouraging.

GROUND-BASED METEOROLOGICAL APPLICATIONS

Water plays a pivotal role in atmospheric processes. The unusually large latent energy associated with water's phase changes significantly affects the vertical stability of the atmosphere and consequently the structure and evolution of storm systems. Water vapor is the most variable and inhomogeneous of the major constituents of the atmosphere and an inability to adequately resolve its distribution is widely considered to be the single greatest obstacle to improved short range precipitation forecasts. Therefore, the ability to measure integrated water vapor at each site in a network of GPS receivers has important implications for the atmospheric sciences (Businger et al., 1995; Chiswell et al, 1995).

In particular, a continuous stream of PW data in near real-time can be assimilated into numerical weather predictions models to provide a powerful constraint on the water vapor distribution and improve analysis of the initial state of the atmosphere at synoptic times. Studies have shown that during the assimilation process numerical models can create a vertical water vapor distribution from the integrated data that is consistent with data implicit to the model (Kuo et al., 1993). GPS PW data can be made available as frequently as every ten minutes, a time scale which makes these data especially well suited to document the rapidly evolving environment of severe thunderstorms. Severe thunderstorms are a frequent hazard over the continental US, especially east of the Rocky Mountains. Coincidentally the deployment of a significant number of GPS receivers, largely for navigational purposes, is planned in the US (Fig. 2).

Because the GPS data represent an integrated value for PW, features in the atmosphere not detectable in traditional surface measurements can be observed with the aid of these data. For example, a classic situation for severe weather in the U.S. Midwest ensues when dry air over the Rockies to the west is advected by westerly a jet stream over a moist southerly flow from the Gulf of Mexico at low levels. When drying and/or cooling aloft is abrupt the leading edge of the transition zone is referred to as a cold front aloft (Businger et al. 1991). Cold fronts aloft, which have been implicated in the triggering of severe squall lines, are not detectable by hygrometers at the surface and radiosondes are released only once every twelve hours. Moreover, satellite radiometers have difficulty providing useful information over land due to the noisy background signal generated by an inhomogeneous underlying surface. Thus a continuous GPS PW data stream becomes especially valuable in monitoring these rapidly evolving, hazardous situations.

SPACE-BASED METEOROLOGICAL APPLICATIONS

In contrast to ground-based data, space-based profiles are discrete in time rather than continuous and are globally distributed rather than restricted to land sites. A single GPS receiver in a suitable low earth orbit satellite (LEO) can observe 500 occultations in a single day. A constellation of 50 such satellites would generate 25,000 refractivity profiles per day. The phenomenal potential importance of space-based GPS meteorology derives from the

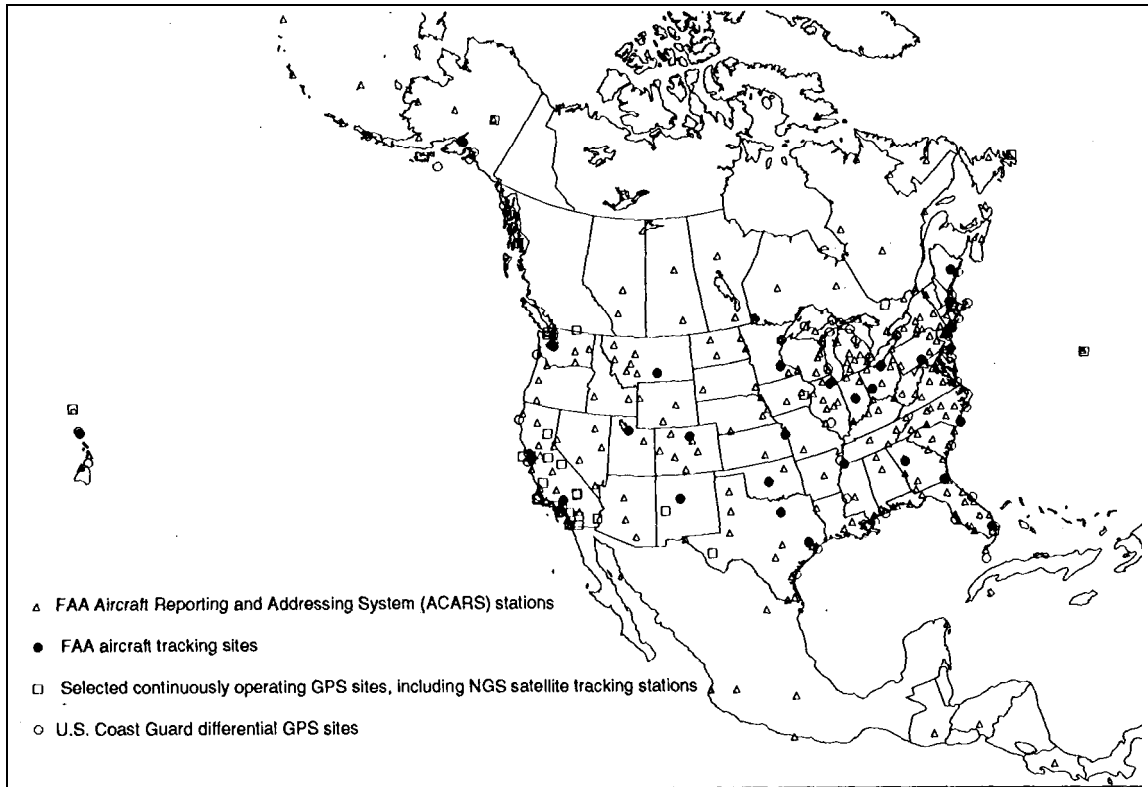


Fig. 2. Location of FAA proposed Aircraft Reporting and Addressing System (ACARS) differential GPS Stations (triangles), proposed FAA aircraft tracking sites (●), selected continuously operating GPS sites including NGS satellite tracking stations (squares), U.S. Coast Guard differential GPS sites (○).

enormous volume of globally distributed observations it could provide. These data, due to their global coverage, will provide the best opportunity to date to monitor the global climate by observing changes in mean refractivity profiles (Yuan et al. 1993). By assimilating the refractivity data directly into numerical weather prediction models, the prospect for improving the definition of the initial state of the atmosphere and subsequent weather forecasts is bright, particularly over open ocean areas where other data sources are extremely sparse.

Analyses of the atmospheric state are constructed in the context of all available data. These analyses form the core data set that is available for a variety of climate and case studies and will benefit greatly from the inclusion of GPS data. Promising applications of the enhanced data set include the study of the ENSO cycle, and tropical cyclogenesis, both of which are impaired by a lack of data over the open ocean.

In regions where the tropospheric temperature distribution is well known, such as over tropical oceans, the contribution of water vapor to the total refractivity profile can be

discerned, allowing a humidity profile to be calculated. Conversely in dry polar regions and above the tropopause, water vapor contributes little to the total refractivity and a temperature profile can be constructed. In this way, GPS data can provide an useful constraint with which to calibrate and supplement satellite-radiometer derived temperature and humidity profiles.

GPS METEOROLOGY AND THE IGS

The most immediate potential for synergy between the IGS and the emerging field of GPS meteorology is associated with the ground-based approach, since it involves networks of continuously operating geodetic GPS receivers. These synergies will be scientific, technological and programmatic. It is increasingly obvious that the geodetic community wishes to utilize increasing numbers of continuously operating GPS receivers in support of its various activities, and that this will require new sources of financial support. This support is more likely to be forthcoming if the networks to be constructed are configured so as to support the widest possible range of activities. GPS meteorology will constitute an important element in a multiple use strategy.

The most obvious way in which the IGS can support ground-based GPS meteorology is to make and disseminate accurate measurements of surface pressure at all of its tracking stations. Surface pressure measurements are essential for the decomposition of the neutral delay into its hydrostatic and wet components, The barometers used should be very precise and very stable so that they will be accurate to, say, 0.5 mbars or better throughout a two-year deployment. Surface temperature is useful in addition, in that it can be used to guide the transformation of zenith wet delay into **precipitable** water. The minimal accuracy requirements for thermometry (0.5 K is probably sufficient) are easily achieved by widely available and inexpensive sensors. Humidity measurements are not used in GPS meteorology per se, but they might prove useful to a meteorological user of a 'GPS met station,' and since they are not expensive, they might as well be included. A meteorological package that would provide digitized observations of pressure, temperature and humidity which could be recorded by a GPS receiver would, at a modest cost (perhaps US\$ 2,500) transform an IGS station into a meteorological station of considerable value. Meteorological observations need not be made more than once every ten minutes, and so need not prove a burden in terms of data telemetry and archiving. Some thought needs to be given to the way in which meteorological observations and atmospheric delay parameters should be incorporated into the RINEX and SINEX formats.

The utility of surface pressure and temperature measurements at IGS tracking stations goes beyond the immediate meteorological significance of the tracking stations themselves. As discussed above, it is useful to incorporate IGS tracking stations into the analysis of small regional GPS meteorological networks in order to promote absolute rather relative measurements of **precipitable** water. Improving the utility of the IGS stations by enabling them to partition the hydrostatic and wet delays will help to promote relatively dense

regional GPS networks constructed at least in part for meteorological applications, thus encouraging the development of continuously operating geodetic GPS networks that can serve to increase the density of the International Terrestrial Reference Frame, as well as serving other geodetic and geophysical functions.

The meteorological applications of GPS fall into two classes - those that require observations in nearly-real time, such as numerical weather prediction, and those, such as water vapor climatology, in which the delay between data collection and data processing is not an important issue. The real-time or nearly-real-time applications will require precise orbit predictions that can be used to support geodetic processing software running more or less continuously as a filter. The Scripps Orbit and Permanent Array Center (SOPAC) has recently initiated a rapid orbit determination, and IGS should consider extending and refining this service. It is not yet clear if predictions based on data collected just once a day will be sufficiently precise for many meteorological applications. These applications may require rapid access to IGS tracking station observations themselves, and to frequently updated orbit predictions, requiring IGS tracking observations to be collected and, processed several times per day, perhaps even hourly in some contexts. Of course it would not be necessary to collect data this frequently from every IGS tracking station, just some suitably chosen subset. This issue requires experimental investigation. Climatological studies make no demands related to timing, but would benefit by incorporating data from as many tracking stations as possible and the highest quality orbits available (which might appear a week or more after the fact). Indeed climatological studies may well drive the installation of continuously operating GPS stations that are essentially off-line, particularly in remote and inaccessible areas undergoing interesting or important climate shifts (e.g., desertification in sub-Saharan Africa).

One concern that arises as one reduces the time delay between data collection and dissemination of corresponding analytical results is the danger of errors slipping through the system and into an operational environment. Interestingly the experimental results from GPS/STORM (Figure 1) suggest a mechanism for checking the quality of rapid orbit determinations. If IGS chose to run WVRs at two or three of its sites, and perform nearly real-time comparisons between PW solutions derived from collocated GPS receivers and WVRs, it could recognize the appearance of systematic errors by detecting divergence between the GPS and WVR results. It would be necessary to suppress the influence of the 'rainfall spikes' (Figure 1) that contaminate WVR solutions by weighing the GPS - WVR comparisons according to the short term repeatability of the WVR time series (Duan et al., 1995).

It is perhaps a little premature to discuss the potential interactions of IGS and a space-based GPS meteorological operation. It seems very likely that it would be useful to incorporate ground-based GPS measurements, made by or in conjunction with the IGS, into data assimilation schemes that absorb space-based measurements into global and regional numerical weather predictions, or into models of climate and climate change. Much of the discussion above concerning rapid data collection and real-time precise orbits carries over from the ground-based into the space-based arena in a fairly obvious way. Once again, the

benefits of a geodetic and meteorological synergy **would** flow in both directions. Much thought needs to be **given** to the potential geodetic significance of dozens of continuously telemetered geodetic GPS receivers orbiting the earth at low elevations, and at no significant cost to the geodetic community!

REFERENCES

- Bevis, M., Businger, S., Herring, T. A., Rocken, C., Anthes, A., and Ware, R., 1992, GPS Meteorology: Remote sensing of atmospheric water vapor using the Global Positioning System, Journal of Geophysical Research, **97**, 15,787-15,801.
- Bevis, M., Businger, S., Herring, T. A., Anthes, R., Rocken, C., Ware, R., and Chiswell, S., 1994, GPS Meteorology: Mapping zenith wet delays onto precipitable water, Journal of Applied Meteorology, **33**, 379-386.
- Businger, S., W.H. Bauman III, and G.F. Watson, 1991: Coastal frontogenesis and associated severe weather on 13 March 1986. *Mon. Wea. Rev.*, 119, 2224-2251.
- Businger, S., S.R. Chiswell, M. Bevis, R. Anthes, C. Rocken, R. Ware, T. VanHove, F. Solheim, 1995: The promise of GPS in atmospheric monitoring. Bulletin of the American Meteorology Society, in review.
- Chiswell, S. R., S. Businger, M. Bevis, J. Duan, C. Rocken, R. Ware, T. VanHove, F. Solheim, 1995, Application of GPS water vapor data in severe weather analysis. Monthly Weather Review, in review.
- Davis, J., G. Elgered, A.E. Neill, C.E. Kuehn, 1993, Ground-based measurement of gradients in the 'wet' radio refractivity of air, Radio Science, **28**, 1003-1018.
- Duan J. , M. Bevis, P. Fang, Y. Bock, S. Chiswell, S. Businger, C. Rocken, F. Solheim, T. Van Hove, R. Ware, S. McClusky, T. Herring, R. W. King, 1995, GPS Meteorology: Direct Estimation of the Absolute Value of Precipitable Water, Journal of Applied Meteorology, in review.
- Eshleman, V. R., G. L. Tyler, J. D. Anderson, G. Fjeldbo, G. S. Levy, G. E. Wood, and T. A. Croft, Radio science investigations with Voyager, **21**, 207 - 232, 1977, '
- Fjeldbo, G., and V. R. Eshleman, 1968, The atmosphere of Mars analyzed by integral inversion of the Mariner IV occultation data, Planetary Space Science, **16**, 123-140.
- Gurvich, A. S., and T. G. Krasil'nikova, Navigation Satellites for Radio Sensing of the Earth's Atmosphere, Soviet Journal of Remote Sensing, 7(6), 1124-1131, 1990.
- Hardy, K. R., D. P. Hinson, G. L. Tyler, and E. R. Kursinski, Atmospheric Profiles from Active Space-Based Radio Measurements, preprint of the 6th Conference on Satellite Meteorology and Oceanography, Atlanta, GA, January 5-10, 1992.
- Herring, T. A., Modeling Atmospheric delays in the analysis of space geodetic data, in Proceedings of Refraction of Transatmospheric signals in Geodesy, eds. J. C. De Munck and T. A. Spoelstra, Netherlands Geodetic Commission Publications on Geodesy. 36, 157P164, 1992.

- Lindal, G. F., G. E. Wood, G. S. Levy, J. D. Anderson, D. N. Sweetnam, H. B. Hotz, B. J. Buckles, D. P. Holmes, P. E. Doms, V. R. Eshleman, G. L. Tyler, and T. A. Croft, The Atmosphere of Jupiter: An Analysis of the Voyager Radio Occultation Measurements, Journal of Geophysical Research, 86,8721-8727, 1981.
- Kuo, Y.-H., Y.-R. Guo, E.R. Westwater, 1993: Assimilation of precipitable water into a mesoscale numerical model. Mon. Wea. Rev. 4, 1215-1238.
- Rocken, C., R. Ware, T. Van Hove, F. Solheim, C. Alber, J. Johnson, M. Bevis, S. Businger, 1993, Sensing atmospheric water vapor with the Global Positioning System, Geophysical Research Letters, 20, 2631-2634.
- Rocken, C., T. Van Hove, J. Johnson, F. Solheim, R. Ware, M. Bevis, S. Chiswell, S. Businger, 1995, GPS/Storm - GPS Sensing of Atmospheric Water Vapor for Meteorology, Journal of Atmospheric and Oceanic Technology, 12, 468-478.
- Rogers, A. E. E., R. J. Cappallo, B. E. Corey, H.F. Hinteregger, A. E. Niell, R. B. Phillips, D. L. Smythe, A. R. Whitney, T. A. Herring, J. M. Bosworth, T. A. Clark, C. Ma, J. W. Ryan, J. L. Davis, I. I. Shapiro, G. Elgered, K. Jaldehag, J. M. Johansson, B. O. Ronnang, W. E. Carter, J. R. Ray, D. S. Robertson, T. M. Eubanks, K. A. Kingham, R. C. Walker, W. E. Himwich, C. E. Kuehn, D. S. MacMillan, R. I. Potash, D. B. Shaffer, N. R. Vandenberg, J. C. Webber, R. L. Allshouse, B. R. Schupler, and D. Gordon, Improvements in the accuracy of Geodetic VLBI, Contributions of Space Geodesy to Geodynamics: Technology, Geodynamics Series, 25, 47P64, American Geophysical Union, Washington, 1993,
- Rothacher, M., Orbits of Satellite Systems in Space Geodesy, Geodätisch-geophysikalische Arbeiten in der Schweiz, 46, 1992.
- Yuan, L., Anthes, R., Ware, R., Rocken, C., Bonner, W., Bevis, M., and Businger, S., 1993, Sensing global climate change using the Global Positioning System, Journal of Geophysical Research, 98, 14,925-14,937.
- Yunck, T. P., G. F. Lindal, and C. H. Liu, The Role of GPS in Precise Earth Observation, Proceeding of the IEEE Position Location & Navigation Symposium, Orlando, Florida, 29 Nov. -2 Dec., 1988.

IONOSPHERIC RESEARCH AND FUTURE CONTRIBUTIONS OF THE IGS NETWORK

N. Jakowski

DLR e. V., Fernerkundungsstation Neustrelitz, Kalkhorstweg 53
17235 Neustrelitz

ABSTRACT

The IGS network of GPS receiving stations can be used for large scale measurements of the Total Electron Content (TEC) of the ionosphere. Various ionospheric phenomena are discussed in view of a potential usage of GPS measurements for more comprehensive studies.

In particular the possibility of large scale TEC monitoring by means of the IGS network is advantageous to study horizontal coupling, transport or propagation processes in the ionosphere.

Requirements for data accuracy and resolution are estimated for various ionospheric phenomena. It is underlined that the scientific value of TEC observations can be enhanced by combining these measurements with data obtained simultaneously by means of ground-based techniques such as ionosonde stations (IS) and incoherent scatter radar facilities (ISR) or by coordination with direct or indirect space-borne plasma probes.

Global or regional TEC maps form the basis for developing, testing and improving empirical and theoretical ionospheric models for different applications. Two proposals for concrete projects in ionospheric research are made which may be considered as a methodological challenge in deriving TEC from IGS network data.

1 INTRODUCTION

The Earth's ionosphere as the ionized part of the upper atmosphere extends from 50 km to about 1000 km altitude. The ionospheric behaviour is affected by a large number of factors due to complex coupling processes with the magnetosphere/thermosphere systems such as electric fields, thermospheric winds, particle precipitation, field aligned currents or mass and heat flows. On the other hand, ionospheric processes influence significantly thermospheric circulation and composition. So the study of solar-terrestrial relationships requires also a careful analysis of ionospheric processes and related feedback mechanisms.

Remote sensing of the ionosphere takes advantage from the interaction of radio waves with the ionospheric plasma what can be troublesome on the other hand in a number of ground- or space-based radio system applications.

Radio beacons onboard satellites have played an important role in studying the temporal and spatial structure of the ionosphere over nearly 3 decades. Related to the Total Electron Content (TEC) of the ionosphere, a quantity which may easily be deduced from two-frequency methods, valuable contributions have been provided for ionospheric research in different fields such as production, loss and transport processes, ionospheric storms, trough, topside/plasmasphere, traveling ionospheric disturbances or small scale irregularities (scintillations). In the following section some of these topics will be discussed to demonstrate under which conditions GPS derived TEC could be used for the exploration of the ionospheric behaviour taking into account that the International GPS Service for Geodynamics (IGS) supports ionospheric research activities (Zumberge et al., 1991).

2 IONOSPHERIC PHENOMENA STUDIED BY RADIO BEACON TECHNIQUES

2.1 Effects due to Solar Radiation Variation

Since the solar extreme ultraviolet (EUV) flux ($10 < \lambda < 130 \text{ nm}$) is the major source of the formation of the ionosphere by photoionization, the ionospheric behaviour is strongly affected by EUV varia-

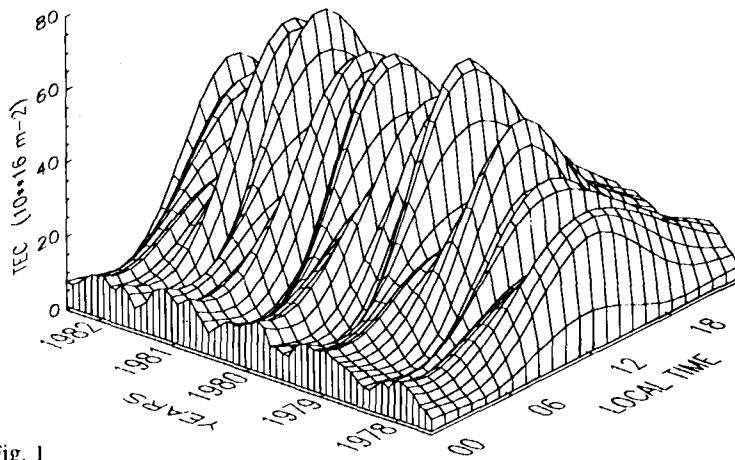


Fig. 1
Smoothed TEC data obtained by Faraday rotation measurements in Neustrelitz using the VHF telemetry beacon of the SIRIO geostationary satellite during the years 1978-1982.

tions, qualitatively indicated by the F10.7 cm solar radio flux index. The ionospheric response to solar activity induced changes of the ionospheric electron content have been studied by a large number of authors. Since accurate EUV data are still missing, correlations were carried out with F10.7 or with the Zurich sunspot number R_z . Although saturation effects at very

high solar activity level were discussed in recent time, linear relationships between TEC and F10.7 are a good approximation (Davies et al., 1994).

The diurnal, seasonal and solar cycle variation of TEC is illustrated in Fig. 1 for 5 years based on Faraday rotation observations carried out in Neustrelitz (53.3°N; 13.1°E) when receiving the VHF radio beacon of the SIRIO satellite. The semiannual variation characterized by maximum noon values around equinoxes indicate close coupling with thermospheric composition (Jakowski and Paasch, 1984).

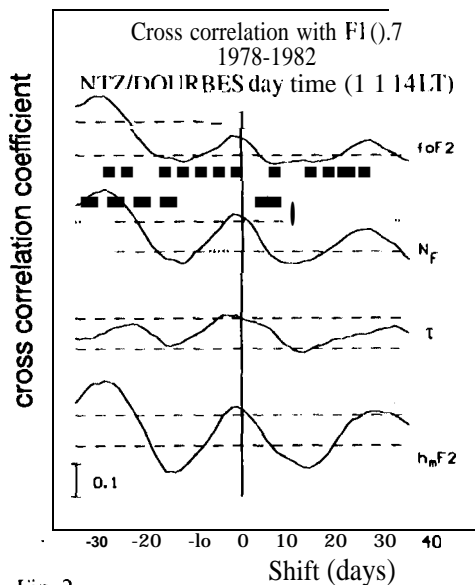


Fig. 2
Cross-correlation function between several ionospheric parameters (foF2, τ , hmF2) observed in Neustrelitz (Faraday -- Polarimeter) and Dourbes (IS) and the solar radio flux F10.7. Negative time shift indicates that the observed parameter is delayed against F10.7.

The sensitive response of TEC to solar irradiance becomes evident in its dependence from solar rotation induced variations of EUV as it is shown in Fig. 2. Both, TEC as well as the ionosonde parameter foF2 and hmF2 indicate the 27 day rotation period of the sun. Of particular interest for ionospheric research is the so-called equivalent slab thickness τ which gives a measure of the width of the vertical electron density profile. This quantity is of particular interest when studying dynamic processes accompanied by expansion or contraction of the electron density profile. The slab thickness τ is defined by:

$$\tau = \text{TEC} / N_m F_2$$

where NmF2 represents the peak electron density related to the critical ionosonde frequency foF2 by $N_m F_2 = 1.24 \cdot 10^{-2} (\text{foF2})^2$ in SI units.

As Fig. 2 shows, the ionospheric response to mid-term solar radiation variations is delayed by 1-2 days. In a first attempt to explain this delay, it is supposed that the atomic oxygen density, which is

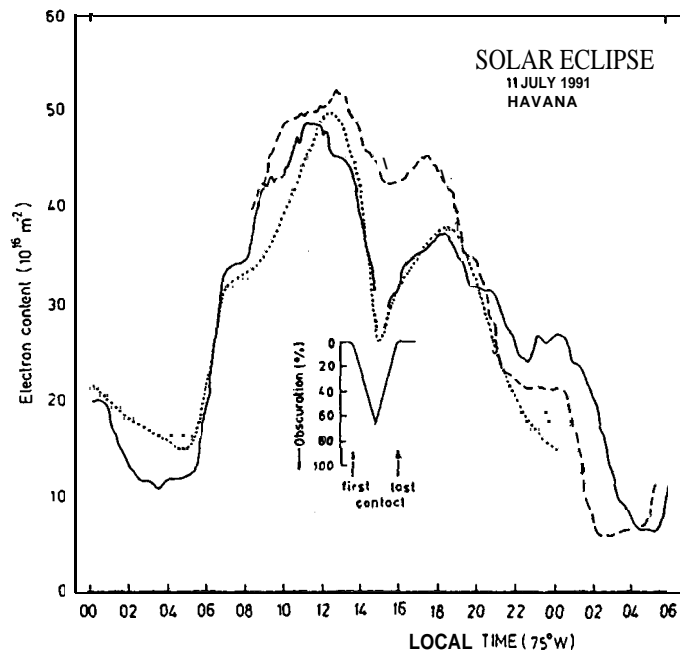


Fig. 3 Total electron content response to the solar eclipse, on July 11, 1991 observed in Havana (23.1°N; 82.5°W). The dashed line represents the observations at quiet pre-storm conditions on July 7–8. Reference is also made to model calculations (dotted line).

Hines', 1971; Jakowski et al., 1983). The ionospheric plasma loss due to the strongly reduced solar radiation during the solar eclipse on July 11, 1991 in Havana is quite evident (see Fig. 3). The model calculations are in reasonable agreement with the TEC variation. As Chimonas and Hines (1971) have pointed out, the fast moving totality zone may generate internal gravity waves which may be detected as Traveling Ionospheric Disturbances (TID's) by ionospheric measuring techniques. However, the attempts to detect such waves during solar eclipses were more or less successfully, indicating that further work is necessary.

A large scale monitoring of TEC by globally distributed IGS stations could follow the movement of the zone of totality in the ionosphere, thus providing a more complex picture of the ionospheric response than it can be done by means of more or less distant singular observations.

2.2 Ionospheric Storms

Ionospheric storms, though studied since more than 50 years, are not yet completely understood. This is due to their close coupling with the thermosphere and magnetosphere and the resulting variability of this phenomenon (e.g. Fuller-Rowell et al., 1994).

Radio beacon studies could improve our knowledge about ionospheric storms particularly in combination with other measuring techniques such as vertical sounding (e.g. Pröls, 1991).

The "classical" F2-layer storm is characterized by a "positive" phase at least during the first few hours after the geomagnetic Storm Sudden Commencement (SSC). During this phase both NmF2 and TEC are increased especially in the evening hours. The positive phase is often followed by a strong loss of F2 layer ionization called the "negative" phase followed by a recovery phase. Such a typical behaviour is illustrated in Fig. 4 for three European stations indicating a latitudinal dependence of the positive phase. A statistical treatment of more than 100 ionospheric storms indicated seasonal differences for average storm pattern in the mid-latitude European sector (Jakowski et al., 1990). Hereafter the positive phase on the first storm day occurs in all seasons positively correlated

also modulated by the solar irradiance variation, lags behind F10.7 (Jakowski et al., 1991).

TEC is also sensitive to short term radiation changes within some minutes as it can be observed during solar flares (e.g. Jakowski and Lazo, 1977).

Although contributions due to X-ray ionization in the lower ionosphere play a certain role, the F2 layer and topside effects which are closer related to EUV, clearly dominate the measured TEC values.

Of particular interest in ionospheric research are solar eclipse observations which provide a unique opportunity to study the ionospheric response to the well-defined variation of the solar radiation. Thus a variety of experimental and theoretical studies are related to this subject (Davis and Da Rosa, 1970; Chimonas and

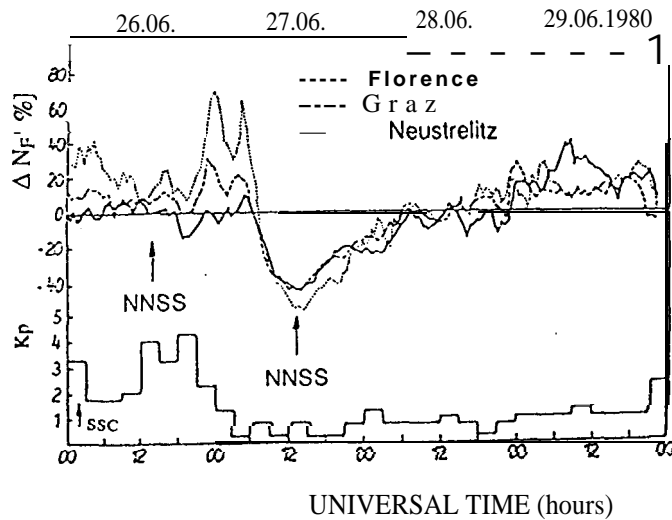


Fig. 4
Percentage deviations of N_F data from their corresponding month] y medians observed at the stations Neustrelitz, Graz and Florence during the storm period June 26-29, 1980.

with the strength of geomagnetic activity. The negative phase is only well pronounced under summer conditions.

The different storm phenomena may be caused by a variety of generation mechanisms depending on the geographic-geomagnetic relationships. Since horizontal transport processes of mass and energy obviously play an important role, global studies are necessary to explore storm mechanisms. Tanaka (1979), analyzing the data of 42 ionosonde stations, has underlined the global character of ionospheric storm events. The global distribution of IGS stations provides good conditions for a large scale description of storm dynamics including high-, mid-, and low-latitudes.

The rather short, but strong perturbation on November 26, 1994 around noon caused a TEC increase of about 100% compared with quiet prestorm conditions (Fig. 5). TEC at subionospheric points was derived from the GPS/IGS data by using special algorithms developed by Sardon et al. (1994). There were 11 European IGS-stations included as TEC data sources (Jakowski et al., 1995). TEC maps have been constructed by combining the irregular distributed TEC data with an empirical regional TEC model NTCM 1 to cover also regions with low data densities (e.g. Jakowski and Jungstand, 1994).

The very similar behaviour of the F2-layer height $hmF2$ and the slab thickness τ after the perturbation onset near sunrise is consistent with a strong uplifting of plasma until about 11 UT followed by a strong downward drift of plasma probably caused by an electric field until 14 UT (decrease of $hmF2$ and τ). The rapid increase of τ after 14 UT is probably due to storm induced composition changes of the neutral gas what is typical for the negative phase. Indeed, as the TEC maps at 12, 13 and 14 UT show, the southward propagating “negative cloud” has reached Juliusruh (54.6°N;13.3°E) at about 14 UT.

Fig. 6 demonstrates the effectiveness of consecutive TEC maps in analyzing horizontal transport processes which may directly visualized in a movie f.i. by using a time resolution of 10 minutes. The worldwide IGS network will provide good conditions for global analysis of storm phenomena.

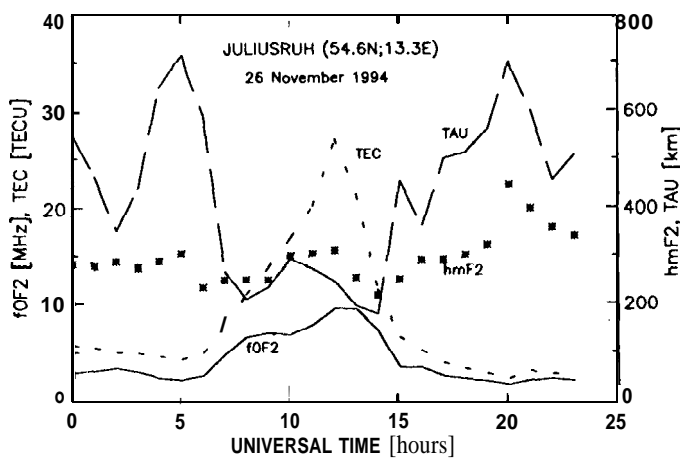


Fig. 5
Comparison of GPS/IGS derived vertical TEC data over Juliusruh for November 26,1994 with corresponding ionosonde data foF2 and $hmF2$ and the equivalent slab thickness $\tau=TEC/NmF2$.

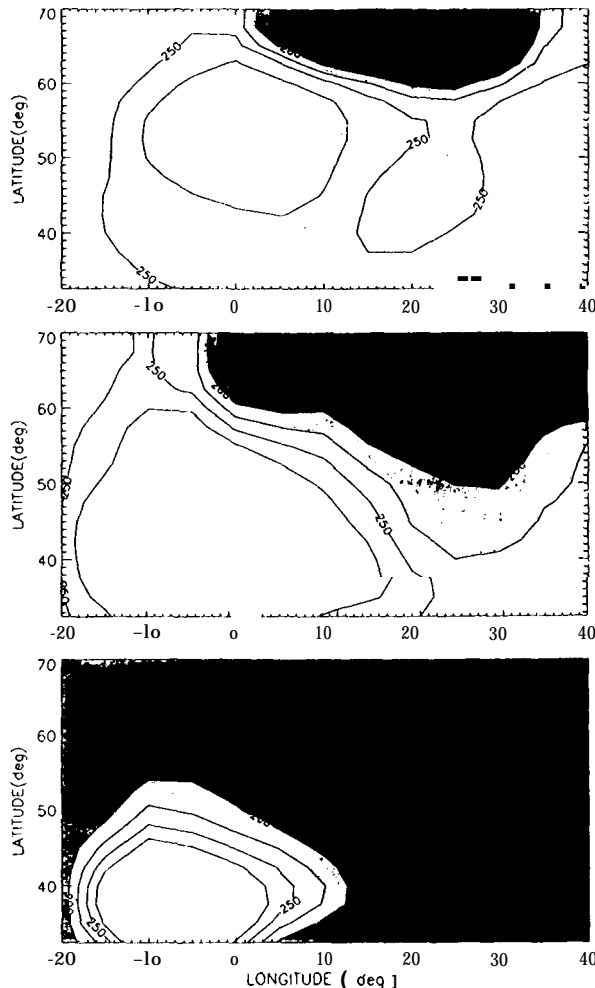


Fig. 6
Sequence of three contour plots of TEC over Europe derived from GPS/IGS station measurements during the ionospheric perturbation on November 26, 1994 at hours 12, 13 and 14 UT (downward). TEC is measured in units of 10^{15}m^{-2} .

over Europe during an ionospheric storm on April 5, 1993 at midnight. This is shown in Fig. 8 indicating also longitudinal asymmetries in the plasma distribution with a nighttime enhancement (NE) effect at about ($36^\circ\text{N}; 10^\circ\text{E}$), probably caused by plasma outflow from the plasmasphere as a consequence of plasmasphere compression due to the enhanced dawn to dusk electric field of magnetospheric origin. Regional ionospheric monitoring of TEC on the basis of GPS/IGS data should be very effective in studying the movement and geographical extension of the trough region.

2.4 The Equatorial Anomaly and Scintillations

The low-latitude ionosphere is characterized by the equatorial anomaly phenomenon which is closely related to the equatorial electrojet. Corresponding electric fields cause a strong uplifting of ionospheric plasma at the geomagnetic equator (e.g. Huang et al., 1989). When drifting down along magnetic field lines, the plasma forms so-called crest regions at both sides of the geomagnetic equator near $\pm 16^\circ$ geomagnetic latitude (fountain effect). In contradiction to the mid-latitude trough where the lowest TEC values may be observed, the crest regions at both hemispheres represent regions with the highest TEC level (e.g. Ezquer and Adler, 1989).

2.3 The Mid-Latitude Trough

The mid-latitude electron density trough is a regular phenomenon in the auroral/subauroral region (e.g. Lyszka, 1967). In this region the electron density is strongly reduced. The trough occurs mainly during night-time with the tendency to move equatorward till midnight and then returning back to higher latitudes. The physical mechanism of the trough is not yet fully understood. Obviously the trough is physically related to the plasmapause which separates the corotating inner plasmasphere from the non-corotating outer magnetosphere. In analogy to the inward motion of the plasmasphere during enhanced geomagnetic activity the pronounced trough structure moves equatorward up to 10° . Since the trough is characterized by the world wide deepest ionization level (a few TECU) it provides a good check for the quality of GPS derived TEC data. This has been done for the night of October 13, 1993 where simultaneous NNSS measurements have been carried out in Neustrelitz. The NNSS-derived TEC data deduced from differential phase measurements on 50/400 MHz are very sensitive to spatial variations along the meridional satellite trace (see Fig. 7).

It is evident that the GPS/IGS data cannot reach the spatial resolution of NNSS observations. However, the trough is also well reflected in the GPS/IGS data.

So its occurrence and movement maybe studied by GPS techniques. An example is given for a well documented trough region

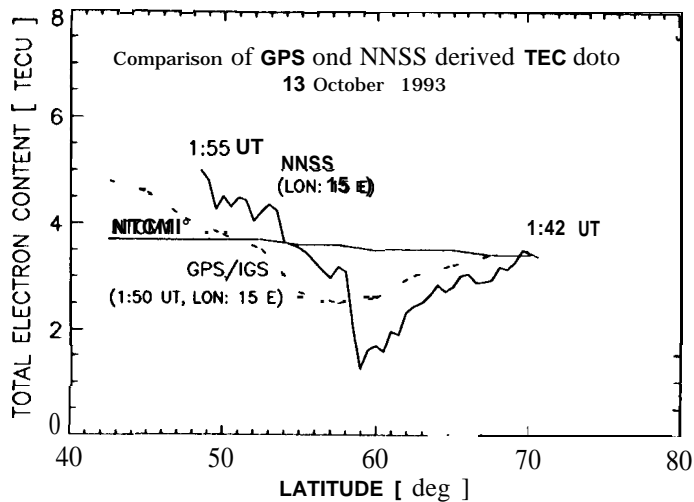


Fig. 7
Comparison of TEC data derived from GPS/IGS station measurements with corresponding NNSS data deduced from NNSS observations in Neustrelitz on October 13, 1993 around 1:50 UT. Reference is also made to the smooth NTCM1 model values.

The equatorial region is also characterized by an enhanced occurrence of small scale irregularities often called ionospheric “bubbles” (e.g. Sobral and Abdu, 1992).

Although the basic processes are known, there remain a variety of phenomena which are not yet fully understood. The high dynamics of the crest and its great sensitivity to geomagnetic activity is illustrated in Fig. 9 where the crest amplitude is shown to reach a level of nearly 140 TECU on April 4, 1994 under geomagnetic perturbed conditions ($A_p=90$) and at a minimum level of solar activity ($F10.7=77.4$).

Such high TEC levels including steep horizontal gradients should also affect the accuracy of geodetic GPS measurements.

Due to strong plasma drifts near the geomagnetic equator there occur plasma instabilities causing scintillations of amplitude, phase and polarization plane of traversing radio waves. Severe scintillations may seriously affect also geodetic GPS measurements (Wanninger, 1993).

High sensitive GPS receiver allowing sampling rates of more than 20 Hz for carrier phase and amplitudes could provide more insight into the physics of ionospheric scintillations.

Due to strong plasma drifts near the

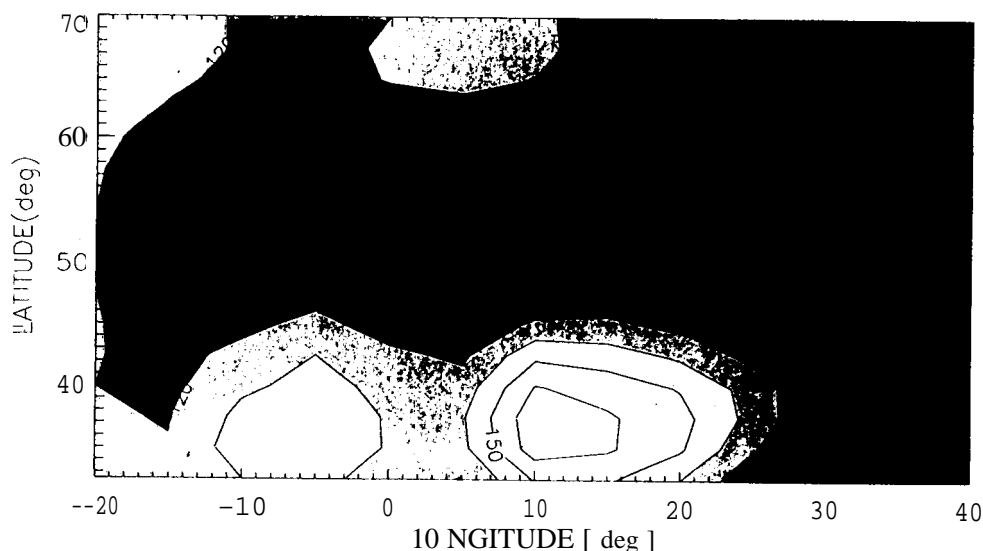


Fig. 8
Illustration of the geophysical extension of the mid-latitude trough during the ionospheric storm on April 5, 1993 at 00:00 UT. TEC contour lines are given in units of $10^{15}m^{-2}$.

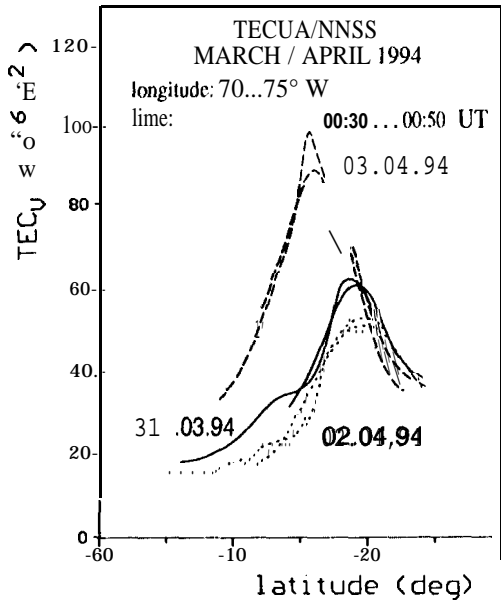


Fig. 9
 Latitudinal profiles of TEC derived from NNSS observations at the Argentinean stations Mendoza, Tucuman and Salta. The observations on March 31 and April 2, 1994 represent geomagnetic quiet conditions whereas April 3 is strongly disturbed.

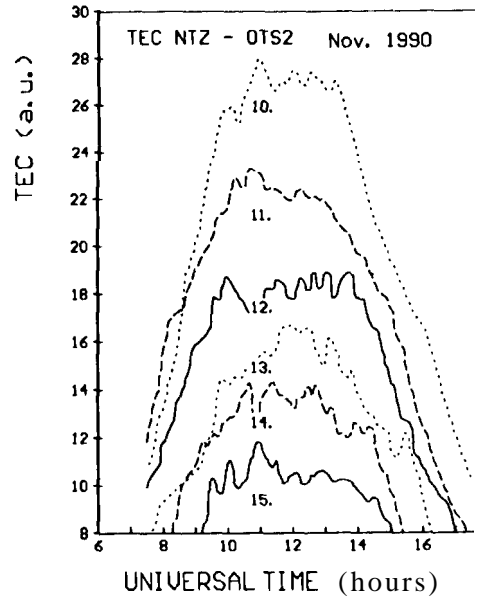


Fig. 10
 Faraday rotation observations during the Super WAGS Campaign during November 10-24, 1990. The observations indicate wave-like structures with amplitudes in the order of 1 TECU and preferred periods at 20, 30, 45 and 90 min.

2.5 Traveling Ionospheric Disturbances (TID's)

Traveling ionospheric disturbances are the ionospheric trace of Atmospheric Gravity Waves (AGW's). A large number of studies has been dedicated to this phenomenon which maybe subdivided into groups of different scale sizes. In particular, generation and propagation processes are still needed to be studied in a more comprehensive way. Here the IGS network offers a good opportunity to get new findings especially in understanding propagation processes. An example for medium scale TID's is given in Fig. 10 where Faraday rotation observations obtained during the Super-WAGS-Campaign in Neustrelitz are shown (Jakowski et al., 1992)

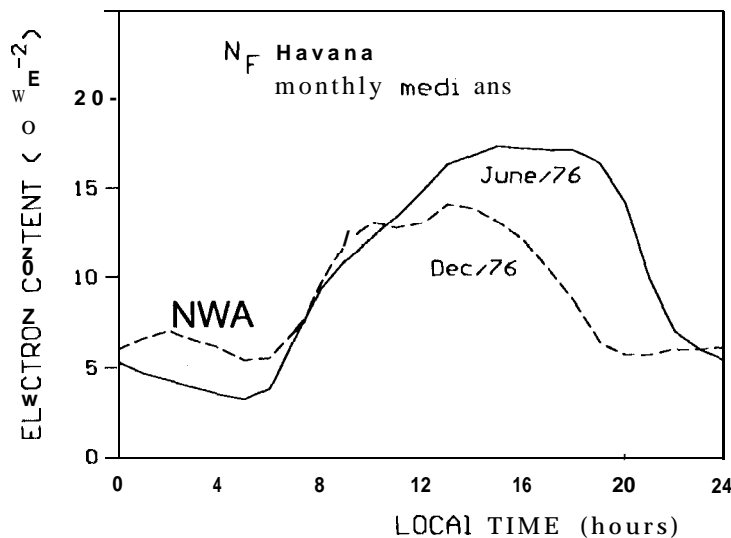


Fig. 11
 Ionospheric electron content data N_F observed by means of the Faraday rotation technique in June and December 1976 ($F_{10.7}=70.6/76.7$). The NWA effect is indicated by higher nighttime ionization in December than in June.

The spectral analysis of the wavelike oscillations revealed TEC amplitudes in the order of 1 TECU (1...3%) and periods in the range 10...120 min. The wave amplitudes A are related to

the wave frequency f by $A \cdot f^{1.5}$. During ionospheric storms large scale TID's (LSTID's) may be generated in the auroral zone then transporting energy towards lower latitudes (Pröls, 1991). The study of TID's by means of GPS techniques is limited to the analysis of carrier phases at the measured original radio link. Coordinated measurements at different radio links may provide new findings in analyzing TID's.

2.6 The Nighttime Winter Anomaly Effect

The Nighttime Winter Anomaly (NWA) effect described in this section is not of fundamental interest in ionospheric research but its systematic study is an interesting challenge for world-wide TEC monitoring using IGS stations.

In analogy to the winter anomaly effect of the daytime F2-layer, the NWA effect is characterized by a higher ionization level during winter nights than during summer nights.

Both effects are subjected to different mechanisms. The NWA effect which is illustrated in Fig. 11 was first described on the basis of ATS-6 radio beacon and vertical sounding observations in Havana (23.1°N, 277.5°E), during the low solar activity years 1974/75 (Jakowski et al., 1981). The appearance of NWA is strongly correlated with the solar activity level ($F10.7 \leq 100$) and with geomagnetic relationships. So NWA will probably be observed only at the North-American and at the South-Asian hemispheres (Jakowski and Förster, 1995).

Since the difference in TEC levels between summer and winter nights amounts to only a few TECU, the check of the reoccurrence of this effect during the low solar activity years 1994-1996 would require high accurate TEC estimations with errors less than 1 TECU. If so, the given interpretation based on close coupling with the plasmasphere and the geomagnetically conjugated ionosphere could be proved very effectively since a latitudinal dependence of the NWA amplitude is expected.

3 TEC OBSERVATION REQUIREMENTS

Depending on the scientific goal, the requirements in TEC accuracy and data coverage are different. Taking into account the special aspects of different ionospheric phenomena discussed in the previous section, some conclusions may be drawn which are summarized in Tables 1 and 2.

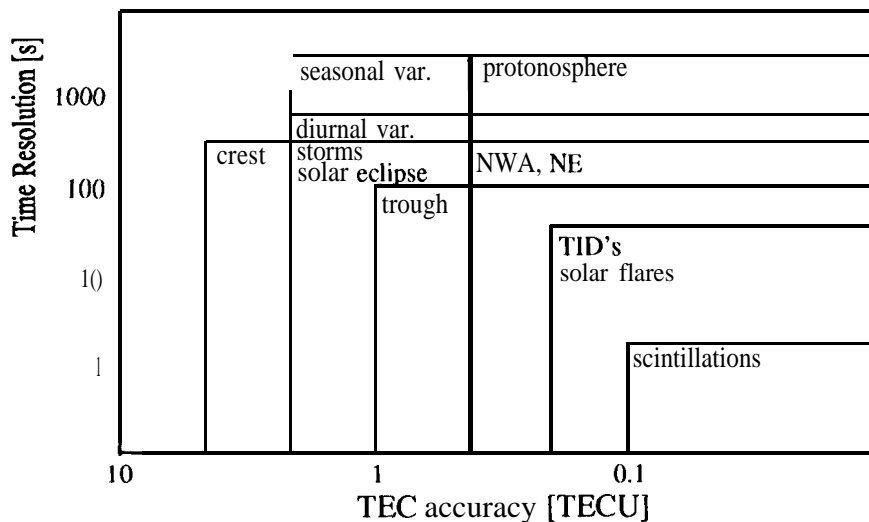


Table 1:

Rough estimation of required time resolution in TEC observations for the investigation of various ionospheric phenomena. The upper left corner of boxes indicates worst case conditions in TEC and time resolution which may be still accepted for the study of the time dependence of the corresponding phenomena.

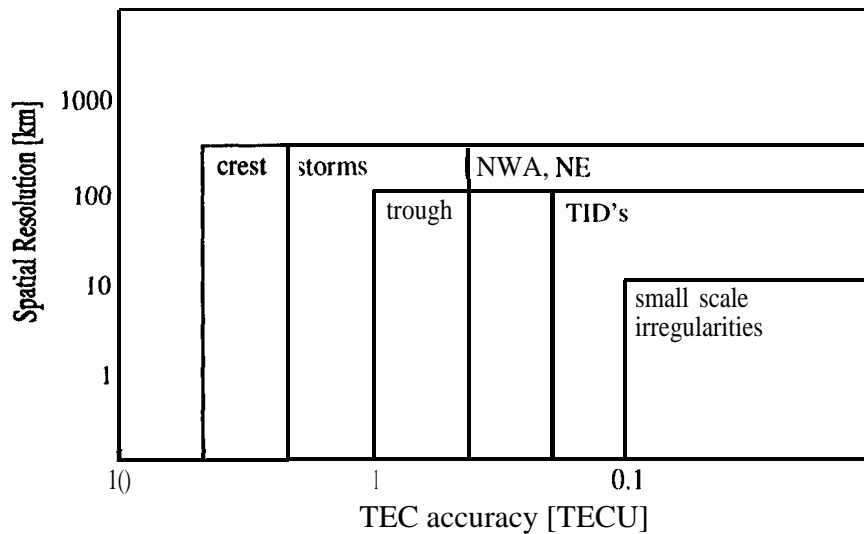


Table 2:
 Rough estimation of required spatial resolution in TEC observations for the investigation of various ionospheric phenomena. The upper left corner of boxes indicates worst case conditions in TEC and space resolution which may be still accepted for the study of spatial structures of the corresponding phenomena.

Table 1 gives a rough estimation of TEC accuracy and time resolution requirements for different ionospheric phenomena which may be effectively be studied by GPS radio beacon technique. In analogy to this, Table 2 gives a rough estimation of required vertical TEC accuracy and spatial resolution for the same phenomena. In most cases a data coverage over large areas up to the entire globe are valuable. For wavelike phenomena (e.g. TID's) and small scale irregularities relative accuracies are sufficient. TID or scintillation observations can be described by original link related phase data. At present some of these requirements can be fulfilled, others not. This is due to several limitations in deriving absolute TEC values from GPS observations related f.i. to hardware biases, multipath, protonospheric content (Klobuchar et al., 1994).

4 COORDINATION OF GPS MEASUREMENTS WITH OTHER IONOSPHERIC MEASURING TECHNIQUES

4.1 Vertical Sounding

As pointed out earlier, vertical sounding parameter such as foF2 and hmF2 enhance the scientific value of TEC data considerably. The slab thickness parameter τ is very helpful in discussing dynamic processes (see Fig. 5). When using the IGS station network for TEC monitoring, it should be useful to include also data from the world wide distributed ionosonde network. At least regional ionosonde networks as f.i. the European should be included in ionospheric research and monitoring tasks. Considerable work has already been done by several ionosonde working groups in developing algorithms for data preprocessing, data exchange and modelling (Bradley, 1992). Information about the electron density profile is helpful to reduce the errors of the mapping function. It is evident that the reduction of the measured slant TEC to the vertical or vice versa depends on the shape of the electron density profile.

4.2 Incoherent Scatter Radar

The incoherent scatter radar technique can provide a lot of information about all ionospheric layers. The main parameters obtainable up to 1000 km are the electron density, the electron and ion temperatures and ion drift velocities. Since this measuring technique works also under extremely perturbed

conditions, the combined analysis of these parameters allows conclusions about the generation and propagation of ionospheric perturbations. World-wide there are 5 Incoherent Scatter Radars (ISR) in operation: at Jicamarca, Arecibo, Millstone Hill, Sondrestrom, and EISCAT.

Since TEC is defined as the integral of the vertical electron density profile, a high correlation with ISR electron density data is expected in the overlapping region. Propagation effects maybe followed outside this region by large scale horizontal TEC maps thus contributing to a better understanding of complex ionospheric processes. The European Incoherent Scatter Radar (EISCAT) is operating in Tromsøe (Norway) with additional receiving stations in Kiruna (Schweden) and Sodankylä (Finland). The IGS stations Tromsøe, Ny Alesund, Metsahovi and Onsala could very effectively be used for coordinated measurements with the EISCAT facility.

4.3 Coordinated measuring campaigns with spacecraft missions

Various Earth satellites currently in operation or planned to be launched during the next years provide information about near earth space plasma by special experiments or as a by-product for which GPS is a good example.

The first category of satellites is mainly related to in situ measurements in space plasma including measurements in the magnetosphere or in the solar wind region.

Spacecraft activities are coordinated within the Solar Terrestrial Energy Program (STEP). Some of such satellites are f.i. INTERBALL, POLAR, CORONAS-F, WIND, CLUSTER, OERSTED, EQUATOR-S.

Satellites of the second category provide ionospheric information as a by-product mainly on the basis of indirect measurements as f.i. GPS, GLONASS, NNSS, PRARE on ERS-2, DORIS and TOPEX / POSEIDON.

By comparing vertical TEC data obtained at low orbiting satellites ($h_s \approx 100$ km) with those obtained by GPS, conclusions about the ionization of the plasmasphere could be drawn. Special arrangements of satellite orbits may be used to get more complete information about the ionosphere/plasmasphere on the basis of radio beacon measurements (Jakowski and Bettac, 1994).

In any case it would be valuable to combine different types of measurements to get more information or to fill data gaps.

5 GENERAL TOPICS OF IONOSPHERIC RESEARCH RELATED TO THE IGS NETWORK

The availability of corrected GPS-data obtained at a number of globally distributed IGS stations provide new chances for ionospheric research (e.g. Coco, 1991). The effective use of IGS stations in regional and/or global monitoring has been demonstrated already by several authors (e.g. Wilson et al., 1992)

In general the reached TEC accuracy lies in the order of 2...5 TECU.

As already discussed in the previous sections in more detail, a number of ionospheric phenomena and processes may be studied under a new point of view. In particular this is possible due to large scale and practically continuous observations of the total ionization of the ionosphere. Since ionospheric research is focussed on the investigation of the polar and equatorial ionosphere, an increasing number of IGS stations in these regions would be valuable. This concerns mainly high latitudes above $\phi=55^\circ$ geographic latitude. Since the orbit inclination of GPS satellites amounts to $i=55^\circ$, for mid-latitude stations there appears a poleward data gap above this latitude.

Besides the investigation of singular events the IGS network provides the unique opportunity to develop and to check both empirical as well as theoretical models of the ionosphere/plasmasphere systems. Such models are necessary to give reliable forecasts f.i. in the frame of a Space Weather Forecast Program.

On the other hand, regional or global models may be helpful in analyzing the GPS data itself.

According to the concept developed in the DLR Remote Sensing Station Neustrelitz (e.g. Jakowski

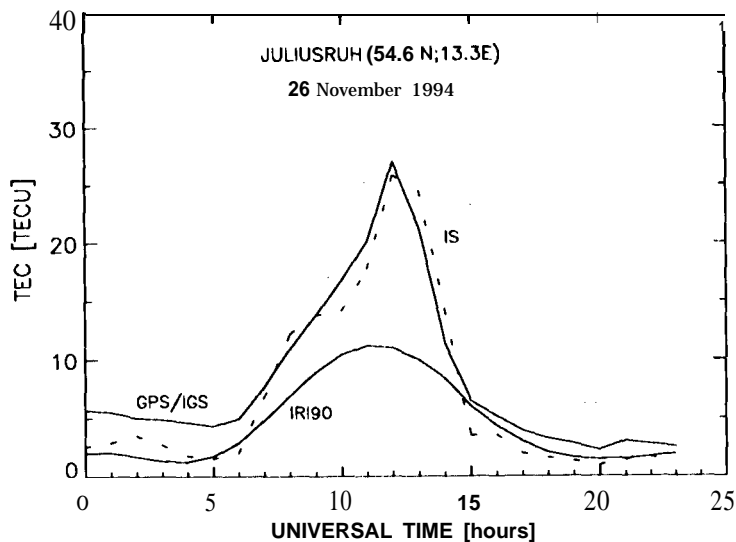


Fig. 12 Comparison of vertical TEC over Juliusruh derived from GPS measurements at European IGS stations with TEC data deduced from the integration of the IRI90 electron density profile up to 1000 km height and by using the model without additional data (IRI 90).

and Jungstand, 1994) an empirical model in combination with actual measurements at different stations is used to produce TEC maps (see Figs. 6 and 8).

Empirical models of the ionosphere need further checking and improvements in accuracy. So the IRI90 model provides some inaccuracies in describing the topside ionosphere (Bilitza et al., 1993). A comparison of actual measured TEC data and those derived by means of IRI is shown in Fig. 12.

TEC data obtained from IGS stations are a tremendous data source for the development of good models both empirical as well as theoretical.

Ionosphere/plasmasphere relationships may be studied in principle by comparing the TEC data

derived from low orbiting satellites with those obtained from GPS. However, such studies require TEC accuracies better than 0.5 TECU. Future low Earth orbit spacecraft missions, planning a well-qualified GPS-receiver onboard, should solve this task much more easier by separated links through the plasmasphere.

6 CONCLUSIONS

As it has been shown in the previous sections, TEC and/or differential phase data derived from IGS network data provide good conditions for more comprehensive studies of the ionosphere.

Valuable contributions may be expected particularly in combination with other well-developed ionospheric measuring techniques such as ionosonde, incoherent scatter radar and various space-based direct and indirect plasma probes. In general TEC accuracies (at present a few TECU) as well as the corresponding resolutions in time and space have to be improved to ensure a broad field of applications in ionospheric research.

If TEC accuracies better than 1 TECU in conjunction with a time resolution better than 1 min and a spatial resolution in the order of 100 km are reached, a large number of ionospheric phenomena may be studied. Further efforts in reducing systematic and noise errors in TEC estimation are necessary to reach this goal. Nevertheless, the accuracies reached at present allow already some studies related to large scale and well-pronounced phenomena such as ionospheric storms or the equatorial crest. The TEC data are also useful for developing and testing ionospheric models and for special tasks in a Space Weather Program.

To define challenging tasks which could enhance the efforts to improve accuracies and resolutions, two projects in ionospheric research are proposed to IGS to be realized within the next 2–3 years: 1. Since the years 1995–1997 will be characterized by a low solar activity level, the NWA effect is predicted to re-appear at mid-latitudes in North-America and in Australian region. To prove this

and, if successfully, to measure the latitudinal dependence of NWA should be an interesting challenge for large scale monitoring by the IGS network.

2. As pointed out in section 2.1, TEC is very sensitive to solar obscuration during a solar eclipse. So it is proposed to define a measuring campaign during a solar eclipse event to follow the trace of the zone of totality in the ionosphere. This would be a unique experiment which should be of great interest for ionospheric modelers. Differential phase data could be used to look for gravity wave induced TID's. Within the proposed time interval only two total eclipses maybe observed: on 24 October 1995 and on 09 March 1997.

Both these projects would involve broad international cooperation.

Acknowledgements:

The author thanks D. Adrian for her help in preparing the manuscript. This study was supported under contract 50 YI9202 with the Deutsche Agentur für Raumfahrtangelegenheiten (DARA).

REFERENCES

Bilitza, D., K. Rawer, L. Bossy, and T. Gulyaeva, International Reference Ionosphere—Past, Present, and Future: 1. Electron Density, *ArJv. Space Res.* **13**, (3)3–(3)3, 1993.

Bradley, P. A., COST238–PRIME (Prediction and Retrospective Ionospheric Modelling over Europe)— First Annual Report, 1992.

Chimonas, G. and C.O.Hines, Atmospheric Gravity Waves Induced by a Solar Eclipse, *J. Geophys. Res.* **76**, 7003–7005, 1971.

Coco, D., GPS–Satellites of Opportunity for Ionospheric Monitoring, *GPS world*, Oct. 1991, pp 47–50.

Davies, K., W. Degenhardt, G.K.Hartmann, N. Jakowski, and R. Leitinger, Relationships between ionospheric electron content and solar fluxes, *Proc. Int. Beacon Sat. Symp.* (Ed.: Min–Chang Lee), MIT, Cambridge, July 6–10, 1992, pp 188–191.

Davis, M. J. and A.V. Da Rosa, Response of the F–region Ionosphere to a Solar Eclipse, *Nature* **228**, 1121–1123, 1970.

Ezquer, R.G. and N.O. de Adler, Electron Content over Tucuman, *J. Geophys. Res.* **94**, 9029–9032, 1989.

Fuller–Rowell, T. J., M.V.Codrescu, R.J.Moffett, and S. Quegan, Response of the thermosphere and ionosphere to geomagnetic storms, *J. Geophys. Res.* **99**, 3893–3914, 1994.

Huang, Yinn-Nien, K. Cheng, and Sen–Wen Chen, On the Equatorial Anomaly of the Ionospheric Total Electron Content Near the Northern Anomaly Crest Region, *J. Geophys. Res.* **94**, 13525–13525, 1989.

Jakowski, N. and B. Laze, Significant Events in TEC Measurements between 20 March and 5 May, 1976, Report UAG–61, WDCA, 232–235, 1977.

Jakowski N., H.–D. Bettac, B. Laze, and L. Lois

Seasonal variations of the columnar electron content of the ionosphere observed in Havana from July 1974 to April 1975, *J. Atmos. Terr. Phys.* **43**, 7–11, 1981.

Jakowski, N., H.–D. Bettac, B.Laze, L. Palacio, and L. Lois, The Ionospheric Response to the Solar Eclipse of 26 February 1979 observed in Havana/Cuba, *Phys. Solariterr.* **20**, 110–116, 1983.

Jakowski N. and E.Paasch, Report on the observations of the total electron content of the ionosphere in Neustrelitz/GDR from 1976 to 1980, *Ann. Geophys.* **2**, 501–504, 1984.

- Jakowski N., E. Putz, and P. Spalla, Ionospheric storm characteristics deduced from satellite radio beacon observations at three European stations, *Ann. Geophys.* 8, 343–352, 1990.
- Jakowski, N., A. Jungstand, B. Fichtelmann, und J. Schwarz, Über das Auftreten von TID's während der Super-WAGS-Kampagne vom 1().-24. November 1990, *Kleinheubacher Berichte* 35,23-30, 1992.
- Jakowski N. and H.-D. Bettac, Proposal for an ionosphere/plasmasphere monitoring system, *Ann. Geophys.* 12,431-437, 1994.
- Jakowski N. and A. Jungstand, Modelling the Regional Ionosphere by Using GPS Observations, *Proc.Int. Beacon Sat. Symp.* (Ed.: L. Kersley), University of Wales, Aberystwyth, 11-15 July 1994, pp 366-369.
- Jakowski, N., E. Sardon, and E. Engler, About Capabilities and Limitations in Using GPS Measurements for Ionospheric Studies, paper presented at the XX. General Assembly of EGS, Hamburg, 3-7 April, 1995.
- Jakowski, N. and M. Förster, About the nature of the Night-time Winter Anomaly effect (NWA) in the F-region of the ionosphere, *Planet. & Space Sci.*, 1995 (in press).
- Klobuchar, J. A., P.H. Doherty, G.J. Bailey, and K. Davies, Limitations in Determining Absolute Total Electron Content from Dual-Frequency GPS Group Delay Measurements, *Proc.Int. Beacon Sat. Symp.* (Ed.: L. Kersley), University of Wales, Aberystwyth, 11–15 July 1994, pp 1-4.
- Liszka, L., **The high-latitude trough** in ionospheric electron content, *J. Atmos. Terr. Phys.* 29, 1243-1259, 1967.
- Pröls, G. W., L.H. Brace, H.G. Mayr, G.R. Carignan, T.L. Killeen, and J. A. Klobuchar. Ionospheric storm effects at subauroral latitudes: a case study, *J. Geophys. Res.* 96, 1275-1288, 1991.
- Sardon. E., A. Rius, and N. Zarraoa, Estimation of the receiver differential biases and the ionospheric total electron content from Global Positioning System observations, *Radio Science*, 29, 577-586.1994.
- Sobral, J.H.A. and M.A. Abdu, Solar activity effects on equatorial plasma bubble zonal velocity and its latitude gradient measured by airglow scanning photometers, *J. Atmos. Terr. Phys.* 53.729--742, 1992.
- Wanninger, I., Effects of the Equatorial Ionosphere on GPS, *GPS worlds*. July 1993. pp 49-54.
- Wilson, B. D., A.J. Manucci, C.D. Edwards, and T. Roth, Global ionospheric maps using a global network of GPS receivers, *Proc.Int. Beacon Sat. Symp.* (Ed.: Min-Chang Lee). MIT. Cambridge. July 6–1 (). 1992. pp 144-147.
- Zumberge, J., R. Neilan, G. Beutler, and W. Gurtner, The international GPS-Service for Geodynamics-Benefits to Users., *Proc. ION GPS-94*, Salt Lake City, September 20-23.199-1.

APPLICATIONS AND USES OF **IGS** INFORMATION

Gordon T Johnston
Chief Surveyor
Racal Survey Limited

Abstract

The advent of data over the Internet and the introduction of a network of GPS reference stations has offered the surveying community a unique opportunity to utilise information to augment and control various surveys. Racal Survey has operated world-wide providing surveying services for over 25 years. As the technology has developed, surveying performance has improved together with the ability to overcome many previous difficulties. The International GPS service for Geodynamics (IGS) has created a network of stations which underpin many commercial geodetic and control surveys. Racal Survey's experience of the process of improving survey schemes with IGS data is described in order to illustrate the opportunities for the IGS and the commercial surveying community to compliment each other's activities. The presentation continues with a review of a number of opportunities which may realise a secure future for both parties.

1.0 Introduction

Racal Survey have operated surveying services throughout the world over the last 25 years, concentrating on offshore surveying and related control surveys. In that time the introduction of satellite based positioning has overtaken the traditional Radio based Positioning Systems enabling greater accuracy and greater production. The development of an international tracking network and reference frame further advances the situation. These benefits have helped Racal Survey to develop globally based Differential GPS (DGPS) and a number of significant geodetic control surveys.

2.0 Who Are **Racal** Survey?

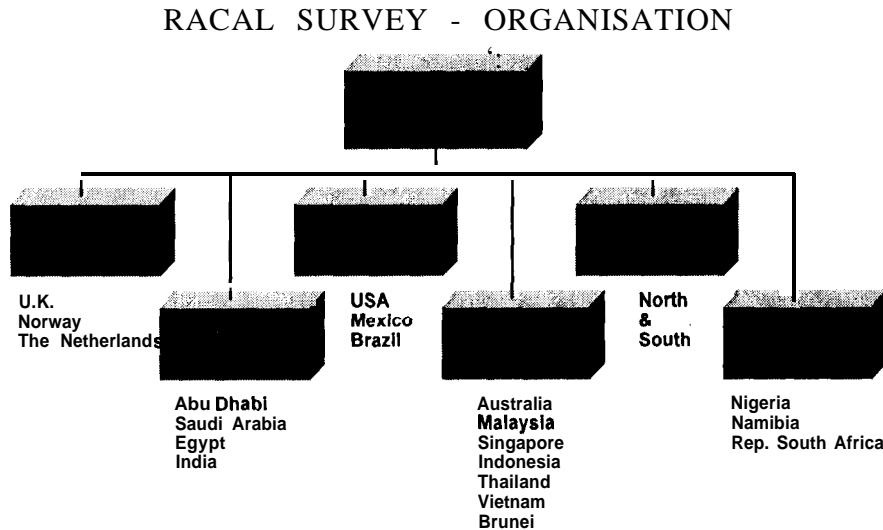
Originally formed out of the Decca Navigator Company, Decca Survey started in the early 1960's offering survey services to the offshore hydrocarbon industry. In these early days the use of Radio Positioning Systems for offshore projects was in its infancy. During the 1960's and 70's Decca expanded into many parts of the world providing a full range of surveying services. In 1980 Decca was purchased by Racal Electronics PLC and the company became Racal Survey Limited. During the 1980's and 1990's the surveying services further expanded in many areas throughout the world until the present. Racal Survey, as part of the Racal Electronics Plc Marine and Energy Group, accounts for over 10% of the £900m revenue.

2.1 The **Racal** Survey Organisation

Racal Survey are represented world-wide by 18 operating companies. These are essentially autonomous units each having responsibility for surveying services within a geographical

area. It has some 700 employees around the world and Figure 1 represents the Survey organisation and describes the geographical spread of these operating companies.

Figure 1



The main areas of survey operations are concentrated where there are offshore hydrocarbon deposits being developed. This reflects the offshore nature of Racal Survey's business however there is an increasing element of land based projects which are typically in remote and difficult areas. The services which Racal Survey currently offer are summarised as:

Differential GPS (DGPS) Services

Racal has developed the Differential links SkyFix and DeltaFix to enable offshore real time positioning in most areas of the world.

Positioning Services - Acoustics

The traditional survey operations offshore relied upon radio positioning systems for precise and accurate data above the water. However the use of acoustic positioning systems for underwater surveys and engineering tasks continues and forms a significant portion of Racal's positioning activities.

Tracking Systems

To accompany certain offshore dynamic positioning requirements Racal have developed a series of Remote Tracking Systems which provide relative positioning, usually based upon GPS, for remote vehicles. Typical applications include the seismic industry and offshore fleet management operations.

Geodetic Control Services

These land based activities are often in support of offshore operations however this trend has been changing. **Racal** Survey are now more active in the co-ordination of control points to provide local mapping, geodetic control, georeferencing of satellite imagery and asset surveys.

Geophysical Surveys

As an offshore survey services company one of the main activities is the execution of geophysical surveys. These surveys are carried out from specialised ships, which carry sensors streamed in the water. Data from the seabed is then remotely sensed and interpreted to provide geological and topographic data to aid in hazard avoidance including sub-seabed gas.

Construction Support Services

With the offshore hydrocarbon industry becoming more mature, **Racal** Survey have developed survey support services for construction operations. These services include the use of underwater remotely operated vehicles (ROV's) for pipeline lays, template installations and jacket settings.

The above activities represent a considerable investment in technology and personnel to offer survey services throughout the world in the offshore environment and, increasingly, on the land.

2.2 GPS Experience

As the use of GPS has developed and expanded so the experience of **Racal** Survey has advanced. Currently **Racal** Survey own and operate over 500 survey grade receivers. These are deployed for real time Pseudo-Range operations and static phase observations. Projects have been carried out in over 55 countries world-wide including geodetic survey activities in Africa, Asia, the Far East and Australia. Deformation studies have been carried out in Europe and on offshore projects, GPS has been used for the timing control of deep water acoustic positioning. However, of the projects regularly carried out, the majority of **Racal's** GPS uses are in real time.

3.0 **Racal** Survey and GPS

As a provider of DGPS services **Racal** Survey is one of the largest. Since 1986 DGPS has been provided using a number of different data links and message formats. Currently services are provided through the **Inmarsat** communications satellites as in Figure 2, Spot Beam communications satellites and radio based terrestrial data links. The reference stations comprise permanent stations which are monitored in real time and which have been co-ordinated in relation to **ITRF 92** in order to provide a consistent approach,

Thus Global DGPS is provided through the SkyFix system and locally operated DGPS is provided through Landstar and DeltaFix. The current coverage is shown in in Figure 3.

Figure 2

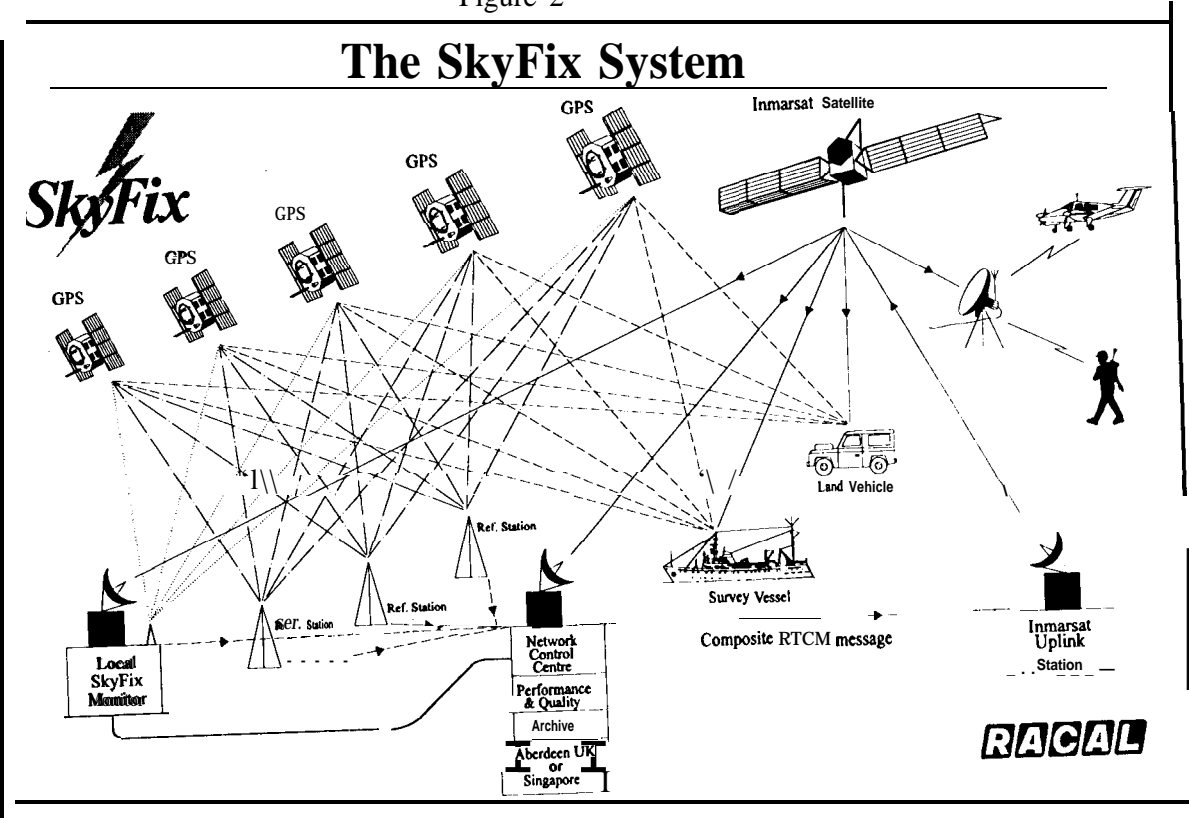
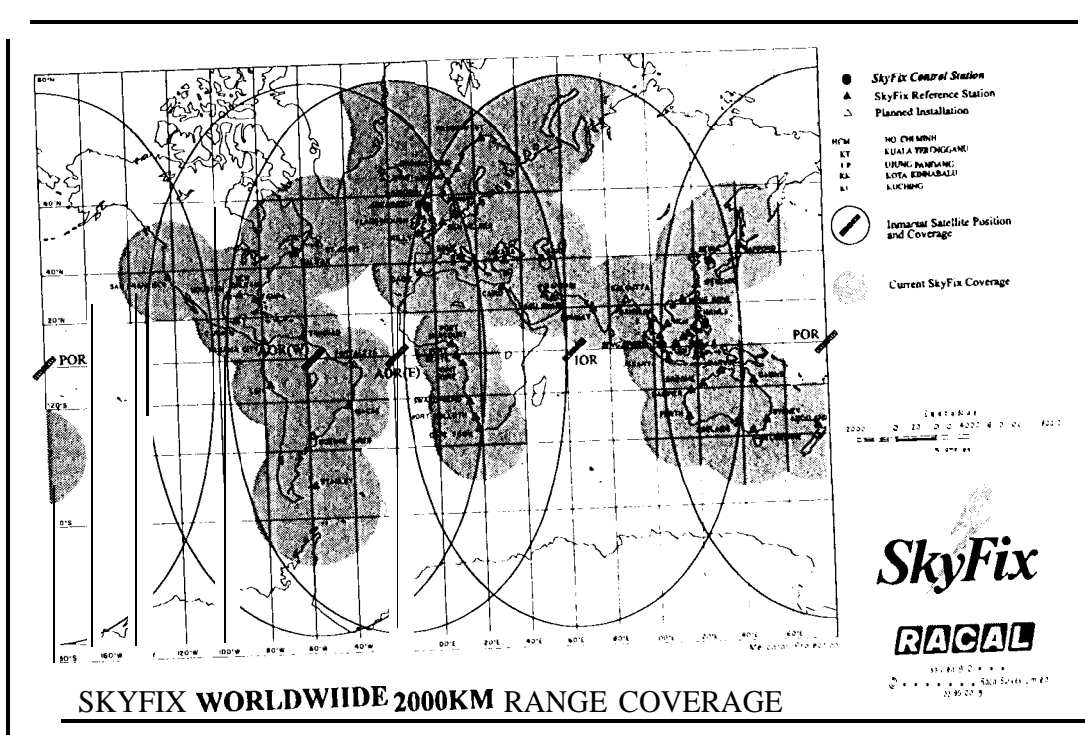


Figure 3



A typical user installation comprises a GPS receiver and equipment to receive and decode the Differential messages. Typically for offshore operations the system utilises a stabilised **Inmarsat** receiving dish, such as that shown in Figure 4.

Figure 4

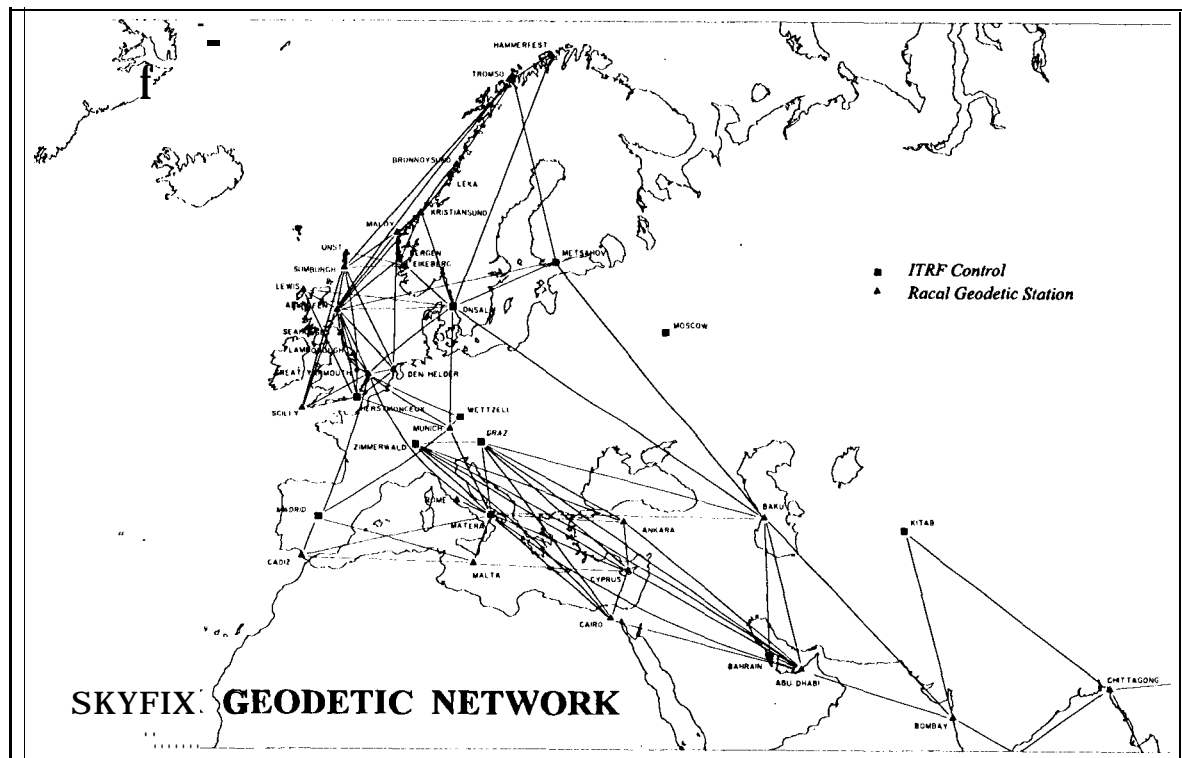


As previously mentioned the SkyFix system is a global Differential GPS service. The current status can be summarised as thus. It comprises some 60 reference stations each of which has been co-ordinated with respect to ITRF. The reference stations utilise the latest digital GPS technology and issue Differential messages to the users over the 4 **Inmarsat** data links. The users can then combine the multiple data sets to develop a single solution based upon multiple stations. The whole system is controlled by two Network Control Centres (NCC's) which are manned 24 hours a day to aid the monitoring of both the system itself and the GPS. Figure 2 provides a schematic diagram of the Skyfix system's components.

Differential GPS has the potential to operate over relatively long baselines, typically in the order of 100 to 2000 Km. Processing of the raw GPS phase data was often hindered by a variety of errors when co-ordinating stations over such long baselines. Consequently the introduction of Precise Ephemeris to overcome one potential source of error proved very useful. Relative accuracies could be contained at the sub 0.5 metre level. The use of this product was supported by the introduction of the tracking network and the development of the International Terrestrial Reference Framework (ITRF). The ITRF has played a vital role in enabling the co-ordinate control to be an order of magnitude more accurate than WGS84 on which the GPS was based. This was a key element in the geodetic approach to the survey for the SkyFix system.

Thus the use of IGS data together with the co-ordinate and Precise Ephemeris products has been a major component in the development of global real time DGPS operations. Figures 5 and 6 illustrate the level to which the geodetic control has been established in order to fully constrain the reference stations introduced,

Figure6



5.0 Racial And IGS

From the above section it might appear that the information is all one way from the IGS to Racial Survey. However this is not quite the case as a number of data sets have been forwarded to IGS related organisations for their use. Examples of this start in 1991 when dual frequency phase data from a Racial projects was offered to support the GIG'91 exercise. This was followed by dual frequency phase data from an African scheme including an IGN site. Latterly data from a variety of Southern Hemisphere stations has been provided to aid in the investigation of temporal effects on different tectonic plates. Currently the data held by

Racal Survey is available to members of the IGS however there has been a lack of supporting documentation. In addition the presence and availability of data is not advertised to IGS members and this is an area which I believe can be improved. An offer was made to the IGS in 1994 regarding the potential installation and operation of a station in one, or more, of the difficult areas as a means of aiding the IGS. To date, however, no firm response or plan has been progressed.

6.0 Future Developments

As technology advanced so the range of services expanded and the distance and accuracy of the Radio Positioning Systems also increased. Similarly the Differential GPS services are extending their range, adding monitoring and reducing their unit costs to subscribers. In this environment Racal Survey have some clear aims and goals to achieve. It is worth just bearing in mind at this stage that the discussion relates to services which support surveying activities and does not cover any life critical safety systems either at sea or in the air.

6.1 Differential GPS - SkyFix

The main feature to be implemented in the near future is the Integrity Monitoring which is required by surveyors to aid in the acceptance of DGPS performance. This task is not straightforward as it requires additional messages to be transmitted over the datalinks and the contents of these messages must have some relevance to the users. The introduction of monitoring has already started and the design no longer requires any investment in hardware but development of software.

Looking further into the future the use of dual frequency GPS receivers has the potential to isolate and reduce certain potential errors. Whilst the current single frequency L 1 based performance is adequate for many applications there is a drive to complete the development of DGPS services with an optimised, dual frequency based, high accuracy system.

In conjunction with this approach to future possible developments the SkyFix reference station distribution lends itself to additional refinements such as the use of Precise Ephemeris and the implementation of a Wide Area DGPS (or WAAS).

As many surveyors will testify the ability to provide a check, either by a method of computation or by additional (secondary) observations, is vital. To aid that concept the really significant addition to a globally based DGPS service would be a similar operation based upon GLONASS. This is an approach which has a subtle distinction between the concept of GLONASS and GPS offered by the avionics industry. For survey purposes it is sufficient to consider the two systems as independent at all levels, not integrated into a single multi-channel receiver.

6.2 GPS Partnerships

There is great potential for future partnerships in the survey industry. As regards GPS and its various uses there are a number of possible elements to be considered. The IGS perform a valuable task in providing reference stations, RINEX data, Precise orbits and other related

information. In the future, one type of data of interest to **Racal** Survey is the **RINEX** data at 1 second epoch interval. The nature of survey operations means that real time data would also be very useful. This move to real time data could be accompanied by products in near real-time such as Ionospheric models and Orbits.

For **Racal** Survey's part the offer to provide several tracking stations remains open. **Racal**'s additional expertise includes knowledge of **datalinks** for the distribution of data in a real time environment and in data compression techniques. Additionally the operational nature of **Racal** Survey's business requires field work to be carried out in remote areas and perhaps the IGS have requirements from some of the surveying projects which would be of benefit to the IGS members. Considering the future requirements for the data and products of the IGS and the pressures to reduce operating costs, there may also be a need for a discrete commercial organisation to link industry and the IGS products so that the interests of the IGS can be preserved for academia in a commercial environment.

6.3 GLONASS

As mentioned above the use of **Glonass** represents an exciting addition to global positioning services, however there is an apparent lack of knowledge regarding the nature of **Glonass** data. This is partly due to the carrier for the phase observations being on a different frequency for each satellite. In addition the differences between the **Glonass** and GPS with regard to time and geodetic reference frames has complicated its adoption for surveying. Receiver manufacturers also had to overcome these difficulties and, without a clear market for a combined **GPS/Glonass** receiver, have not perceived a financial return to exist.

Racal Survey wish to further their understanding and use of **Glonass** and to this end are investigating the nature of Differential **Glonass**. It may be useful in the future to deploy a number of reference stations throughout the world, similar to that of SkyFix, in order to offer a secondary positioning system. The reference stations and their real time data links back to a central hub may benefit the IGS who could incorporate the data into a scheme for deriving an Ionospheric model or datum shifts. In addition the IGS role could include the expansion of the **Glonass** tracking stations thus creating an enhanced ITRF network related to **SGS-90**. The culmination of such a scheme would be the generation of Precise Orbit and Ephemeris products which add to the development of real time Ionospheric models.

7.0 Conclusions

The use of IGS data and products has been instrumental to the development of survey activities on a global scale. **Racal** Survey's SkyFix DGPS service is an example of such a use. The benefits to date have generally been to the commercial survey organisation who has been able to use the products to facilitate surveys and gain improved performance. It is however recognised that this situations unlikely to continue. The increased demands made of organisations to be fully accountable for their costs means that the **IGS** must analysis its funding and operations.

In this climate of economic uncertainty in the surveying world it is the author's belief that the time is opportune to develop partnerships enabling a secure future for both the academic

interests and commercial interests derived from geodetic surveys and geodetic data. The business development strategy of a group such as **Racal Survey** is never presented for public debate however the **IGS** must also recognise certain potential benefits from an alliance with organisations such as **Racal Survey**. In order to best develop the future management of GPS data and make it's future secure, a closer working relationship must benefit all parties.

THE UNIVERSITY NAVSTAR CONSORTIUM: GLOBAL POSITIONING FOR GEOSCIENCES RESEARCH

Randolph H. Ware
University Navstar Consortium
POB 3000, Boulder, CO 80307 USA

ABSTRACT

Academic investigators established the University Navstar Consortium (*UNAVCO*) a decade ago to support their use of global positioning for **crustal** deformation research. More recently, the International Association of Geodesy established the International *GPS* Service for **Geodynamics** (*IGS*) to develop and operate an international *GPS* tracking network for geodetic and geophysical research applications. As a result of continuing improvements in *GPS* surveying accuracy and the establishment of *GPS* tracking networks, a variety of geoscience research opportunities are emerging. This paper describes *UNAVCO* and introduces some new opportunities for geosciences research using global positioning.

GLOBAL POSITIONING SATELLITES AND NETWORKS

Soon after the space age began, it was recognized that satellite orbits provide a valuable reference frame for global navigation. Today, the 24-satellite Global Positioning System (*GPS*) operated by the U.S. Department of Defense is the most widely used system, followed by the Russian *GLONASS* system. These systems may be augmented in the future by commercial low Earth orbit communication and positioning satellite services.

Reference frames of satellite orbits and the Earth's crust can be linked using **ground-based** tracking networks. The first global *GPS* tracking network was established more than 15 years ago, includes five tracking stations and is used to determine *GPS* orbits with an accuracy of about 10 m. More recently, the *IGS* established a second global network including more than 50 tracking stations, to support geodetic and geophysical *GPS* applications (e.g. **Zumberge** et al, 1994). The *IGS* network provides high accuracy *GPS* orbits (-10 cm), allowing users to place *GPS* monuments in the International Terrestrial Reference Frame with centimeter accuracy. *IGS* orbits are available within 2 to 3 weeks via anonymous ftp ([igsch.jpl.nasa.gov](ftp://igsch.jpl.nasa.gov)) or World Wide Web (<http://igsch.jpl.nasa.gov>). The *IGS* includes more than 50 international organizations.

UNAVCO AND CRUSTAL DEFORMATION RESEARCH

Scientists from seven universities formed the University Navstar Consortium (*UNAVCO*) in 1984. The Consortium's original scientific goal was to use signals broadcast by global positioning satellites to map deformation of the Earth's crust with unprecedented accuracy and spatial coverage. In pursuit of this goal, the Consortium acquired *GPS* receivers, established a facility to manage their optimal use, and began to support academic investigators using *GPS* for **crustal** deformation research.

Since that time the *UNAVCO* Consortium, its Facility, and the science associated with them have undergone continuous growth. The Consortium now includes 63 institutions, more than a third of them international, and the Facility manages more than 120 *GPS* receivers. The Facility has supported more than 150 major experiments involving *GPS* measurements of **crustal** deformation in worldwide locations (Figs. 1-9).

Governance of *UNAVCO* is based on a Memorandum of Understanding between members and its managing institution, the University Corporation for Atmospheric Research. Member Representatives elect a Steering Committee to provide program guidance and establish policy. *UNAVCO* is supported through peer-reviewed grants from the U.S. National Science Foundation (*NSF*) and National Aeronautics and Space Administration (*NASA*). Additional information regarding *UNAVCO* can be obtained via its Home Page on the World Wide Web (<http://unavco.ucar.edu>).

MULTI-DISCIPLINARY USE OF GLOBAL POSITIONING

High accuracy *GPS* positioning has been improved by two orders of magnitude during the past decade, and now millimeter accuracies are being routinely achieved. In addition, continuous global positioning satellite tracking networks are being established by the *IGS* and other local, regional and international organizations to provide basic infrastructure for space-age navigation, surveying, science, engineering, and atmospheric sensing. These networks, including 400 currently operating and 1400 proposed tracking sites (Table 1), present opportunities for tectonic, earthquake, volcano, Earth rotation, sea-level, satellite altimetry, **glaciology**, meteorology, global climate, ionosphere, hydrology and ecology studies (e.g. Ware and Businger, 1995). Many of these applications are described in the report: *Geoscientific Research and the Global Positioning System* (1994). This report is available via the *UNAVCO* Home Page (<http://unavco.ucar.edu>) or via anonymous ftp.

Table 1. Estimated number of sites operating and proposed in various tracking networks. Regional networks address civil and scientific applications in localized areas, national networks address aviation and coastal navigation, and international networks contribute to global tracking objectives.

NETWORKS	CURRENT SITES	PROPOSED SITES
Regional	70	360
National	250	875
International	75	125
Subtotals	395	1360
Total Current and Proposed		1755

Some new applications for *GPS* networks are rapidly developing. For example, tracking sites designed for geodetic positioning can be equipped with surface meteorological (*surface met*) sensors that record pressure, temperature and humidity. Data from such sites can be analyzed to provide accurate estimates of precipitable water vapor (*PWV*). *PWV* data are valuable for meteorological research and weather forecasting (Bevis et al, 1992; Kuo et al, 1995; Rocken et al, 1995) and for climate studies (Yuan et al, 1993; Elliott and Gaffen, 1995). A global climate monitoring instrument could be created by equipping *IGS* sites with *surface met* sensors. A prototype *surface met* package designed for use at *GPS* tracking sites and applications for *GPS*-sensed *PWV* will be discussed during this *IGS* workshop (Rocken et al, 1995).

Another new application for the *IGS* network is double differencing of network and orbiting *GPS* receiver data to sense atmospheric path delays. These delays can be converted to atmospheric refractivity, temperature, and moisture profiles (Ware, 1992). A demonstration of this concept was initiated in April, 1995, with the successful launch of a Turborogue receiver modified for use in space as a part of the *GPS/MET* project (Ware et al, 1993). Information including procedures for accessing data can be found on the *GPS/MET* Home Page (<http://poccc.gpsmet.ucar.edu>). The *GPS/MET* data are expected to be useful for weather research and forecasting (Kuo et al, 1995) and for climate studies (Gaffen et al, 1991; Yuan et al, 1993).

REFERENCES

- Bevis, M., S. Businger, T. Herring, C. Rocken, R. Anthes, and R. Ware, *GPS Meteorology: Remote Sensing of Atmospheric Water Vapor using the Global Positioning System*, Journal of Geophysical Research, 97, 15,787-15,801, 1992.
- Bevis, M., S. Businger, S. Chiswell, T. Herring, R. Anthes, C. Rocken, and R. Ware, *GPS Meteorology: Mapping Zenith Wet Delays onto Precipitable Water*, J. Appl. Meteorology, 33,379-386, 1994.
- Businger, S., S. Chiswell, M. Bevis, J. Duan, R. Anthes, C. Rocken, R. Ware, T. Van Hove, and F. Solheim, *The Promise of GPS in Atmospheric Monitoring*, submitted to the Bulletin of the American Meteorological Society, 1995.
- Businger, S., S. Chiswell, M. Bevis, and J. Duan, C. Rocken, T. Van Hove, J. Johnson, F. Solheim, R. Ware, *GPS/STORM: An Experiment in Using the Global Positioning System to Remote Sense Atmospheric Water Vapor*, Bulletin of the American Meteorological Society, in press, 1995.
- Chiswell, S., S. Businger, M. Bevis, J. Duan, C. Rocken, R. Ware, F. Solheim, T. Van Hove, *Application of GPS Water Vapor Data in Analysis of Severe Weather*, Monthly Weather Review, in press, 1995.
- Davis, J., G. Elgered, A. Neill, and C. Kuehn, *Ground-based measurement of gradients in the "wet" radio refractivity of air*, Radio Science, 28, 1003-1018, 1993.
- Elliott, W., and D. Gaffen, *Chapman Conference Probes Water Vapor in the Climate System*, EOS, 76,67, Feb. 14, 1995.
- Gaffen, D., T. Barnett, and W. Elliott, *Space and Time Scales of Global Tropospheric Moisture*, Journal of Climate, 4,989-1008, 1991.

- Gutman, S., R. Chadwick, D. Wolfe, A. Simon, T. Van Hove, and C. Rocken, *Toward an Operational Water Vapor Remote Sensing System Using GPS*, NOAA Forecast Systems Lab (FSL) Forum, 12-19, September 1994.
- Kuo, Y., Y. Guo, and E. Westwater, *Assimilation of Precipitable Water Measurements into a Mesoscale Numerical Model*, Mon. Wea. Rev. 121, No. 4, April 1993.
- Kuo, Y., X. Zou, and Y. Guo, *Variational Assimilation of Precipitable Water Using a Nonhydrostatic Mesoscale Adjoint Model Part I: Moisture Retrieval and Sensitivity Experiments*, submitted to Mon. Wea. Rev., March 1995.
- Rocken, C., R. Ware, T. Van Hove, F. Solheim, C. Alber, and J. Johnson, *Sensing Atmospheric Water Vapor with the Global Positioning System*, Geophys. Res. Lett., 20,2631-2634, 1993.
- Rocken, C., T. Van Hove, J. Johnson, F. Solheim, R. Ware, M. Bevis, S. Chiswell, and S. Businger, *GPS/STORM-GPS Sensing of Atmospheric Water Vapor for Meteorology*, **Journal of Atmospheric and Ocean Technology**, in press, June, 1995.
- Rocken, C., F. Solheim, R. Ware, and M. Rothacher, *Application of IGS Data to GPS Sensing of Atmospheric Water Vapor for Weather and Climate Research*, Proceedings of the IGS Workshop "Special Topics and New Directions", Potsdam, May 15-17, 1995.
- Geoscientific Research and the Global Positioning System, Recent Developments and Future Prospects*, University Navstar Consortium, 1994. This report is available via anonymous ftp (unavco. ucar. edu /pub/UNAVCO.doc/SciencePlan94.ps) Or World Wide Web (http: //unavco. ucar. edu).
- Ware, R., *GPS Sounding of Earth's Atmosphere*, **GPS World**, 3,56-57, September, 1992.
- Ware, R., M. Exner, B. Herman, W. Kuo, and T. Meehan, *Active Atmospheric Limb Sounding with an Orbiting GPS Receiver*, EOS, 74,336, 1993.
- Ware, R., C. Rocken, F. Solheim, T. Van Hove, C. Alber, and J. Johnson, *Pointed Water Vapor Radiometer Corrections for Accurate Global Positioning System Surveying*, Geophys. Res. Lett., 20,2635-2638, 1993.
- Ware, R., and S. Businger, *Global Positioning Finds Applications in Geosciences Research*, EOS, in press, 1995.
- Yuan, L., R. Anthes, R. Ware, C. Rocken, W. Bonner, M. Bevis, and S. Businger, *Sensing Climate Change Using the Global Positioning System*, Journal of Geophysical Research, 98, 14,925-14,937, 1993.
- Zumberge, J., R. Neilan, G. Beutler, and J. Kouba, *The International GPS Service for Geodynamics - Benefits to Users*, Proceedings: Institute of Navigation, 7th Technical Meeting, September 1994.
- Zou, X, Y.-H. Kuo, and Y.-R. Guo, *Assimilation of Atmospheric Radio Refractivity Using a Nonhydrostatic Mesoscale Model*, submitted to Mon. Wea. Rev., January 1995.

Fig. 1. UNAVCO Archive, 1,400 monuments & 5,600 station-days since 8/92.

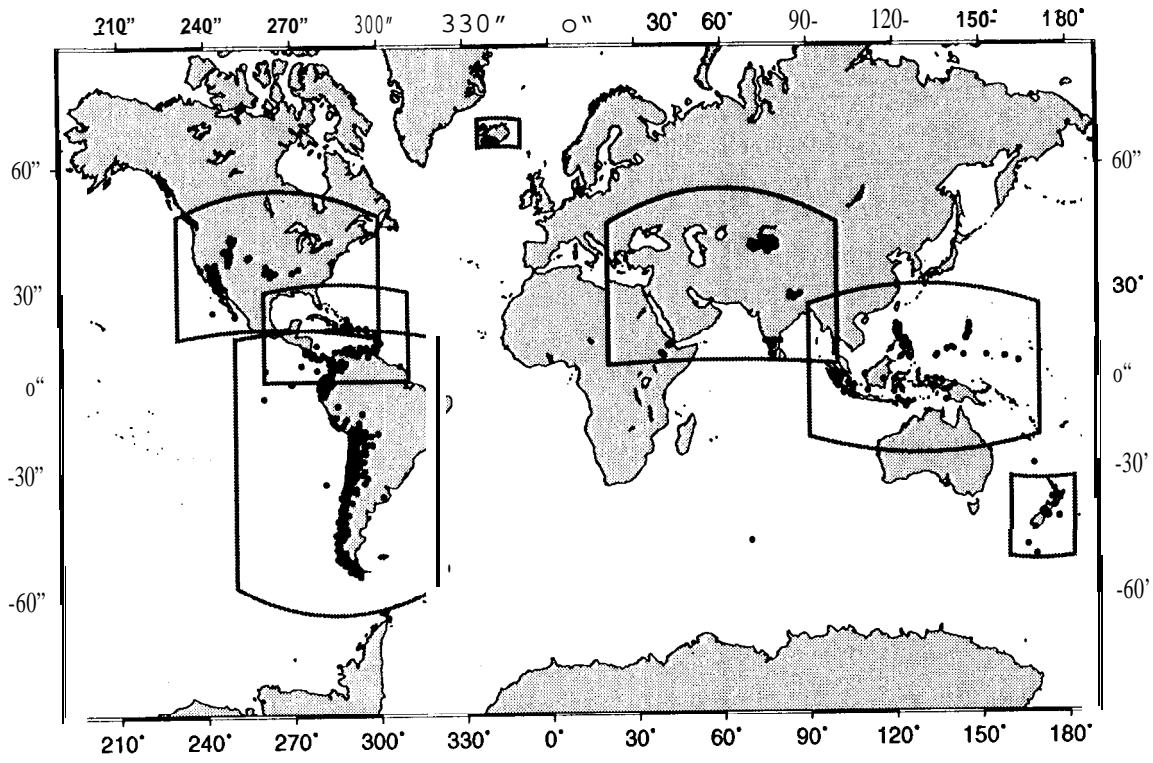


Fig. 2. Central Asia, 150 monuments archived since 8/92.

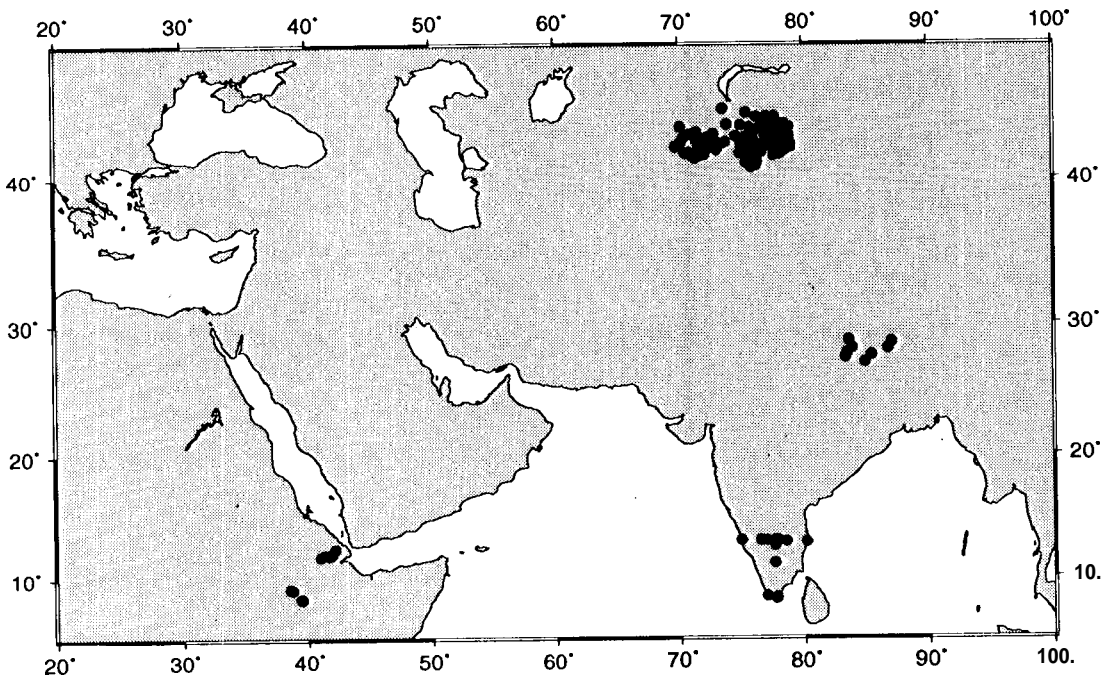


Fig. 3. South America, 425 monuments archived since 8/92.

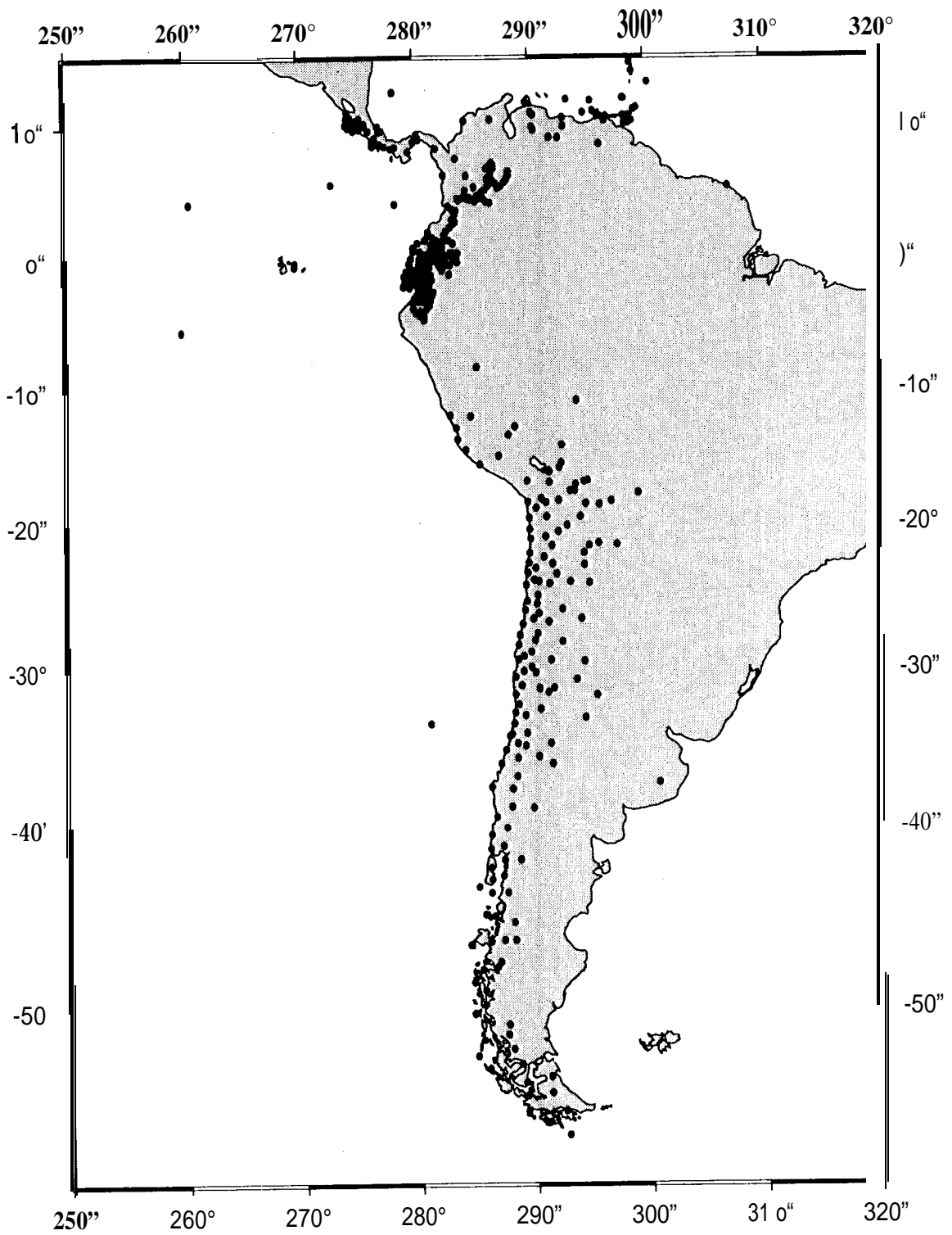


Fig. 4. Central America/ Caribbean, 197 monuments archived since 8/92.

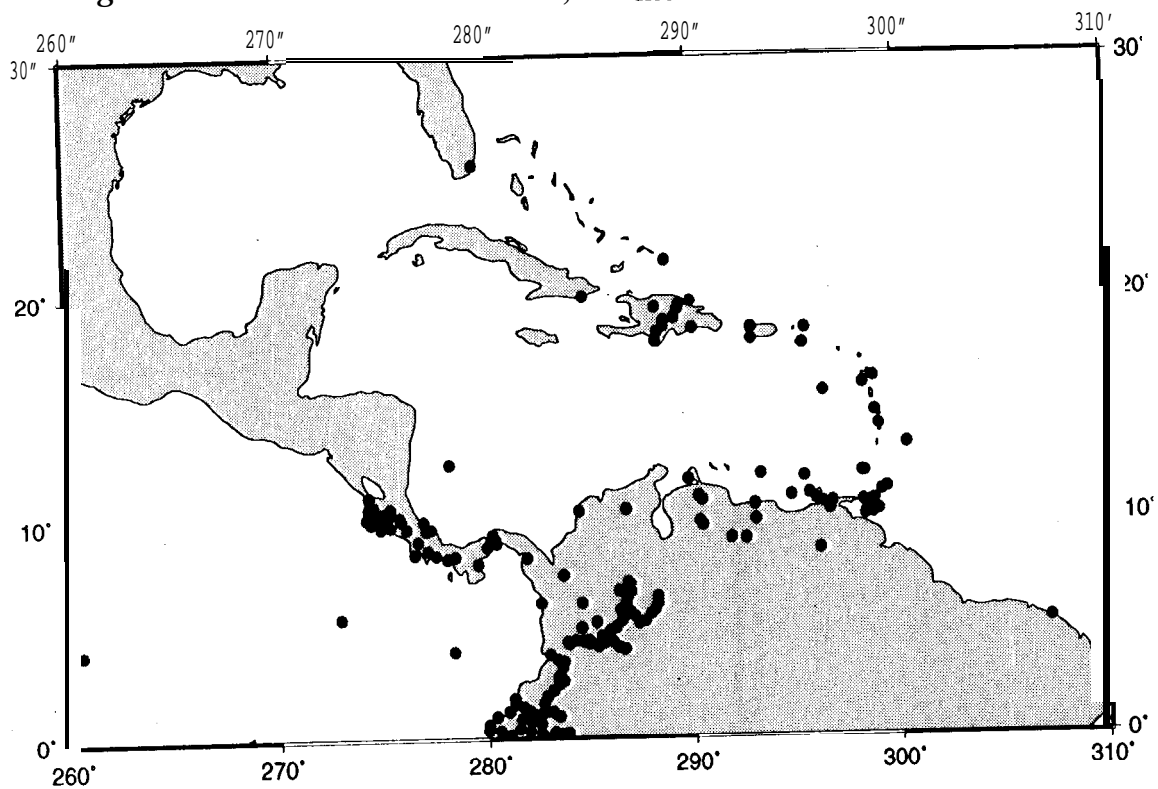


Fig. 5. Iceland, 41 monuments archived since 8/92.

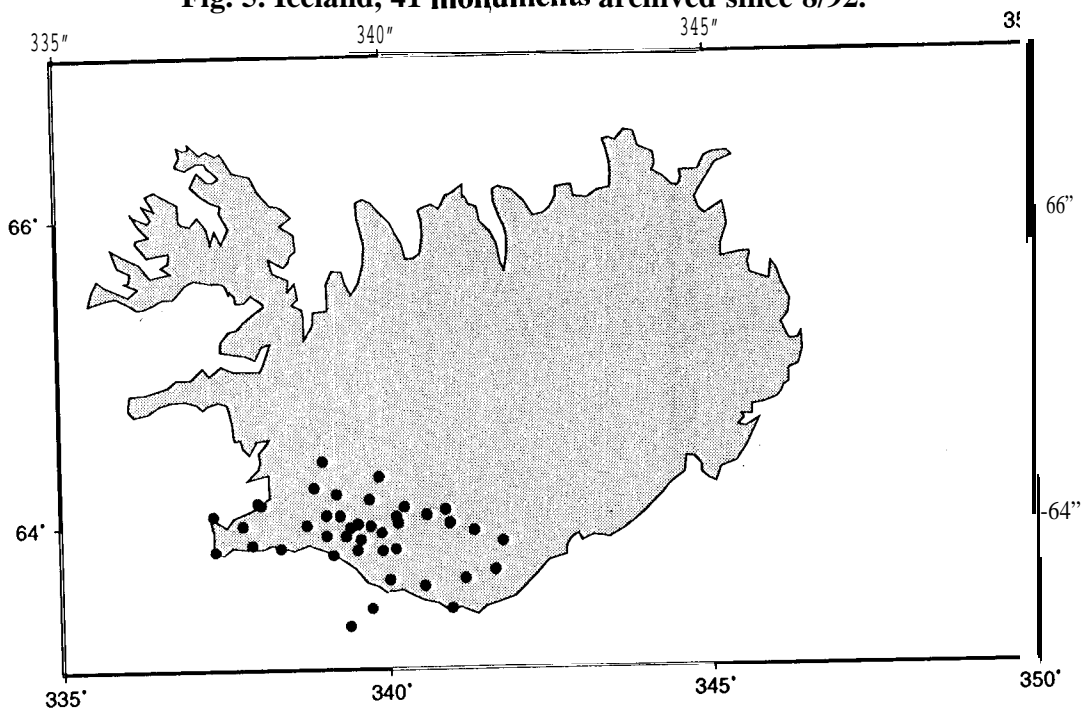


Fig. 6. Indonesia, 262 monuments archived since 8/92.

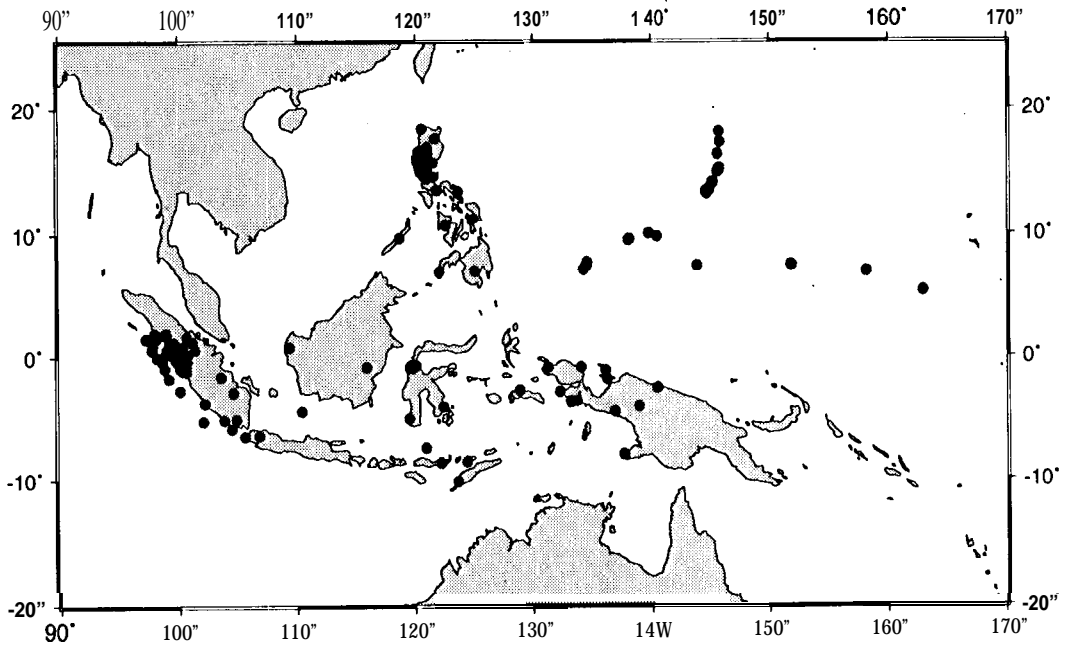


Fig. 7. New Zealand, 161 monuments archived since 8/92.

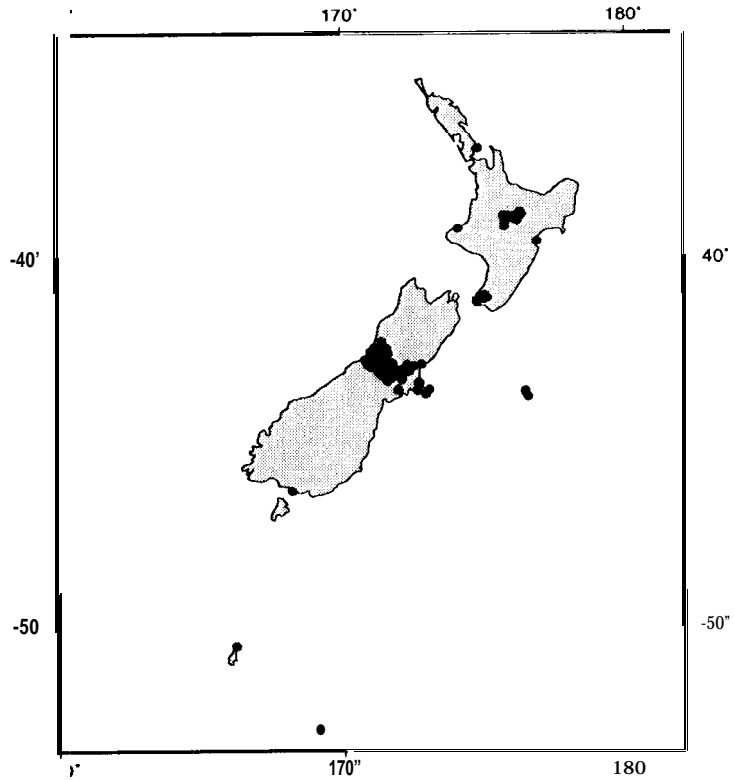


Fig. 8. North America, 334 monuments archived since 8/92.

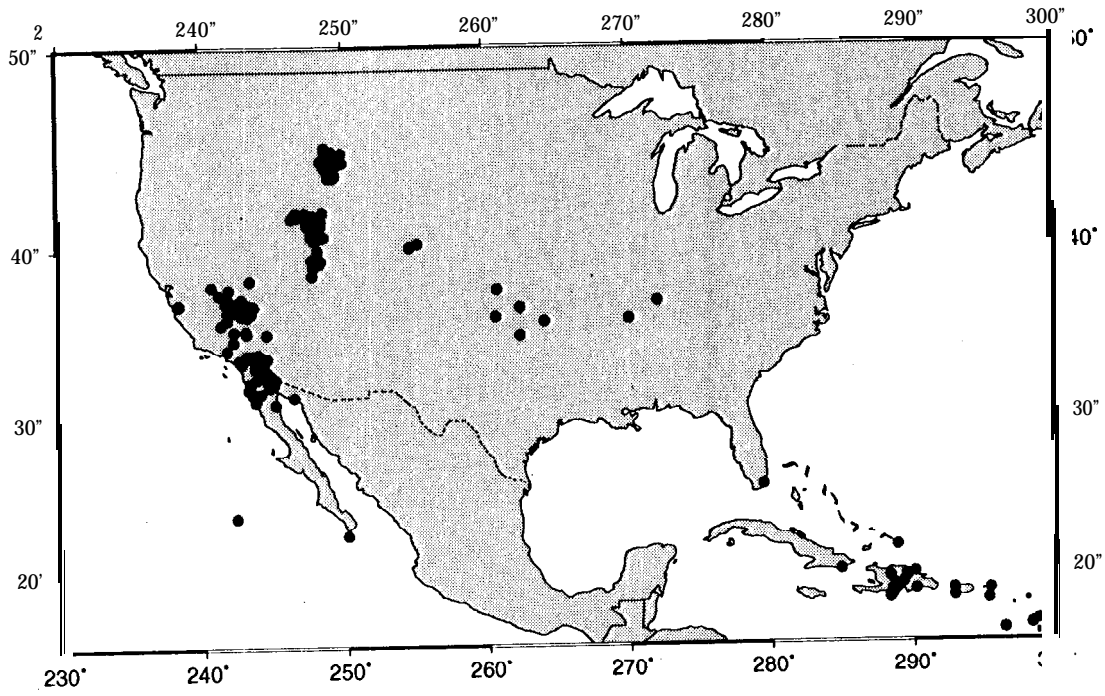
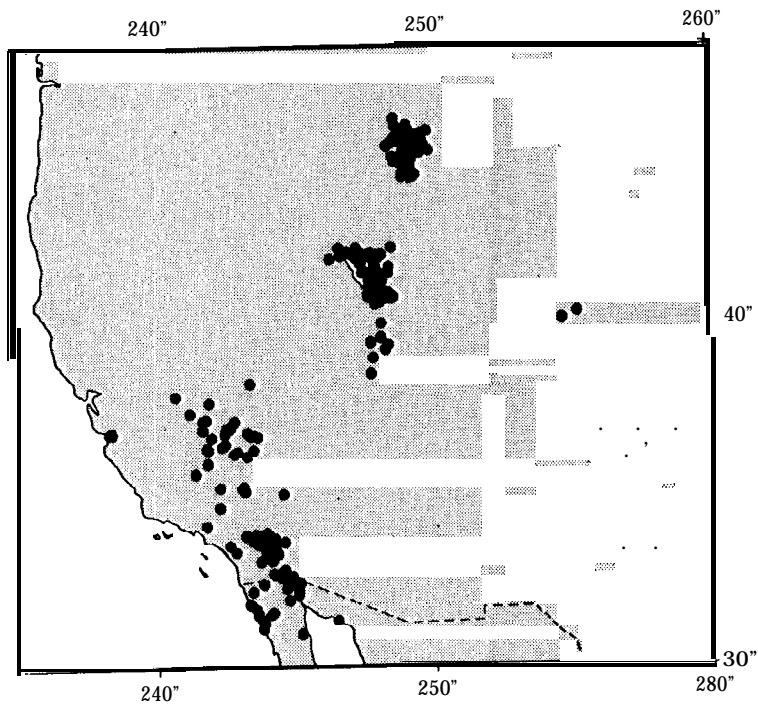


Fig. 9. Western United States, 294 monuments archived since 8/92.



Global Monitoring of Ionospheric Total Electron Content Using the IGS Network

Anthony J. Mannucci, Brian D. Wilson, Dah-Ning Yuan,
Ulf J. Lindqwister, and Thomas F. Runge
Jet Propulsion Laboratory, California Institute of Technology
Pasadena CA 91109 USA

ABSTRACT

The GPS satellites and a world-wide network of dual-frequency GPS receivers **allow** one to measure ionospheric total electron content (**TEC**) on global scales. This paper describes a method for generating global ionospheric maps (**GIM**) using data from the IGS network. Our method uses a **Kalman-type** filter and random-walk process noise to generate global TEC maps at time intervals of one hour or less. The accuracy of the maps has been assessed by comparing the computed vertical TEC to independent measurements from the dual-frequency altimeter onboard the **TOPEX/POSEIDON** ocean altimetry satellite. Computed root-mean-square (**RMS**) differences between global ionospheric maps and TOPEX are 4 TECU (1 TECU = 1×10^{16} el/m²) when the TOPEX ground track comes within 500 km of a GPS receiver. Comparisons along the entire TOPEX track generally yield larger RMS differences (5-10 TECU), indicating that the global maps become less accurate in regions far from GPS receivers.

1. INTRODUCTION

The IGS global network currently consists of more than 60 high-precision dual-frequency global positioning system (**GPS**) receivers distributed around the world. Data from this network has been used to produce global ionospheric maps (**GIM**) which are “snapshots” of the Earth’s zenith total electron content (**TEC**) distribution [Mannucci, *et al.* 1993]. Global ionospheric maps are useful for monitoring the global TEC distribution for scientific studies, model development and calibration of ionospheric delay.

In addition to the GPS network, vertical TEC measurements covering a significant portion of the Earth’s oceans are available from instruments onboard the **TOPEX/POSEIDON** ocean altimetry satellite. These instruments include a dual-frequency ocean altimeter and a dual-frequency range-rate (**DORIS**) capability. The TOPEX data can be used to study the accuracy of the **GPS-based** global maps, or incorporated into the mapping algorithm to improve accuracy. In this paper, we present a preliminary assessment of the accuracy of the global maps by performing comparisons between the mapped TEC and the ionospheric measurements available from the dual-frequency altimeter.

$$I_{rs}(t) = F(E) \sum_{i=1}^3 W_i(\phi_{pp}, \lambda_{pp}) V_i + b_r + b_s \quad (1)$$

where $I_{rs}(t)$ is the GPS line-of-sight measurement from receiver r and satellites at time t , V_i is the value of the TEC at vertex i (i.e. parameter i), and b_r and b_s are the receiver and satellite instrumental delays [Wilson and Mannucci, 1993]. The placement of the vertices is based on a triangular tessellation of a spherical shell. The factor $W_i(\phi_{pp}, \lambda_{pp})$ is a weighting function which depends on the distance between vertex i and the ionospheric pierce point of the measurement, whose latitude and longitude is $(\phi_{pp}, \lambda_{pp})$. Each measurement only affects the three vertices of the intersected tile. $F(E)$ is the elevation mapping function relating slant delay to vertical. The simplest “thin-shell” mapping function is given by:

$$F(E) = \{1 - [\cos E / (1 + h/R_E)]^2\}^{-\frac{1}{2}} \quad (2)$$

where E is the elevation angle, h is the height of the shell (350 km) and R_E is the mean Earth radius. There are several more realistic mapping functions which can still be expressed analytically in closed form, including a uniform slab of finite width and an extended slab (a slab with exponential tails).

A Kalman-type filter is used to estimate the vertex and instrumental bias parameters based on the linear observation equation 1. The vertex parameters are re-estimated every hour (more frequent updates are possible) allowing the maps to follow short term TEC changes of the ionosphere. An animated sequence of maps can show the time evolution of the global ionosphere. The errors for vertex values not updated with new data grow as a random walk (square root of time).

Local to each GPS receiver, the accuracy of the maps is affected by multipath noise at low elevations; the accuracy of the instrumental bias determinations for the GPS receivers and satellites; errors made in the elevation mapping function; and errors of interpolation between the ionospheric pierce points of the GPS measurements (some of these factors are discussed by Klobuchar *et al.*, 1993).

The large-distance interpolation between the local GPS measurements is made more accurate by fixing the grid points in a “solar-geomagnetic” coordinate system. In this system, each vertex has a fixed geomagnetic latitude and nearly sun-fixed longitude, so the grid does not co-rotate with the Earth. The value of a grid point represents the TEC value for a given local time, not a given geographical position. All geographic regions, whether populated with GPS stations or not, sample the full range of local times over the course of a day. Therefore, in areas far from receivers, the TEC value at a given local time is determined by measurements obtained at that same local time from receivers in a geomagnetic latitude band surrounding the vertex. In effect, interpolation of the distribution over large distances is replaced with “local-time prediction”.

3. TOPEX COMPARISONS

3.1 The TOPEX dual-frequency altimeter

To assess the accuracy of the GPS-based global maps, we used the ionospheric measurements from the TOPEX dual-frequency radar altimeter (TPXALT). This data set, available from the satellite since October of 1992, measures vertical TEC up to a height of about 1330 km, which is above almost all of the daytime ionosphere. Since the global ionospheric maps (GIM) provide vertical TEC covering all latitudes and times, the GIM evaluated along the TOPEX ionospheric pierce points can be compared to the altimeter measurements. An example of such a comparison plot is shown in Figure 2. The TOPEX orbital period is approximately 110 minutes.

3.2 Comparison Overview

The TOPEX/GIM comparison has been done in two ways. First, we have restricted the comparisons to times when the TOPEX ground track comes within 500 kilometers of a GPS station (a so-called “over-flight”). This tests the accuracy of the maps local to a GPS receiver. We have also compared the GIM and TOPEX measurements over the entire day-time portion of each ground track. The TOPEX altimeter data is only available over the water, where the average distance to the nearest station is typically several thousand kilometers. Therefore, the whole track comparisons assess the accuracy of the interpolation in areas far from GPS receiver sites.

Data from three periods was used in this study: March 13-15 of 1993, August 13-15 of 1993 and January 23, 24, 26 and 27 of 1994. The station locations for the current network are shown in Figure 1. The global geomagnetic index A_p for each day is shown in Figure 3. All comparisons were performed for local daytime (6 am-6 pm) conditions so that the accuracy numbers represent an upper limit (undiluted by the low nighttime TEC values).

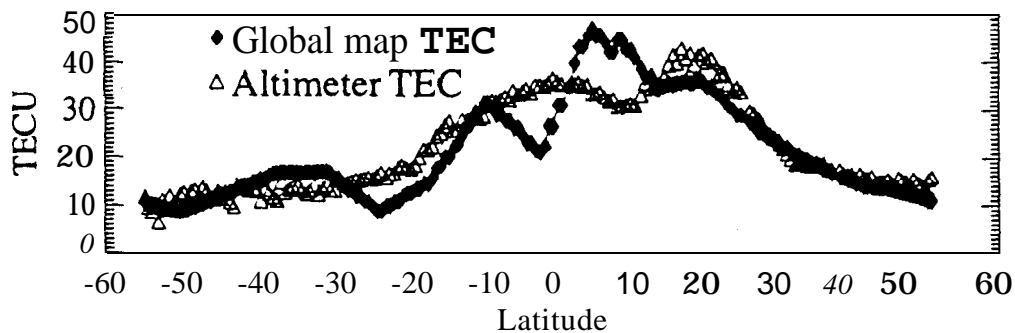


Figure 2: A plot showing the TOPEX-derived TEC measurements and the GIM map evaluated along the TOPEX track. Data from August 14, 1993 is shown. The track was at its southern-most point at 13:00 local time and crossed the equator at 16:25 local time.

3.3 Over-flight analysis: assessing GIM near GPS receivers

Comparing GIM and TPXALT during over-flights allows a comparison between the “instantaneous” ionosphere measured by each technique with a minimum of interpolation error. An over-flight occurs when the TOPEX ground track comes within 5 degrees (500 kilometers) of a GPS receiver; 36 daytime over-flight opportunities from 18 receiver sites were analyzed, and the results for mid and low latitude sites are summarized in Table 1. The nine mid-latitude sites used in this study were situated between 30 and 55 degrees, north or south. The nine equatorial sites were within 30 degrees of the geographic equator. The RMS differences were computed between the GIM TEC values and the TPXALT measurements for every 10 second altimeter data point during the 1-2 minute duration of each over-flight.

	Low Latitude	Mid Latitude
RMS Difference	4.0	4.1
Mean Difference	-1.9	-3.5

Table 1: RMS and mean differences between TPXALT and GIM for 36 over-flight opportunities in March and August of 1993 and January of 1994. Vertical TEC differences in units of TECU.

The RMS difference between the GPS and TOPEX-derived TEC is about 4 TECU, and does not differ for the two latitude bands (1 TECU = 1 TEC unit = 1×10^{16} el/m²). Some contribution to this RMS difference is due to the finite accuracy of the TOPEX measurements, estimated to be about 3 TECU [Callahan, 1993]. If the TPXALT and GIM errors are summed in a root-sum-square manner, then a global map error of 2.6 TECU near the receivers is consistent with a TPXALT error of 3 TECU and an overall RMS difference for the over-flights of 4.0 TECU.

The negative mean difference between GIM and TPXALT indicates that the global map TEC was on average lower than the altimeter-derived TEC. This is surprising since the GPS satellites orbit at 22,000 km altitude while the TOPEX altitude is 1330 km. One possibility is that the TOPEX altimeter TEC data is biased too high. Another possible explanation is that the estimates for the GPS receiver or satellite instrumental delays are larger than the true values. Since the bias between two independent measurement types is an upper limit on the accuracy of each technique, agreement at the level of 2–3.5 TECU is encouraging and suggests that the estimated instrumental delays for the GPS receivers and satellites are accurate to at least that level. The GPS instrumental bias estimates may improve in the near future with the use of an improved elevation mapping function.

For these over-flights, the satellite and receiver instrumental biases were estimated along with the TEC distribution for all but three receivers. The receiver biases in Goldstone, California, Madrid, Spain and Tidbinbilla, Australia were fixed to hardware calibration values. Of these three, only the Tidbinbilla station was used in the over-flight comparisons.

3.4 Accuracy comparison along the TOPEX orbit as a function of latitude band

The TEC differences between GIM and TOPEX along the entire daytime portion of the TOPEX orbits have also been computed. The orbital ground tracks span a latitude range of approximately 66S to 66N geographic and have a Sun-relative angle (local time) that varies only about 2 degrees per day. The differences have been analyzed as a function of latitude region. We expect local-time prediction to be less accurate in the low latitude region where the ionospheric F2 layer is more variable than for the mid-latitudes. Another latitude-dependent factor which may affect accuracy is the number of sites in each latitude band: there are more northern mid-latitude sites as compared to the low and southern mid-latitudes.

Figure 3 shows the RMS differences between GIM and TOPEX as a function of latitude band for the three time periods studied. As expected, the RMS differences along the entire track are generally larger than for the over-flights. This results from the additional interpolation error required to produce GIM values far from the stations. For most days, the low latitude band contains the largest RMS differences.

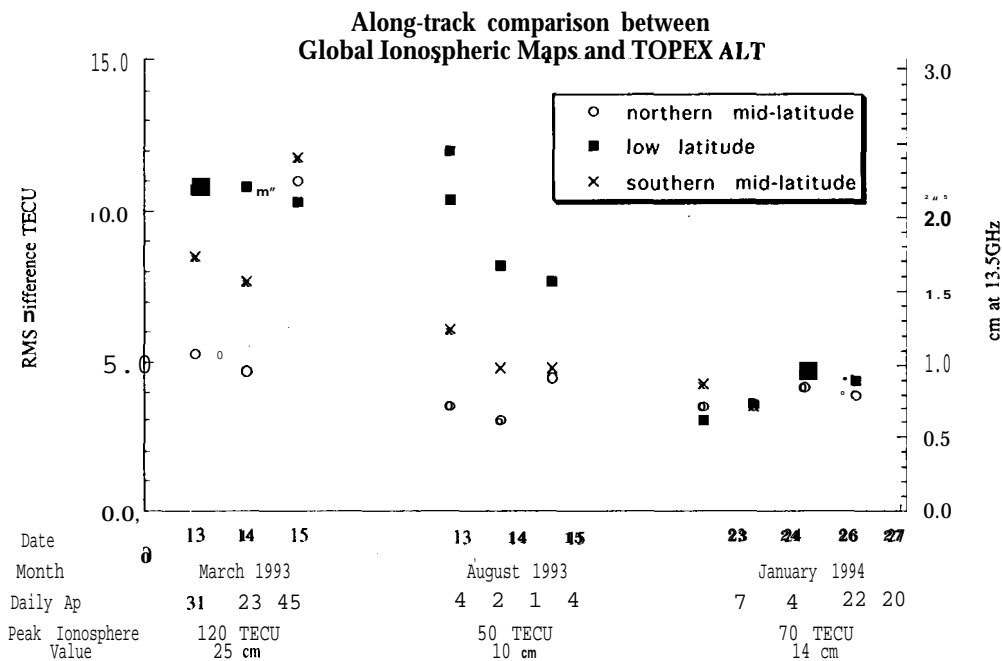


Figure 3. Daily RMS differences between TPXALT and GIM along the entire daytime portion of the altimeter ground track. The latitude bands are defined as follows: northern mid-latitude = 60N-30N geographic; low latitude = 30N-30S; southern mid-latitude = 30S-60S.

The RMS error for each latitude band decreases going from March 1993 to January 1994. This is not surprising since the number of stations in the network increased from March to January. However, the differences in the RMS errors are probably related to the differences in local times for the three periods. The daytime TOPEX passes were around local noon during March 1993, 4:30 PM local time during August 1993, and 8 AM during January 1994. The number of days studied is too few to draw any firm conclusions. The accuracy of the global maps is a function of the number and distribution of the receiver sites and the temporal variability of the ionosphere, which tends to reduce the accuracy of local-time prediction,

4. CONCLUSION

This study is a preliminary effort to assess the accuracy of the global ionospheric maps. Since the TEC data available from the altimeter onboard the TOPEX/POSEIDÓN satellite covers a broad range of latitudes, it is a valuable tool in such a study. Unfortunately, no data is available above 66 degrees latitude due to the satellite inclination and no data is available over land.

A comparison between GIM and TOPEX was done for “over-flights”, when the TOPEX ground tracks came within 500 km of a GPS receiver. This comparison reveals an RMS difference between TPXALT and GIM of about 4.0 TECU. The results are the same for equatorial and mid-latitude over-flights. Given that the TOPEX accuracy is considered to be about 3 TECU, the RMS error of the vertical TEC measured by GIM near the receivers may be 2.6 TECU.

The global maps were also compared to the TOPEX measurements along the entire daytime portion of the TOPEX orbit for three latitude ranges. As expected, the RMS differences were generally larger than for the over-flights and were usually larger in the low latitude region than in the mid-latitudes. Since several factors contribute to the accuracy of the global maps, a more comprehensive study is in progress to analyze how the accuracy varies as a function of local time, geographic region, distance from the receivers, and geophysical conditions.

ACKNOWLEDGMENTS

This analysis was made possible by the high quality of both the global GPS and TOPEX data sets, the result of a collaborative effort involving many people at JPL and at other centers around the world. The research described in this paper was performed by the Jet Propulsion Laboratory, California Institute of Technology, under contract with the National Aeronautics and Space Administration.

REFERENCES

Callahan, P., TOPEX GDR user's handbook, JPL D-8944 Rev. A, 3-19, 1993.

Klobuchar, J. A., S. Basu, P. Doherty, Potential limitations in making absolute ionospheric measurements using dual-frequency radio waves from GPS satellites, Proceedings of the Seventh International Ionospheric Effects Symposium, J. Goodman, cd., Alexandria, VA, May 1993.

Mannucci, A. J., B. D. Wilson, C. D. Edwards, A new method for monitoring the Earth's ionospheric total electron content using the GPS global network, Proceedings of the Institute of Navigation GPS-93, Salt Lake City, Utah, September 22-24, 1993.

Wilson, B. D., A. J. Mannucci, C. D. Edwards, Instrumental biases in ionospheric measurements derived from GPS data, Proceedings of the Institute of Navigation GPS-93, Salt Lake City, Utah, September 22-24, 1993.

MONITORING IONOSPHERIC DISTURBANCES USING THE IGS NETWORK

Lambert Wanninger
Geodetic Institute, TU Dresden
D-01062 Dresden
Germany

ABSTRACT

Small-scale ionospheric irregularities disturb GPS signals in two ways: they produce fluctuations in signal strength (amplitude scintillations) and rapid changes in ionospheric delay (phase scintillations). GPS observation data provided by the IGS network are an excellent resource for monitoring phase scintillation occurrence. Examples of phase scintillation occurrence maps produced from IGS data demonstrate their importance not only for ionospheric research but also for GPS users.

INTRODUCTION

The ionosphere is well known by GPS users as a source of refraction errors which can effectively be corrected by simultaneous dual-frequency observations. The highest total ionospheric electron contents (TEC) and thus the largest ionospheric refraction delays are found in the equatorial region (Fig. 1, Fig. 3). They not only cause **single-frequency coordinate errors but also difficulties in single-frequency and dual-frequency carrier phase ambiguity resolution**. In relative positioning, large-scale gradients of the vertical TEC often produce larger errors than absolute TEC.

This paper, however, deals with the effects of the disturbed ionosphere on GPS signals and GPS positioning. It concentrates on small-scale irregularities in the electron density which cause signal scintillation. Since the early days of GPS it has been known that signal scintillation is by far the most serious problem in transionospheric propagation (Parkinson *et al.* 1977). Scintillation degrades GPS receiver performance: an increased number of cycle slips and even the inability to track the GPS signals (data loss) can occur. The effects of ionospheric scintillation on GPS

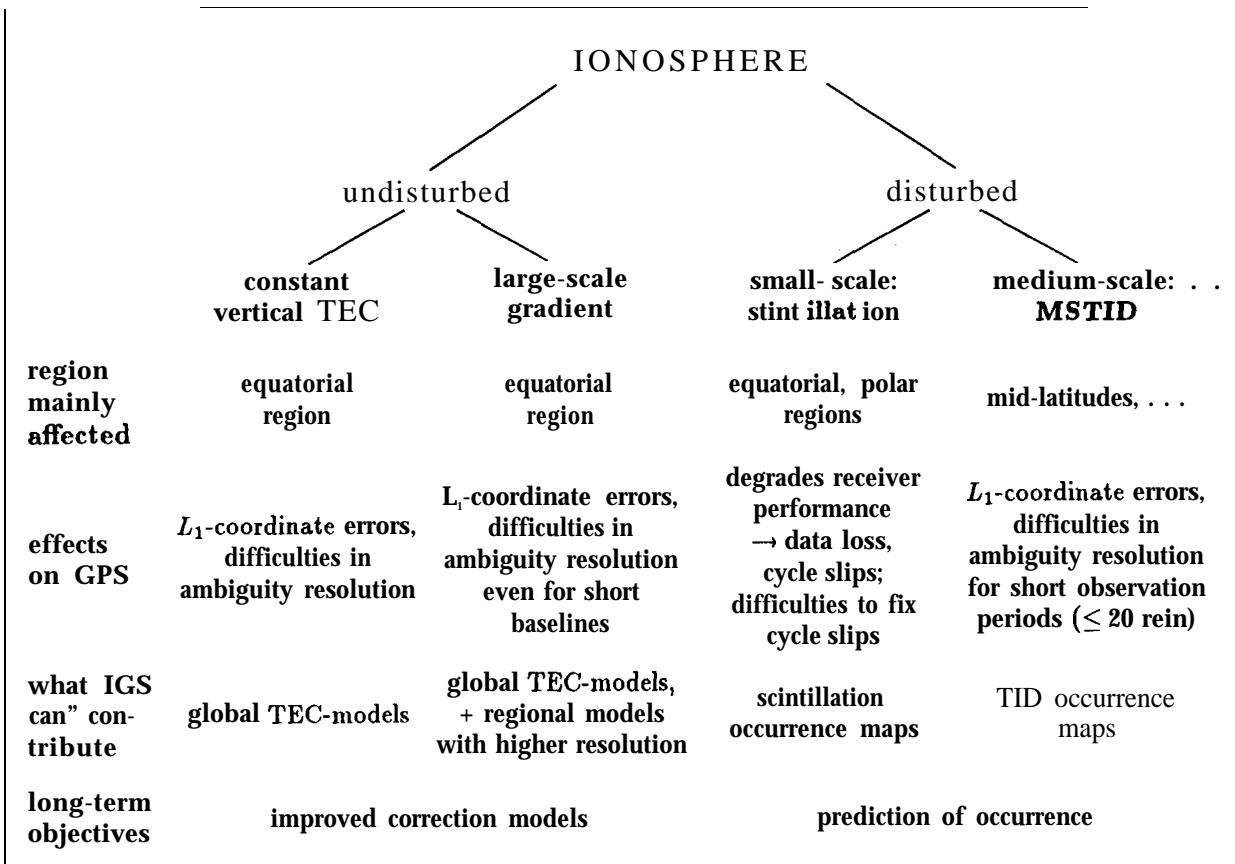


Fig. 1: GPS, IGS, and the ionosphere.

signals can be detected in GPS observations and thus the geographical and temporal occurrence of small-scale ionospheric irregularities can be monitored.

SCINTILLATION EFFECTS ON GPS

Severest effects of small-scale ionospheric irregularities are signal fading and signal enhancement, collectively known as amplitude scintillations. As a result of these scintillations, the level of a GPS signal can drop below a receiver's lock threshold. This threshold depends on the bandwidth of the GPS receiver system and on the type of tracking channel. Amplitude scintillations can be monitored by interpretation of time series of S/N values provided by many GPS receivers. Rapidly changing values indicate scintillation activity (Fig. 2). Missing S/N values for the disturbed satellite pass indicate that the receiver could not continuously track the GPS signal. Data loss and an increased number of cycle slips are a consequence of this scintillation activity.

Phase scintillations result from sudden changes in ionospheric refraction or from diffraction effects. Because of these scintillations, the phase of both the L_1 and L_2 carriers can change by several cycles between two measurements spaced by, for

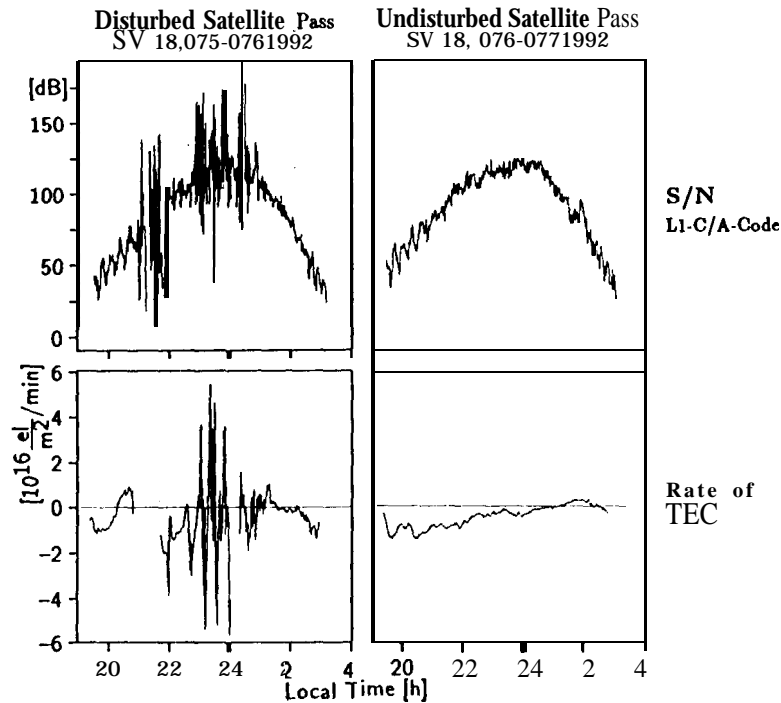


Fig. 2: Effects of equatorial scintillations on GPS measurements from southern Brazil: amplitude scintillations, phase scintillations (*Wanninger 1993b*).

example, 30 seconds. Such perturbations complicate cycle slip detection and repair. They can easily be detected in continuous dual-frequency phase data. The lower two panels of Figure 2 show the change of ionospheric refraction from one minute to the next as derived from dual-frequency phase data. Missing values for the disturbed satellite pass show that no continuous dual-frequency phase data were available for a considerable time period.

The scintillation effects shown in Figure 2 belong to the worst effects to be expected for GPS signals. They were observed in **Curitiba** (Brazil) in March of 1992, thus few degrees south of the magnetic equator during an equinox month and in a year of high solar activity. Most probably no such severe effects have disturbed any IGS data till today. In 1995, with some IGS stations close to the magnetic equator (**Arequipa**, **Fortaleza**, **Bangalore**), solar activity is at its minimum level and thus such severe effects are not expected. But in 1992, with a higher level of solar activity, no IGS stations existed in the center of the equatorial region. With the advent of the next period of high solar activity around the end of this decade, those effects will be observable at many equatorial IGS stations.

OCCURRENCE OF SMALL-SCALE DISTURBANCES

The region of equatorial scintillations extends 30° on either side of the earth's magnetic equator (Fig. 3). The strongest effects are found at approximately 10° N and

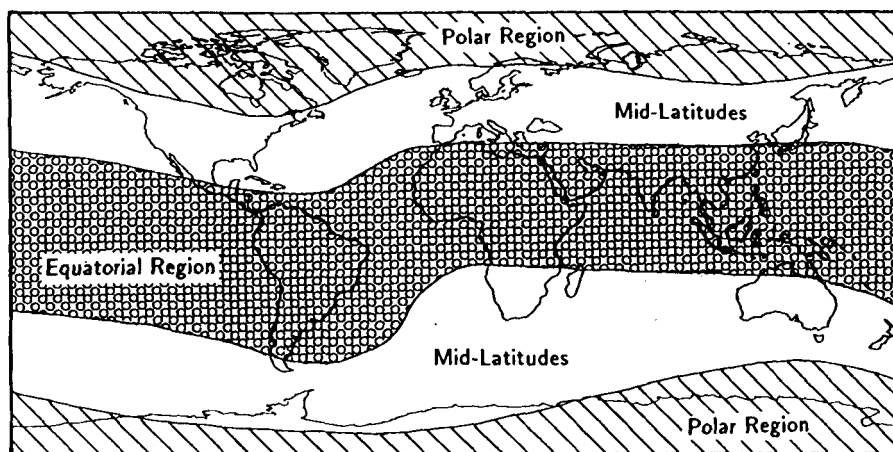


Fig. 3: Ionospheric regions of the world.

S. There is a clear diurnal variation: scintillations occur between approximately one hour after sunset and midnight and occasionally continue until dawn. In addition, there is a seasonal dependence: strongest effects are found in equinox months. A high level of occurrence is observed between September and April in the longitude band stretching from the Americas to Africa. In the Indian and Pacific region, however, a high level of occurrence is found between March and October (*Basu et al. 1988, Aarons 1993*).

Polar scintillations are not as strong as those near the equator. Their occurrence is closely related to magnetic storm activity. The strongest ionospheric activity does not take place in the polar cap regions but rather in the **auroral** zones situated at the boundary of polar regions and mid-latitudes between magnetic latitudes of about 64° and about 70° . During strong magnetic storms, these **auroral** effects can extend well into the mid-latitudes. The equatorward extension of polar scintillation activity is of primary interest to GPS users in the mid-latitudes,

Furthermore, scintillation effects depend on the 11-year solar cycle. Their level of occurrence and their intensity increase with an increase in the solar sunspot numbers. From 1989 to 1992, they were especially strong due to the maximum of solar cycle No. 22. From 1994 to 1997, minimal occurrence and minimal strength can be expected. But around the year 2000, scintillation effects will increase again.

GPS SCINTILLATION MONITORING

Amplitude scintillations can be detected in time series of S/N values provided by many GPS receivers. Unfortunately, when raw data (in a binary receiver dependent format) are converted to RINEX format, most of the S/N information gets lost as the S/N values are projected onto the interval 1 to 9. Since all IGS observations are available in RINEX format only, no use can be made of this valuable information of the GPS signal strength.

Phase scintillations can easily be detected in continuous dual-frequency GPS phase

observations. The vast amount of such data in the IGS archives presents an important resource for research on ionospheric phase scintillations.

Other desirable features for scintillation monitoring are the ability to record phase (and amplitude) observations at a rate of at least 1 Hz and with a tracking loop bandwidth of some Hz. These characteristics are needed to investigate the structure and dynamics of small-scale irregularities. These features, however, do not exist for the IGS data (**30 seconds recording rate, small tracking loop bandwidth**).

In summary, the IGS network does not provide ideal GPS observations for scintillation monitoring, but the dual-frequency phase data can be used for phase scintillation detection and can therefore give indications of the geographical and temporal occurrence of small-scale irregularities.

DETECTION OF PHASE SCINTILLATION IN IGS DATA

Phase scintillations can easily be detected in the time- differenced ionospheric (“geometry-free”) linear combination of single-station dual-frequency phase observations. This unambiguous observable provides the rate of change of ionospheric delay, which is converted to the rate of change of the total ionospheric electron content (Rate of TEC - RoT [$10^{16}m^{-2}min^{-1}$]):

$$RoT = 9.52 \cdot ((\Phi_1 - \Phi_2)_{t_j} - (\Phi_1 - \Phi_2)_{t_i}) \quad (1)$$

with

$$\Delta t = t_j - t_i = 1 \text{ min}. \quad (2)$$

Φ_1 and Φ_2 [m] are the measured carrier beat phase observable of L_1 and L_2 respectively, t_i and t_j are the measurement epochs, the scaling factor converts the ionospheric delay difference to units of [$electrons/m^2$](*Wanninger 1993a*).

All frequency independent errors are removed by forming the ionospheric linear combination. Significant remaining errors are **multipath**, which can reach up to $0.3 \cdot 10^{16}m^{-2}min^{-1}$, and random observation errors, which usually do not exceed $0.07 \cdot 10^{16}m^{-2}min^{-1}$. Cycle slips have to be detected in the pre-processing. They do not need to be estimated, but time- differencing is performed for continuous observations only. Similar observable are found in several publications or software-packages (e.g. *Wild et al. 1989, UNAVCO 1994, Doherty et al. 1994*). They mainly differ in respect to epoch rate and units. Their information content concerning phase scintillations is identical.

The **RoT-values** of complete satellite passes and various ionospheric conditions are shown in Figure 4. They illustrate (from left to right) undisturbed ionospheric conditions, polar scintillations, equatorial scintillations, and equatorial scintillations with receiver tracking difficulties causing data gaps. Low frequency spectral components are caused by vertical TEC and by large-scale gradients of vertical TEC.

In order to simplify scintillation detection, a phase scintillation index I_{GPS} is computed from RoT values. In a first processing step, the RoT time series are high

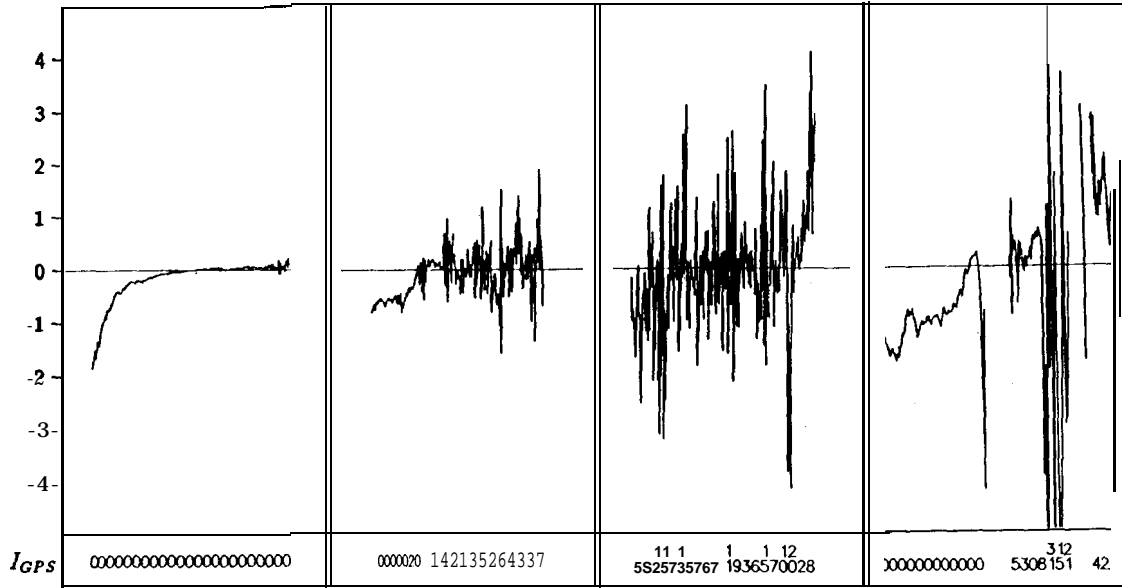


Fig. 4: Rate of change of TEC (RoT in $[10^{16} m^{-2}min^{-1}]$) and phase scintillation index I_{GPS} .

pass filtered in order to remove low frequency components. The index is computed as RMS over n epochs of the remaining components of RoT time series (RoT):

$$I_{GPS} = 10 \cdot \sqrt{\frac{1}{n} \sum_{epochs} \overline{RoT}^2}. \quad (3)$$

Examples of I_{GPS} values of 15 minute blocks of observations are presented in Fig. 4. Other kinds of index definitions should also be considered and should be tested against **this RMS-type index**.

It is expected that small-scale irregularities in the electron content cause larger phase scintillations for signals coming from satellites at low elevation compared with scintillations for signals arriving from zenith direction. However, such an elevation dependence could not be confirmed with actual GPS observations. Thus, no reduction of I_{GPS} values to zenith direction is performed. Further investigations on the elevation dependence of GPS phase scintillations are needed.

In a last processing step spatial information is assigned to every index value. Having just one observation site, it is sufficient to use the satellite's azimuth and elevation which provide the direction to the area sampled. However, in order to combine index values of several sites, sub-ionospheric coordinates have to be computed. They consist of latitude and longitude (or local time) of the intersection points of the GPS signals with an ionospheric shell in a certain height above the earth surface. Since the actual height of small-scale irregularities, which could be as low as 250 km or as high as 600 km, is usually not known, an average height (400 km) is taken for coordinate computations. The examples presented below were computed with this ionospheric height.

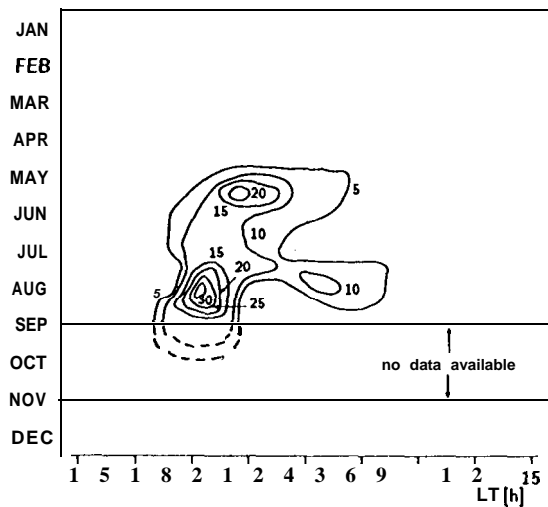


Fig. 5:
 Percentage occurrence of
 phase scintillations at
 Kokee Park, Hawaii 1992:
 $I_{RoT} \geq 3$ in periods of 30
 minutes, elevation mask 15° ,
 mid-month marked, local time
 of sub-ionospheric points
 (400 km).

Example 1: Kokee Park, Hawaii 1992

Hawaii is located at 20°N magnetic latitude. It belongs to the ionospheric equatorial region. Though the main scintillation activity takes place around $\pm 10^\circ$ magnetic latitude, Hawaii is also expected to be affected. Of major interest is the temporal (seasonal, diurnal) distribution of the disturbances.

Kokee Park data are available for the whole of 1992, with the exception of a data gap from mid-September to mid-November. Figure 5 shows the percentage occurrence of phase scintillations as derived from phase scintillation index values I_{GPS} (Wanninger 1993a).

No scintillation occurrence was detected from January to April and in November and December. The observed scintillation activity from March to September/October was not as severe as scintillation activity monitored closer to the magnetic equator (compare Fig. 2). The figure reveals that the main activity was limited from sunset to local midnight, but on occasion continued until dawn. A maximum percentage of 20 to 30 indicates that disturbances occurred in maximum every third to fifth night. A similar picture of the seasonal and diurnal distribution of scintillation occurrence can be expected in every year. Thus, this kind of phase scintillation monitoring helps those GPS user who are interested in highest accuracy to avoid these disturbances.

Example 2: Magnetic Storm April 1993

GPS observations from mid-latitudes sites are usually not affected by ionospheric scintillations. Only in the case of major magnetic storms, small-scale irregularities can penetrate from the polar regions into the mid-latitudes. Several questions arise, for example: How far does the area of ionospheric irregularities extends into the mid-latitudes under storm conditions? Is scintillation occurrence in the polar regions, in the auroral regions, and in the equatorial region correlated with magnetic storms? These questions can be answered with the help of phase scintillation index maps derived from IGS data.

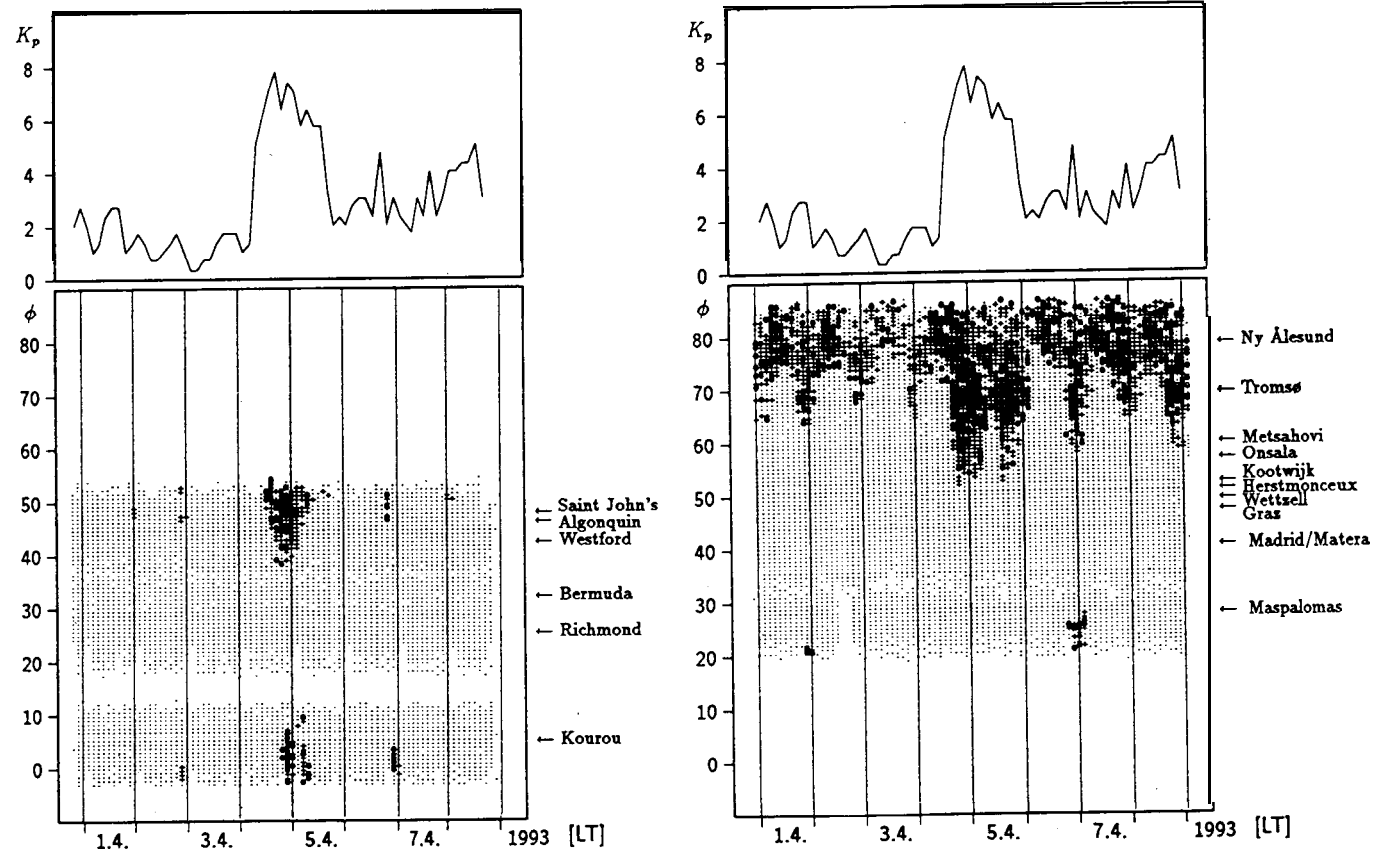
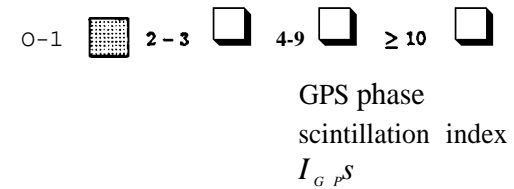


Fig. 6: The development and effects of a major magnetic storm (April 4 and 5, 1993): three-hourly planetary index of geomagnetic activity K_p (upper panels), phase scintillation index I_{GPS} (lower panels) in a coordinate system of local time and geographic latitude (20° elevation mask, 400 km ionospheric height). **Fig.6a** (left): I_{GPS} from sites at the east coast of the Americas. **Fig.6b** (right): I_{GPS} from European sites.



An example has been produced for a major magnetic storm which took place on April 4 and 5, 1993. Figures 6a and 6b present the storm effects in the American latitude region and in the European latitude region respectively. The three-hourly planetary index of geomagnetic activity K_p (*SGD 1993*) reveals the development of the storm. It suddenly commenced on April 4, 1993 forenoon local time in America and around noon local time in Europe and lasted for about 2 days (upper panels in Fig. 6a and 6b). The lower two panels show phase scintillation index maps in a coordinate system of geographic latitude and local time and indicate the latitudes of IGS sites used. The vertical lines mark local midnights. Whereas in the European longitude sector, IGS sites very well cover the latitudes from the polar region (Ny Ålesund) to the northern edge of the equatorial region (Maspalomas), no further sites can be found closer to the center of the equatorial region. At the Atlantic coast of the Americas, the site located furthest north is Saint John's in the northern mid-latitudes. No polar IGS sites exist in this longitude region.

In the European polar region (Ny Ålesund), ionospheric disturbances could be found all day long in the period from April 1 to April 8. Their intensity seems not to be correlated with K_p . In the auroral region (Tromsø), disturbances occurred every night around midnight. During the storm they were very intense and they continuously lasted for about 2 days. In the northern mid-latitudes, no midnight disturbances were detected. But on April 4 and 5, small-scale irregularities extended south to a geographic latitude of 50°. They were not as severe as in the auroral region and they did not occur around noon of April 5. In the northern equatorial region (Maspalomas), disturbances were detected in two night but not during the storm. Their occurrence seems not to be correlated with K_p .

In the American longitude region, the northern mid-latitudes were affected by small-scale irregularities during some nights and especially during the storm. Then, these irregularities extended equatorward to a geographic latitude of less than 40°. In the equatorial region (Kourou), disturbances were detected during three nights with severest effects occurring during the storm. Here, longitudinal differences in scintillation occurrence were found in the equatorial region. Whereas no phase scintillations were detected at Maspalomas on the days of the storm, the GPS observations of Kourou, located at about the same magnetic latitude but 40° further west, were affected.

CONCLUSIONS

Ionospheric scintillations are detectable in GPS signal amplitude observations and GPS phase observations. Since RINEX-formatted observations contain only very little information on the signal amplitude, amplitude scintillations are not detectable in IGS data. The vast amount of IGS continuous dual-frequency GPS phase observations, however, presents an important resource for research on the temporal and geographical occurrence of small-scale ionospheric irregularities. Phase scintillation occurrence maps – as presented in this paper – provide important information for ionospheric research and for users of precise GPS who want to avoid ionospheric disturbances.

REFERENCES

- Aarons, J. (1993), The longitudinal morphology of equatorial F-layer irregularities relevant to their occurrence, *Space Science Reviews*, **63**:209-243.
- Basu, S., E. MacKenzie, S. Basu (1988), Ionospheric constraints on VHF/UHF communications links during solar maximum and minimum periods, *Radio Science*, **23**:363-378.
- Bishop, G., Coco, D. S., Coker, C., Fremouw, E. J., Secan, J. A., Greenspan, R. L., Eyring, D. O. (1992), GPS Application to Global Ionospheric Monitoring: Requirements for a Ground-Based System, in *Proceedings of ION GPS-92*, September 16-18, 1992, Albuquerque, New Mexico, pp.339-353.
- Doherty, P. A., Raffi, E., Klobuchar, J. A., El-Arini M.B. (1994), Statistics of Time Rate of Change of Ionospheric Range Delay, in *Proceedings of ION GPS-94*, pp.1589-1598.
- Parkinson B. W., Lassiter, E. M., Cretcher, C.K. (1977), Ionospheric Effects in NAVSTAR GPS, in *A GARD Conference Proceedings 209: Propagation Limitations of Navigation and Positioning Systems*.
- SGD (1993), *Solar Geophysical Data, Prompt Reports, No 586-I*, June 1993.
- UNAVCO (1994), *QC v3 Users Guide*, University NAVSTAR Consortium (UNAVCO), Boulder, March 1994.
- Wanninger, L. (1993a), Ionospheric Monitoring using IGS data, in *Proceedings of the 1993 IGS Workshop*, March 25-26, 1993, Bern, Switzerland, pp.351-360.
- Wanninger, L. (1993 b), Effects of the equatorial ionosphere on GPS, *GPS World*, July 1993, pp.48-54.
- Wild, U., Beutler, G., Gurtner, W., Rothacher, M. (1989), Estimating the ionosphere using one or more dual frequency GPS receivers, in *Proceedings of the Fifth International Geodetic Symposium on Satellite Positioning*, Las Cruces, New Mexico, pp.724-736.

REAL-TIME MONITORING OF THE IONOSPHERE

E. Engler, E. Sardón, N. Jakowski, A. Jungstand, D. Klähn

Deutsche Forschungsanstalt für Luft- und Raumfahrt e.V.
Deutsches Fernerkundungsdatenzentrum
Fernerkundungsstation Neustrelitz
Kalkhorstweg 53
17235 Neustrelitz
Germany

ABSTRACT

In **this** paper we describe our approach to monitor the total electron content (TEC) in the ionosphere using GPS data in real-time. **These** real-time TEC values are used in combination with an ionospheric model to provide a regional **TEC** map for other possible users. **We** have used data with a rate of 10 seconds **from** our Turbo-Rogue **receiver** in **Neustrelitz** to estimate the **TEC** and a subset of the **IGS** (International GPS Service for **Geodynamics**) network with a rate of 30 seconds to estimate the differential instrumental biases in the **GPS** satellites and receivers. As we are assuming that those biases are very stable over short periods, we present a study of their stability. **We** also show some comparisons between the results obtained using the same **GPS** data in post-processing vs real-time, **We** have selected several values for some processing parameters in the real-time routine (like minimum number of epochs used for cycle-slip detection and ambiguity estimation, elevation mask, etc.) and we have checked the different results against the post-processing ones. **We** have found that the **rms** of the differences in **TEC** between post-processing and real-time estimations are about 4 **TECU**, for instance, when using a mask elevation of 20 degrees, 10 epochs for cycle slip detection and 90 epochs for ambiguity estimation.

INTRODUCTION

The **ionosphere** introduces a delay in the Global Positioning System (**GPS**) observations that is proportional to the ionospheric total electron content (**TEC**) along the propagation **path** and inversely proportional to the squared frequency. The dispersive nature of this effect makes possible to measure the **TEC** using dual frequency **GPS** data (**Lanyi** and **Roth**, 1988, **Coco** et al., 1991, **Sardón** et al., 1994). In the study presented **here** we have used dual **GPS** phase and pseudorange measurements to monitor the **TEC** in real-time and to produce **TEC** maps. The main applications of the **TEC** estimated in real-time can be for high precision differential navigation in aircraft landing approach or in wide-area differential systems. In the first case, the **TEC** of the reference station can be directly used, but in the case of wide-area applications several measuring stations are needed to increase the coverage of the **TEC** map.

The main differences in the estimation of **TEC** using **GPS** data in post-processing and real-time are in the detection of cycle-slips and in the estimation of the ambiguity terms in the phases. In post-processing mode, some observations before and after a possible cycle-slip can **be** checked to decide

if it is a real cycle-slip and to estimate it. In real-time mode, we only have the observations previous to the possible cycle-slip, so we have to rely only in those observations or, if we want to use also some observations **after** the cycle-slip, we have to wait and produce no TEC estimation for those observations. In any case, we have to minimize the number of epochs used for cycle-slip detection and estimation, For the estimation of phase ambiguities, in post-processing a complete arc of data (a period without cycle-slips, or with corrected cycle-slips) can be used. But in real-time, only the first epochs per arc are used, and this number have also to be minimized. In the next sections we describe our approach for the detection of cycle-slips and estimation of phase ambiguities.

The biggest sources of error in the estimation of **TEC** using GPS observations are the differential instrumental biases in the satellites and the receivers. The **combined** receiver and satellite instrumental biases can reach up to few nanoseconds, Only for some GPS receivers it is possible to **determine** the differential instrumental bias by internal calibration, For the satellites, a prelaunch calibration is made, but those biases show a poor **agreement** with the values estimated using later observations (**Coco et al. 1991**). Therefore, the combined receiver and satellite instrumental biases are usually estimated simultaneously with the **TEC**.

The best estimation of the instrumental biases can be obtained combining data from several GPS stations due to the increased number of observations. But that is not so easy in real-time **TEC** estimation. In that case we have two possibilities: to estimate the instrumental biases simultaneously with the TEC using only one station, or to use **predetermined** biases estimated in post-processing with data from several stations. We have chosen the later approach, but in this case, we have to check the stability in time of the biases, to know how old the **predetermined** values can be. The stability in time of the instrumental biases is discussed in one of the next sections.

TEC ESTIMATION IN REAL-TIME

For real-time monitoring of the ionosphere we are using GPS data from a Turbo-Rogue SNR 8100, which is implemented at the reference station in **Neustrelitz (Germany)**. We are using dual pseudorange and phase measurements with a sample rate of 10 seconds because no higher data rates under AS are achieved with **the** receiver firmware V2.83.

The ionospheric delay can be derived as a first approximation from differential pseudorange measurements, but it is strongly influenced by **multipath**, noise and instrumental delays. The more accurate phase measurements have smaller noise and **multipath** effects but contain **unkown** initial phase ambiguities and sometimes a change or reset of this initial terms (cycle-slips, tracking losses). **Therefore** the pseudorange observations are necessary to estimate the ambiguities and to derive an absolute TEC **from** the phase measurements. Using uncorrected pseudorange measurements results in a transfer of **multipath**, noise and biases into the estimated terms: TEC, A (sum of frequency independent terms like geometric range, clock errors and tropospheric delay) and N 1 and N2, ambiguities in each frequency. Due to the stability of the instrumental biases, which will be shown later, it is possible to **remove** the most of their influence using predicted values. **The** influence of noise and **multipath** on **the** estimates depends on the elevation mask and the number of epochs used for first ambiguity fixing. Increasing the elevation mask to 20 or 30 degrees reduces **multipath** effects but also decreases the number of observed satellites at each epoch. As we are working with data from only one station is rather important to keep as many observations per epoch as possible. **Therefore** it's necessary to find the best compromise between the minimum elevation mask and the provided accuracy or to try to estimate the **multipath** effects in the observable.

A flow chart of the real-time TEC estimation algorithm is shown in Fig. 1. In the **START.INI** the processing parameters like epochs for cycle-slip **determination**, epochs for first ambiguity fixing,

elevation mask, data rate and also **further** information to control the data flow (firmware type) are set. The predicted **instrumental** biases are available in a table. The box “Pseudomultipath” offers the **multipath** correction for our reference station, which is under development. The whole **real-time** algorithm is working without the use of any **TEC** model. But at the end the real-time slant **TEC** can be used for updating the regional TEC model NTCM 1 (**Jakowski et al., 1994**) to produce a **TEC** map. Therefore we enter here the coefficients (mainly the solar radio flux F 10.7) to apply the **NTCM1** model. With respect to the time **behaviour** pseudomultipath and instrumental biases can be updated every day.

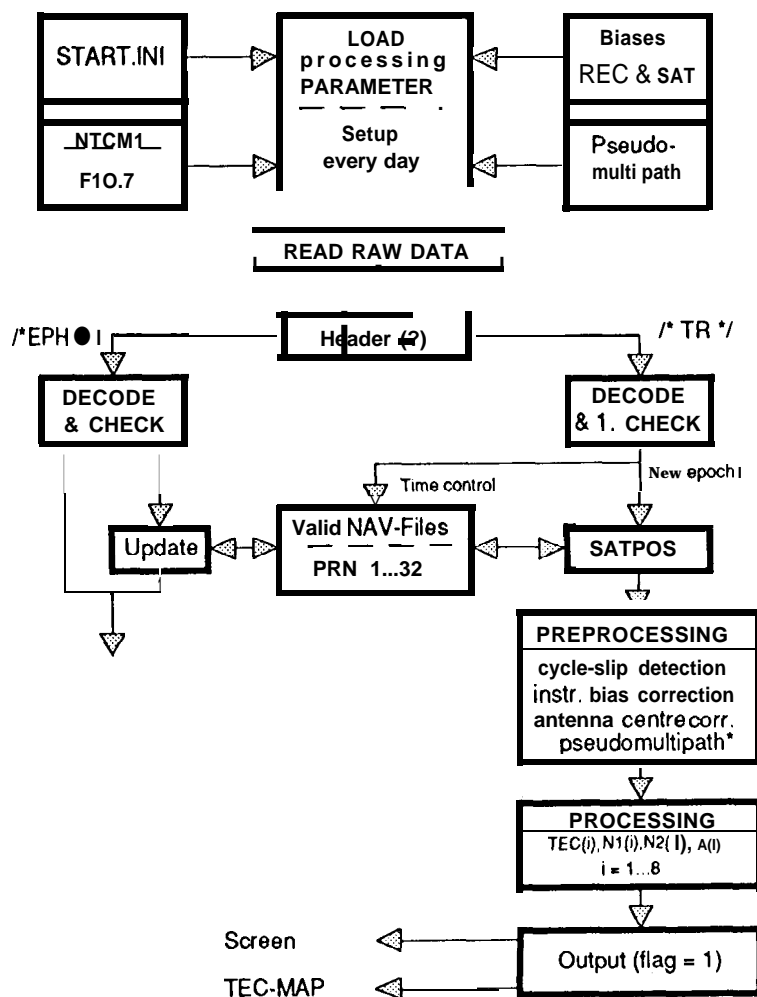


Fig. 1 Flow chart of the TEC estimation in real-time

The **received** different file types (ephemerides **/*EPH***, observations **/*TR***, . . .) are detected by their header. The ephemerides are only used during the TEC estimation routine to determine the elevation and azimuth of the tracked satellite, the longitude and latitude of the **subionospheric** point (intersection of the signal path and the mean ionosphere layer) and to display the difference between the expected and measured range for the operator. During the “**DECODE & FIRST CHECK**” module the code and phase measurements are transformed into ranges and outliers are removed. During the “**DECODE & CHECK**” module the ephemerides files are decoded and if

those are detected as a new information and the included flag is healthy they are loaded in to the NAV-Files. At every new observation epoch this NAV-Files are checked to remove obsolete files. The preprocessing starts with the detection of cycle-slips and tracking losses. The distinction between cycle-slip (temporary change of ambiguities) and tracking losses (reset of the phase counter) is based on the different reaction of the algorithm. A reset of the phase counter normally occurs if the satellite was not tracked for several epochs. Cycle slips are observed during continuous tracking. But both events are visible at the phase difference $L_1 - L_2$. The use of several epochs of the **phase** difference terms allows to estimate the TEC rate and to predict the TEC value of the next epoch. If the difference between the predicted and the measured phase difference is greater than 5.4 cm (change of both ambiguities N_1 and N_2 by 1) then a possible change of ambiguities is detected, This epoch is excluded for the next prediction and also for **TEC** determination. If a certain number of successive epochs (set in **START.INI**) are detected as cycle slips then a calculation of the TEC rate and also the ambiguity fixing is restarted. In the case of tracking losses (**more** than 10 epochs without raw data recording at the same satellite) the processing routine restarts also. As an example Fig. 2 shows the total amount of detected **cycle-**

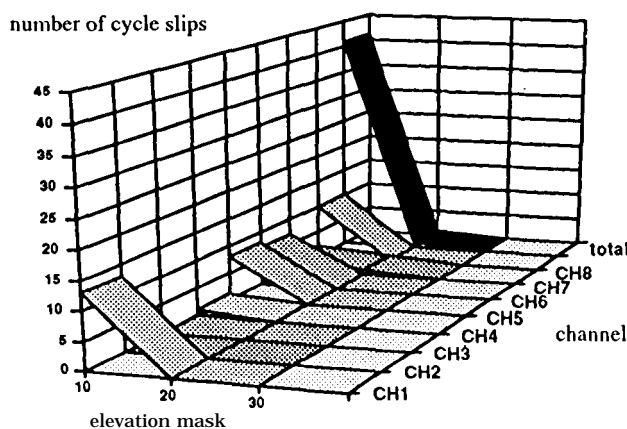


Fig. 2 Observed cycle-slips at 26.11.1994

slips for 26 Nov 1994 . Less than 0.05% of all observations are disturbed by cycle slips working with a elevation mask of 10° under activated Anti-Spoofing. For higher elevations the number of cycle slips decreases. Tracking losses, which can result **from** temporary fall of SNR or **from** a change of the tracked satellites, result in a reduced number of **observat ions**, because after the restart we must use several epochs for cycle slip detection and also for the new first ambiguity fixing. During this time no results are available for this tracked satellite.

In the next step, the observations that are free of cycle slips are corrected by the predicted receiver and satellite instrumental biases, which are determined in post-processing with two or three days of delay using GPS data **from** several IGS stations, and by the **antenna** phase center correction, If there is a **multipath** correction map for the reference station or if the **multipath behaviour** was derived **from** previous measurements, it may be possible to decrease the number of necessary epochs before the first ambiguity fixing. **This** is under development.

The estimation of TEC is done on the base of measuring intervals free from cycle-slips and tracking losses. Using the phase measurements to derive the rate of A and TEC gives the possibility to estimate the temporary **behaviour** of the **pseudomultipath** (sum of **multipath** and noise) (Engler, 1994, Jungst and et al., 1995). If the instrumental biases are removed successfully, then only the mean value of **pseudomultipath** related to this interval influences the ambiguity fixing. It is clear, that small number of epochs increases the influence of **pseudomultipath** on the fixed

ambiguities and therefore on the TEC estimation. This dependence will be shown later, The number of used epochs for fixing the ambiguities is a parameter of the **START.INI** that we can change to get experience and to find a compromise between accuracy and available TEC values for each epoch.

At each epoch we have now 3 to 8 TEC values from the successfully tracked satellites. For users, which are close enough to the reference station (-10 km, satellites are observed with identical elevation) it is possible to use the slant TEC values directly for ionospheric corrections. For other users it is necessary to describe the ionosphere of the region. This is done using the TEC values derived at the reference station to modify the regional TEC model NTCM 1 to estimate the instantaneous ionospheric conditions. The use of only one station results mainly in a modification of the basic level of the model.

The result of the last processed epoch is displayed at the screen (Fig. 3). The PRN of the tracked satellite, the number of successive epochs and the status of the last observation (1 =ok, 5= no ephemerides or elevation below mask, ...) related to each channel is given. For successful observations with fixed ambiguities the measured range and vertical TEC at the subionospheric point are shown. The control parameter, which give an impression of the data quality, are pseudomultipath estimations for the pseudoranges P1 and P2 (dm 1 and dm2), and the observed range error by Selective Availability (d_AS). The parameter dha and dht describe the offset for the A term and the TEC, respectively, between two real-time solutions (one using only specified number of epochs, and the other using all the available observations in that moment). If therefore a satellite track is finished, the end values of dha and dht are the necessary parameters to determine the offset between real-time and post-processing. These offsets represent the error in the ambiguity fixing of real-time estimation and is therefore constant for the whole measuring interval.

fix_d	:	90	time	:	10:4500				
CH		CH(1)	CH(2)	CH(3)	CH(4)	CH(5)	CH(6)	CH(7)	CH(8)
PRN		24	19	4	7	14	15	18	29
flag		5	5	1	5	1	5	1	1
epo		1182	738	530	977	1461	1812	446	918
ran	:(m)	o	o	21304918	0	21256821	0	21017884	20404354
VTEC	:(TECU)	0,000	0,000	19,152	0,000	13,297	0,000	17,056	15,677
ele	:(°)	14,549	8,331	52,702	12,105	50,805	2,826	53,962	79,511
azi	:(°)	318,426	180,614	286,605	240,542	101,947	153,838	226,806	99,946
Quality Control Parameter									
dm 1	:(m)	0,000	0,000	0,252	0,000	0,423	0,000	0,474	-0,201
dm2	:(m)	0,000	0,000	-0,323	0,000	0,007	0,000	0,786	-0,918
d AS	:(m)	0,000	0,000	11,930	0,000	23,158	0,000	76,438	64,876
dha	:(m)	0,000	0,000	0,196	0,000	-0,746	0,003	-0,301	-0,503
dht	:(TECU)	0,000	0,000	-1,311	0,000	4,652	0,000	1,284	2,949
TEC map is produced for:		261194		10:4500		(4)			
VTEC(REF) = 16.45 TECU									

Fig. 3 Screen example of the real-time TEC estimation routine (26.11.94, elevation mask 20°)

elevation mask, data rate and also further **information** to control the data flow (firmware type) are set. The predicted instrumental biases are available in a table. The box “Pseudomultipath” offers the **multipath** correction for our reference station, which is under development. The whole **real-time** algorithm is working without the use of any TEC model. But at the end the real-time slant **TEC** can be used for updating the regional **TEC** model NTCM 1 (Jakowski et al., 1994) to produce a TEC map. **Therefore** we enter **here** the coefficients (mainly the solar radio flux $F10.7$) to apply the **NTCM1** model. With respect to the time **behaviour** pseudomultipath and instrumental biases can be updated every day.

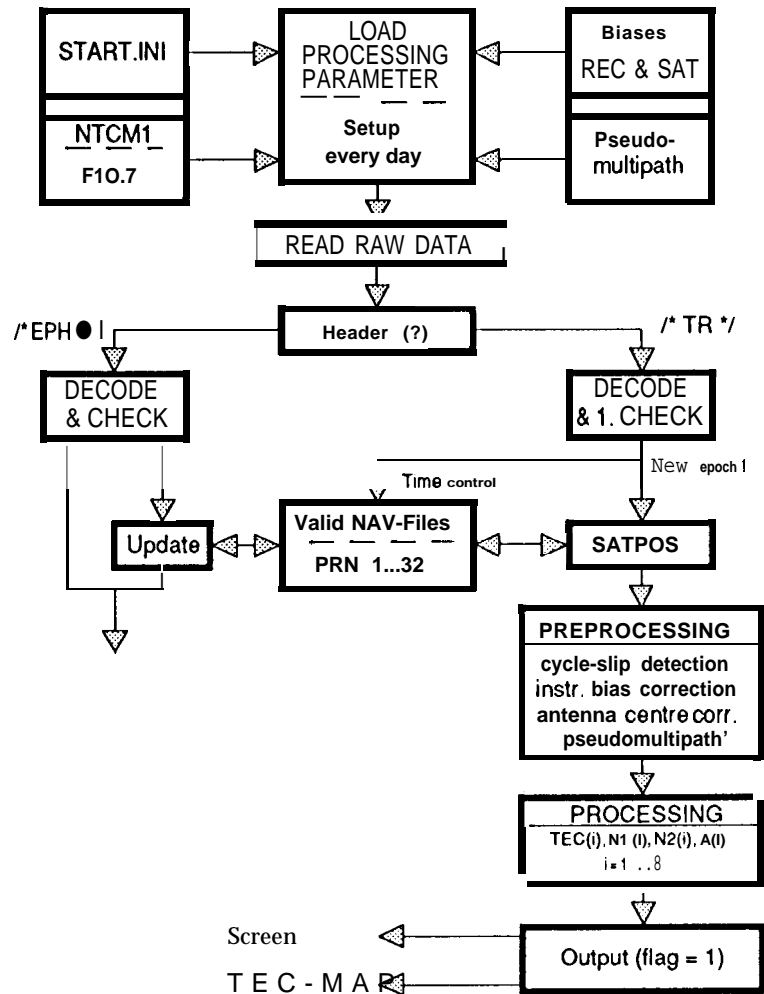


Fig. 1 Flow chart of the TEC estimation in real-time

The received different tile types (ephemerides /*EPH*/, observations /*TR*/, ...) are detected by their header. The ephemerides are only used during the TEC estimation routine to **determine** the elevation and azimuth of the tracked satellite, the longitude and latitude of the **subionospheric** point (intersection of the signal path and the mean ionosphere layer) and to display the difference between the expected and measured range for the operator. During the “DECODE & FIRST CHECK” module the code and phase measurements are transformed into ranges and **outlayers** are removed. During the “DECODE & CHECK” module the ephemerides files are decoded and if

INSTRUMENTAL BIAS STABILITY

We are assuming that the instrumental biases in the GPS satellites and receivers are enough stable in time to work in real-time estimation with the biases **determined** two or three days ago using data from several stations. In **this** section we discuss the **stability** of those biases.

Sardón et al. (1994) found that the variation in time of the GPS satellite instrumental biases (relative to the **mean** of them) was below 1 ns, using different epochs during 1-year period (September 1990 to September 1991). In **Jungstand et al. (1995)**, we also presented a study of the stability of the GPS satellite biases over long **periods**, and we found that the variation in time of those biases (also relative to the mean) estimated in different epochs during about 1.5 years (January 1993 to September 1994) was below 1.5 ns.

Here we want to discuss the variation of the combined **receiver** and satellite instrumental biases in periods of consecutive days, because those biases are the ones that we plan to use for the **real-time** monitoring of TEC. Since February 1995 we are processing GPS data **from** several IGS stations **plus two receivers at Neustrelitz in a daily routine analysis. All stations are equipped with Rogue** or Turbo-Rogue receivers. For each day we produce, in post-processing, hourly maps of the vertical **TEC** over the central European region, and also a set of instrumental biases. **These** are the instrumental biases that we use for the real-time estimation of **TEC**.

If no internal calibration is available for the receivers, then it is not possible to separate the satellite bias **from** the receiver bias. We have arbitrarily chosen the receiver at Madrid (**ds60**) as reference, and then, for the satellites we have the combined Madrid receiver plus satellite bias and for the other receivers, we have the difference **between** the receiver bias and the bias for Madrid. Table 1 shows, for each GPS satellite, the **rms** of the corresponding bias (satellite plus reference station) from February 1st to March 31th in nanoseconds (1 ns = 2.86 TECU).

PRN	1	2	4	5	6	7	9	12	14	15	16	17	18
rms [ns]	0.16	0.14	0.12	0.11	0.12	0.11	0.10	0.11	0.12	0.15	0.15	0.18	0.11
PRN	19	20	21	22	23	24	25	26	27	28	29	31	
rms [ns]	0.14	0.13	0.16	0.18	0.16	0.13	0.16	0.12	0.13	0.22	0.14	0.17	

Tab. 1 RMS of combined biases (Madrid plus satellites)

For the same period, Table 2 shows, for each station used, the rms of the corresponding bias (station minus reference station bias), also in nanoseconds.

stat ion	dslo	ds42	brus	bor1	mate	nzre	nzmo	onsa	pot s	trom	Wtz l
rms [ns]	0.25	0.37	0.29	0.29	0.31	0.40	0.23	0.98	0.45	0.58	0.28

Tab. 2 RMS of receiver bias (receiver minus Madrid)

Some examples of the biases estimated in February and March are displayed in Fig. 4. The largest **rms** is for satellite PRN 28 and it is due to the larger noise between day 51 and 65. From day 51 on AS was turn off for PRN 28, and on days 66 and 67 PRN28 was unusable due to maintenance. After that, it seems that PRN 28 goes back to a “normal” level. For the station biases, the largest rms corresponds to **Onsala**, as can be seen in Fig. 5 due to a jump in the bias of that station in day 80. In fact, the **receiver** at **Onsala** had some problems and it was replace by another one (Jan **Johansson**, **Onsala** Space Observatory, private communication), so what we are seeing are the biases of two different receivers. But, in all cases, the variation of the combined biases from one

day to the two or three consecutive days is small enough, usually less than 0.5 TECU, to allow us to use predetermined biases (few days ago) for the real-time estimation of TEC.

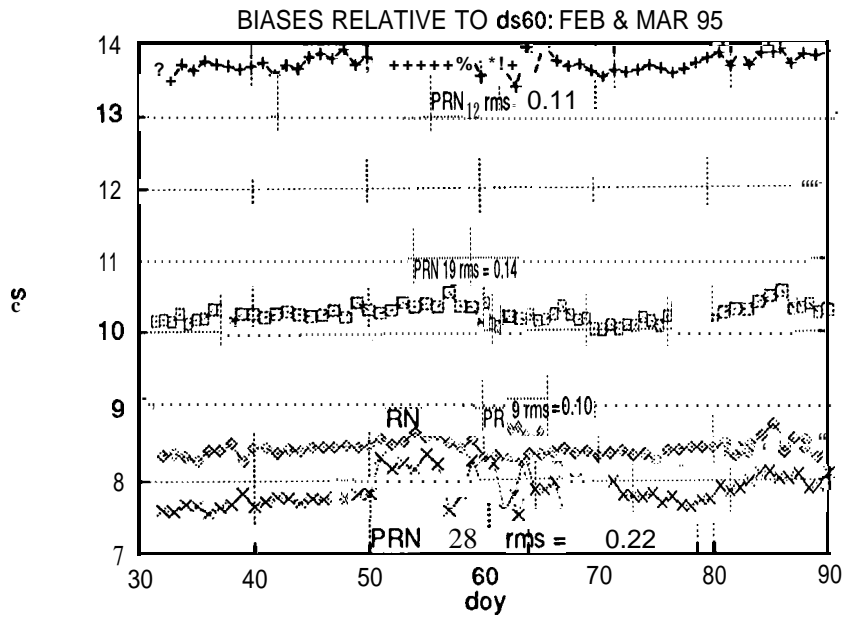


Fig. 4 Combined bias for several satellites (in ns) for February and March, 1995. X axis is day of year.

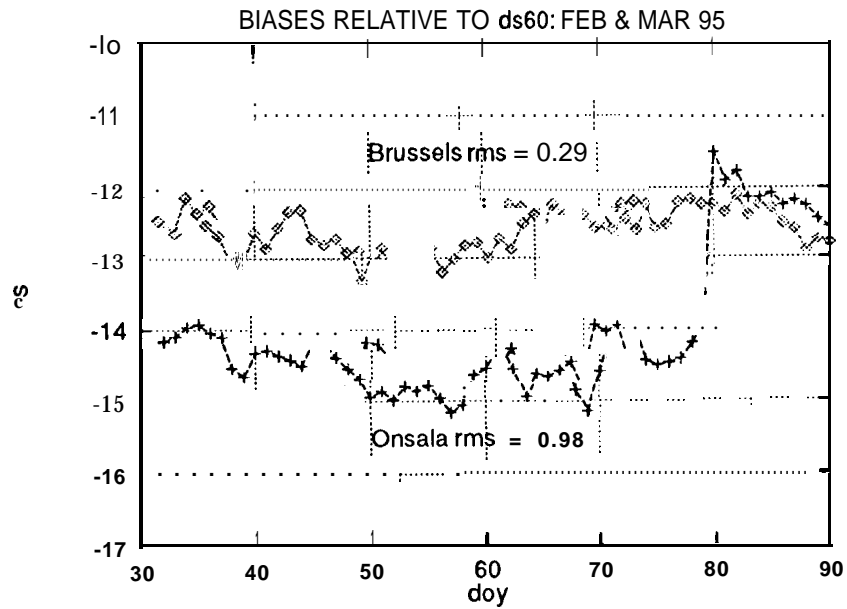


Fig. 5 Receiver bias at Brussels and Onsala relative to Madrid (inns) for February and March, 1995. X axis is day of year.

COMPARISONS OF THE TEC ESTIMATED IN REAL-TIME AND IN POST-PROCESSING

In order to check the accuracy of the estimates in real-time we have compared the TEC and the A term with those that can be obtained using the same GPS data but in a **post-processing** mode.

Besides, in our real-time approach we can choose between different processing parameters like the elevation mask, the minimum number of epochs for the detection of cycle-slips and the estimation of ambiguities. Then, the real-time processing of a sample day (26 November 1994) was simulated using different **combinations** of those processing parameters and the **TEC** and A term obtained was compared with the **TEC** and A term estimated in post-processing. On the 26th of November 1994 there was an ionospheric storm, so the results can be seen as a first worst case study.

In **Fig. 6** the comparison of A terms between the real-time and the post-processing values are shown for several elevation masks (10° , 20° , 30°) in **dependence** of used epochs for first ambiguity fixing as maximum error and **rms**. The corresponding **TEC** differences (Slant) are plotted in **Fig. 7**.

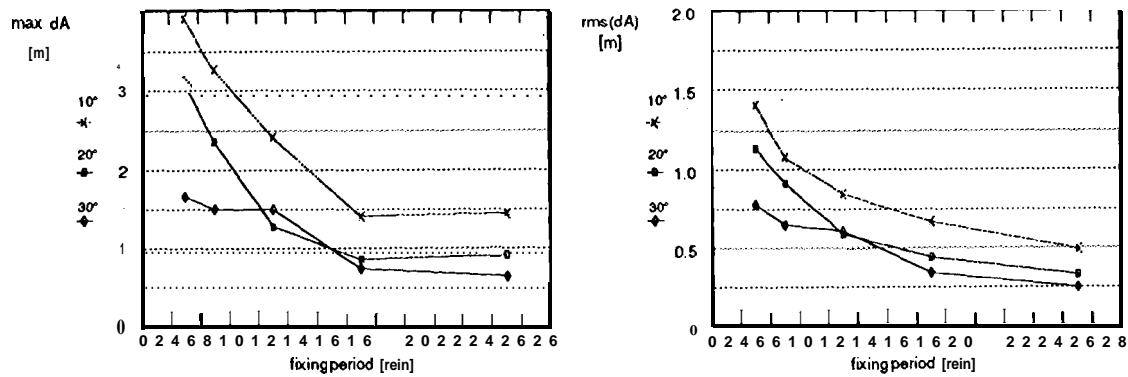


Fig. 6 Differences of the A term between real-time- and post-processing

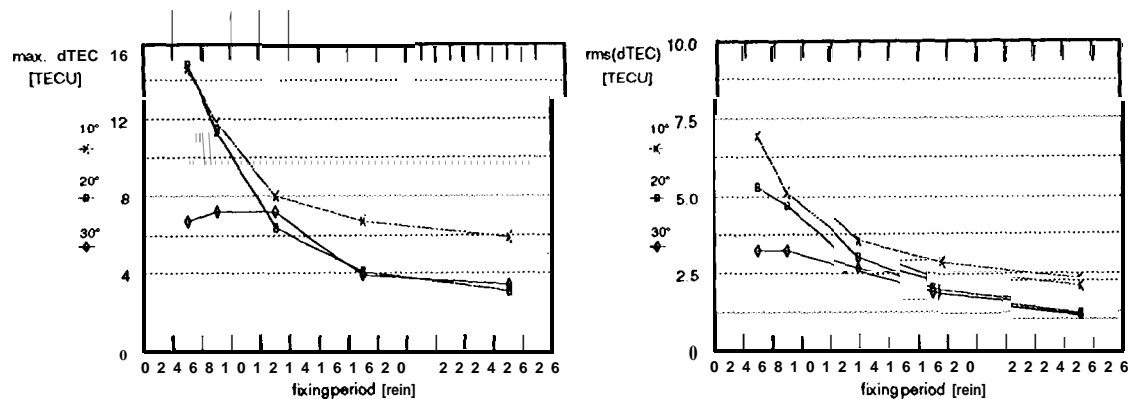


Fig. 7 Differences of the Slant **TEC** between real-time- and postprocessing

In both cases it is seen, that using more than 90 epochs (15 rein, data sample each 10 see) results only in a slight improvement in contrast to the change from 2 min up to 15 min. The increase of the elevation mask **from** 20° to 30° yields only for fixing periods less than 9 min to a remarkable

gain in accuracy. But working with high elevation masks reduces the number of TEC and A values per epoch (Tab. 3).

elevation mask	T_fix [rein]	Average of observations per epoch				
		3	5	9	15	25
10°		6.39	6.32	6.19	5.99	5.69
20°		4.97	4.92	4.82	4.68	4.44
30°		3.85	3.80	3.71	3.58	3.36

Tab. 3 Average of observations per epoch [26.11.94, nzro]

Therefore we can conclude, that an elevation mask of 20° and fixing periods of 15 min (90 epochs) are a good compromise between the available observations and reachable accuracy. In this case the

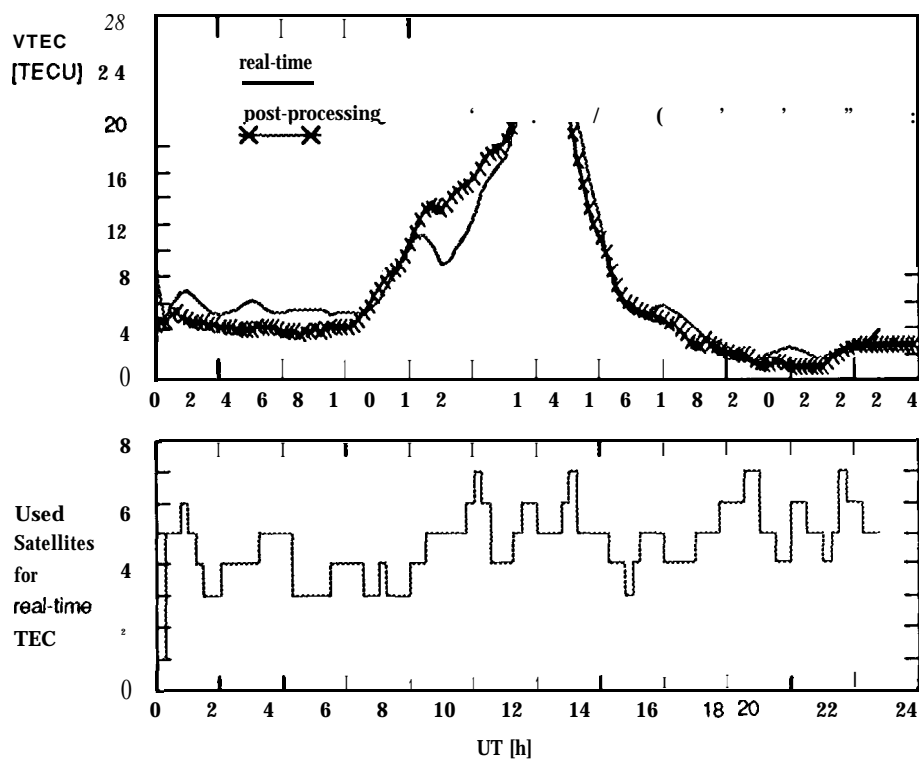


Fig. 8 Estimated vertical TEC at reference station [26.11.94]

maximum TEC error observed is 4.1 TECU and the rms is 2.1 TECU. If the TEC monitoring should start at lower elevation angles anti/or using only few epochs for first ambiguity fixing the multipath error must be handled by models or by prediction.

The estimated vertical TEC in real-time at the reference station, calculated on the base of modified NTCM1 model, is shown in Fig. 8. In this case we have used a 20° elevation mask and 90 epochs for the first ambiguity fixing. In Fig. 8 we also show the post-processed TEC estimated for that day without NTCM 1. It is seen, that the difference between the post-processed and the real-time TEC is in the order of 2 TECU. At 9 o'clock the largest offset of 4 TECU was observed.

CONCLUSIONS

This paper has described the developed real-time TEC monitoring routine. The reached accuracy in comparison with post-processing was shown at a storm day as a worst case study. We have determined that 20° elevation mask and periods of 15 min for the first ambiguity fixing are a good compromise between accuracy and available TEC values per epoch if no multipath correction is implemented. The main error of TEC estimation, the instrumental satellite and receiver biases, are removed by predicted values. The necessary stability of instrumental biases was proved for several stations and satellites. In all cases the variation of the combined biases (sum of receiver and satellite) from one day to the two or three consecutive days is less than 0.5 TECU. This allows us to work with predetermined biases for the real-time estimation of TEC. In comparison to post-processing the maximum TEC error (slant) observed is 4.1 TECU and the rms is 2.1 TECU. The results can be improved by the implementation of multipath corrections using models or prediction routines.

REFERENCES

1. Lanyi, G.E., Roth, T., 1988, "A comparison of mapped and measured total ionospheric electron content using Global Positioning System and beacon satellite observations", *Radio Science*, Vol. 83 (4), 483-492
2. Coco, D. S., Coker, C., Dahlke, S.R., Clynch, J.R., 1991, "Variability of GPS satellite differential group delay biases", *IEEE Transactions on Aerospace and Electronic Systems*, 27(6), 931-938
3. Sardon, E., Rius, A., Zarraoa, N., 1994, "Estimation of the transmitter and receiver differential biases and the ionospheric total electron content from GPS observations", *Radio Science*, 29 (3), 577-586
4. Jakowski, N., Jungstand, A., 1994, "Modelling the Regional Ionosphere by Using GPS Observations", *International Beacon Satellite Symposium*, Aberystwyth, UK.
5. Engler, E., 1994, "Der Einfluß von Multipath auf die TEC Bestimmung mittels GPS", presented paper at the *DGON Meeting*, FA Weltraumtechnik, Hannover, Germany.
6. Jungstand, A., Engler, E., Sardon, E., Kfähn, D., 1995, "Error Separation Concept in Experimental TEC Monitoring Network", *ION Technical Meeting 1995*, Anaheim (CA), USA.

GLOBAL AND REGIONAL IONOSPHERE MODELS USING THE GPS DOUBLE DIFFERENCE PHASE OBSERVABLE

Stefan Schaer, Gerhard Beutler, Leos Mervart, Markus Rothacher
Astronomical Institute, University of Berne
CH-3012 Bern, Switzerland

Urs Wild
Federal Office of Topography
CH-3084 Wabern, Switzerland

ABSTRACT

The CODE¹ Analysis Center of the *International GPS Service for Geodynamics (IGS)* produces orbits, Earth orientation parameters, station coordinates, and other parameters of geophysical interest on a daily basis using the *ionosphere-free linear combination* of the double difference phase observable. Consequently, *clean* (i. e. *cycle-slip-free*) portions of the L1 and the L2 phases are readily available for every day. The difference L1–L2 in meters contains *only* differential ionospheric refraction effects *and* in the ambiguity- unresolved case a constant bias due to the initial carrier phase ambiguities in L1 and L2.

Here we use exactly this observable to extract ionospheric information from the IGS network. On one hand it is *not* ideal to use the difference L1–L2 on the *double difference level* — the differencing reduces the ionospheric signal considerably. On the other hand we have the advantage of a clean signal. Also, processing is simplified because satellite and receiver specific biases cancel out to the greatest extent in our approach.

As usual we model the ionospheric *Total Electron Content (TEC)* with a *single-layer model* which is based on the corresponding mapping function. As opposed to earlier attempts (local ionosphere models using Taylor series expansions in latitude and sun-fixed longitude) we develop the vertical TEC into a series of spherical harmonics. We may use the geocentric latitude and the sun-fixed longitude or an equivalent set in the solar-geomagnetic system as independent arguments. These models have the advantage — over Taylor series expansions — to be well suited for *regional and for global* models.

First results using one week of regional (European) and global data (entire IGS network) from the CODE Analysis Center seem to indicate that under *normal* ionospheric conditions the ionosphere models are very useful for single-frequency GPS users, i.e. ionospheric refraction effects are greatly reduced if these TEC models are taken into account.

¹Center for Orbit Determination in Europe

INTRODUCTION

Ionospheric refraction was considered as an important aspect within the GPS group of the *Astronomical Institute of the University of Berne (A IUB)* for a long time. In the time period when usually only *single-band* (L1) receivers were available it was important to get insight into the biases introduced in a GPS network by *unmodeled* ionospheric refraction (Beutler et al., 1988). Later on, it became obvious that short period variations in ionospheric refraction could harm GPS analyses even if *dual-band* receivers were available (Beutler et al., 1989). In the latter paper there were also clues that valuable information about the ionosphere could be extracted from dual-band GPS data.

Modeling and monitoring the ionosphere was the main topic of the Ph.D. thesis (Wild, 1994). In this thesis it could be shown that local ionosphere models like those presented by (Georgiadiou and Kleusberg, 1988) are very efficient to remove --- or greatly reduce --- the *scale bias* for single-band receivers operating in the vicinity of dual-band receivers, the data of which were used to establish a local ionosphere model. (Wild, 1994) computed such local ionosphere models for a number of IGS sites over an extended time period. He also describes a procedure to assess the *stochastic* behaviour of the ionosphere in the vicinity of a GPS station. The principal conclusion was that essential information concerning the ionosphere might be extracted from the IGS network. Local ionosphere models have proved their usefulness on many occasions. However, the concept of having as many ionosphere models as stations in a network like that of the IGS is hardly operational. The modeling techniques used by (Wild, 1994) had to be modified in one important respect before it became possible to replace *N local models* by *one regional* or *global model* based on the data of *N* stations.

Let us briefly review the modeling features as used by (Wild, 1994) and as used below. Wild uses the so-called *single-layer model* where it is assumed that all free electrons are concentrated in a shell of infinitesimal thickness. This *thin shell* is located in a height *H* above a spherical Earth. The height *H* of this idealized layer is usually set to 350 or 400 kilometers, which corresponds approximately to the peak height of the electron density profile in the F-region of the ionosphere. The electron density *F* - the surface density of the layer is assumed to be a function of the geocentric latitude β and the *sun-fixed* longitude *s*

$$F(\beta, s) = \sum_{i=0}^n \sum_{j=0}^m P_{ij} \cdot (\beta - \beta_0)^i \cdot (s - s_0)^j \quad (1)$$

where

- n, m are the maximum degrees of the *n*-dimensional Taylor series expansion in latitude and in *sun-fixed* longitude,
- P_{ij} are the (unknown) coefficients of the Taylor series, and
- β_0, s_0 are the coordinates of the origin of the development.

The single-layer model defined by equation (1) does *not* provide a modeling of the time dependence in the *sun-fixed* reference frame because the “frozen” ionosphere is co-rotating with the Sun. Nevertheless, there is always a time dependence in the *earth-fixed* frame. Note

that short-term variations of the ionospheric TEC are *not* modeled by equation (1). They will be interpreted as noise of the *geometry-free* GPS observable.

The representation (1) is *not* well suited for *regional* or *global* TEC models because of limitations in the (β, s) -space. Based on the above considerations we decided to use a new approach to model the ionosphere in the following way (details explained in the next section):

- (i) The single-layer *model* is used as previously.
- (ii) The mapping junction is taken over without change.
- (iii) The *zero-difference* observable was replaced by the *double-difference* observable due to operational considerations.
- (iv) Instead of using a *Taylor series* development a development into *spherical* harmonics was used.

As already mentioned above we are fully aware of the fact that by using *double* instead of *zero* differences we lose parts of the ionospheric signal but we have the advantage of a *cleaned* observable. Moreover we are *not* affected by a degradation of the code observations under the AS-regime. This advantage may be “lost” when the next generation of precise P-code receivers will become available.

THE “NEW” IONOSPHERE MODELING TECHNIQUE

The *double-differenced observation equation* for the *geometry-free linear combination* ϕ_4 of the carrier phase measurements (ϕ_1 and ϕ_2) referring to a set of *two* receivers and *two* satellites may be written as

$$\text{dd}(\phi_4) + v_4 = -\alpha \left(\frac{1}{\nu_1^2} - \frac{1}{\nu_2^2} \right) \text{dd}(F(z) \cdot E) + B_4 \quad (2)$$

where

$\text{dd}(\dots)$ is the *double-difference operator*,

$\phi_4 = \phi_1 - \phi_2$ is the *geometry-free* phase observable (in meters),

v_4 is the corresponding residual,

$\alpha = 4.03 \cdot 10^{17} \text{ m S}^2 \text{TECU}^{-1}$ is a constant (TECU stands for Total Electron Content Unit²),

ν_1, ν_2 are the frequencies associated with the carriers L1 and L2,

$F(z)$ is the mapping function evaluated at the zenith distance z ,

E is the *vertical* Total Electron Content (in TECU), and

²One TEC Unit corresponds to 10^{16} free electrons per square meter.

$B_4 = \lambda_1 N_1 - \lambda_2 N_2$ is a *constant* bias (in meters) due to the initial phase ambiguities N_1 and N_2 with their corresponding wavelengths λ_1 and λ_2 ; if new ambiguities were set up for one satellite, a new parameter of this type has to be introduced.

In the *ambiguity-resolved* case the (integer) double-difference ambiguity parameters N_1 and N_2 as well as the (real-valued) parameter B_4 are known. All *unresolved* ambiguity parameters B_4 — auxiliary parameters only — and the ionosphere model parameters have to be estimated simultaneously.

The *single-layer* or *thin-shell* mapping function $F(z)$ simply may be written as

$$F(z) = \frac{1}{\cos z'} = \frac{1}{\sqrt{1 - \sin^2 z'}} \quad \text{with} \quad \sin z' = \frac{R}{R+H} \sin z \quad (3)$$

where

- z, z' are the (geocentric) zenith distances at the station and at the single layer,
- R is the mean Earth radius, and
- H is the height of the single layer above the Earth's surface.

We develop the surface density E of the ionospheric layer into a series of spherical harmonic functions of maximum degree n_{\max} and maximum order $m_{\max} \leq n_{\max}$:

$$E(\beta, s) = \sum_{n=0}^{n_{\max}} \sum_{m=0}^n \tilde{P}_{nm}(\sin \beta) \cdot (a_{nm} \cos ms + b_{nm} \sin ms) \quad \text{with} \quad t \in [t_i, t_{i+1}] \quad (4)$$

where

- β is the geocentric latitude of the intersection point of the line receiver-satellite with the ionospheric layer,
- $s = \lambda - \lambda_0$ is the *sun-fixed* longitude of the ionospheric pierce point, which corresponds to the *local solar time* neglecting an additive constant π (or 12 hours),
- λ, λ_0 are the *geographic* longitude of the ionospheric pierce point and the *true* (or *mean*) longitude of the Sun,
- t is the time argument,
- $[t_i, t_{i+1}]$ is the specified period of validity (of the i -th model),
- $P_{nm} = \Lambda(n, m)$. P_{nm} are the *normalized* associated Legendre polynomials of degree n and order m based on the *normalization function* Λ and the *unnormalized* Legendre polynomials P_{nm} , and
- a_{nm}, b_{nm} are the *unknown coefficients* of the spherical harmonic functions, i.e. the global (or regional) ionosphere model parameters.

We may use the geocentric latitude β and the sun-fixed longitude s in the *geographical* coordinate system or an equivalent set (β', s') in the *solar-geomagnetic* coordinate system

as independent arguments. Using simply the *mean* longitude of the Sun, the sun-fixed *mean* longitude s of the ionospheric pierce point in the geographical system reads as

$$s = \lambda - \lambda_0 = \lambda - (\pi - t) = \lambda + t - \pi \quad (5)$$

where t is the *Universal Time UT* (in radians).

The *normalization function A* is defined as follows:

$$\Lambda(n, m) = \sqrt[2]{\frac{2n+1}{1+\delta_{0m}} \frac{(n-m)!}{(n+m)!}} \quad \text{with } \Lambda(0, 0) = 1 \quad (6)$$

where δ denotes the Kronecker Delta.

The zero-degree coefficient a_{00} may be interpreted on a *global* scale as the *mean* TEC E_0 by forming the surface integral of the TEC distribution (4)

$$E_0 = \frac{1}{4\pi} \int_S E \, dS = \frac{1}{4\pi} \int_{-\frac{\pi}{2}}^{+\frac{\pi}{2}} \int_0^{2\pi} E(\beta, s) \cos\beta \, d\beta \, ds = \Lambda(0, 0) a_{00} = a_{00} \quad (7)$$

Multiplying the coefficient a_{00} (in TECU) by the surface area of the ionospheric layer (in m^2) we obtain the total number of free electrons n_E (in 10^{16}) within the ionospheric shell

$$n_E = 4\pi R'^2 a_{00} \quad \text{with } R' = R + H \quad (8)$$

where R' is the geocentric radius of the ionospheric layer.

The number n_P of ionosphere model parameters a_{nm} and b_{nm} (per parameter set) is given by the expression

$$n_P = (n_{\max} + 1)^2 - (n_{\max} - m_{\max})(n_{\max} - \text{inn},, + 1) \quad \text{with } m_{\max} \leq n_{\max} \quad (9)$$

or by

$$n_P = (n_{\max} + 1)^2 \quad \text{i f } n_{\max} = m_{\max} \quad (10)$$

Both TEC models (1) and (4) represent a *static* (or “frozen”) ionosphere in the sun-fixed reference frame. However, the parametrization of the ionospheric coefficients a_{nm} and b_{nm} as time-dependent parameters — for instance as piece-wise linear functions in time ensuring the continuity — allow us theoretically to model a (*low-*)*dynamic* ionosphere $E(\beta, s, t)$. In summary, we are able to set up in our procedure a set of constant ionosphere parameters per specified time interval $[t_i, t_{i+1}]$ or a parameter set per specified reference epoch t_i while the ionosphere coefficients $a_{nm}(t)$ and $b_{nm}(t)$ are interpolated linearly in time between subsequent epochs t_i . This modeling technique was not followed up in detail. Attempts were made specifying each 24 hours reference epochs t_i to generate a sequence of *quasi-static* ionosphere models *continuously* varying in time.

The *global ionosphere model parameter* type as presented here has been implemented into the parameter estimation program GPSEST of the *Bernese GPS Software*, where the parameter estimation algorithm is based on a least-squares adjustment.

FIRST RESULTS

At present (mid 1995), the CODE Analysis Center is processing the data of about 60 globally distributed sites of the GPS tracking network of the IGS. Figure 1 shows the present state of the IGS core network. Notice in particular the station distribution in latitude with *Ny Alesund* as the IGS station furthest north (78.9° N) and *McMurdo* as the station furthest south (77.8° S).

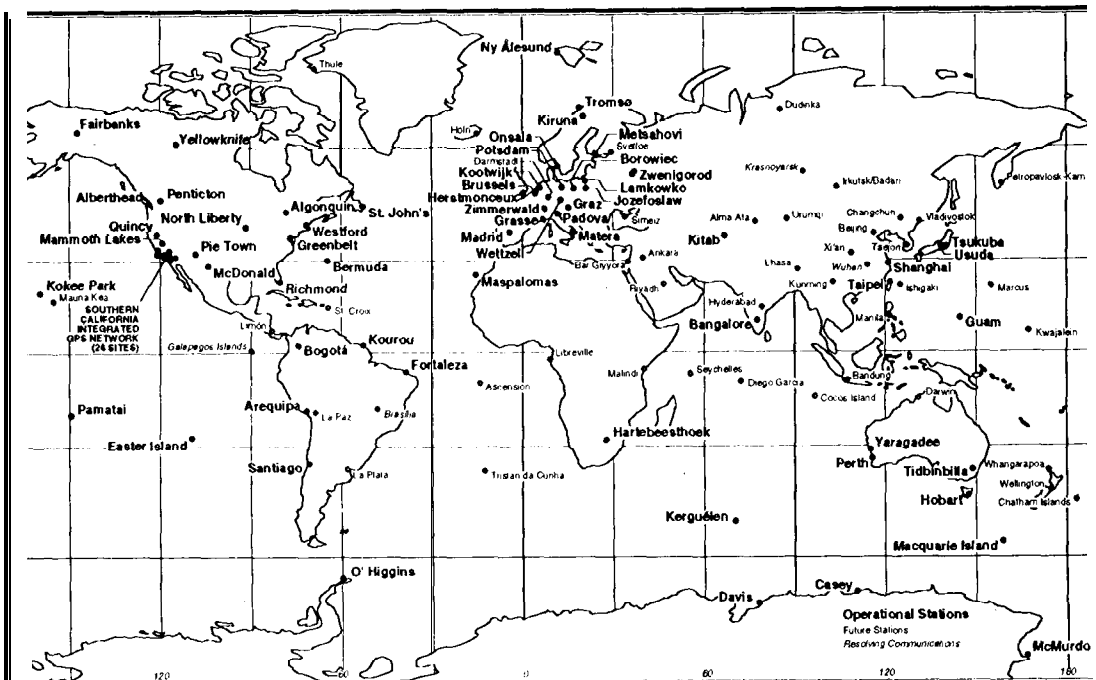


Figure 1. GPS tracking network of the *International GPS Service for Geodynamics (IGS)* – operational and planned stations (May 1995)

Looking at Figure 1 the *inhomogeneous* distribution of the IGS sites and even the *sparse* coverage in the *southern* hemisphere can be clearly seen. Obviously, a high-temporal resolution of the TEC structure without any gaps over the *entire* globe will *not* be possible, because each GPS station “observes” the ionosphere within a radius of 1000 (1 500) kilometers only when using an elevation angle cutoff at 20 (15)°.

Global Ionosphere Models

Below we discuss results using a data set of April 23-29, 1995 (GPS week 798, DOY 113-119). Let us summarize some important aspects first. For all subsequent computations, a single-layer height H of 400 kilometers is assumed. Furthermore all ionosphere models (or maps) are derived from *double-differenced* GPS phase data using an elevation angle cutoff at 20° — as used for our routine processing — and a sampling rate of one epoch per 4 minutes³.

An 8th-degree spherical harmonics expansion (4) is normally performed for a 24-hour *global ionosphere model*. Consequently, this 24-hour model represents a *time-averaged* TEC structure, which is a *static* (or “frozen”) one in the *sun-fixed* reference frame. According to formula (10) the number of ionosphere parameters per such a TEC model is 81.

In order to illustrate *ionosphere maps*, the results for April 23, 1995 are included in this paper. Figure 2 shows the *global ionosphere map* based on the *geographical* coordinate system in the *ambiguity-free* and *ambiguity-fixed* case respectively. In both cases the *maximum* TEC is about 47 TECU (explicitly plotted in Figures 4a and 4b). The sun-fixed longitudes s of the ionospheric pierce points have been computed according to the simplified relation (5) as *mean* longitudes. In Figure 2 (and 3) the latitude band of the ionospheric pierce points is indicated by the two dashed lines.

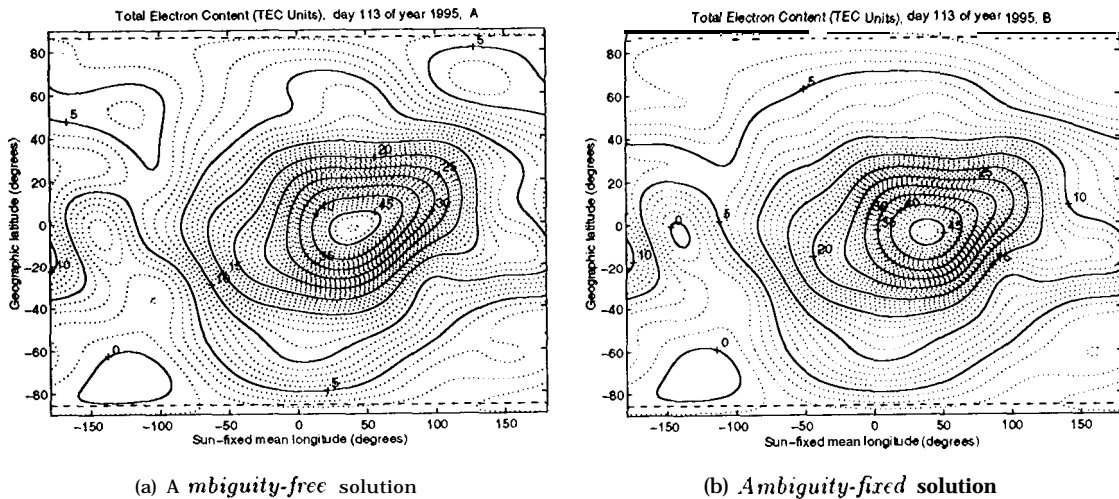


Figure 2. *Global ionosphere map* for April 23, 1995 based on the *geographical* coordinate system (with 81 coefficients, i. e. $n_{\max} = m_{\max} = 8$)

On day 113 about 48 % of roughly 2200 ambiguity parameters B_4 (see observation equation (2)) were resolved (i. e. known). Ambiguity resolution⁴ *without* using the P-code measurements is performed up to baseline lengths of 2 000 kilometers (Mervart, 1995): where

³One epoch per 30 seconds would be available.

⁴We use the so- called *Quasi-Ionosphere-Free (QIF)* ambiguity resolution strategy.

typically about 85 (90)% of the ambiguities are resolved for baseline lengths $l < 500$ km, 80 (85) % for $1 < 1000$ km, and 70 (75) % for $1 < 2000$ km when *Anti-Spoofing (AS)* is turned on (off). By resolving the ambiguities we achieve primarily a drastic reduction of the number of *unknown* parameters as well as an improvement in accuracy of the remaining parameters. Since June 25, 1995 (GPS week 807, DOY 176) - after an experimental phase of several months - the *official* IGS products from the CODE Analysis Center are based on (partly) *ambiguity-fixed* solutions.

To study the effect of choosing the *geographical* and the *solar-geomagnetic* coordinate system respectively, we have compared global ionosphere models based on each coordinate system for all days of GPS week 798. However, we could *not* recognize any significant difference in terms of the root-mean-square (RMS) error of the unit weight. Figure 3 shows the ionosphere map for April 23, 1995 based on the *solar-geomagnetic* coordinate system in the *ambiguity-fixed* case.

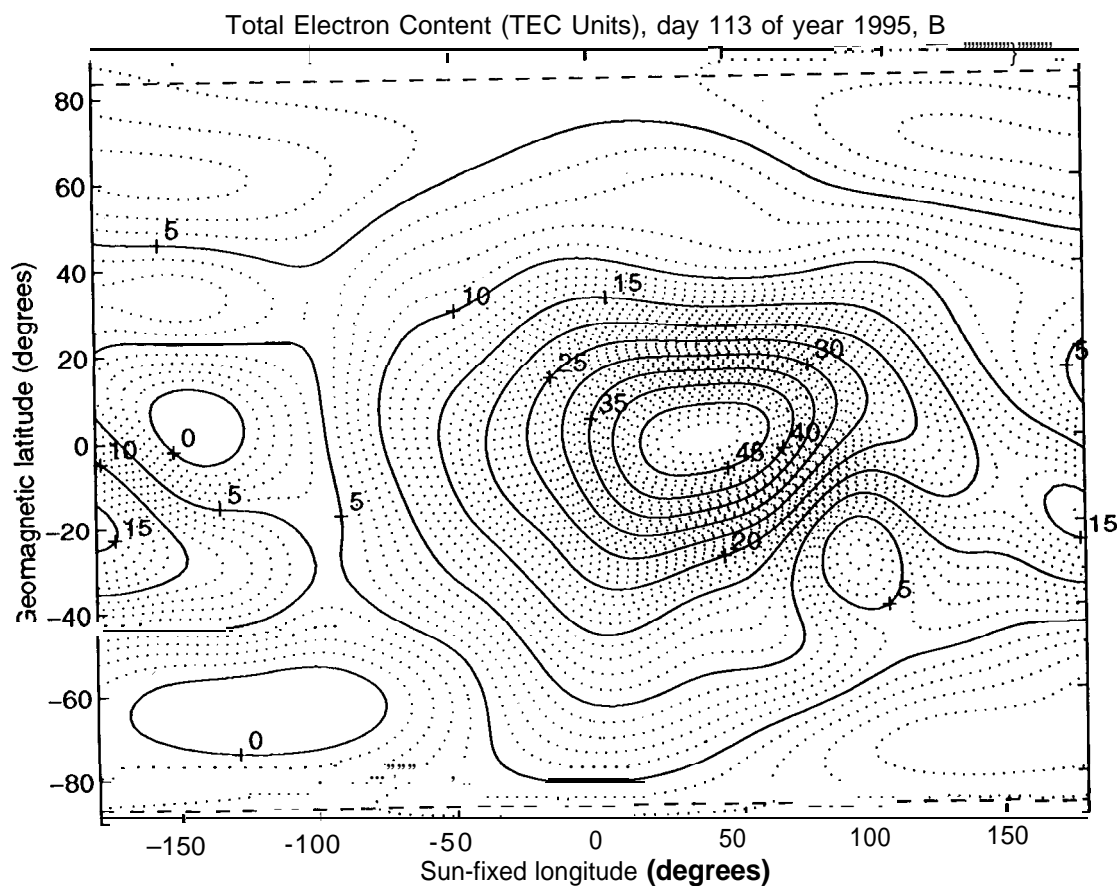


Figure 3. Global ionosphere map for April 23, 1995 based on the *solar-geomagnetic* coordinate system (with 81 coefficients, i. e. $n_{\max} = m_{\max} = 8$)

Comparing Figure 3 with Figure 2b both contour line maps look similar. Note that the *geomagnetic* latitude of the Sun varies considerably (ea. $\pm 1.09^\circ$) as opposed to the geo-

graphical system, where the latitude of the Sun remains nearly constant over the time span of 24 hours.⁵

The development in time of three special quantities namely the *maximum*, *mean*, and “*minimum*” TEC is shown in Figure 4. The values coming from solutions based on both the *geographical* and the *geomagnetic* frame are very similar, hence the values of the first set only are plotted.

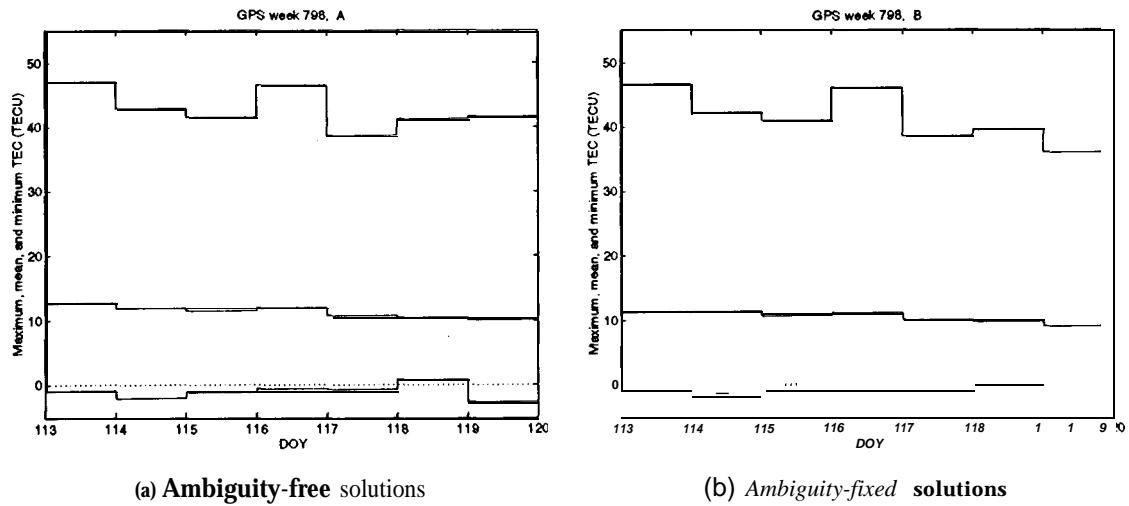


Figure 4. Development in time of the daily *maximum*, *mean*, and “*minimum*” TECS during GPS week 798

According to the surface integral (7) the *mean* TEC E_0 is represented by the zero-degree coefficient a_{00} . Using the simple relation (8) we can convert a_{00} (or E_0) into the total number n_E of free electrons within the ionospheric shell: e.g. $n_E = 6.5.1031$ at day 113. The *mean* TEC (or the *time-averaged* total number of free electrons) steadily decreasing during GPS week 798 (see Figure 4) seems to be quite stable (small variations). After fitting the “observed” ionospheric coefficients a_{00} by a first-degree polynomial in time, we have got residuals with an RMS error of 0.3 TECU, which is a first criterion for the quality of the special ionosphere parameter a_{00} (or E_0). Theoretically the quantity E_0 should be a good indicator for the solar activity. One may expect that this ionospheric parameter is strongly correlated with the *Sun spot number*. We should mention that the solar activity was quite *weak* (*low* Sun spot number) during this test week.

By definition the TEC must be greater than *zero*. Accordingly, the “*minimum*” TEC estimates are never significantly below *zero*, which is a sign of success, too (we have *never* applied any a priori constraints on the ionosphere model parameters).

⁵The current geographic latitude of the *geomagnetic pole* is about 79.10.

Regional Ionosphere Models

When processing data from tracking stations located within a *narrow* longitude band, the ionosphere modeling technique (4) yields *regional* ionosphere models. An example of a regional ionosphere map is shown in Figure 5a compared with the corresponding detail (latitude band) of the *global* TEC map (see Figures 2b and 5b). Both maps are based on *ambiguity-fixed* GPS solutions using the *geographical* coordinate system.

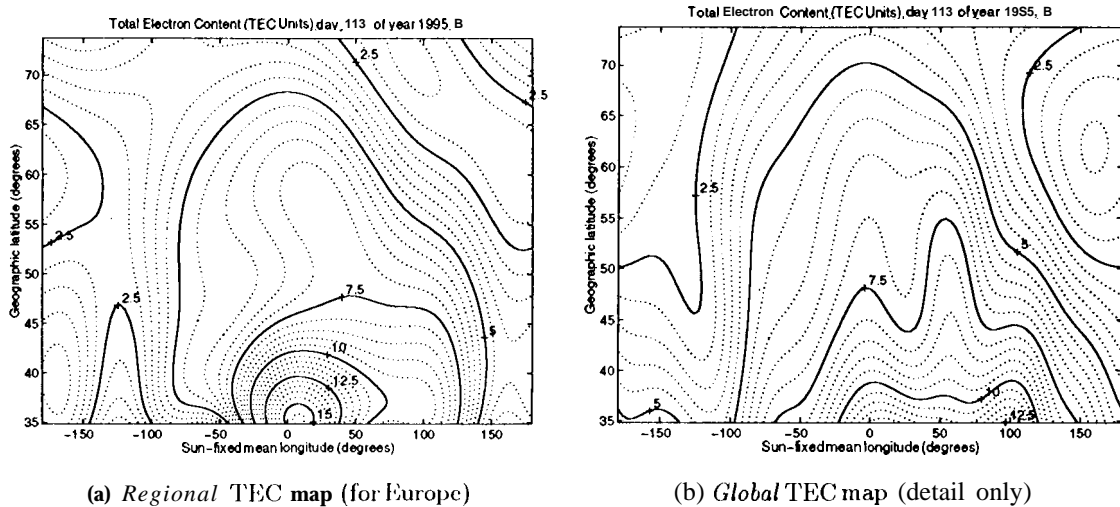


Figure 5. The *regional* TEC model (with $n_{\max} = 5$) for April 23, 1995 is based on data of 16 European IGS stations (listed in Tables 1 and 2), whereas the *global* TEC model (with $n_{\max} = 10$) is based on data of 50 globally distributed IGS stations (including the European ones).

The TEC model (4) -- its specified period of validity assumed to be not longer than 24 hours (i.e. $t_{i+1} - t_i \leq 24$ h) --- provides for a *regional* model a real modeling of the time dependence in the *sun-fixed* reference frame because by definition the longitude band $[\lambda_{\min}, \lambda_{\max}]$ of the monitor stations is small, i.e.

$$\lambda_{\max} - \lambda_{\min} \ll 2\pi \quad (11)$$

Therefore the monitor stations of a *regional* network “probe” at every time only a *narrow* longitude band of the ionosphere co-rotating with the Sun. A restriction of the latitude band would not be necessary, but is given by the station geometry. Considering these restrictions the *regional* ionosphere model (Figure 5a) is applicable only for GPS stations lying within the latitude band $[40^\circ \text{ N}, 70^\circ \text{ N}]$ and strictly speaking within the “narrow” longitude band $[4^\circ \text{ W}, 37^\circ \text{ E}]$, as opposed to the *global* model (Figure 5b), where we assume the TEC to be longitude-independent. Notice that Figure 5a shows the (wider) latitude band of the ionospheric pierce points.

The special case of processing individual baselines (two stations) only to generate so-called *baseline-specific* ionosphere models was already considered in (Schaer, 1994). The following Figures 6a, 6b, and 7b (from (Schaer, 1994)) are based on results of 1,1- L2-solutions containing station coordinates, ambiguities (N_1 and N_2), tropospheric zenith path delay parameters, stochastic ionosphere parameters, and last but not least deterministic ionosphere parameters according to TEC model (4) with $H = 350$ km. Figure 6 illustrates the *baseline-specific* ionosphere model for the baseline Kootwijk-Wetzell (Europe) *before* and *after* ambiguity resolution respectively. The “bulge” at (local) early afternoon as well as a gradient in north-south direction are clearly recognizable. The ionospheric activity at that time seems to have been much stronger than 15 months later as seen in the TEC map for Europe (Figure 5a).

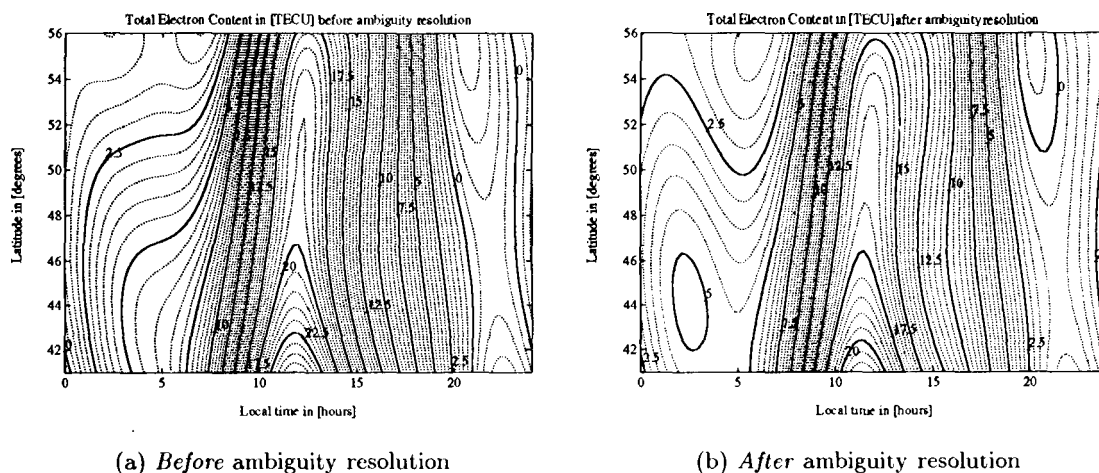


Figure 6. *Baseline-specific* ionosphere model with 36 parameters ($n_{\max} = 5$) for baseline Kootwijk-Wetzell ($l \approx 600$ km) at January 25, 1994

The fractional parts of the *wide-lane* ambiguities $N_5 = N_1 - N_2$ just before fixing are shown in Figure 7b. Note that our “fractional parts” are *not* generally the differences with respect to the next integer but the differences between *true* and *biased* ambiguity parameters; therefore they may be greater than *half* a cycle (see Figure 1’s). Assuming that the station coordinates and the troposphere parameters (or the “geometrical” parameters) are well determined, these fractional parts are proportional to the biases due to the ionospheric refraction.⁶ The dispersion of the fractional parts of the ambiguities N_5 is consequently an excellent indicator for the *unmodeled* ionospheric influence or the quality of the ionosphere modeling of course — at least on differential level. Comparing Figures 7a and 7b the decreasing of this dispersion when TEC is modeled is clearly visible.

⁶ One wide-lane cycle ($\lambda_5 = 86$ cm) corresponds approximately to 4.1 TECU (at $z = 0$).

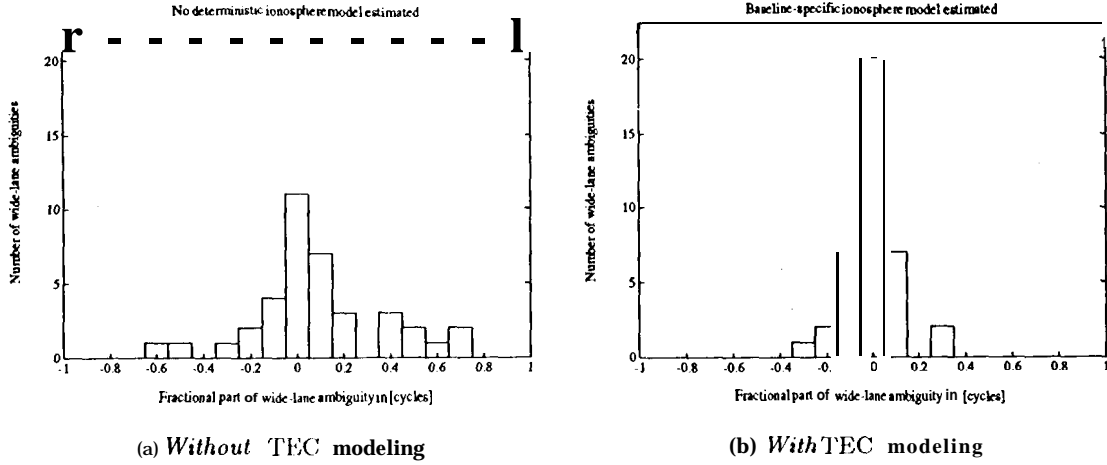


Figure 7. Histogram of the fractional parts of the *wide-lane* ambiguities for one-day single-baseline solution - *without* or *with* TEC modeling (Figure 6a)

Quality Checks

Applying the ionosphere model (4) the *ionospheric range correction* (in meters) for the *z-em-difference* GPS observation of the *i*-th frequency is given by

$$\Delta_i(\beta, s, z) = \mp \frac{\alpha}{\nu_i^2} F(z) \cdot E(\beta, s) \quad \text{with } i = 1, 2 \quad (12)$$

where one has to select the *negative* sign for *phase* observations and the *positive* for *code* observations (see also equations (2) and (3)). It is very important to use in relation (12) the same height *H* of the single layer the TEC model (4) is based on, whereas GPS results are nearly insensitive to the value itself of the height *H* (Wild, 1994). Nevertheless, the *absolute* calibration of the *TEC E* strongly depends on the assumed height *H* of the single layer.

In order to get a first impression of the quality of our large-scale ionosphere models we computed regional single-frequency (L1) solutions with European data with and without *regional* and *global* ionosphere models respectively applied according to the above formula (12). Note that the maximum extent of this IGS sub-network evaluated is about 3500 kilometers in diameter. The baseline shortening introduced into GPS results by neglecting the ionospheric refraction is on the average 0.08 ppm/TECU when the L1 phase observable is processed with an elevation mask at 20° (Beutler et al., 1988). We expect an *apparent* network contraction of the same order.

Analyzing the scale biases estimated and the residuals of the coordinates coming from Helmert transformations with respect to ITRF⁷ coordinates, we observed for every day of

⁷IERS (International Earth Rotation Service) Terrestrial Reference Frame

the test week that when applying our ionosphere models not only the scale bias has been reliably removed (on the 10-ppb level) but also the RMS variance of the residuals could be reduced significantly. No perceptible quality difference between *regional* and *global* ionosphere models could be detected by these criteria. Results of the seven parameter Helmert transformation between ITRF coordinates and the station coordinates of the *regional* single-frequency solution for the first day of the test week are shown in Table 1. The scale bias estimated is given at the bottom of the table: -0.25 ppm (without) and -0.02 ppm (with TEC model). The *global* TEC model illustrated in Figure 2b was used. The statistics of the corresponding six parameter Helmert transformation (no scale bias estimated) is given in Table 2. A dramatic increase of the standard deviation of the station coordinates when no TEC model is used has to be expected.

Table 1. Seven parameter Helmert transformation between ITRF coordinates and the coordinates of the *regional* L1 solution processing European IGS data from April 23, 1995

<i>Global</i> TEC model applied	No			Yes		
Station name	Residuals (cm)			Residuals (cm)		
	North	East	up	North	East	up
JOZE Jozefoslaw	2.1	-0.4	6.6	1.8	-3.7	4.4
BRUS Brussels	-4.6	-4.5	9.2	-2.7	-2.8	3.2
BOR1 Borowiec	1.0	0.7	7.3	1.0	-1.2	3.3
GRAZ Graz	4.9	1.4	-3.3	4.6	-1.8	-4.1
HERS Herstmonceux	-6.7	-3.4	-1.4	-5.4	-0.7	-1.5
KOSG Kootwijk	0.5	-4.4	9.2	0.3	-3.6	5.6
MADR Madrid	12.8	2.7	-9.8	15.2	8.8	-4.5
MATE Matera	2.2	10.0	-19.6	1.1	4.3	-5.0
TROM Tromso	2.4	11.3	-24.5	-2.0	13.4	-13.0
WETT Wettzell	3.3	-1.9	7.2	3.2	-3.4	3.4
ZIMM Zimmerwald	-8.4	-2.2	-6.7	-7.2	-1.6	-9.1
ONSA Onsala	-8.1	0.4	13.7	-7.8	2.0	12.1
METS Metsahovi	-3.3	1.0	-6.3	-2.9	4.2	-4.4
POTS Potsdam	1.4	-0.9	7.1	0.8	-1.2	3.1
LAMA Lamkowko	-1.7	1.9	10.8	-1.8	-0.7	6.8
MDVO Mendeleev	2.4	-11.7	0.6	1.7	-12.1	-0.3
RMS per component (cm)	5.4	5.4	11.1	5.4	5.8	6.4
RMS of transformation (cm)	8.2			6.2		
Degree of freedom	41			41		
Scale factor (mm/km)	-0.252 ± 0.020			-0.018 ± 0.015		

This method to perform quality checks indicates GPS-internal consistency of the ionosphere models. The same is true for the analysis of the fractional parts of wide-lane ambiguity parameters (Figure 7b). In order to check the *absolute* calibration of our TEC models, comparisons with models established by other groups using other techniques or even other than GPS observations will have to be made.

Table 2. Six parameter Helmert transformation (*no* scale factor permitted) between ITRF coordinates and the coordinates of the *regional* L 1 solution processing European IGS data from April 23, 1995

Global TEC model applied	No			Yes		
Station name	Residuals (cm)			Residuals (cm)		
	North	East	up	North	East	up
JOZE Jozefoslaw	2.2	13.0	5.1	1.8	-2.7	4.3
BRUS Brussels	-1.1	-20.2	8.0	-2.4	-3.9	3.1
BORI Borowiec	1.2	7.3	5.4	1.0	-0.7	3.2
GRAZ Graz	19.7	5.7	-4.5	5.6	-1.5	-4.1
HERS Herstmonceux	-4.5	-26.1	-1.8	-5.2	-2.3	-1.5
KOSG Kootwijk	0.4	-17.1	7.7	0.3	-4.5	5.5
MADR Madrid	41.6	-34.1	-4.9	17.3	6.2	-4.2
MATE Matera	34.7	17.4	-18.2	3.4	4.9	-4.9
TROM Tromso	-45.6	16.9	-19.1	-5.4	13.8	-12.6
WETT Wettzell	12.4	-2.5	5.4	3.9	-3.4	3.2
ZIMM Zimmerwald	6.6	-13.2	-7.6	-6.1	-2.4	-9.2
ONSA Onsala	-22.2	-1.6	12.3	-8.8	1.8	12.0
METS Metsahovi	-26.4	16.5	-5.9	-4.6	5.3	-4.4
POTS Potsdam	1.4	-1.1	5.0	0.8	-1.3	3.0
LAMA Lamkowko	-6.5	14.2	9.4	-2.2	0.2	6.7
MDVO Mendeleevo	-13.9	24.9	3.7	0.5	-9.5	-0.1
RMS per component (cm)	21.7	17.6	9.4	6.1	5.4	6.3
RMS of transformation (cm)	17.6			6.2		
Degree of freedom	42			42		

CONCLUSIONS AND OUTLOOK

The world-wide IGS network of permanent tracking dual-frequency GPS receivers provides a unique opportunity to *continuously* monitor the *Total Electron Content (TEC)* on a *global* scale. First results using one week of *GPS phase data* as used by the CODE Analysis Center seem to indicate that under *normal* ionospheric conditions we are able to estimate *plausible* ionosphere models using the *double-difference approach*. Results were illustrated by several *ionosphere maps* for April 23, 1995.

An 8th-degree spherical harmonics expansion seems to be adequate for a 24-hour global TEC model. This 24-hour model represents a *time-averaged* global TEC structure. To verify the GPS-internal consistency of our TEC models we computed *regional* single-frequency (1.1) solutions with European data with and without using *regional* and *global* models, respectively. Comparisons by Helmert transformations between the station coordinates stemming from the different L1 solutions and the corresponding ITRF coordinates revealed that when applying our ionosphere models not only the *scale biases* could be reliably removed, a significant reduction of the residuals could be observed as well for every day of the test week. *No* quality difference between *regional* and *global* ionosphere models could be detected. In order to check in detail the quality as well as the *absolute* calibration of our TEC models, comparisons with models established by other groups will have to be made.

The assumptions of the thin-shell model -- the height H of the shell in particular — are essential for *absolute* calibration. If a smaller (larger) height than the “effective” (or actual) height H_0 is adopted, larger (smaller) zenith distances at the ionospheric sub-points will cause the TEC values to be underestimated (overestimated). This means that in principle the determination of the single-layer height H as an additional *unknown* parameter would be possible.

The use of the double-difference *approach* will give us the capability to produce very “low-cost” one-day ionosphere models (and maps) on a routine basis — even under *Anti-Spoofing (AS)*. The ionosphere modeling technique presented in this paper will be implemented at the CODE Analysis Center in the very near future. An additional fully-automatic procedure will be set up to create ionosphere model files for every day. These daily *average ionosphere models* should potentially support our so-called *Quasi-Ionosphere-Free (QIF)* ambiguity resolution strategy (Mervart and Schaer, 1994). By statistically analyzing the *fractional parts* of the *wide-lane ambiguities* we will get another quality check indicator for our ionosphere models. After ambiguity resolution we will be able to generate ionosphere models which are based on (partly) *ambiguity-fixed* solutions.

The ionosphere model parameters (*global* ionosphere maps only) will *not* be sent to the *IGS Global Data Centers*, but will be made available in an *Anonymous FTP* account at the CODE processing center.⁸ Such an *ionosphere service* providing day by day TEC models is of interest for all GPS users, which are analyzing and evaluating *small* high-precision control networks using the L 1 observable only instead of the *ionosphere -free LC* for reasons of accuracy (see e.g. (Beutler et al., 1995)). Finally, let us not forget that we will obtain information related to the ionosphere (and the solar activity) like mean TEC, maximum TEC, etc. for long-term studies.

REFERENCES

- Beutler, G., I. Bauersima, W. Gurtner, M. Rothacher, T. Schildknecht, 1988, *Atmospheric Refraction and Other Important Biases in GPS Carrier Phase Observations*, Monograph 12, School of Surveying, University of New South Wales, Australia.
- Beutler, G., I. Bauersima, S. Botton, W. Gurtner, M. Rothacher, T. Schildknecht, 1989. Accuracy and biases in the geodetic application of the Global Positioning System. *Manuscript Geodaetica*, Vol. 14, No. 1, pp. 28–35.
- Beutler, G., I. I. Mueller, R. Neilan, 1994, The International GPS Service for Geodynamics (IGS): Development and Start of Official Service on 1 January 1994, *Bulletin Géodésique*, Vol. 68, No. 1, pp. 43–51.
- Beutler, G., M. Cocard, A. Geiger, M. Müller, M. Rothacher, S. Schaer, D. Schneider, A. Wiget, 1995, Dreidimensionales Testnetz Turtmann 1955–1993: Teil 11, *Geodätisch-geophysikalische Arbeiten in der Schweiz*, Band 51.
- Georgiadiou, Y. and A. Kleusberg, 1988, On the effect of ionospheric delay on geodetic relative GPS positioning, *Manuscripta Geodaetica*, Vol. 13, pp. 1–8.

⁸The next version of the *Bernese GPS Software* will be able to process directly these ionosphere files.

- Lanyi, G. E. and T. Roth, 1988, A comparison of mapped and measured total ionospheric electron content using global positioning system and beacon satellite observations, *Radio Science*, Vol. 23, No. 4, pp. 483-492.
- Mannucci, A. J., B. D. Wilson, D.-N. Yuan, 1994, Monitoring Ionospheric Total Electron Content Using the GPS Global Network and TOPEX/POSEIDON Altimeter Data, *Proceedings of the Beacon Satellite Symposium*, Aberystwyth, Wales, July 1994.
- Mervart, L., G. Beutler, M. Rothacher, U. Wild, 1993, Ambiguity Resolution Strategies Using the Results of the International GPS Geodynamics Service (IGS), *Bulletin Géodésique*, Vol. 68, No. 1, pp. 29-38.
- Mervart, L. and S. Schaer, 1994, *Quasi-Ionosphere-Free (QIF) Ambiguity Resolution Strategy*, Internal report, Astronomical Institute, University of Berne, Switzerland.
- Mervart, L., 1995, *Ambiguity Resolution Techniques in Geodetic and Geodynamic Applications of the Global Positioning System*, Ph.D. thesis, Astronomical Institute, University of Berne, Switzerland.
- Rothacher, M., G. Beutler, W. Gurtner, E. Brockmann, L. Mervart, 1993, *The Bernese GPS Software Version 3.4: Documentation*, Astronomical Institute, University of Berne, Switzerland.
- Rothacher, M., R. Weber, E. Brockmann, G. Beutler, L. Mervart, U. Wild, A. Wiget, C. Boucher, S. Botton, H. Seeger, 1994, *Annual Report 1994 of the CODE Processing Center of the IGS*.
- Schaer, S., 1994, *Stochastische Ionosphärenmodellierung beim Rapid Static Positioning mit GPS*, Diplomarbeit, Astronomisches Institut, Universität Bern.
- Wild, U., 1993, Ionosphere and Ambiguity Resolution, *Proceedings of the 1993 IGS Workshop*, March 25-26, 1993, Berne, Switzerland, pp. 361-369.
- Wild, U., 1994, Ionosphere and Satellite Systems: Permanent GPS Tracking Data for Modelling and Monitoring, *Geodätisch-geophysikalische Arbeiten in der Schweiz*, Band 48.
- Wilson, B. D. and A. J. Mannucci, 1993, *Instrumental Biases in Ionospheric measurements Derived from GPS Data*, Paper presented at ION GPS 93, Salt Lake City, September 22-24, 1993.

APPLICATION OF IGS DATA TO GPS SENSING OF THE ATMOSPHERE FOR WEATHER AND CLIMATE RESEARCH

C Rocken, F S Solheim, R H Ware, M Exner, D Martin
UNAVCO/UCAR, POB 3000,
Boulder CO 80307-3000, USA

M Rothacher
Astronomical Institute, University of Bern,
CH-3012, Bern, Switzerland

ABSTRACT

Water vapor is one of the most important constituents of the atmosphere as it is the principal mechanism by which moisture and latent heat are transported. Consequently, accurate and sufficiently frequent and dense **sampling** of water vapor is needed for weather and climate research as well as operational weather forecasting. It has been demonstrated that GPS data can be used to measure atmospheric water vapor. The worldwide International GPS Service (**IGS**) network of GPS tracking stations can be used to sense global atmospheric water vapor **if** adequate pressure and temperature data are available at these sites. Addition of pressure sensors accurate to 0.3 **mbars** and temperature sensors accurate to several degrees Kelvin at IGS stations would allow sensing of **precipitable** water vapor (**PWV**) over 30 minute intervals with an accuracy better than 2 mm. This paper describes the main ground and space-based applications of GPS to atmospheric sciences and discusses current and future developments and the important role of the IGS. Specifically we will discuss: (a) importance of global water vapor measurements for climate studies; (b) accuracy considerations and suggested design of pressure, temperature and humidity sensors for installation at **IGS** sites; (c) suggested solutions for meteorological data flow and download issues; (d) conversion of estimated GPS path **delay** to zenith water vapor; (e) a suggestion for combining delays from all IGS processing centers; and (f) PWV time series - a new **IGS** product?

INTRODUCTION

Tropospheric water vapor plays an important role in the **global** climate system and is a key variable for short-range numerical weather prediction. Despite significant progress in remote sensing of **wind** and temperature, cost-effective monitoring of atmospheric water vapor is still lacking. Data from the Global Positioning System (**GPS**) have recently been suggested to improve this situation (i.e. **Bevis et al.**, 1992). Figure 1 illustrates the prob-

lem of current satellite systems for reliably measuring atmospheric water vapor and the promise of ground-based GPS systems.

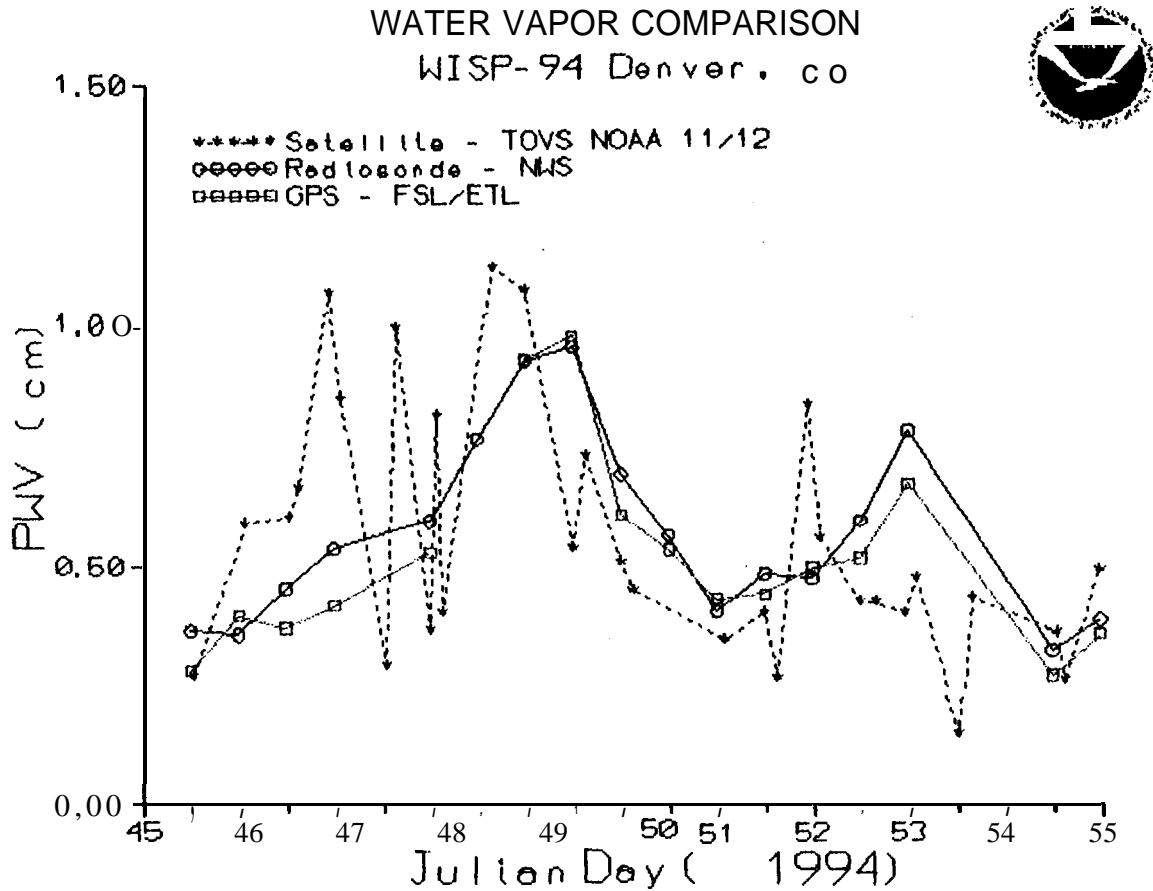


Figure 1. Comparison of satellite, radiosonde and GPS estimates of integrated water vapor during the joint NOAA/UNAVCO WISP-94 experiment. The figure shows that GPS estimates correlate strongly with the radiosonde while the satellite data is less reliable. (Figure courtesy of Russ Chadwick of NOAA/FSL).

The GPS signal is sensitive to the refractive **index** of the atmosphere, and because this index is a function of pressure, temperature, and moisture, GPS can be used directly for sensing properties of the atmosphere. Small amounts of atmospheric water vapor significantly affect GPS signal propagation velocities. Thus GPS is especially well suited for sensing atmospheric water vapor.

Recent studies have demonstrated (i.e. Rocken *et al.*, 1993, 1995, Duan *et al.*, 1995) that GPS can reliably be used to estimate PWV with 1-2 mm accuracy and 30-minute temporal resolution. The first GPS network, dedicated to PWV estimation, has been established by the National Oceanic and Atmospheric Administration (NOAA) in the **United States** (Figure 2). Results from operating this network for over 100 days confirm that PWV can be computed reliably from GPS data at the 1-mm rms level.

PWV FROM GPS, WVR, and SONDES
GPS · WVR · SONDES ◻

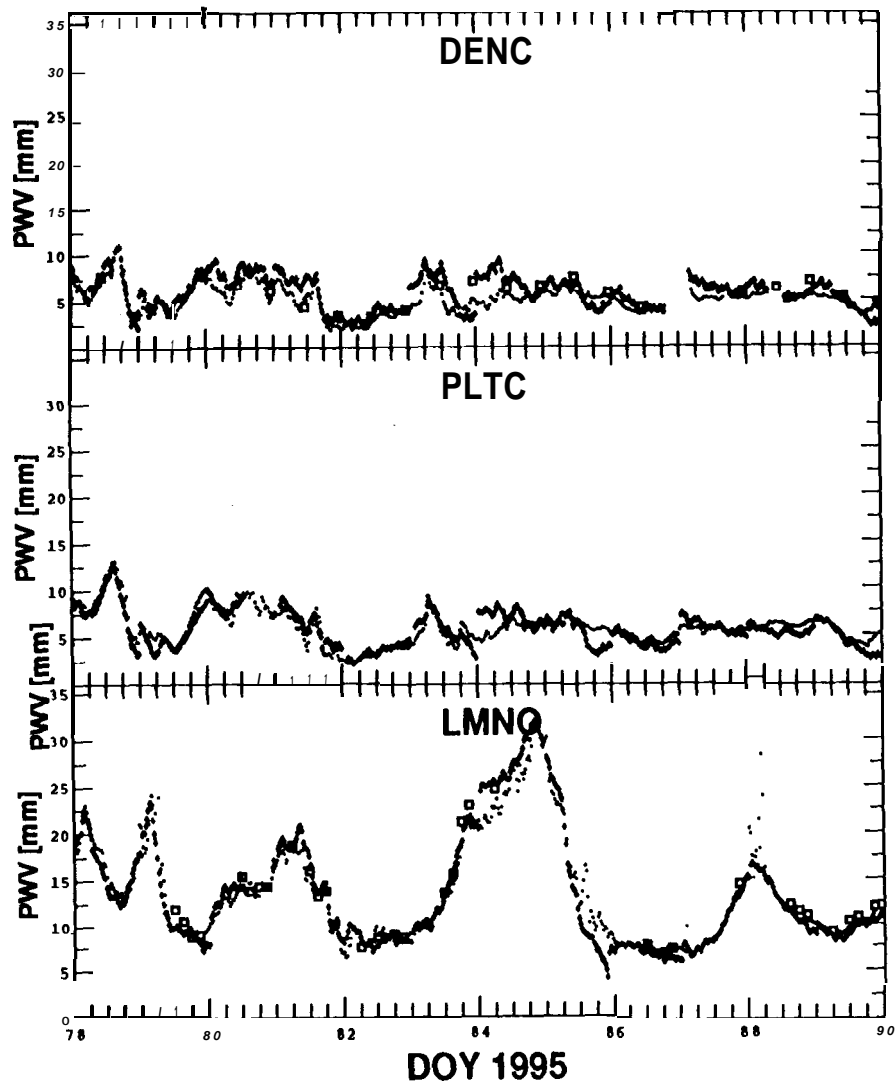


Figure 2 GPS-estimated values of precipitable atmospheric water vapor during March, 1995 for three NOAA/FSL windprofiler sites in the central United States (Denver, CO, Platteville, CO, and Lament, OK). GPS estimates are compared to Water Vapor Radiometers (WVR) and radiosonde data.

Atmospheric scientists have shown that GPS determined integrated water vapor from ground-based observations can significantly improve weather forecasting accuracies (Kuo *et al.*, 1992, 1995). Scientists have reported a worldwide increase in atmospheric water vapor between 1973-1985 (Figure 3, Gaffen *et al.*, 1991). That study was conducted with radiosonde data only, and similar studies in the future could greatly benefit from GPS PWV estimates, because of the inher-

ent homogeneity of the GPS data and their long-term stability.

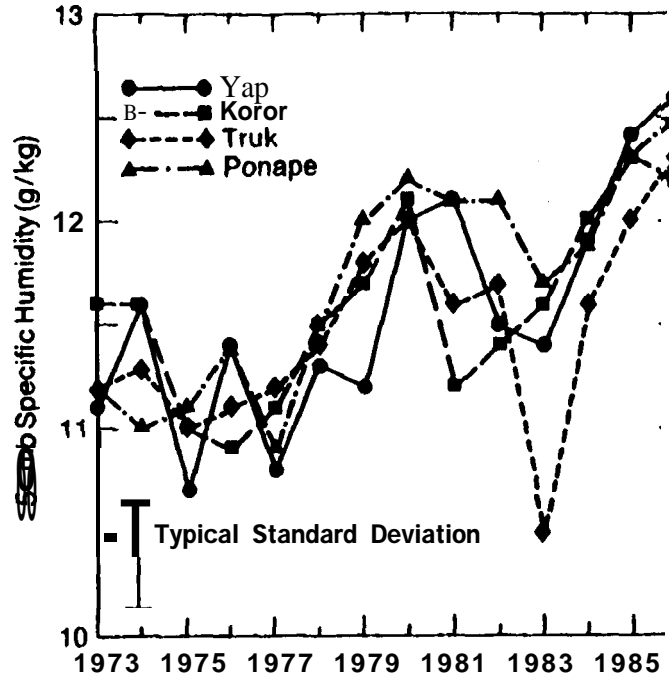
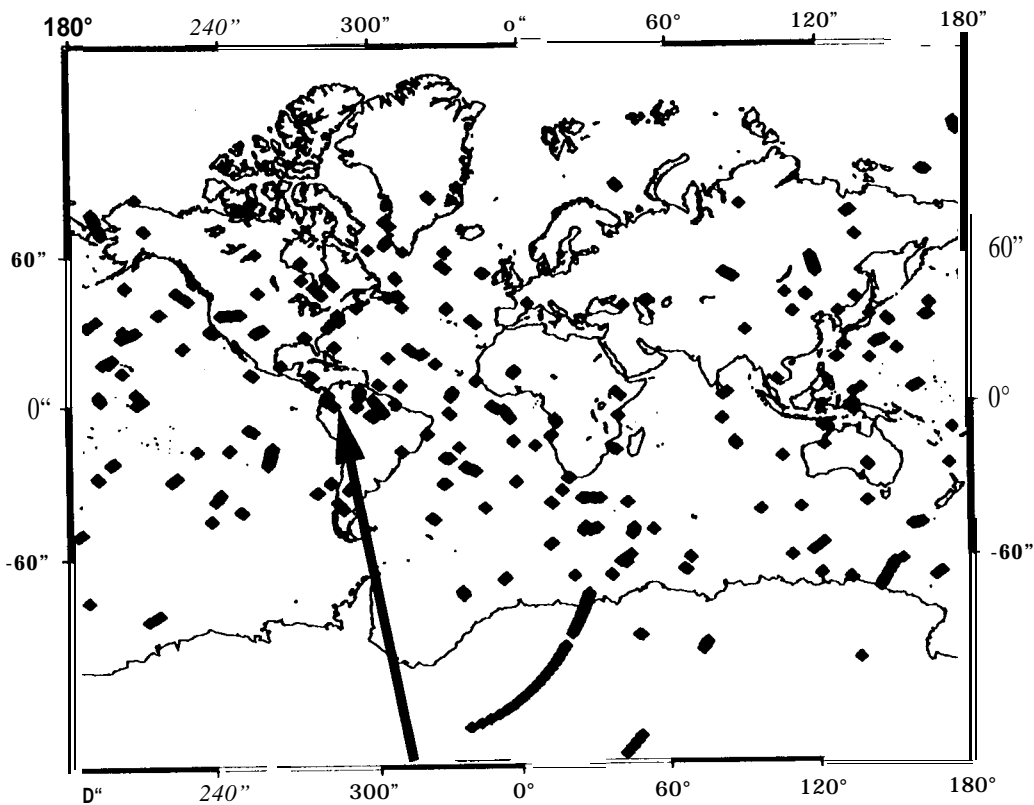


Figure 3 (from Gaffen *et al.*, 1991). The mean annual specific humidity (g kg^{-1}) at four tropical stations from 1973 to 1986 is shown. The error bar represents a typical value of the standard deviation for the monthly means used to calculate the annual values. Similar data for monitoring the global atmosphere could be collected from the IGS network in the future.

While data from ground based GPS stations typically provide integrated PWV, data from a GPS receiver in Low-Earth-Orbit (LEO) can be inverted to measure atmospheric profiles of refractivity, which in turn can provide tropospheric humidity profiles if temperature profiles are known. These space-based atmospheric measurements exploit the fact that a GPS signal that is traveling from a GPS satellite to a LEO is bent and retarded as it passes through the earth's atmosphere.

Yuan *et al.*, 1993. demonstrate that space based GPS measurements could provide a sensitive "thermometer" for global atmospheric change. The first such instrument for global atmospheric soundings was successfully launched on April 1995, by a team of GPS/MET scientists from the University Corporation for Atmospheric Research (UCAR/UNAVCO), the Jet Propulsion Labo-

ratory (JPL), and the University of Arizona (Figure 4).



**"Dry Air" GPSMET Inversion Comparing GPSMET
Temperatures to Radiosonde Temperatures**

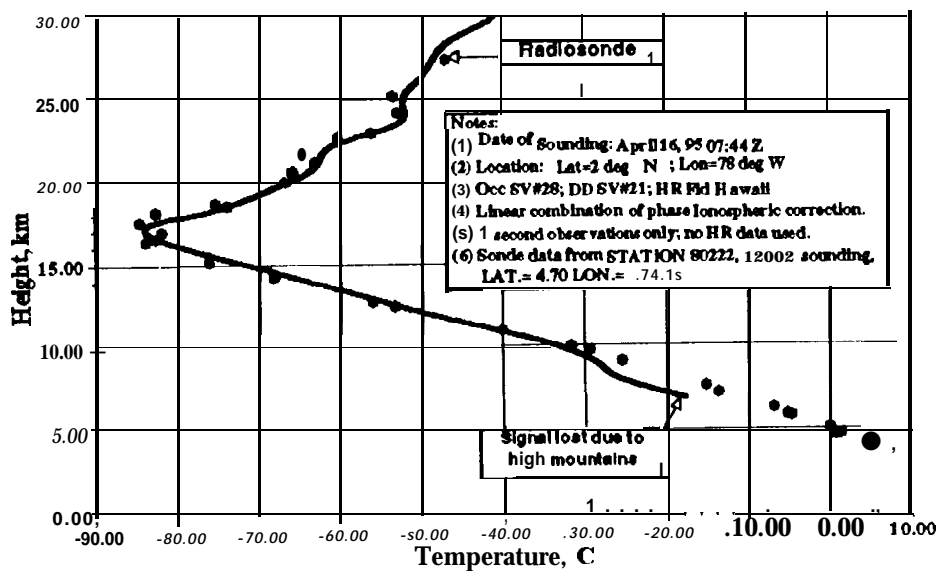


Figure 4 shows in the top panel the locations of radio occultation soundings during a 12-hour time period on April 16, 1995. The bottom panel compares the results of an initial inversion for a location above the Andes, as indicated by the arrow.

THE IGS AND ATMOSPHERIC SCIENCE

Ground-based and space based meteorological GPS applications already benefit from the services provided by the **IGS**. Ground based analysis often uses **IGS** orbits, and data from the **IGS** network are of critical importance for the analysis of **GPS/MET** LEO data.

In addition to these current services to the atmospheric community, the **IGS** can also directly provide time series of mm-level **precipitable** water vapor if the following were done:

- (a) **IGS** data sites would collect surface pressure, temperature, and humidity data.
- (b) These surface meteorological measurements were made available to the data and processing centers together with the GPS data.
- (c) The **IGS** processing centers would compute tropospheric zenith delay corrections at agreed upon time intervals.
- (d) The delay corrections from **all** processing centers should be converted to **precipitable** water vapor and combined into weekly time series of **precipitable** water vapor to be published by the **IGS**.

The **IGS** water vapor time series would become available several days to weeks after real-time and would be most useful for climate studies rather than weather prediction.

The **IGS** could contribute to weather forecasting if high-quality GPS satellite orbits were made available in real-time. These rapid orbits could be used for PWV estimation by regional GPS networks dedicated to weather prediction.

PWV ACCURACY CONSIDERATIONS

High accuracy GPS software estimates the total tropospheric delay in the zenith direction at regular time intervals. This delay is approximately 250 cm at sea level and has two components. Wet delay is caused by atmospheric water vapor, and dry or hydrostatic delay by all other atmospheric constituents. The hydrostatic delay of a zenith GPS signal traveling to an atmospheric depth of 1000 mb is approximately 230 cm. Assuming hydrostatic equilibrium, this delay can be predicted to better than 1 mm with surface pressure measurement accuracies of 0.5 mb. The error introduced by the assumption of hydrostatic equilibrium depends on winds and topology but is typically of the order of 0.01 %. This corresponds to 0.2 mm in zenith delay. Extreme conditions may cause an error of several mm (Elgered, 1993).

Wet GPS signal delay ranges from 0 to 40 cm in the zenith direction. Zenith wet delay (**ZWD**) is highly variable and cannot be accurately predicted from surface observations. PWV is the depth of water that **would** result if all atmospheric water vapor in a vertical column of air were condensed to liquid. One centimeter of PWV causes approximately 6.5 cm of GPS wet signal delay. This 6.5-fold “amplification” effect is important for accurate PWV measurement with GPS.

Tests during which we biased pressure measurements by known amounts showed that an error in pressure measurement can be related to the resulting error in estimated PWV as:

$$\delta PWV = 0.4X \delta Pressure \quad (1)$$

where δPWV is the error in PWV in units of mm and $\delta Pressure$ is the pressure error in mb. Thus to keep the contribution of the pressure error below 0.1 mm PWV a barometer should be calibrated to better than 0.25 mb.

Because GPS software estimates the delay due to the wet troposphere (ZD), this delay has to be converted to PWV. This conversion can be accomplished without incurring any significant additional errors using the equation (Bevis *et al.*, 1992):

$$PWV = \Pi \times ZD_{GPS} \quad (2)$$

The factor Π is approximately 0.15. This value varies with location, elevation and season by as much as 20%, but can be determined to ~2% if Π is computed as a function of surface temperature. Thus the requirement for the measurement of surface temperature at the GPS site. Temperature accuracy requirement is not very strict and -2 degrees K is sufficient.

Using the NCAR/Penn State mesoscale model, Kuo *et al.*, 1995, have shown that the combination of PWV and surface humidity data benefit numerical models significantly. 20% improvement in numerical weather forecasting accuracy was achieved when PWV time series were introduced. Almost as much additional improvement was achieved when the surface humidity was available. We therefore recommend that the IGS sites should collect 3 meteorological data types: pressure (P), temperature (T), and humidity (H). Accuracy requirement for relative humidity is ~2%. Estimates of the effect of the major error sources on PWV estimation are summarized in Table 1.

**Table 1: ERROR SUMMARY
FOR 30-MINUTE GPS/PWV ESTIMATION**

ERROR-SOURCE	SIZE OF ERROR [MM]		COMMENT
	δPWV	δZD	
ORBIT	0.2	1.3	10 CM ORBIT RMS, 1000-KM BASELINE
PHASE MULTIPATH	0.3	2.0	SITE AND ANTENNA DEPENDENT
COORDINATE ERRORS	0.5	3.0	1 -CM VERTICAL ERROR ASSUMED
BAROMETRIC PRESSURE	0.1	0.6	0.25 MB MEASUREMENT ACCURACY
“HYDROSTATIC ASSUMPTION”	0.0	0.2	CAUSED BY WIND+ TOPOLOGY
SURFACE TEMPERATURE ERROR	0.0	0.0	NO SIGNIFICANT EFFECT ON DRY DELAY
DELAY TO PWV CONVERSION	<0.1	-	2% ERROR IF SURFACE TEMP. KNOWN
REFERENCE WVR ERROR	0.9	6.0	INSTRUMENT + RETRIEVAL ERROR

The orbit error effect in Table 1 was estimated based on the assumption that GPS orbit errors of 10 cm cause baseline length errors of about 4 mm over distances of 1000 km. We assumed further that the vertical baseline coordinate error caused by orbit errors for the long baseline is also 4 mm. This vertical coordinate error corresponds to a zenith delay error of about 1.3 mm and thus to **an** error in PWV of 0.2 mm (**Rothacher**, 1992). These errors increase with increasing orbit error. The contribution of a 50-cm orbit error for a 1000 km baseline would be **1** mm PWV. For long baselines highest orbit accuracies are therefore required.

The effect of phase **multipath** was evaluated by computing the differential PWV between two sites separated by only a few meters. For such short baselines zenith delay and PWV are identical at both ends of the baseline and any differences in estimates of this delay are due to **multipath** (if identical GPS antennas are used).

Coordinate and barometric pressure errors were discussed above, and errors due to the hydrostatic assumption, temperature error and delay to water vapor conversion error are small.

One important error **listed** in Table 1 is the 6 mm delay (or 0,9 mm PWV) error due to a water vapor radiometer (Gary *et al.*, 1985, Westwater *e/ al.*, 1989). For small GPS networks of **significantly** less than 500 km aperture a water vapor radiometer (**WVR**) at one reference site in the network is required for levering. Levering is the process to correct for errors in the zenith delay that are common at all stations in the network, For larger networks, with baselines of ~ 1000 km levering is generally not required.

THE CLIMATE AND METEOROLOGICAL “CLAM” SENSOR PACKAGE

We have built a prototype “Climate and Meteorological Sensor Package” (CLAM) for suggested installation at **IGS** sites. The most important features of the CLAM are:

- (1) 0.2 mb accuracy, less than 0,02 mb/year drift (> 5-year calibration cycle)
- (2) 0.5 K temperature accuracy
- (3) 2% humidity accuracy - biannual simple inexpensive sensor chip change-out
- (4) 2 watts at 40-250 VAC, or 12 to 30 VDC
- (5) Writes surface meteorology data directly to the GPS receiver - uses the GPS receiver as data logger
- (6) Since data are in the GPS data file, data retrieval protocol from field sites to the data centers requires minimal or no changes
- (7) Price of each CLAM is about **US\$2.5 k** in parts (**US\$1.8K** for pressure sensor)

The most expensive component of the CLAM is the pressure sensor. However, we selected a very accurate sensor with low drift rate to avoid the requirement for **re-calibration** of the instrument.

The CLAM is controlled by a microprocessor, which is programmed to go through the following steps every 10 minutes (this time interval can be changed). First the time will be read from the GPS receiver, and then P, T, and H will be read from the sensors. With this information CLAM generates a 39-character string of Year: Month: Day: Hour: Minute: Second P [rob] T [K] H [%], such as the suggested example string: “#@&95 042618 :30:001013.1121.1 36”.

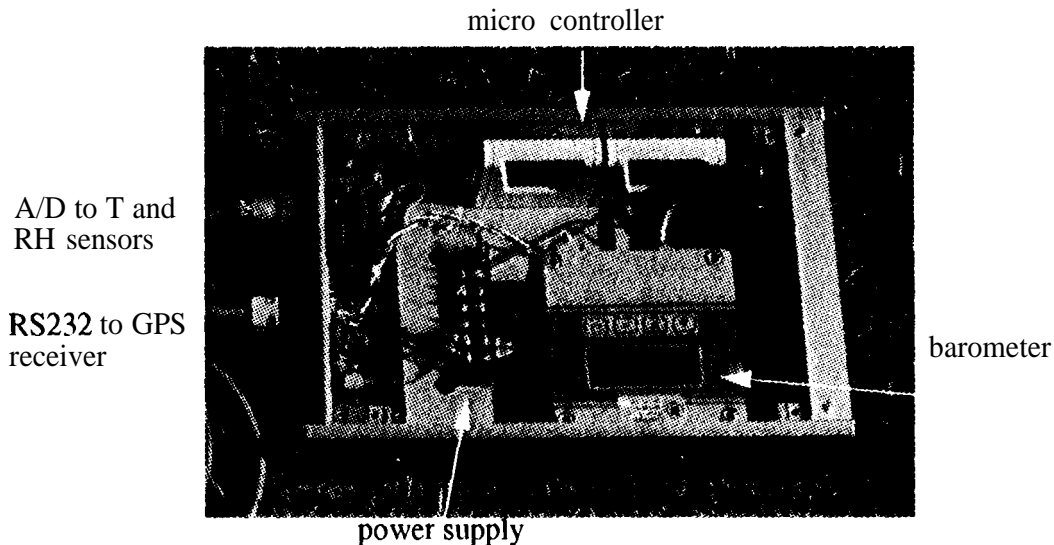


Photo of the prototype Climate and Meteorological Sensor package (CLAM) suggested for installation at IGS sites. Temperature and relative humidity sensors and pressure port inlet are at the end of a 10-meter cable for outdoor installation.

This string is written to the GPS receiver. When data from the receiver is downloaded this information appears currently in the RINEX observation files as comment lines. The special characters “#@&” at the beginning of the string are identifiers to allow simple extraction of these strings from the RINEX data files.

Thus the meteorological data will be downloaded and sent to the IGS data centers without any changes in current IGS procedures. Users interested in these meteorological data can strip this information from the GPS data file and write it to RINEX meteorological files.

The IGS community should decide at which point to separate meteorological and GPS observation data. This could be done during downloading, during translation of the observation data to RINEX or at a later stage.

The CLAM has so far been tested with the AOA TurboRogue receiver only. Microprocessor programs to operate the CLAM with other receivers can be written. The current setup should be considered a prototype. Ultimately the meteorological data, will be stored and time-tagged by the GPS receiver, and it should be written directly into RINEX meteorological data files during downloading.

ZENITH DELAY AND PWV COMPUTATION AT THE IGS PROCESSING CENTERS

We propose that the **IGS** analysis centers agree on specific times for which to compute GPS zenith correction values. The GPS community should seek input from atmospheric scientists to select a reasonable time interval.

Each analysis center could provide the total zenith delay used in its analysis every $N \cdot \Delta t$ hours starting at 00:00 UTC." N could be a different **integer** number for different processing centers, Δt is the shortest reasonable time interval between different zenith delay estimates,

It is important that all analysis centers provide estimates of total delay, and not incremental corrections computed by their software relative to an *a priori* delay based, for example, on default atmospheric parameters. Total tropospheric delay values determined at the processing centers and formal errors, should be included in **SINEX** solution files, currently under development.

The processing centers could use the surface meteorological data available from the IGS sites to separate dry and wet delay and to compute PWV.

Alternatively, a new type of associate data processing center could take on the task of correctly combining the delays computed at the various processing centers, applying the meteorological data and computing combined IGS time series of **precipitable** water vapor. These time series could be made available to the meteorological and atmospheric research communities at the same time as other **IGS** products become available.

SUMMARY AND CONCLUSION

Ground based and space based GPS applications to atmospheric monitoring are already strongly supported by the activities of the **IGS**. In addition time series of accurate PWV from the global **IGS** network could be produced by the **IGS** community with a small amount of additional effort. These PWV time **series** would be of great value for scientists involved in climate, weather, aviation, and hydrology research.

IGS analysis centers compute zenith **delay** corrections for GPS data analysis. If surface meteorological data were available from **IGS** sites these delay estimates could be converted to estimates of integrated atmospheric **precipitable** water vapor. An associate **IGS** processing center could be selected to combine the time series of delay, estimated by the various centers, to provide the combined **IGS** PWV time series.

We have developed a prototype meteorological sensor package CLAM with three major design priorities: (a) Ease of installation and integration with current **IGS** operations, (2) High accuracy and low pressure sensor drift, (3) Low cost. We propose to operate CLAM at a trial IGS site while preparing for the installation at a larger number of sites world-wide.

Acknowledgments We thank Russ Chadwick and others of the GPS team at NOAA/ERL for use of the data from their **windprofiler** network. Processing of the ground based PW data was supported by NOAA. Development of the CLAM was supported by the National Science Foundation.

REFERENCES

- Bevis M., S. Businger, T.A. Herring, C. Rocken, R.A. Anthes and R.H. Ware, 1992: GPS Meteorology: Remote Sensing of Atmospheric Water Vapor using the Global Positioning System, *J. Geophys. Res.*, 97,15,787-15,801.
- Duan, J., M. Bevis, P. Fang, Y. Bock, S.R. Chiswell, S. Businger, C. Rocken, F. Solheim, R.H. Ware, T. A. Herring and R. W. King, 1995: Remote sensing atmospheric water vapor using the Global Positioning System, in review,
- Elgered, G., 1993: Tropospheric radio-path delay from ground-based microwave-radiometry, in *Atmospheric Remote Sensing by Microwave Radiometry*, Wiley, ISBN 0-471-62891-3,215-258.
- Gaffen, D.J., T. P. Barnett, and W. P. Elliott, 1991: Space and time scales of global tropospheric moisture, *Journal of Climate*, Vol .4, No. 10.
- Gary. B. L., S.J. Keihm, and M.A. Janssen, 1985: Optimum Strategies and Performance for the Remote Sensing of Path-Delay using Ground-Based Microwave Radiometers, *IEEE Trans. Geosci. and Rem. Sens.*, GE-23, No. 4,479-484.
- Kuo, Y.-H., Y.-R. Guo, and E. R. Westwater, 1993: Assimilation of Precipitable Water Measurements into Mesoscale Numerical Models, *Mon. Wea. Rev.*, 121, 1215-1238.
- Kuo, Y.-H., X. Zou and Y.-R. Guo, Variational Assimilation of precipitable water using a nonhydrostatic Mesoscale Adjoint Model Part 1: Moisture Retrieval Sensitivity Experiments: 1995, submitted to *Mon. Wea. Rev.*
- Rocken, C. R. H. Ware, T. Van Hove, F. Solheim, C. Alber, J. Johnson, M. Bevis, S. Businger, 1993: Sensing Atmospheric Water Vapor with the Global Positioning System, *Geophys. Res. Letters*, Vol. 20, No. 23, pp 2631-2634, Dec.
- Rocken, C. T. Van Hove, J. Johnson, F. Solheim, R. H. Ware, M. Bevis, S. Businger, S. Chiswell: 1994, GPS/STORM - GPS Sensing of Atmospheric Water Vapor for Meteorology, *Journal of Atmos. and Ocean. Tech.*, accepted for publication.
- Rothacher, 1992: M., Orbits of Satellite Systems in Space Geodesy, *Geodaetisch-geophysikalische Arbeiten in der Schweiz*, Vol. 46, Ph.D. Thesis, Published by the Schweizerischen Geodaetischen Commission, ETH Zuerich, Switzerland, 243 pages.
- Westwater, E. R., M. J. Falls, and I.A. Popo Fotino, 1989: Ground-Based Microwave Radiometric Observations of Precipitable Water Vapor: A Comparison with Ground Truth from Two Radiosonde Observing Systems, *J. Atmos. Ocean Technol.*, 6, pp 724-730.
- Yuan L., R. A. Anthes, R.H. Ware, C. Rocken, W. D. Bonner: 1993, M. G. Bevis and S. Businger, Sensing Climate Change Using the Global Positioning System, *Journal of Geophys. Res.*, Vol. 98, No. D8, pp 14,925-14,937.

A Review of the NOAA Geosciences Lab's Automated Water Vapor Project

M. S. Schenewerk, G. L. Mader,
NOAA, SSMC4, 1305 East-West Highway
Silver Spring, MD 20910
301-7 13-2854; e-mail: mark @tony.grdl.noaa.gov

T. M. vanDam,
NOAA, CIRES/University of Colorado
Boulder CO 80309
303-492-5670; e-mail: tonic @roberson.colorado.edu

W. E. Carter
NOAA, SSMC4, 1305 East-West Highway
Silver Spring, MD 20910
301-7 13-2844; e-mail: bcarter@geo.grdl.noaa.gov

ABSTRACT

NOAA's Geosciences Laboratory (GL) has operated GPS tracking stations at NOAA's Test Facility in Sterling, VA and NASA's Wallops Flight Facility on Wallops Island, VA since July, 1994. These facilities were selected because they are radiosonde launch sites which provide independently determined water vapor measurements for evaluation of the GPS derived estimates. These sites serve as a test-bed for equipment and processing techniques whose purpose is reliable, automated, and timely **precipitable** water vapor measurements from GPS. This project has successfully provided reliable estimates of **precipitable water vapor with high time resolution. In addition, GL is collaborating with** NOAA's Forecast Systems Lab which operates seven GPS sites in the mid-west U.S. dedicated to monitoring atmospheric water vapor. Together, these sites provide a unique data set suitable for weather and climate studies.

This presentation will provide an overview of the GL water vapor project. The Wallops and Sterling sites, equipment, data, and accessibility will be described along with an evaluation of the quality and reliability of these data. The water vapor measurements will be shown and comparisons made to radiosonde observations. The plans for a 1995 intensive campaign will also be described.

INTRODUCTION

GPS tropospheric path length corrections are nuisance parameters for geodetic measurements but a potential product for weather and climate studies. GPS tropo delays can be incorporated as data into atmospheric models or converted into estimates of integrated precipitable water vapor (PWV) over individual sites. The high time resolution of GPS compliments the satellite imagery and radiosonde data. Therefore, if this GPS product can be made available with sufficient speed and reliability, it becomes useful in weather forecasting, particularly in forecasting the dynamic changes of severe weather. The anticipated growth in the number of GPS tracking sites will result in continuous measurements over entire continents. Many of these GPS sites could be made compatible for tropospheric monitoring at a relatively small expense and the necessary observations routinely generated as part of network quality control or routine orbit production.

NOAA's Geosciences Laboratory (GL) began a multi-year project in July 1994 to measure PWV using GPS at two sites. Since then, collaboration with NOAA's Forecast Systems Laboratory (FSL), which independently had begun a similar project, has extended the effort to include a subset of the Wind Profiler Demonstration Network (WPDN). Figure 1 shows the locations of these sites. A key to the site ID's is given in Table 1. The focus of the GL involvement is the development of automated data retrieval and processing tools which can produce reliable estimates in a timely manner. In particular, the generation of PWV measurements as by-products of other routine processing is being evaluated. The GPS measurements are being examined for accuracy under a variety of weather, diurnal signals, and seasonal differences. In addition, the effects of tropo modeling on vertical repeatability of GPS baseline estimates are being explored.

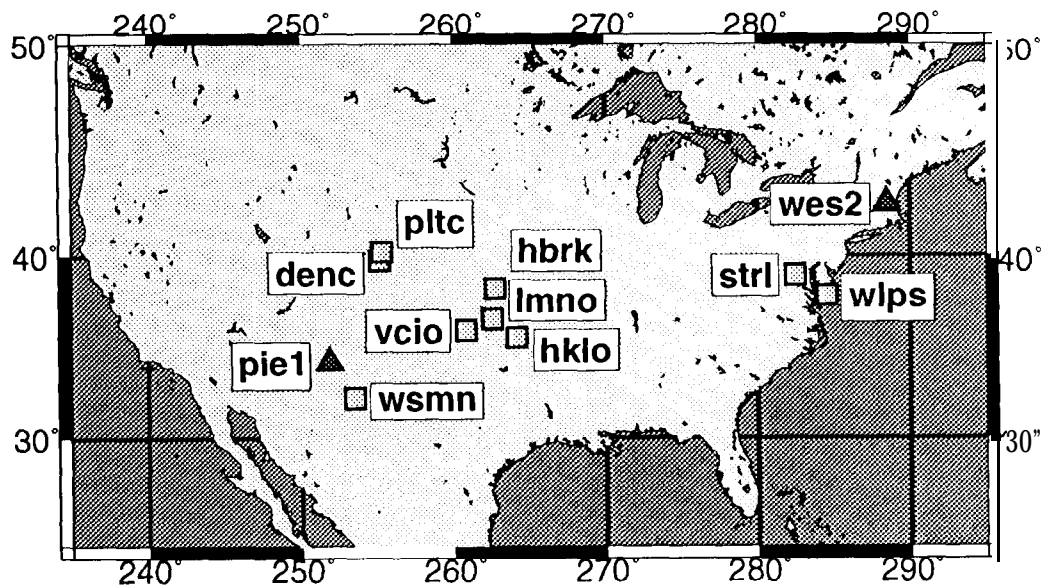


Figure 1: Sites used in this study

Table 1: Site names, ID's and receiver types

Denver, CO	dent	Trimble SSE
Haskell, OK	hklo	Trimble SSE
Hillsboro, KS	hbrk	Trimble SSE
Lament, OK	lmno	Trimble SSE
Pietown, NM	piel	Rogue 8000
Platteville, CO	pltc	Trimble SSE
Sterling, VA	strl	Rogue 8000
Vici, OK	vcio	Trimble SSE
Wallops Island, VA	wlps	Rogue 8000
Westford, MA	wes2	Rogue 8000
Whitesands, NM	wsmn	Trimble SSE

This presentation will provide a review of GL activities related to monitoring PWV. The sites, equipment and data accessibility will be described. An evaluation of the quality and reliability of these data will be given. The PWV measurements will be shown and, where possible, comparisons made to radiosonde observations. Finally, the continuing development and expansion of this project will be discussed.

SITES AND EQUIPMENT

The GL supports GPS tracking sites at the NASA Wallops Flight Facility, Wallops Island, VA and at the NOAA Test Facility, Sterling, VA. These near-sea level, mid-Atlantic sites provide wide variations in atmospheric water vapor. Collocated at weather balloon launch facilities, twice daily radiosonde measurements are available for evaluation of the GPS results. The close proximity to GL at the NOAA campus in Silver Spring, MD makes these sites a convenient test-bed for equipment. One TurboRogue GPS receiver with Dome Margolin T antenna and one Parasonics barometer were installed at each site. Each site also has a UPS, PC, modem and phone line enabling remote operation and minimizing down time. The GPS and local pressure data are automatically transferred to the GL daily. These data are available from the GL Data Center by anonymous ftp from `grac ie. grdl.noaa. gov`. Westford, designated with a triangle in Figure 1 is used as a reference for processing data from Sterling and Wallops Island.

The WPDN sites are located in the mid-west U.S. and will sample some of the most dynamic weather systems in North America. Built to monitor upper air wind fields, a subset of the WPDN sites are equipped with Trimble SSE receivers and Trimble GEODETIC L1/L2 (SST) antennas. Surface temperature, pressure, and humidity data in RINEX format as well as GPS data are available from these sites. These data are continuously downloaded to the FSL facilities in Boulder, CO. Currently, these GPS and met files are transferred daily to the CORS data distribution system. From CORS, the

data are available by anonymous ftp from proton. ngs. noaa. gov. Pietown, shown as a triangle in Figure 1, is used as a reference for processing the WPDN data.

PROCESSING

The procedure described is automatically initiated after midnight. The last day processed is identified and the data distribution computer is queried for the NOAA precise ephemeris for the next day. The assumption is that if the precise ephemeris is found, sufficient time has elapsed for all available data to be retrieved. Next, the RINEX files from the designated PWV sites are retrieved. The number of available sites are checked and, if sufficient (at least one baseline can be formed), the processing commences. If insufficient sites are found, an error message is electronically mailed (emailed) to one of the authors (MSS).

Coordinates of the GPS Monitoring Sites

The initial stage of the processing is to estimate site coordinates, the results of which are used for data quality assessment. If minor difficulties are detected such as marginally high or low post-fit RMS or number of observations, a warning message is emailed, but processing continues. If major difficulties are found, an error message is emailed and processing stops. Terminal conditions include no solution, very high RMS or very low number of observations.

The site coordinate estimates use 28 hours of data; 4 hours from the previous day plus 24 hours of the current day. The observable is double-differenced, ionosphere-free phase. The data interval is 30 seconds with a 15° observation elevation cutoff. The data are organized by baseline and automatically edited. The original RINEX files are then **removed leaving the clean data**. The *page3* program (Schenewerk, et al., 1994) is used for the baseline solutions. As implied above, the NOAA precise ephemeris is used with no additional orbit adjustment. The reference site coordinates are held fixed. The phase biases, monitoring site coordinates, and 4 hour piece-wise continuous, linear tropo scaling factors for all sites are estimated. If processing is deemed successful, the output from this solution is saved for use in future, more comprehensive determinations of site coordinates.

Integrated Precipitable Water Vapor Estimates

The second stage of the automated processing generates the PWV estimates. The edited data files created during the first stage are reused. Again, 28 hours of double-differenced, ionosphere-free phase data are processed; 4 hours from the previous day plus 24 hours of the current day. The data interval is 30 seconds with a 15° observation elevation cutoff. The NOAA precise ephemeris is used with no additional orbit adjustment. A specialized variant of the *page3* program is used for this solution. This variant uses the NMF dry and wet mapping functions (Neil, 1993) with the Saastemoinen dry and wet zenith delay models (Saastemoinen, 1972). All site coordinates are held fixed. These coordinates are

generated from a weighted mean of the daily estimates and are updated periodically. Phase biases are estimated. 15 minute piece-wise continuous, linear tropo scaling factors are estimated at the reference sites. At the PWV monitoring sites, the local barometric pressure measurements are used to model and remove the hydrostatic component of the troposphere. 15 minute piece-wise continuous, linear estimates of the “wet” zenith path length delays are, generated for the PWV monitoring sites and stored. In a separate file, the first and last 2 hours from these daily estimates are removed to minimize “edge” effects, converted to PWV using a standard value of 6.5 (Bevis et al., 1992), and concatenated to an existing file forming a continuous series.

The automated procedure then cleans-up and stores the files created in the processing. In principle, all files except the position, PWV, and processing log could be removed thereby reducing the final storage requirements to a few kilobytes per day. This procedure is currently in testing, and the files required to reprocess the data are kept.

INTEGRATED **PRECIPITABLE** WATER VAPOR TIME SERIES

Figure 2 shows the PWV time series for the Sterling and Wallops Island monitoring sites. The PWV estimates from the co-located balloon data are shown for comparison using diamonds connected by a thick line. No attempt to vertically align the data sets has been made. Blow-ups of small portions of each series are also shown. The agreement evident in the blow-ups is typical of these series. The GPS receivers at these sites were obligated to another project between March 11 and April 4, 1995 causing a break in the series during this period. Two points not readily evident are worth making. First, GPS gave slightly lower PWV values, 1 -3 mm, than radiosondes for the first three months of this comparison. This probably reflects the weak temperature dependence of the value for converting between path length and PWV. Both the magnitude and sign of the difference agrees with the functional form for that conversion value given by Bevis et al. (1992). Second, the only weather related vulnerability so far identified (ignoring the physical destruction of equipment by lightning strikes etc.) is snow and ice cover on the GPS antennas. Figure 3 shows the complete GPS series for the period February 19 through March 5, 1995. One of the few snow storms of the winter moved through the northeast U.S. on February 28 and March 1. Evidence indicates that the antenna at Westford became snow covered for the duration of this storm. The overall RMS of fit and number of observations during period were within normal limits but the position estimates for Sterling and Wallops Island and PWV estimates are in error by centimeters. Without the cross-check of the position estimates, the erroneous PWV estimates would have been unknowingly included in the series.

The Denver, Lament and Plattville WPDN sites have only been available through the CORS data center since January 23, 1995; Haskell, Hillsboro, and Vici since April 21; and Whitesands since May 4. The reliability of these sites is expected to be excellent. Figures 4, 5, and 6 show the PWV series for all sites for 1995. Radiosonde data, diamonds connected by a thick line, are shown for comparison where possible. Denver

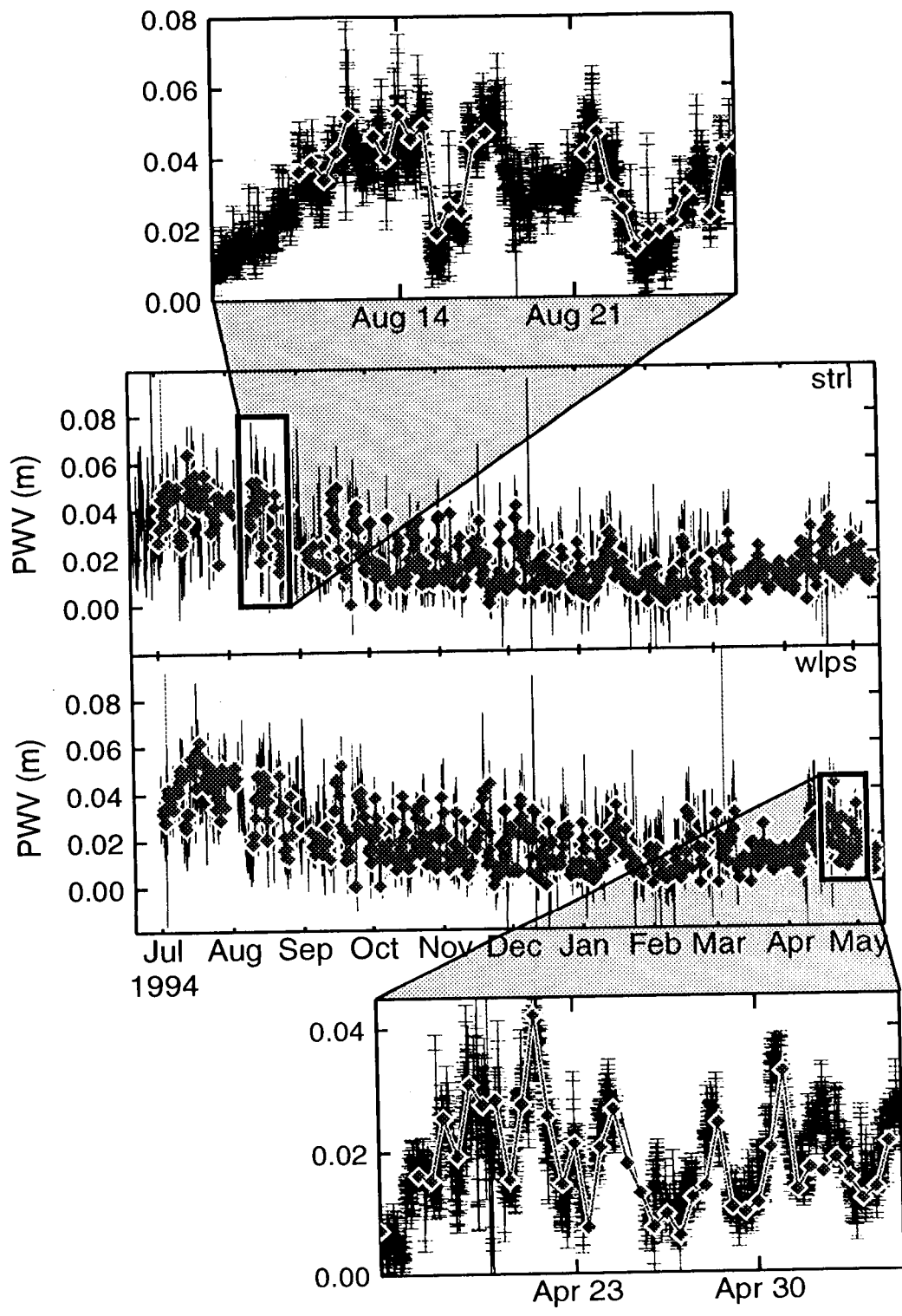


Figure 2: PWV time series for Sterling and Wallops Island

has nearby radiosonde data; however, Lament is shown with radiosonde data from Norman, OK, approximately 150 km to the south. Detailed conclusions for Lament should be guarded.

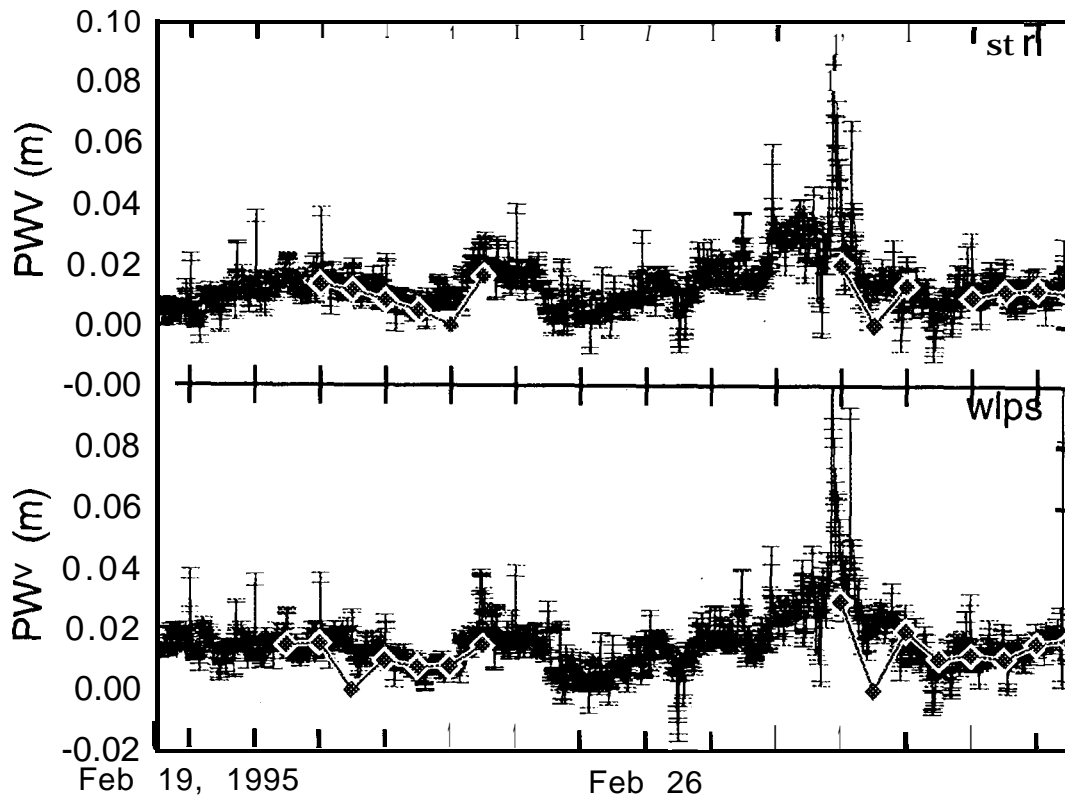


Figure 3: Effects of snow cover on Westford GPS antenna

FUTURE PLANS

The GL intends to participate in this project with site support, data redistribution and software development for several years. The support for other NOAA projects and the potential value to geodetic research make GPS monitoring of PWV an excellent compliment to other research projects. Outfitting other NOAA continuously tracking sites with met sensors is being considered. Discussions with the U.S. Coast Guard on the feasibility of similarly equipping those sites have begun. The production of PWV or wet delay values as part of the routine quality check of the NOAA and U.S. Coast Guard sites will be evaluated this summer. A one to two month intensive campaign is being planned between GL and FSL. Six or more additional WPDN sites will be equipped with GPS receivers during this period and near-real time processing tested.

REFERENCES

- Bevis, M., Businger, S., Herring, T. A., Rocken, C., Anthes, R. A., and Ware, R. H., GPS Meteorology: Remote Sensing of Atmospheric Water Vapor Using the Global Positioning System, *JGR*, 1992, pp. 15787-15801.
- Neil, A. E., New Approach for the Hydrostatic Mapping Function, in *Proc. Intern. Workshop for Reference Frame Establishment and Technical Development in Space Geodesy*, Communications Research Laboratory, Tokyo, pp. 61-68.
- Saastamoinen, J., Atmospheric Correction for the Troposphere and Stratosphere in Radio Ranging of Satellites, *Geophysical Monograph 15*, ed. Henriksen, pp. 247-251.
- Schenewerk, M., Kass, W., Mader, G., and Spofford, P., *IGS Analysis Center Questionnaire*, 1994.

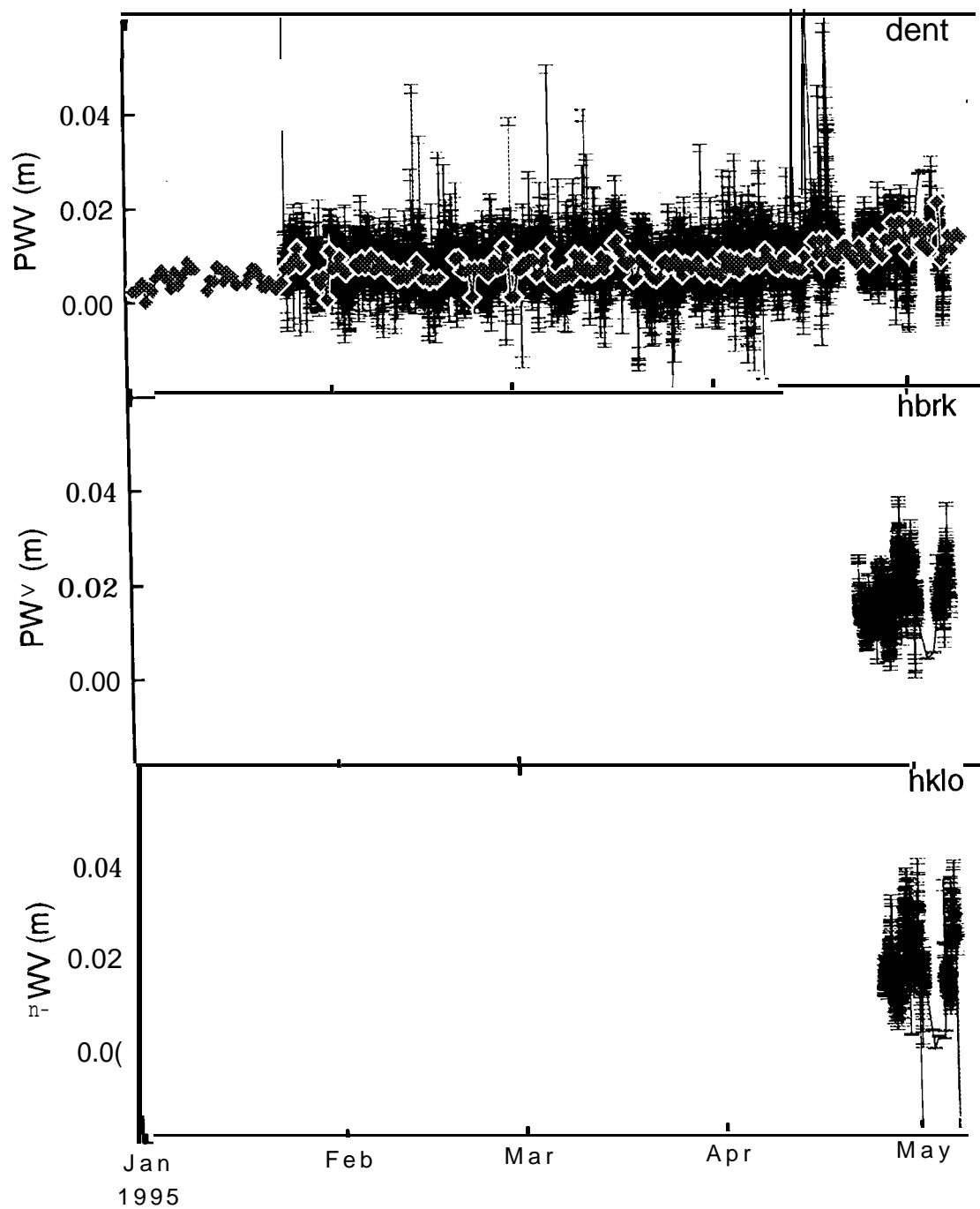


Figure 4: 1995 PWV time series for Denver, Hillsboro, and Haskell

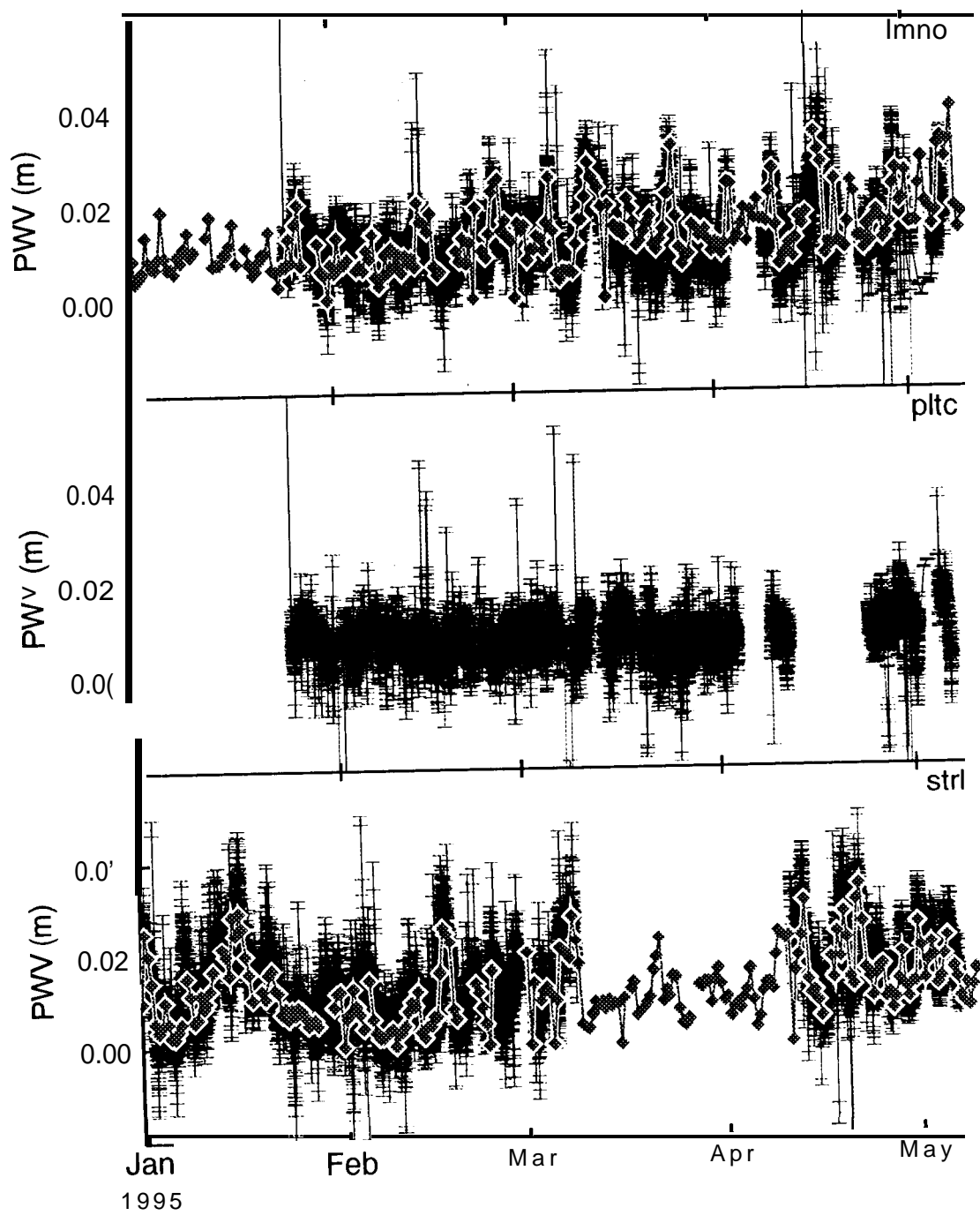


Figure 5: 1995 PWV time series for Lament, Plattville, and Sterling

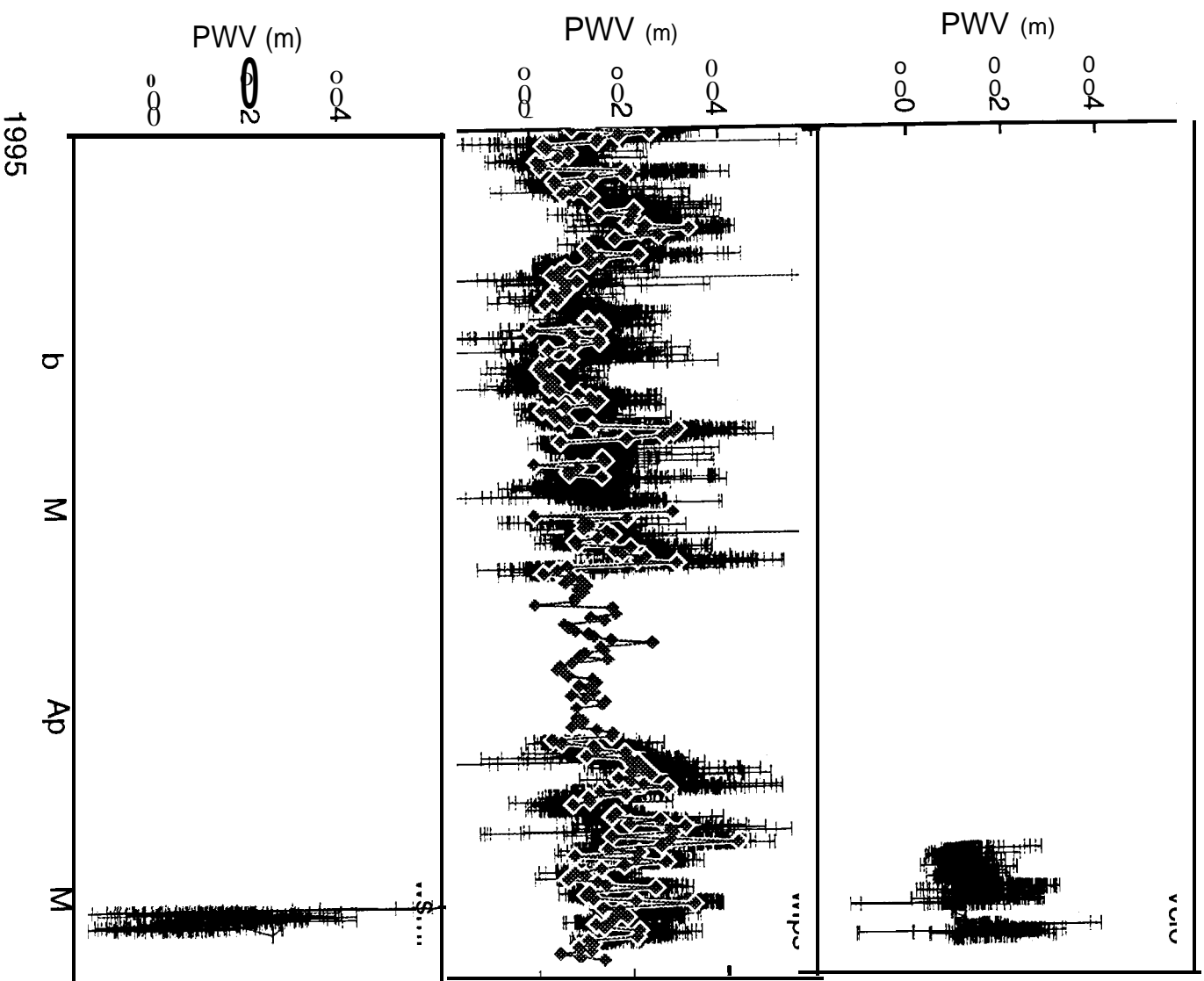


Figure 6: 1995 PWV time series for Vici, Wallops Island, and Whitesands

CONSISTENCY IN THE TROPOSPHERE ESTIMATIONS USING THE IGS NETWORK

Gerd Gendt¹ and Gerhard Beutler²

¹GeoForschungsZentrum Potsdam, Aufgabenbereich 1,
Telegrafenberg A17, D-14473 Potsdam, Germany

²Astronomical Institute, University of Berne,
Sidlerstrasse 5, CH-3012 Berne, Switzerland

ABSTRACT

Seven IGS Processing Centers are routinely determining the orbits, earth orientation and rotation parameters (**ERPs**), and the coordinates of the **IGS** tracking stations. In order to produce these parameters of geodetic and geodynamic interest tropospheric refraction has to be modeled by all processing centers. Different methods are used by different centers (estimation of site- and time-specific troposphere parameters, stochastic troposphere estimation). In addition different minimum elevation angles, different mapping functions, different weighting schemes for the observations (zenith distance dependent or independent weighting), different observations (phase and code, or phase only), different combinations of observations (zero difference or double difference), and last but not least different sets of stations are used by different analysis centers.

So far, the troposphere parameters were considered as 'nuisance parameters within the **IGS**. In view of the growing interest of meteorologists in the wet component of the troposphere and in view of the **inhomogeneous** modeling/processing situation it seems advisable to study the consistency of troposphere estimates as produced by different **IGS** analysis centers.

Forced by the limited amount of time and resources, we decided to look only into the tropospheric zenith delay estimates of **CODE** and **GFZ**, and to focus on **GPS** weeks 781, 782, and 783. We found that the biases between **GFZ** and **CODE** estimates for individual stations are in general below 1 cm; the associated rms errors are of the same order of magnitude. Biases and rms error are even smaller (about 1-3 mm for the biases, about 5 mm for the rms error) for differences of tropospheric zenith delays associated with sites in the same continent (estimates relative to a reference site). We conclude that a systematic comparison of tropospheric zenith delay estimates, which eventually might lead to a combined **IGS** troposphere for the **IGS** tracking stations, should be considered within the **IGS**.

INTRODUCTION

Water vapor is a crucial parameter in atmospheric modeling. Continuous and well distributed measurements of water vapor is of fundamental interest for the weather forecast and climatology. With radiosondes relative humidity can be measured with an accuracy of -3.5%. The vertical resolution is good, but the **spatial** and temporal (twice a day) coverage is rather sparse. The cost of this technique restricts the number of launches (Bevis, et al.,1992). GPS networks are capable of providing a rather dense and nearly continuously measured water vapor data. Even if this is only the integrated water vapor (no vertical resolution) this will be an important information. The accuracy should be -5%. Ground-based systems like GPS can provide a good temporal coverage, The number of permanently operating GPS receivers has steadily increased so that in many regions (North America, Europe, Japan, Australia) a rather good spatial distribution already now exists and in the next years a further **dramatical** improvement (DGPS, navigational networks) may be expected. Other ground-based systems with the capability of continuous monitoring like Water Vapor Radiometer (WVR) and Very Long Baseline Interferometric (VLBI) are too expensive for a wide-scale use. They could, be used to calibrate the GPS derived results. Space-borne systems like NIMBUS (space-borne WVR) or GPSMET (occultations of low orbiting satellite) do not have good temporal coverage, but a good spatial and vertical resolution, respectively.

Radio techniques like GPS and VLBI are sensitive to water vapor in the atmosphere. Knowing the mapping function (i.e. dependency of path delay from elevation) and assuming azimuthal symmetry of the atmosphere around the site and assuming that the wet component changes little over short periods of time simultaneous measurements in different elevations can be used to determine the zenith path delay (ZPD). The ZPD is the sum of the hydrostatic and wet components. Using the surface pressure it is possible to remove the hydrostatic zenith delay, which may reach values up to about 2.3 m, with an accuracy of a few millimeters or better. So we may assume to compute from the ZPD the zenith wet path delay (ZWD) without introducing any additional error. Furthermore the error in the mapping function for elevations above 20° is not a significant part of the error budget for the ZWD.

The parameter of interest for the meteorologist is not the ZWD but the vertically integrated water vapor in terms of **precipitable water (PW)**, the length of an equivalent column of liquid water. With the knowledge of the surface temperature only, this transformation from ZWD to PW may be done with an accuracy of 2%, using a 3-dimensional temperature model even with 1% (Bevis et al., 1994). Having all this in mind we conclude that it is sufficient to look at the error in the ZPD determination, the directly estimated parameter of the adjustment, to get insight into the accuracy of the water vapor determination using the GPS.

The daily variability of the wet delay usually exceeds that of the hydrostatic delay by an order of magnitude, and reaches values of up to 5 cm PW, typically not bigger than 1 to 2 cm. The PW cannot be accurately predicted from surface measurements. An accuracy of 5% corresponds to an error of 1-2 mm for PW which is equivalent to 5 -15 mm in ZWD (rule of thumb transformation factor -6.4), and as explained above in ZPD too.

From previous experiments, e.g. the CONT 94, we have some estimations of the accuracy which can be reached with the GPS technique (Freedman et al., 1994; MacMillan et al., 1994). In the CONT 94 experiment simultaneous measurements of GPS, VLBI and WVR were performed. The ZPD differences between GPS and VLBI had a bias in the range of 3-8 mm and the rms scattering was 5-10 mm, but discrepancies of a few cm on some sites for some days have also been observed. Differences between GPS and water vapor radiometer (**WVR**) were in the range of 1 cm, but also here we saw over hours discrepancies of some cm.

In this paper an attempt is made to assess the accuracy that could be obtained using the IGS network. For this purpose the ZPD results of two **IGS** Analysis Centers (AC), CODE and GFZ, will be compared.

DATA AND SOFTWARE

Both, the CODE and the GFZ processing centers (reprocessed the same data as in their respective **IGS** routine analyses. The data used are given in Table 1 (extracted from the weekly summary files distributed through the IGSREPORT series). At that time the total number of stations analysed by the CODE and GFZ processing centers were 49 and 40, respectively. But, as one may see from Table 1, not **all** were available (in time) for the processing. Marked station were fixed (constrained on sub-millimeter level) for the processing.

The CODE processing center uses the Bernese GPS Software Version 3.6 to analyse the **IGS** network (Rothacher et al., 1994). It is based on the double difference approach. Several models for the tropospheric zenith delay may be selected by the user. For the present analysis (and for all the **IGS** processing performed so far by CODE) the **Saastamoinen** model (including the corresponding mapping function) was used as an a priori model. The surface met data temperature T , pressure p , and humidity h needed by the **Saastamoinen** model were not taken from actual met measurements, but from a height dependent model based on sea-level values for p , T , and h (Gurtner et al, 1989). Because the mapping function is identical for the dry and the wet component of the tropospheric delay one may solve for one or more ZPD for each station and add them to the a priori value for the particular station. The total delay (a priori plus estimate) may easily be compared with the corresponding quantity stemming from another processing center. The software allows it to select the number of troposphere parameters for each station. It is also possible to constrain the estimates of the troposphere parameters (in an absolute sense for each parameter, and differentially between consecutive parameters). At present the CODE one-day solutions (not made available to the scientific community) are all based on **2h-sampling** intervals for the ZPD. No constraints are imposed, The three-day solutions are formed using the normal equation systems pertaining to three consecutive days (Beutler et al, 1995). In this process the three one-day-arcs are combined into one three-day-arc, and the number of troposphere parameters per station is reduced from 12 to 4 per day

Table 1. Subset of IGS Network used by CODE and GFZ processing centers in GPS weeks 781, 782, 783. (c g X: used by CODE, GFZ or both; -: data not available). Sites fixed are marked with **c,g,X** in the header.

	GRAZ	MADR ^x	METS	TROM ^x	DRAO	KOKB ^x	RCM5 ^o	YELL ^x	TIDB ^x	PAMA	USUD	JOZE
	HERS	MAS1 ^o	NYAL	WETB ^x	FAIR ^x	PIET	STJO	KOUR	HOB2	YAR1 ^x	ZIMM	FORT
	KOSG ^x	MATE ^o	ONSA	ALGO ^x	GOLD ^x	QUIN	WES2	SANT ^x	MCMU	TAIW ^o	HART ^x	BRMU
	BRUS	MDO1	TSKB	AREQ	BORO	DAV1	SEIS	KIT3	CAS1	POTS	BOGT	KERG
	LAMA	MAC1	NLIB	JPLM								

359	ccXcc	XXXXg	XcXXg	xxx-g	Xxc	XcXX	XXX-	Xxx-	Xxxx	Cxxx	xc--	Cxxx
360	-cXcc	Xxxxg	XcXXg	xxx-g	XXXc	XcXX	XXX-	Xxxx	Xxxx	Cxxx	Xc--	cXXX
361	ccXcc	XXXXg	XcXXg	XXXXg	XXX-	XcXX	xxx-	Xxxx	Xxxx	Cxxx	Xc--	Cxxx
362	ccXc-	XXXXg	XcXXg	XXXX9	XXX-	XcXX	xxx-	Xxxx	Xxxx	-xxx	Xc--	cxx-
363	-cXc-	Xxxxg	XcXXg	Xxxxg	XXX-	XcXX	XXX-	Xxxx	x-xx	-xxx	xc-x	cxx-
364	ccXcc	XXXXg	XcXXg	Xxxxg	Xxc	XcXX	xxx-	Xxxx	x-xx	cXX-	XC-X	C-X-
365	ccXc-	XXXX-	XcXXg	Xxxxg	XXX-	XcXX	XXX-	Xxx-	x-xx	cXX-	xc-x	cXX-
1	ccXcc	X-XX-	XcXXg	Xxxxg	XXX-	XcXX	XXX-	XXX-	X-xx	xxx-	xc-x	cxx-
2	c-Xcc	X-XX-	XcXXg	Xxxxg	Xxc	XcXX	xxx-	xxx-	x-xx	xxx-	xc-x	Cxxx
3	c-xc-	X-XX-	XcXXg	XXXXg	Xxc	XcXX	XXX-	Xxx-	x-xx	xxx-	xc-x	Cxxx
4	c-Xcc	XXXX-	XcXXg	Xxxxg	XXX-	XcXX	XXX-	XXX-	X-xx	xxx-	xc-x	Cxxx
5	c-Xcc	XXXX-	XcXXg	Xxxxg	XXX-	XcXX	xxx-	Xxxx	x-xx	Xxxx	xc-x	-xxx
6	ccXcc	XXXX-	XcXXg	XXXXg	XX-C	XcXX	XXX-	XXXC	X-XX	-XXX	Xc--	Cxxx
7	ccXcc	XXXX-	-cXXg	XXXXg	Xxc	XcXX	XXX-	Xxxx	x-xx	Xxxx	-c--	Cxxx
8	cc-cc	XXXX-	-cXXg	XXXXg	Xxc	XcXX	xxx-	Xxxx	x-xx	xx-x	Xc--	Cxxx
9	ccXcc	XXXX-	-cXXg	Xxxxg	Xxc	XcXX	xxx-	Xxxx	x-xx	Xxxx	xc-x	Cxxx
10	ccXcc	XXXX-	XcXXg	Xxxxg	XXX-	XcXX	xxx-	XXX-	Xxxx	Xxxx	xc-x	Cxxx
11	ccXcc	XXXX-	XcXXg	XcXXg	XXX-	XcXX	xxx-	xxx-	Xxxx	Xxxx	xc-x	Cxxx
12	ccXcc	XXXX-	XcXXg	Xxxxg	Xxc	XcXX	XXX-	Xxxx	Xxxx	x-xx	xc-x	Cxxx
13	cc-cc	XXX-	XccXg	XXXXg	Xxc	XcXX	XXX-	XX--	Xxxx	x-xx	Xc--	Cxxx
14	ccXcc	XXXX-	XccXg	XXXXg	Xxc	XcXX	XXX-	Xxxx	Xxxx	Xxxx	Xc--	Cxxx

(corresponding to a 6h-sampling interval) in the routine processing, For the present analysis the three-day-arcs were generated as in the CODE routine analysis with the exception that the 2h-sampling intervals were retained. This made it easy to compare the results to those of theGFZ. Some comparisons of the results obtained using the 2h- resp. the 6h-sampling intervals for the troposphere are presented in the next section. A minimum elevation angle of 20° was used to generate the CODE results.

The GFZ processing center uses theEPOS .P.V2 software developed at GFZ (Gendt et al.,1995). It is based on the analysis of undifferenced phase observations. The orbital arc length used is 32 hours, overlapping by 8hours from day to day. Forthe IGS analysis the Saastamoinen model was used too. Because no surface met data are available, standard pressure values were taken which correspond to the station height, the other values were T=290°K, h=60%. In the average the ZPD corrections were in the order of5 -10 cm and were added to the model values to give the total ZPD. No constraints are imposed to the tropospheric parameters. The software uses the Helmert-blocking method, where each parameter may be solved for selected time intervals. In the routine IGS analysis the ZPD for each station are solved-for in intervals of 4hours, for this study 2 hours were taken.

The principal difference between the CODE and GFZ procedures thus has to be seen in the zero- resp. double- difference approach and in the arc-length. It should also be mentioned that the network analysed by CODE and GFZ are not identical. Mapping functions, a priori troposphere models, and minimum elevation angles on the other hand are identical (with the exception of the definition of the a priori meteorological parameters).

The ZPD was estimated for 2h intervals, independently from interval to interval. This interval length was chosen, because it is on the one hand short enough to follow most water vapor fluctuations and on the other hand long enough to be used without random walk constraints. This makes the comparison easier, having not too many parameters which influence the results.

RESULTS

First of all it should be pointed out that no attempt is made to assess the absolute accuracy of water vapor determination achievable using the IGS network. Only the internal consistency of the ZPD-estimations derived from different ACS using different approaches is studied. A high consistency will be the prerequisite for a high quality water vapor determination, and may be an indicator for the accuracy which can be reached. Three types of results are presented in this section:

- (1) The impact of the sampling interval (2h resp. 6h) is studied using CODE results.
- (2) The consistency of troposphere parameters in the overlap interval of consecutive solutions produced by the GFZ are studied.
- (3) The ZPD estimates of CODE and GFZ (based on the 2h intervals) are compared.

We should point out already here that the comparisons of type (1) and (2) are side issues, that the consistency tests of type (3) are the key issue.

Let us first look into the impact of the length of the sampling interval using the CODE results. Figure 1 shows the 2h-estimates and the 6h-estimates for the station Wettzell (WETB). We see that the 6h-curve is a smoothed version of the 2h-curve; the 6h-estimates are essentially the (weighted) averages of the corresponding three 2h-estimates. This behaviour allows it to compare results from processing centers using different sampling intervals for the troposphere parameters. The behaviour in Figure 1 is representative for all other stations, too.

What is the optimum sampling interval for station-specific troposphere parameters ? (Continuous estimation using constrained random walk processes are not considered here.) The answer to this question may be different for different applications: if the troposphere parameters are of primary interest a high temporal resolution may be of interest, if the other parameters (orbits, ERPs, coordinates) are in the focus a high temporal resolution may not be required. In Table 2 we can see that the rms error a posteriori of one single difference phase observation (formally referred to the L1 frequency) is getting slightly better (about 10%) in the case of the 2h-troposphere sampling interval. Let us add that the improvement is marginal if the sampling interval is further reduced.

Based on Table 2 one has to conclude that the solution with the 2h-interval is slightly superior. If we are interested in the other parameters (ERPs, station coordinate, and orbits) the conclusion is not really clear. Let us include Table 3 as an example. It shows the transformation error per satellite coordinate of the middle days of our three-day-arcs of seven parameter similarity transformations between the combined IGS orbit, the CODE

Table 2. Rms of single difference observation (L1) a posterior for 2h- resp. 6h-troposphere sampling intervals

doy	rms	of	sd	doy	rms	of	sd	doy	rms	of	sd
1994	phase		obs	1995	phase		obs	1995	phase		obs
	2h		6h		2h		6h		2h		6h
359	3.2		3.4	1	3.0		3.3	8	3.2		3.5
360	3.1		3.4	2	3.0		3.2	9	3.2		3.4
361'	3.1		3.4	3	3.1		3.4	10	3.2		3.4
362	3.1		3.4	4	3.2		3.4	11	3.2		3.4
363	3.1		3.4	5	3.2		3.4	12	3.1		3.4
364	3.2		3.4	6	3.2		3.4	13	3.2		3.4
365	3.1		3.4	7	3.1		3.4	14	3.2		3.5

solutions based on the 6h- resp. 2h-sampling intervals for the troposphere. The last column in Table 3 shows that the differences are small indeed between the two CODE solutions. The two preceding columns are more difficult to interpret: The errors for the transformation IGS -> 6h-soln are slightly better than those for the transformation IGS -> 2h-soln. One has to take into account on the other hand that the 6h-soln was one of the contributors to the IGS combined solution! It is not possible to clearly conclude from Table 3 which would be the best sampling interval. Tables 2 and 3 together probably would favour the 2h-binning.

Similar analyses might be performed (and actually were performed using different data spans) for the coordinates and earth rotation parameters. Our conclusion is that the actual

Table 3. Rms of seven parameter Helmert transformations between the official IGS orbits, and the CODE solutions based on 6h- resp. 2h- sampling intervals for troposphere parameters

MJD	RMS per Satellite Coordinate Of 7-Parameter-Similarity Trafo of Daily Orbit Files		
	IGS -> 6h-soln	IGS -> 2h-soln	6h soln -> 2h-soln
49713.0	0.117 m	0.123 m	0.056 m
49714.0	0.111 m	0.119 m	0.054 m
49715.0	0.109 m	0.128 m	0.058 m
49716.0	0.127 m	0.128 m	0.069 m
49717.0	0.135 m	0.145 m	0.066 m
49712.0	0.097 m	0.109 m	0.064 m
49718.0	0.113 m	0.111 m	0.048 m
49719.0	0.141 m	0.131 m	0.050 m
49720.0	0.132 m	0.138 m	0.057 m
49721.0	0.124 m	0.131 m	0.052 m
49722.0	0.119 m	0.126 m	0.049 m
49723.0	0.109 m	0.111 m	0.044 m
49724.0	0.112 m	0.108 m	0.050 m
49725.0	0.121 m	0.129 m	0.043 m
49726.0	0.112 m	0.120 m	0.038 m
49727.0	0.110 m	0.123 m	0.047 m
49728.0	0.106 m	0.114 m	0.039 m
49729.0	0.121 m	0.135 m	0.038 m
49730.0	0.115 m	0.119 m	0.049 m
49731.0	0.100 m	0.101 m	0.042 m

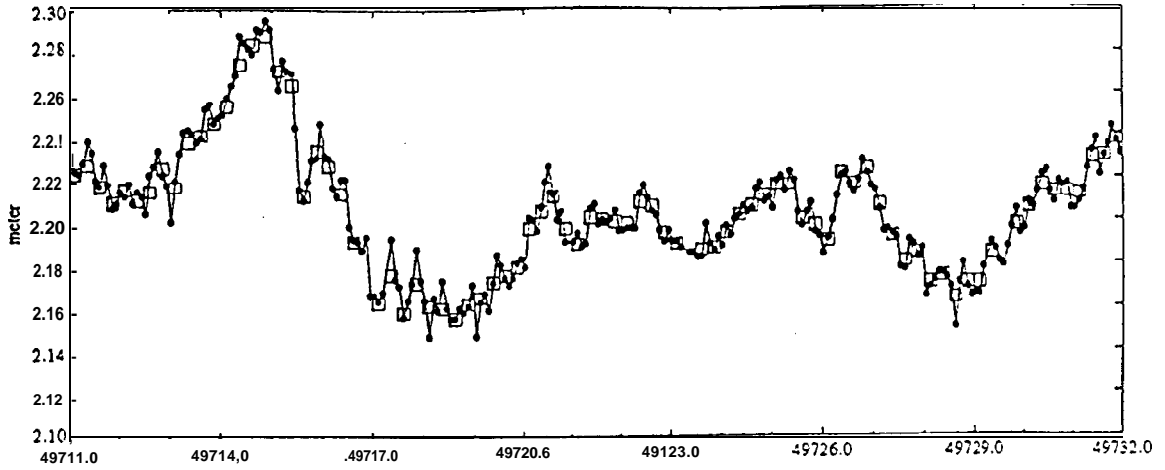


Fig. 1. Total path delay based on 2h-resp.6h- sampling intervals for the station WETB. (● - 2h, □ - 6h; AC: CODE)

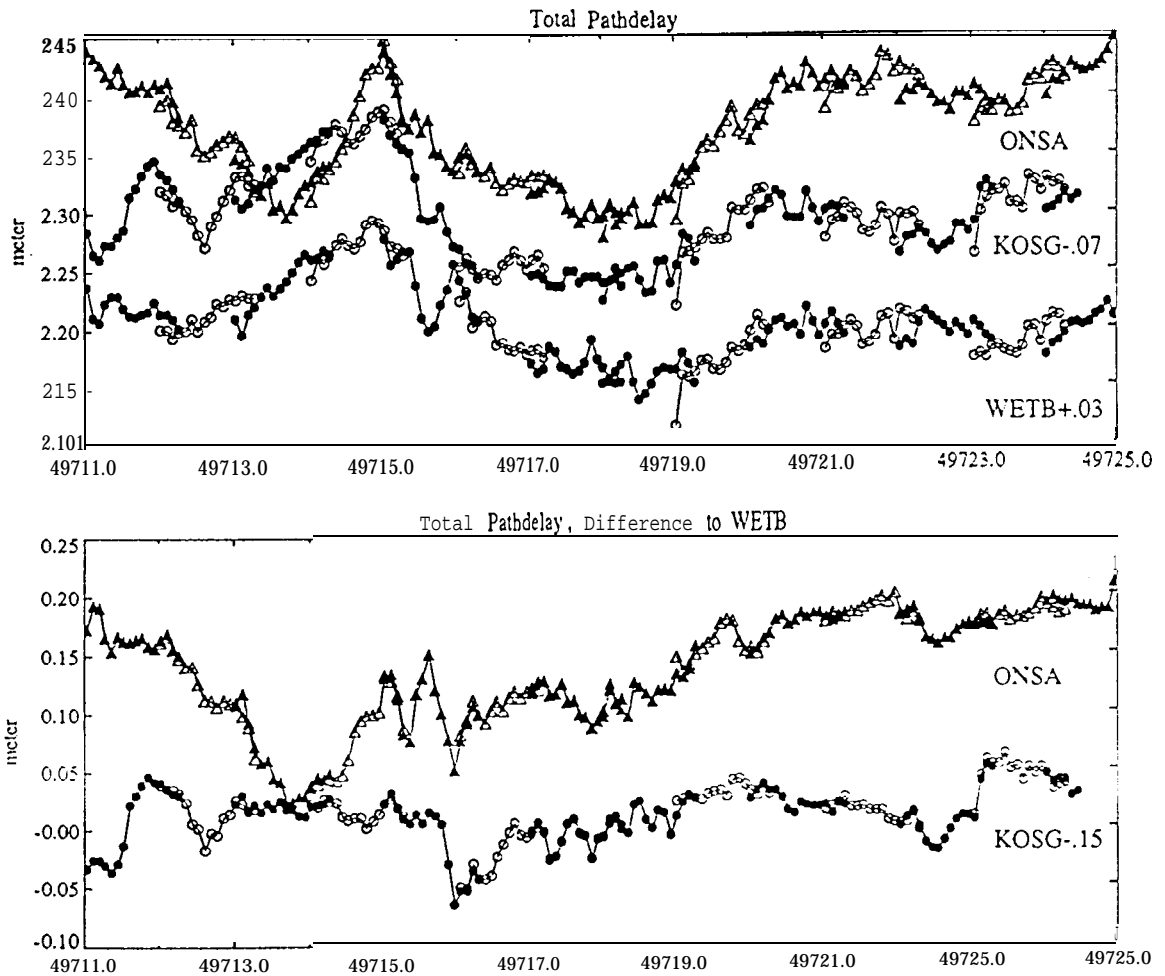


Fig. 2. Total zenith path delay for selected sites (results of GFZ) to demonstrate the consistency in the daily overlapping. Common effects can be reduced when a reference site is subtracted (bottom)

Table 4. Overlap differences of ZPD using 8h orbit overlap of GFZ (4 values in 2h intervals)

Sites:	EURO	NOAM	EURO - WETB	NOAM - WES2
Week 1	12	20	6	10
Week 2	19	18	9	8
Week 3	20	22	11	9

sampling interval (as long as it is not longer than about half a day) is not of great importance if the **geodynamical** parameters are considered, The situation may be different for high precision height determinations, e.g. for height variation studies (land uplift, global warming, tide gauge calibrations), Here special investigations should be performed.

A first impression of the achievable accuracy of the **ZPD** estimation may be obtained using the overlapping parts of adjacent arcs from the GFZ solutions. The results for parameters like orbital state, ERP and length of day are rather independent, having only 25% of the data in common, and therefore the ZPD values may be considered as independent. From the 8 hour overlaps one gets 4 values of ZPD to compare, The differences of selected sites over 2 weeks can be seen from Figure 2. Clearly visible are systematic effects which influence all sites in the same way. The results are summarized in Table 4. The rms-differences are about 2 cm. Subtracting a reference site (**WETB** in Europe and **WES2** in North America) the overlap differences come down to a level of 1 cm and better.

Let us now come to the main topic, the analysis of the consistency of the CODE- and GFZ troposphere parameters. The total ZPD estimations are taken for this comparison. The daily solutions of both AC are composed to form a weekly series of ZPD for each site, without any corrections from the overlapping time interval between consecutive solutions, The consistency of those series can be seen from Figure 3 and 4 for selected sites in North America and Europe, respectively. For each week the bias (one parameter for the whole week) and the rms of the ZPD differences between CODE and GFZ series were computed for all stations separately. The results for each of the three weeks are shown in Figure 5 (only the absolute value of the bias is considered), It is clearly seen that the differences are smaller for regions with a good site distribution (the only exception is **RCM5**). This is more pronounced for the rms than for the bias, which can easily be seen from the summary in Table 5. For most sites the bias is about 5 mm and the rms 10 mm, The origin of the larger bias for **RCM5** could not identified yet.

Looking in more detail into the results systematic effects in the differences are found which are almost identical for nearby sites. Computing relative ZPD values, relative to a reference site, one gets for sites in the neighborhood of this reference site (some 1000 km radius) a much better agreement. An example is given for the European region in Figure 6 where **WETB** was chosen as a reference. The results for all European sites are summarized in Figure 7 and Table 5. We found a significant improvement, for the bias

Table 5. Weekly bias and rms of ZPD differences between CODE and GFZ (units mm, only the absolute value of the bias is considered)

Sites:		All	EURO	NOAM*	Other	EURO - WETB
Bias	Week 1	6	5	5	6	2
	Week 2	7	4	3	8	1
	Week 3	7	6	6	7	3
Rms	Week 1	11	8	7	14	6
	Week 2	11	9	8	14	6
	Week 3	12	9	7	15	5

* w/o RCM5

Table 6. Mean daily bias and rms of ZPD differences between CODE and GFZ (units mm, only the absolute value of the bias is considered)

Sites:		All	EURO	NOAM*	Other
Bias	Week 1	6	6	5	6
	Week 2	6	4	4	6
	Week 3	7	5	5	7
Rms	Week 1	9	8	6	10
	Week 2	9	8	6	10
	Week 3	9	7	6	10

* w/o RCM5

in particular. The bias and rms are of the order of 2 mm and 6 mm. There is no big difference between the weekly and mean daily rms (cp. Table 5 with 6), which is an indication that the bias between CODE and GFZ estimates for the ZPD is rather stable from day to day.

SUMMARY, CONCLUSION, RECOMMENDATIONS

The troposphere estimates stemming from CODE and GFZ analyses using the observations of the **IGS** network from GPS weeks 781-783 show a consistency of about 5 mm (bias) and about 10 mm (**rms**) for single sites. The consistency is better by about a factor of two **if the ZPD is analyzed relative to a reference site within a continent**. This underlines that GPS is an **interferometric** space technique.

We could furthermore show that the length of the sampling interval for site-specific troposphere parameters is not critical to obtain highest accuracy for the parameters of

geodynamic and/or geodetic interest (may be the height component needs special investigation). We saw that the time development of the troposphere parameters is nearly identical in both, the CODE and the GFZ solutions, Keeping in mind the completely different **pre-processing** strategies this result is most encouraging. We conclude, that at least down to time intervals of two hours GPS is capable to give good estimates for the time evolution of the ZPD for single stations.

We recommend that a similar analysis should be performed using the material of more -- if possible all -- **IGS** processing centers. Of special interest are centers using stochastic troposphere estimates (**JPL**, NR Can) and centers using different weighting schemes for the observations (NR Can). In view of the experiences gained with different lengths of the sampling intervals there can be little doubt that the estimates of all **IGS** centers should be consistent on the same level as those of CODE and GFZ.

Should there be sufficient interest of the meteorological community in the ZPD emerging from the routine IGS analyses we would recommend the establishment of a routine ZPD comparison/combination service through the IGS. As usual the establishment of such a service would ask for a considerable amount of coordination including the use of high quality barometers, the organization of the transfer of met data from the stations of interest to the IGS processing centers, and possibly the adoption of common physical models for the ZPD. We are convinced that such an effort would lead to physically meaningful estimates of the **precipitable** water content in the environment of the IGS sites but NOT to a substantial improvement for the parameters of primary interest to the IGS (orbits, earth rotation parameters, and coordinates).

The aspect that the troposphere estimates are more consistent with respect to a reference site in a continent should be further explored. One should e.g. look at the rms errors (a posteriori) for the differences between troposphere estimates. We believe -- without being **able to** prove it -- that these relative estimates are one order of magnitude more reliable (in the sense of a physical model) than the absolute ZPD values established by the GPS.

The assessment of the quality of the absolute GPS derived ZPD values must include other techniques like Water Vapor Radiometers (**WVR**) and Satellite Laser Ranging (**SLR**) to those GPS satellites equipped with Laser reflectors and/or **radiosondes**.

REFERENCES

- Beutler, G., E. Brockmann, U. Hugentobler, L. Mervart, M. Rothacher, R. Weber (1995). Combining n Consecutive One-Day-Arcs into one n-Day s-Arc., Submitted for publication to Manuscript **Geodaetica**, October 1994.
- Bevis M, S. **Businger**, T. A. Herring, Ch. Rocken, R. A. Anthes, R. H. Ware (1992). GPS Meteorology: Remote Sensing of Atmospheric Water Vapor Using the Global Positioning System. *Journal of Geophysical Research*, Vol 97, No D14, 15787-15801, 1992.
- Bevis M, S **Businger**, S Chiswell (1994), GPS Meteorology: Mapping Zenith Wet delays onto **Precipitable** Water. *Journal of applied meteorology*, Vol.33 (1994),379-386

Freedman, A P, K Schulz, R S Gross, T A Herring, J W Ryan (1994). Precipitable water vapor derived from archived GPS zenith path delay estimates. Paper presented at AGU Fall Meeting, San Francisco 1994.

Gendt, G, G. Dick, Ch. Reigber (1995). IGS Analysis center at GFZ Potsdam. *IGS Annual Report*. in press.

Gurtner, W., G. Beutler, S. Botton, M. Rothacher, A. Geiger, H.-G. Kahle, D. Schneider, A. Wiget (1989). The use of the GPS in mountainous areas, *Manuscripta Geodaetica*, Vol. 14, pp. 53-60.

MacMillan, D.S, R M Elowitz (1994). Atmospheric delays estimated from GPS and VLBI during CONT94. Paper presented at AGU Fall Meeting, San Francisco 1994.

Rothacher, M., G. Beutler, W. Gunner, E. Brockmann, L. Mervart (1995). Bernese GPS Software Version 3.5., *Druckerei der Universitaet Bern*.

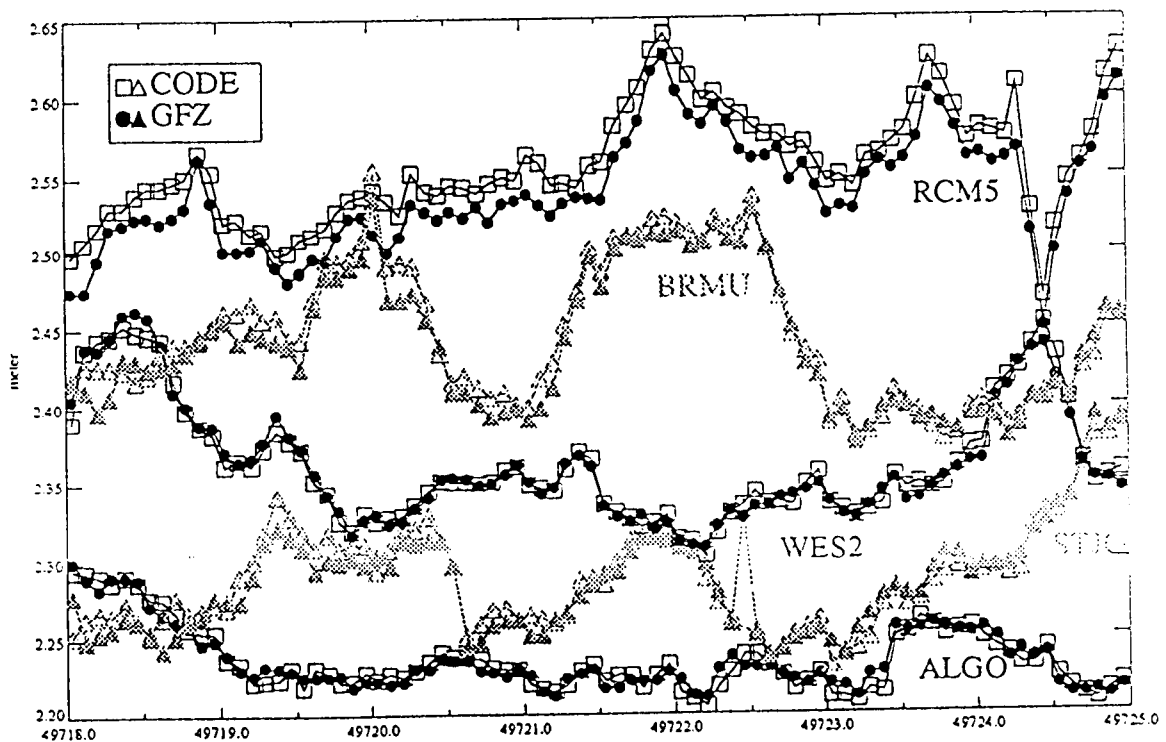


Fig. 3. Comparison of total zenith path delay (ZPD) from CODE and GFZ for selected North American sites.

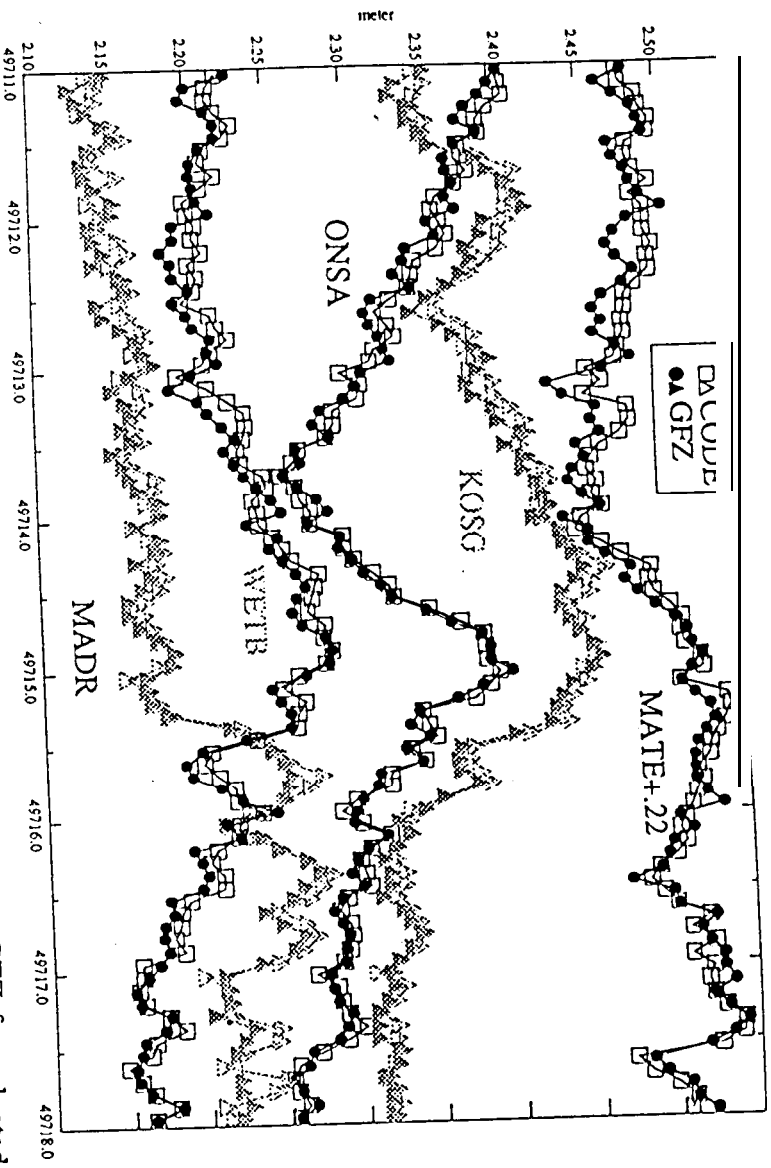


Fig. 4. Comparison of total zenith path delay (ZPD) from CODE and GFZ for selected European sites.

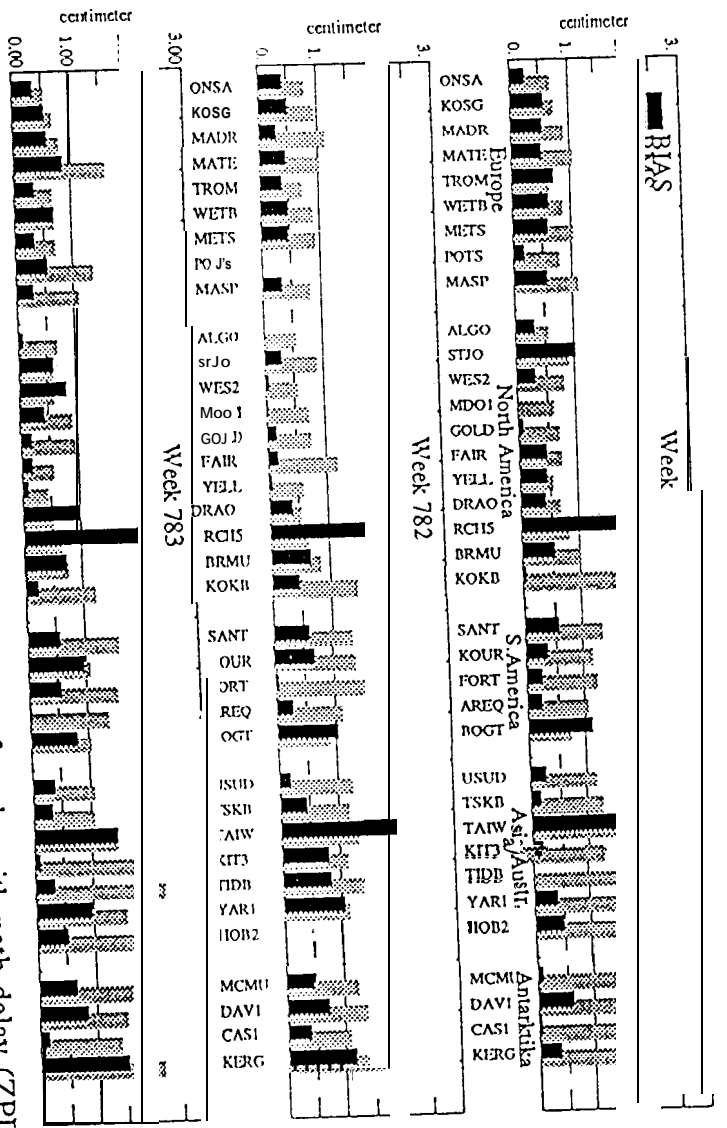


Fig. 5. Weekly bias and rms values of the differences of total zenith path delay (ZPD) from CODE and GFZ for all sites (only the absolute value of the bias is given)

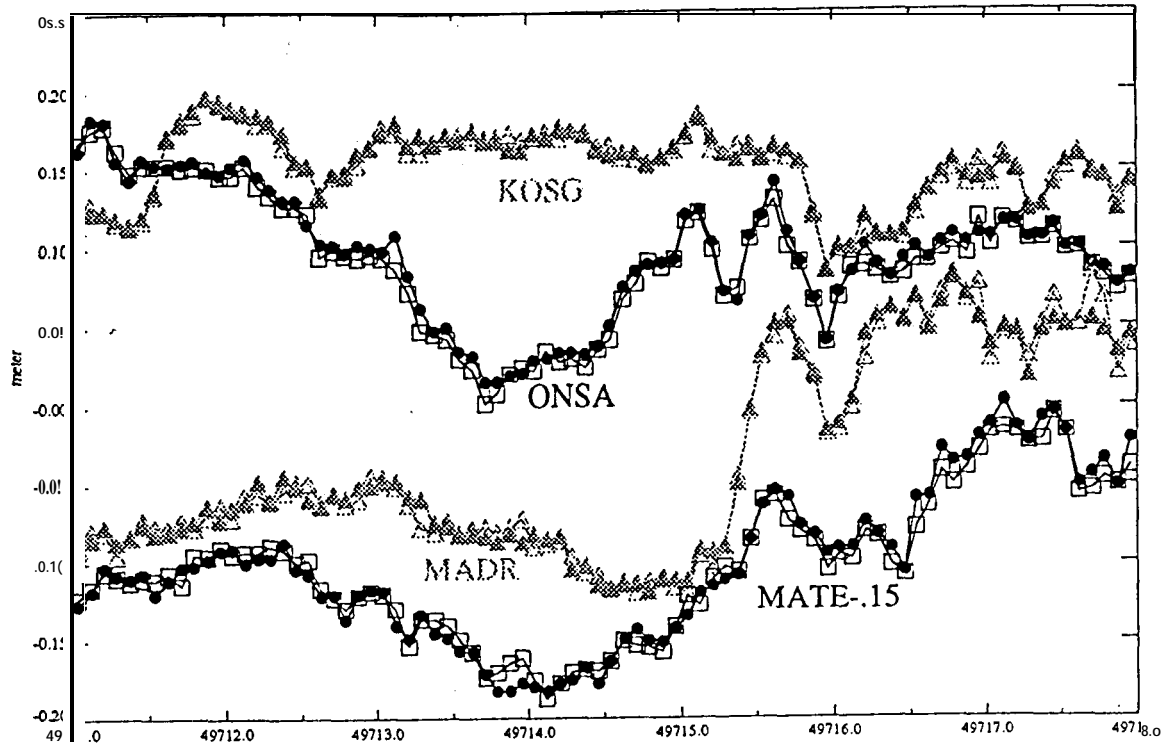


Fig. 6. Comparison of the total zenith path delay from CODE and GFZ for selected European sites. Values relative to WETB.

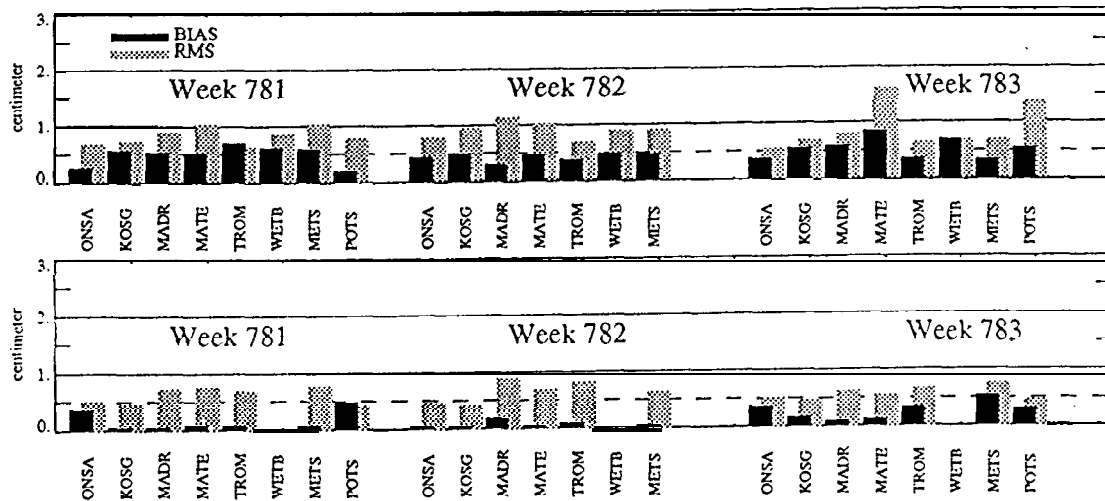


Fig. 7. Weekly bias and rms values of the differences of total zenith path delay from CODE and GFZ for European sites. Differences of original estimations (top) and estimates relative to a reference site (bottom) (only the absolute value of the bias is given)

A NEW MODEL FOR GPS YAW ATTITUDE

Yoaz E. Bar-Sever
Jet Propulsion Laboratory, California Institute of Technology
Pasadena, CA 91109 USA

ABSTRACT

Proper modeling of the GPS satellite yaw attitude is essential in high-precision geodetic applications. This fact is illustrated here as a new model for the GPS satellite yaw attitude is introduced. The model constitutes a significant improvement over the previously-available mode] in terms of efficiency, flexibility and portability. The model is described in detail and implementation issues, including the proper estimation strategy are discussed. The performance of the new model is analyzed and an error budget is presented. The evolution of the yaw attitude of the GPS satellites since the implementation of the yaw bias by the US Air Force is reviewed and operational aspects of modeling the yaw attitude are discussed.

INTRODUCTION

On June 6, 1994, the US Air Force implemented a yaw bias on most GPS satellites. By January 1995 the implementation was extended to all the satellites except SVN 10. The yaw bias was introduced as a way to make the yaw attitude of the GPS satellites **modelable** during shadow crossings (Bar-Sever et. al., 1995). The yaw attitude of a biased GPS satellite during eclipse seasons is markedly different from the yaw attitude of a **non-eclipsing** satellite, or from that of an unbiased satellite. The yaw attitude of the GPS satellite has a profound effect on precise geodetic applications. **Mismodeling** the satellite attitude can cause decimeter-level error in the positioning of ground stations with certain GPS-based techniques. This required the development of a special attitude model for biased GPS satellites. In addition to the yaw bias effects, that model also corrected other **mismodeling** that existed in the old model, namely, that of the "noon turn".

The first attitude model written for the biased constellation (Bar-Sever et. al., 1995) was made freely available to the GPS community in the form of a collection of FORTRAN subroutines and programs (Bar-Sever, 1994). For simplicity we will refer to this model throughout this paper as GYM94 (for "GPS Yaw attitude Model - 94"). GYM94 was implemented in **JPL's GIPSY** software and, **in** various forms, in other high-precision geodetic packages elsewhere. The model was successfully used within **JPL's Flinn** process to produce daily GPS orbits and ground stations coordinates of the highest quality. The model had some drawbacks, though. Mainly, it is cumbersome **to** implement and very demanding in computer resources, namely, memory and CPU time.

In this paper we describe a new model for the GPS satellite attitude, named here GYM95. The model is analytic, in contrast to the numerical nature of GYM94 that required sequential processing in time. A time series of yaw rates estimated by the Flinn process will be analyzed to demonstrate the need to estimate the yaw rates. Finally, The current state of the GPS constellation with respect to the yaw bias will be described as well as its evolution since the implementation of the yaw bias. Operational questions regarding the stability of the system and disseminating relevant information will finally be discussed,

BACKGROUND

The analysis that led to the implementation of the yaw bias on GPS satellites is described in Bar-Sever et. al. (1995). A general description of the first yaw attitude model can also be found there. For completeness, we give here a brief summary.

The nominal yaw attitude of a GPS satellite is determined by satisfying two constraints. First, that the navigation antennae point toward the geocenter and second, that the normal to the solar array surface will be pointing at the Sun. To meet these two conditions the satellite has to yaw constantly. The yaw attitude algorithm described above is singular at two points - the intersections of the orbit with the Earth - Sun line. At these points the yaw attitude is not single-valued as any yaw angle allows optimal view of the Sun. In the vicinity of these singular points the yaw rate of the spacecraft, required to keep track of the Sun, is unbounded. This singularity problem was by and large ignored prior to the release of GYM94. While this mismodeling problem could be easily fixed through the realization of a finite limit on the spacecraft yaw rate, a bigger problem existed that could only be addressed by changing the Attitude Control Subsystem (ACS) on board the spacecraft. The ACS determines the yaw attitude of the satellite by using a pair of solar sensors mounted on the solar panels. As long as the Sun is visible, the signal from the solar sensors is a true representation of the yaw error. During shadow, in the absence of Sun light, the output from the sensors is essentially zero and the ACS is driven in an open loop mode by the noise in the system. It turns out that even a small amount of noise can be enough to trigger a yaw maneuver at maximum rate. To make the yaw attitude of the GPS satellites modelable the ACS had to be biased by a small but fixed amount. Biasing the ACS means that the Sun sensor's signal is superposed with another signal (the bias) equivalent to an observed yaw error of 0.5° (the smallest bias possible). As a result, during periods when the Sun is observed, the satellite yaw attitude will be about 0.5° in error with respect to the nominal orientation . During shadow, this bias dominates the open loop noise and will yaw the satellite at full rate in the direction of the bias. Upon shadow exit, the yaw attitude of the satellite can be calculated and the Sun recovery maneuver can also be modeled.

GYM94 accounted for the yaw bias as well as the limit on the yaw rate. It computed the satellite yaw angle through numerical integration of a control law. Its output was a large file containing the yaw attitude history and, optionally, partials of the yaw attitude with respect to the yaw rate parameter. This file could later be interpolated to retrieve a yaw angle at the requested time, This process required relatively large amounts of computer memory and CPU time. In addition, the model's complex control law - a simulation of the on-board attitude determination algorithm, did not allow much insight into the problem and was hard to tune. To overcome all these deficiencies the GYM95 model was written.

GYM94 was used operationally in JPL's Flinn process since September 1994. The design of the new attitude model draws on the experience accumulated with GYM94. GYM95 is simple enough to be described by a small set of formulas, allowing easy implementation in different computing environments. Its analytic nature, as opposed to the numerical nature of GYM94, allows queries at arbitrary time points with great savings in computer resources. Finally, it allows more flexibility in tuning and adapting it to the changing conditions of the GPS constellation.

THE EFFECTS OF GPS SATELLITE YAW ATTITUDE ON PRECISE GEODETIC APPLICATIONS

Both carrier phase and pseudo-range are sensitive to GPS satellite yaw. Both are effected by the variation of the transmit antennae phase center with time. Unmodeled phase center variations due to yaw can cause up to 8 cm in range error both in the carrier-phase and pseudo-range observable (Bar-Sever et. al., 1995). In addition, mismodeling the phase wind-up can lead to a decimeter-level range error (Wu et. al. 1994). The wind-up error cancels out with double differencing but is present otherwise. In precise point-positioning - the process by which fixed GPS orbits and clocks, say, the JPL solution, are used to solve for individual station position - the wind-up error compounds with the phase center error, resulting in large errors in station positions. The actual error will depend on the amount and quality of data and on the estimation strategy. JPL routinely uses its daily orbit and clock solutions to point-position a globally distributed sub-set of the IGS network. To demonstrate the possible positioning errors that result from mismodeling GPS satellite yaw, the following experiment was performed. 51 globally distributed stations were point-positioned in three different ways. First, with the full yaw attitude model and the estimated yaw rates, then, with the yaw attitude model but with nominal yaw rates and, finally, without the yaw attitude model. The resulting errors, assuming that the positions obtained with the full yaw attitude model are "truth", are presented in Table 1.

Precise knowledge of satellite attitude is also essential for orbit modeling. In particular, the solar pressure force is sensitive to the attitude. Eclipsing satellites violate the attitude algorithm prescribed with the ROCK models (Fliegel & Gallini, 1992). This implies that the solar pressure is mismodeled for these satellite during parts of the orbit. The only remedy for this situation is to redesign the solar pressure model. This project is currently under work. In the mean time orbit errors should be soaked up with suitable fudge factors.

Table 1. 3D errors in positioning 51, globally distributed, stations on April 6, 1995. In centimeters. Positioning was done using the the JPL IGS solutions for satellites and clocks for that day. 8 GPS satellites were eclipsing. Most of the error is in height.

	Position Errors - Nominal Rates	Position Errors - No Yaw Model	Formal Errors - Any Method
Mean	0.3	0.7	0.6
Std. Dev.	0.3	0.9	0.4
Max	1.8	5.9	3.0

THE NEW YAW ATTITUDE MODEL (GYM95)

Overview

The yaw attitude of a GPS satellite can be divided into four regimes: nominal attitude, shadow crossing, post-shadow maneuver and noon turn. Most of the time (and for non-eclipsing satellites all the time) the satellite is in the nominal attitude regime. The post-shadow maneuver begins immediately after emerging from the earth shadow and lasts until the satellite has regained its nominal attitude. This can last from zero to 40 minutes. Noon turn maneuver does not occur until the beta angle goes below about 5° and it can last between zero and 40 minutes.

We will start by defining few important terms and then describe the yaw attitude during each of the four regimes including the governing formulas. Finally we will describe how to tie all the regimes together into one functional model and analyzed the built-in errors.

Definitions

Orbit-Midnight: The point on the orbit furthest from the Sun.

Orbit-Noon: The point on the orbit closest to the Sun.

Orbit Normal: Unit vector along the direction of the satellite's angular momentum, treating the satellite as a point-mass. (= position \times velocity where the order of the cross product is important)

Sun vector: The direction from the spacecraft to the Sun.

Beta angle: The acute angle between the Sun vector and the orbit plane. It is defined as positive if the Sun vector forms a sharp angle with the orbit normal and negative otherwise.

Orbit angle: The angle formed between the spacecraft position vector and Orbit-Midnight, growing with the satellite's motion.

Yaw-Origin: A unit vector that completes the spacecraft position vector to form an orthogonal basis for the orbit plane and is in the general direction of the spacecraft velocity vector.

Spacecraft-fixed Z axis: The direction of the GPS navigation antennae.

Nominal spacecraft-fixed X axis: A unit vector orthogonal to the Spacecraft-fixed Z axis and such that it lies in the Earth-spacecraft-Sun plane and points to the general direction of the Sun. (Note: this definition is not single valued when the Earth, spacecraft and Sun are collinear.)

Spacecraft-fixed X axis: A spacecraft-fixed vector, rotating with the spacecraft, such that far enough from Orbit-Noon and Orbit-Midnight it coincides with the Nominal Spacecraft-fixed X axis. Elsewhere, it is a rotation of the Nominal Spacecraft-fixed X axis around the Spacecraft-fixed Z axis.

Nominal yaw angle: The angle between the Nominal spacecraft-fixed X axis and the Yaw-origin direction, restricted to be in $[-180,180]$. It is defined to have sign opposite to that of the beta angle.

Yaw angle: The angle between the spacecraft-fixed X axis and the Yaw-Origin direction, restricted to be in $[-180,180]$. Also termed "actual yaw angle".

Yaw error: The difference between the yaw angle and the nominal yaw angle, restricted to be in $[-180,180]$.

Midnight turn: The yaw maneuver the spacecraft is conducting from shadow entry until it resumes nominal attitude sometime after shadow exit

Noon turn: The yaw maneuver the spacecraft is conducting in the vicinity of Orbit-Noon when the nominal yaw rate is higher than yaw rate the spacecraft is able to maintain. It ends when the spacecraft resumes nominal attitude

Notations

μ - The orbit angle
 β - The beta angle
E - The Earth-Spacecraft-Sun angle
b - The yaw bias inserted in the satellite ACS
B - The actual yaw angle induced by b
Y - The actual yaw angle
 Ψ_n - The nominal yaw angle
t - Current time, in seconds
 t_i - Time of shadow entry
 t_e - Time of shadow exit
 t_n - Start time of the noon-turn maneuver
 t_s - The spin-up/down time
 Ψ_i - Yaw angle upon shadow entry
 Ψ_e - Yaw angle upon shadow exit
R - The maximal yaw rate of the satellite
RR - The maximal yaw rate rate of the satellite

Angle units, i.e., radians or degrees, will be implied by context. Radians will be usually used in formulas and degrees will be usually used in text.

FORTTRAN function names are used whenever possible with the implied FORTRAN functionality, e.g., ATAN2(a,b) is used to denote arc-tangent(a/b) with the usual FORTRAN sign convention.

The nominal attitude regime

The realization of the two requirements for the satellite orientation, mentioned above, yield the following formula for the nominal yaw-angle:

$$\Psi_n = \text{ATAN2}(-\text{TAN}(\beta), \text{SIN}(\mu)) + B(b, \beta, \mu) \quad (1)$$

where β is the beta angle, μ is the orbit angle, measured from orbit-midnight in the direction of motion and B is the yaw bias (see below). It follows from this formula that the sign of the yaw-angle is always opposite that of the beta angle.

Ignoring the time variation of the slow-changing beta angle leads to the following formula for the yaw rate (there are simpler formulas but they contain removable singularities which are undesirable for computer codes):

$$\dot{\Psi}_n = \text{TAN}(\beta) * \text{COS}(\mu) * \dot{\mu} / (\text{SIN}(\mu)^2 + \text{TAN}(\beta)^2) + \dot{B}(b, \beta, \mu) \quad (2)$$

where $\dot{\mu}$ varies little in time and can safely be replaced by 0.0083 degrees/second. Notice that the sign of the nominal yaw rate is the same as the sign of the beta angle in the vicinity of Orbit-Midnight ($\mu = 0$).

The singularity of these two formulas when $\beta = 0$ and $\mu = 0, 180$ is genuine and cannot be removed.

The yaw bias

Like any medicine, the yaw bias has its side effects. Outside shadow it introduces yaw “errors” that are actually larger than 0.5° . To understand this we have to describe the ACS hardware, which is beyond the scope of this paper. The underlying reason is that the output of the solar sensor is proportional not to the yaw error but to its sine and it is also proportional to the sine of the Earth-Spacecraft-Sun angle, E. So, in order to offset a bias of b degrees inserted in the ACS the satellite has to actually yaw B degrees where B is given by:

$$B(b, \beta, \mu) = B(b, E) = \text{ASIN}(0.0175 * b / \text{SIN}(E)) \quad (3)$$

0.0175 is the hardware-dependent proportionality factor and the Earth-Spacecraft-Sun angle, E, the beta angle, β and the orbit angle, μ , satisfy the following approximate relationship:

$$\text{COS}(E) = -\text{COS}(\beta) * \text{COS}(\mu) \quad (4)$$

and E is restricted to $[0, 180]$. Formula (3) becomes singular for E less than 0.5013° . This has no effect on the actual yaw because a small value of E implies that the spacecraft is in the middle of a midnight turn or a noon turn and is already yawing at full rate. The value of B does have a significant effect, though, on the timing of noon turn entry and on the yaw angle shortly before that. For example, for $E = 5^\circ$ which is the typical threshold value for noon turn entry, the actual yaw bias is $B \approx 6^\circ$.

The bias rate, B, is given by:

$$\dot{B}(b, \beta, \mu) = 0.0175 * b * \text{COS}(E) * \text{COS}(\beta) * \text{SIN}(\mu) * \dot{\mu} / (\text{COS}(B) * \text{SIN}(E)^3) \quad (5)$$

The ACS bias, b, can be $\pm 0.5^\circ$ or 0° . With few exceptions, to be discussed below, the bias is always set to $b = -\text{SIGN}(0.5, \beta)$ since this selection was found to expedite the Sun recovery time after shadow exit.

The shadow crossing regime

As soon as the Sun disappears the yaw bias is steering the satellite. On most satellites the yaw bias has a sign opposite to that of the beta angle. To “correct” for the bias-induced error the satellite has to reverse its yaw rate upon shadow entry. For those satellites with bias of equal sign to that of the beta angle there is no yaw reversal. The bias is large enough to cause the satellite to yaw at full rate until shadow exit when the bias can be finally compensated for. The yaw angle during shadow crossing depends, therefore, on three parameters: The yaw angle upon shadow entry, Ψ_i ; The yaw-rate upon shadow entry, $\dot{\Psi}_i$, and the maximal yaw rate, R. Let t_i be the time of shadow entry and let t be the current time. Define:

$$t_1 = (\text{SIGN}(R,b) - \dot{\Psi}_i) / \text{SIGN}(RR,b) \quad (6)$$

to be the spin-up/down time. Then the yaw angle during shadow crossing is given by:

$$\Psi = \begin{cases} \Psi_i + \dot{\Psi}_i * (t - t_1) + 0.5 * \text{SIGN}(RR,b) * (t - t_1)^2 & t < t_1 \\ \Psi_i + \dot{\Psi}_i * t_1 + 0.5 * \text{SIGN}(RR,b) * t_1^2 + \text{SIGN}(R,b) * (t - t_1) & \text{Else} \end{cases} \quad (7)$$

Using this formula, we avoid the singularity problem of the nominal attitude at midnight.

The **post-shadow maneuver**

This is the trickiest part of the yaw attitude model, The post-shadow maneuver depends critically on the yaw angle upon shadow exit. The ACS is designed to reacquire the Sun in the fastest way possible. Upon shadow exit the ACS has two options: one is to continue yawing at the same rate until the nominal attitude is resumed, or two, to reverse the yaw rate and yaw at full rate until the nominal attitude is resumed. In this model we assume that the decision is based on the difference between the actual yaw angle and the nominal yaw angle upon shadow exit. Denote this difference by D. If t_e is the shadow exit time then:

$$D = \Psi_n(t_e) - \Psi(t_e) - \text{NINT}((\Psi_n(t_e) - \Psi(t_e)) / 360) * 360 \quad (8)$$

and the yaw rate during the post-shadow maneuver will be $\text{SIGN}(R,D)$.

Given the yaw angle upon shadow exit, the yaw rate upon shadow exit, $\text{SIGN}(R,b)$, and the yaw rate during the post-shadow maneuver, we can compute the actual yaw angle during the post-shadow maneuver by using formula (7) with the appropriate substitutions. This yields:

$$t_1 = (\text{SIGN}(R,D) - \text{SIGN}(R,b)) / \text{SIGN}(RR,D) \quad (9)$$

$$\Psi = \begin{cases} \Psi(t_e) + \text{SIGN}(R,b) * (t - t_e) + 0.5 * \text{SIGN}(RR,D) * (t - t_e)^2 & t < t_e + t_1 \\ \Psi(t_e) + \text{SIGN}(R,b) * t_1 + 0.5 * \text{SIGN}(RR,D) * t_1^2 + \text{SIGN}(R,D) * (t - t_e - t_1) & \text{Else} \end{cases} \quad (10)$$

The post-shadow maneuver ends when the actual yaw attitude, derived from formula 10, becomes equal to the nominal yaw attitude. The time of this occurrence is computed in GYM95 by an iterative process that brackets the root of the equation $\Psi(t) = \Psi_n(t)$, where the time dependence of $\Psi_n(t)$ is introduced by substituting $\mu = \mu_e + 0.0083 * (t - t_e)$ in formula 1. This equation can be solved as soon as the satellite emerges from shadow. Once the time of resuming nominal yaw is reached we switch back to this regime.

The **noon turn regime**

The noon turn regime starts in the vicinity of orbit-noon, when the nominal yaw rate reaches its maximal allowed value and it ends when the actual yaw attitude catches up with

the nominal regime. First we have to identify the starting point and this can be done by finding the root, t_n , of the equation $\dot{\Psi}_n(t) = -\text{SIGN}(R, \beta)$, where $W.(t)$ is the nominal yaw rate from formula 2. After the start of the noon-turn the yaw angle is governed by formula (7), again, with the proper substitutions. This yields:

$$\Psi = \Psi_n(t_n) - \text{SIGN}(R, \beta) * (t - t_n) \quad (11)$$

The end time is found by the same procedure that is used to find the end time of the post-shadow maneuver.

The complete model

Satellite position and velocity, as well as the timing of shadow crossings are a required input to GYM95. The model is able to bootstrap, though, if these input values are unavailable far enough into the past. For example, if the satellite is possibly in the post-shadow regime upon first query, there is a need to know the shadow entry time so that all the input to Formulas (9) and (10) be known. If this shadow entry time is missing from the input the model can compute it approximately as well as the shadow exit time. Once all the timing information is available, yaw angle queries can be made at arbitrary time points. The model will decide what is the relevant yaw regime and compute the yaw angle using the correct formula. Given the above formulas it is an easy matter to compute the partials of the yaw angle with respect to any parameter of the problem, the most important of which is the maximal yaw rate, R .

Model fidelity

The fidelity of the model is a measure of how accurately it describes the true behavior of the satellite. This is hard to measure because there is no high quality telemetry from the satellite and because the estimated values of the main model parameter, namely, the yaw rate, depend on many other factors beside the model itself data, estimation strategy and other models for the orbit and the radiometric measurements. Nevertheless, based on the experience accumulated thus far with this model and its predecessor, GYM94, it is possible to come up with an educated guess as to the built-in inaccuracies of GYM95.

The nominal attitude regime is believed to be very accurate. The only source of error is misprinting of the satellite which is little understood and relatively small (of the order of 1" around the pitch, yaw and roll axes). Compensations for this error source were discussed by Kuang et. al. (1995) and Beutler et. al. (1995) where it was treated, properly, within the context of the solar pressure model.

Modeling the midnight-turn accurately is difficult. Inherent uncertainties like the exact shadow entry and exit time are a constant error source. Inaccuracies in shadow entry time are more important than inaccuracies in shadow exit time because errors in the former are propagated by the model throughout the midnight-turn maneuver. In contrast, error in the shadow exit time will effect the post-shadow maneuver only. Either way, the inaccuracy will be manifested through a constant error in the yaw angle, something that can be partially compensated through the estimation of the yaw rate. The length of the penumbra region is usually about 60 seconds. Sometime during this period the yaw bias kicks in. GYM95 puts that time midway into penumbra. The maximum timing error is, therefore, less than 30

seconds. A worst-case scenario, ignoring the short spin-up/down period and using a yaw rate of 0.13 degrees/second, will give rise to a constant yaw error of $30 \times 0.13 \approx 4$ degrees throughout the midnight turn. A more realistic estimate is 3", even before applying yaw rate compensation, after which the RMS error will remain the same but the mean is expected to vanish. Another error source is the uncertainty in the value of the maximal yaw rate rate, RR. This parameter is not very observable and therefore is hard to estimate. The nominal value used in GYM95 is 0.00165 degrees/sec² for Block HA satellites and 0.0018 for Block 11 satellites and is believed to be 70% accurate. The long-term effects of a yaw rate error can be computed from the second part of Formula (7) to be:

$$\Psi(RR) = [\dot{\Psi}_i * \text{SIGN}(R,b) - 0.5 * \dot{\Psi}_i^2 - 0.5 * \text{SIGN}(R,b)^2] / \text{sign}(RR,b)$$

A worst-case scenario assuming $\dot{\Psi}_i = -\text{SIGN}(R,b) = 0.13$ and 30% error in the yaw rate rate would give rise to a yaw error of about 5°. But these assumption also imply a very short shadow so the error will not be long-lasting. For long shadow events $\dot{\Psi}_i \approx 0$ and the resulting yaw error is about 10. Again, this error can be partially offset by estimating the yaw rate.

The main error source for the noon turn is the timing uncertainty of the onset of the maneuver. This uncertainty is not expected to be larger than two minutes. A 2-minute error will cause a constant yaw error of about 15°, assuming a yaw rate of 0.13 deg/sec. The relatively short duration of the noon turn diminish somewhat the effects of such a large error. Estimating the yaw rate will decrease the error further.

The value of the yaw rate is not considered here as an error source. Any nominal value stands to be at least 10% in error (see below). Since errors due to yaw rate grow in time this parameter must be estimated or, alternatively, a previously-estimated value should be used. For example, an error of 0.01 deg/sec in the yaw rate will give rise to a 30° error in yaw at the end of a 50-minute shadow event.

Although unlikely, errors from different sources can augment. In that case the maximal error for each regime is as follows: 2" for the nominal yaw regime, 9° for the midnight turn regime and 15° for the noon turn regime. Actual errors are expected to be smaller than half of these values.

THE ESTIMATED YAW RATES

As part of the implementation of the GYM models at JPL the yaw rates of all eclipsing satellites are estimated for every midnight turn and every noon turn. In JPL's GIPSY software this is done by treating the yaw rate as a piece-wise constant parameter for each satellite. The parameter value is allowed to change twice per revolution, mid-way between noon and midnight. Since a small error in the yaw rate can cause a large yaw error over time and since our a-priori knowledge of the yaw rate is not sufficiently accurate, we found it necessary to iterate on the yaw rate value. JPL routinely publish the final estimates for the yaw rates. They are available as daily text file via anonymous ftp to 128.149.70.41, directory "pub/jpligsac". Unfortunately, due to a series of software bugs, all of the yaw rates for dates prior to February 16, 1995, were either lost or in error. This leaves a period of about two months when the estimated yaw rates are available. Figure 1 depicts the

estimated yaw rates for each eclipsing satellite, for each midnight turn and for each noon turn, from February 16 to April 26, 1995. The accuracy of the estimates depends on the amount of data available during each maneuver and this, in turn, is proportional to the duration of the maneuver. The longer the maneuver the better the estimate. The effect of a reduced estimation accuracy during short maneuvers is mitigated by the fact that the resulting yaw error is also proportional to the duration of the maneuver. For long maneuvers, e.g., midnight turn at the middle of eclipse season, the estimates are good to $0.002^\circ/\text{sec}$ which lead to a maximal yaw error of about 6° . A similar error level is expected for short maneuvers. Noon turns occur only during the middle part of the eclipse season. In Figure 1 they can be distinguished from midnight turn rates by the larger formal error associated with them, since they are typically short events - 15 to 30 minutes long. As a result, the scatter of the noon-turn rates is larger than that of the midnight turn rates. Toward the edges of the eclipse season the quality of the yaw rate estimates drops, again, because of the short duration of the shadow events. The most striking feature in Figure 1 is the jump discontinuity of the estimated yaw rates in the middle of eclipse season, corresponding to the beta angle crossing zero. No plausible explanation is currently available for this jump. Observe the following facts: SVN 29 is the only satellite that does not have a jump discontinuity. This is also the only satellite that does not undergo a bias switch in the middle of eclipse season. SVN 31 is the only satellite with a jump from high yaw rates to low yaw rates as the beta angle transitions from positive to negative. There is nothing otherwise special about SVN 31. The ratio of the high yaw rate values to the low yaw rate values is about 1.3 for all satellites.

Within each half of the eclipse season the midnight yaw rates are fairly constant, varying by 10% or less. The noon turn yaw rates seem to be more variable. This is not only a consequence of the weak observability but also of the fact that the spacecraft is subject to a varying level of external torque during the noon turn as the eclipse seasons progresses.

The modeling of the post-shadow maneuver is a perennial problem that has not found a satisfactory solution yet. The source of the problem is that the presence of the post-shadow regime makes the estimation of the yaw rate into a non-linear problem. There is always a critical value of the yaw rate such that for higher values the spacecraft will reverse its yaw upon shadow exit and for lower values the spacecraft will retain its yaw rate until the end of the midnight turn. If this critical value falls in the range of feasible yaw rates - which it often does - it becomes very hard to figure out what kind of maneuver the satellite is doing upon shadow exit. To avoid this post-shadow ambiguity we have been rejecting measurement data from shadow exit until about 30 minutes thereafter.

OPERATIONAL ASPECTS

The ACS of the GPS satellites has been changing continuously in ways that effect the yaw attitude. The changes are due to yaw bias variations and occasional hardware problems. This section reviews the changes in the GPS constellation *via-a-vis* the yaw attitude since the initial implementation of the yaw bias on June 6, 1994.

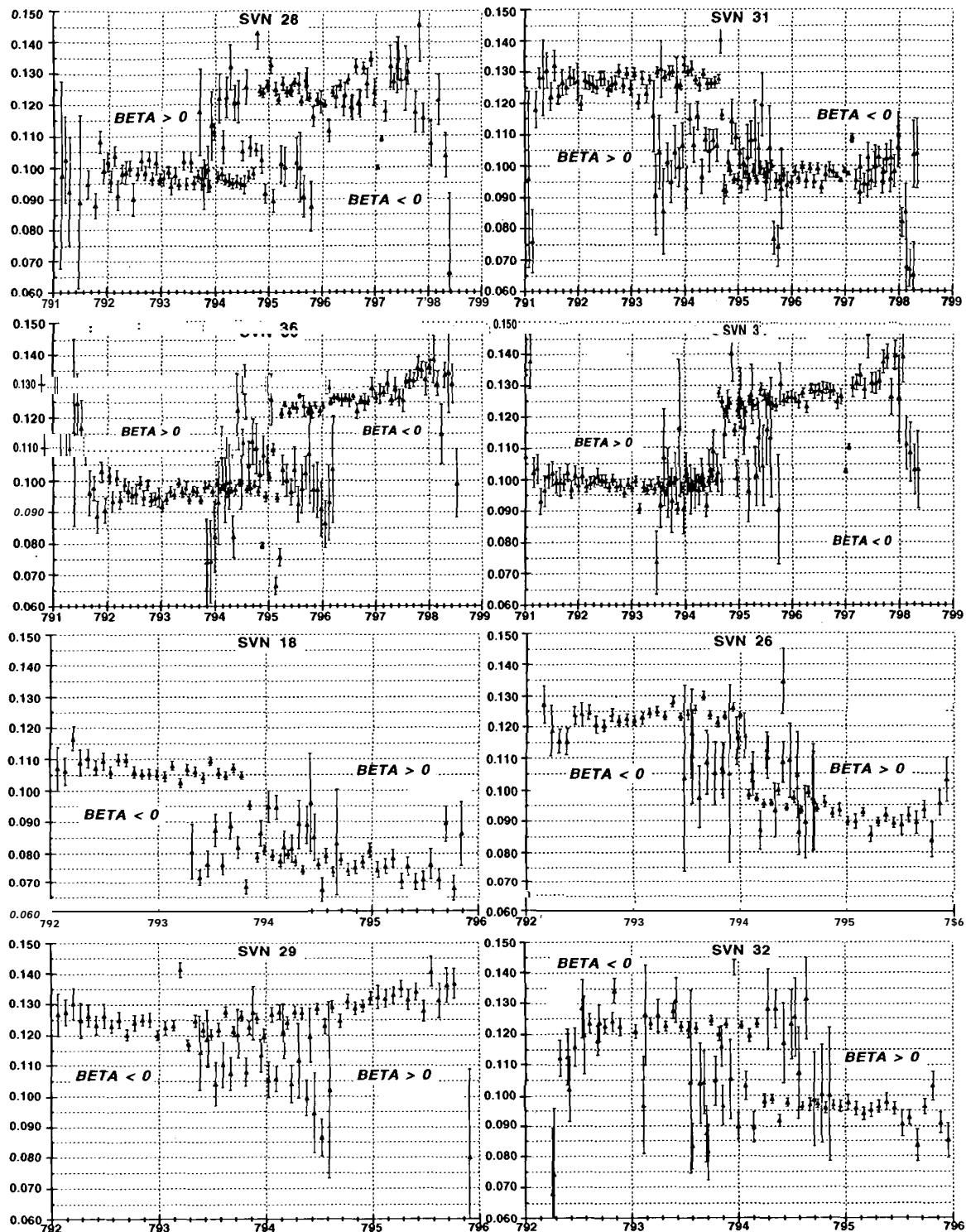


Figure 1. Estimated yaw rates (deg/second) with their formal errors vs. GPS week. SVNS 28,31, 36,37 are coplanar (C-plane). So are SVNS 18,26,29 and 32 (F-plane).

Initially the yaw bias was inserted into all GPS satellites except those with a reaction wheel failure (SNVS 14, 18 and 20 at the time). SVN 10 does not allow for a yaw bias. On January 9, 1995, a reaction wheel failure on SVN 16 forced the GPS operators to switch off its yaw bias. Then on January 31 the Air Force has agreed to extend the implementation of the yaw bias to the satellites with a reaction wheel failure but, due to operators error, the implementation was carried out only a week later. Currently, all 24 operational satellites are yaw biased. The four satellites with reaction wheel failure cannot yaw at the same rate as a healthy satellite. Their yaw rate is about 23% smaller.

The yaw bias could be set positive or negative. It can be shown that if the sign of the yaw bias is opposite that of the beta angle, the Sun reacquisition time after shadow exit is minimized. Therefore, whenever the beta angle of a satellite crosses zero the operators switch the sign of the yaw bias such that $b = -\text{SIGN}(0.5, \beta)$. Unfortunately it is impossible to carry out this switch exactly when $\beta = 0$ due to operational constraints. The Air Force will execute the switch within 24 hours of the beta angle sign change but the actual time is known only shortly before the upload. A hardware problem on SVN 29 makes it an exception to the bias sign rule, After January 9, 1995 the bias on this satellite remained positive and it will not change until further notice.

The changes in the ACS of the GPS satellites, described in the paragraphs above, require a reliable, fast and accessible communication channel through which announcements of upcoming changes can be delivered. So far this function has been fulfilled by the author but as the community of users of the yaw attitude model expands there may be a need to improve this process and to make it more automated and fast. This issue can be taken up with the Air Force, which has been extremely cooperative so far. Tables recording the history of the yaw bias on every satellite and the relevant nominal yaw rates, that are suitable for automated reading, can be downloaded from directory "pub/GPS_yaw_attitude on node 128.149.70.41.

ACKNOWLEDGMENTS

The help and cooperation of the US Air Force 2SOPS at Falcon AFB throughout this project was essential to its success and is greatly appreciated. The work described in this paper was carried out in part by the Jet Propulsion Laboratory, California Institute of Technology, under contract with the National Aeronautics and Space Administration.

REFERENCES

- Bar-Sever, Y., 1994. Improvement to the GPS Attitude Control Subsystem Enables Predictable Attitude During Eclipse Seasons. IGS Mail #0591, May, 1994.
- Bar-Sever, Y., Anselmi, J., Bertiger, W., Davis, E., 1995. Fixing the GPS Bad Attitude: Modeling GPS Satellite Yaw During Eclipse Seasons. Proceedings of the ION National Technical Meeting, Anaheim, CA, January 1995.

- Beutler, G., Brockmann, E., Gurtner, W., Hugentobler, U., Mervart, L., Rothacher, M., Verdun, A., 1995.** Extended Orbit Modeling technique at the CODE Processing center of the International GPS Service for **Geodynamics (IGS): Theory and Initial Results.** Manuscript **Geodaetica**, to appear.
- Fliegel, H. F., Gallini, T. E., 1992.** Global Positioning System Radiation Force Model for geodetic applications. *Journal of geophysical research*, Vol 97, No. B 1.
- Kuang, D., Rim, H. J., Schutz, B. E., Abusali, P. A.M., 1995.** Modeling GPS Satellite Attitude Variation for Precise Orbit Determination. Manuscript **Geodaetica**, to appear.
- Wu, J.T., Wu, S. C., Hajj, G. A., Bertiger, W. I., Lichten, S.M., 1993.** Effects of Antenna Orientation on GPS Carrier Phase. Manuscript **Geodaetica** 18.
- Zumberge J. F., Bertiger, W. I., 1995,** The Global Positioning System - Theory and Application. Vol. I, Chapter 16, "Ephemeris and Clock Navigation Message Accuracy", Senior Editors: **B.W. Parkinson, J.J. Spilker Jr.**; Editors: **P. Axelrad, P. Enge.** In press.

ESTIMATION OF PRECISE GPS CLOCK BIAS VALUES BY THE ESOC IGS ANALYSIS CENTRE

Tomás J. Martín Mur

European Space Operations Centre, European Space Agency
D-64293 Darmstadt, Germany

ABSTRACT

The **ESOC IGS Analysis Centre** has been providing precise estimated values of the clock biases of the GPS satellites from January of 1994. These clock biases are estimated in post-processing together with the receiver clock biases using pseudo-range and phase observable. The intended reference for the biases is GPS time. These clock biases have been used for precise off-line point-positioning for ground and space applications and for time-transfer experiments.

This presentation introduces the ESOC approach to clock bias estimation, including daily estimation of pseudo-range biases **and** highlights the difficulties of estimating very precise clock biases when Anti-spoofing is activated.

INTRODUCTION

To obtain precise GPS orbits, the estimation of precise clock biases for the GPS satellites is not needed if double difference observable are used. The only clock biases that need to be estimated are the receiver clock biases and not necessarily with a very high accuracy. Receiver clock biases are needed because they affect the time tag of the observations. The level of accuracy needed to correct double difference carrier phase observations is in the order of **100ns**. The satellite clock bias corrections broadcast in the GPS navigation message have this accuracy in general, but occasionally they may be worse or not available for some satellites.

The error in the clock bias corrections in the GPS navigation message can be separated into two terms. The first term will be that due to the error in the estimation and prediction of the clock bias. This term will be influenced by the accuracy with which the clock biases can be estimated by the GPS Master Control System and by the accuracy with which the behavior of the time and frequency standards on-board the GPS satellites can be predicted for the time of validity of the corrections. The second term is the intentional **modelling** error introduced by describing the evolution of the clock over some hours only in terms of bias, drift, and aging. As is well known the clock bias of the satellites that are performing Selective Availability

(SA) changes significantly in minutes, with a typical peak to peak variation of 300ns (~100 m range error). The changes in clock drift due to SA have a typical peak to peak variation in the order of 3×10^{-9} (~ 1 m/s range rate error). These errors are introduced in order to deny **non-**authorized users from obtaining the full precision achievable with the Precise Positioning Service (**PPS**). There are several ways of avoiding the effect of SA for very precise applications. One is to use additional simultaneous measurements from a station whose position is known with a better accuracy than the one we need for our application and to perform differential GPS. Another is to use measurements from a network of stations in order to estimate the clock corrections.

Our typical customer, the geodesy user, does not need very precise knowledge of the GPS satellites clock biases, but there are some other applications for which precise clock biases are needed. ESOC in particular is interested in the use of GPS for the navigation of low Earth orbit spacecraft. We want to be able to monitor the GPS signals at the same time that they are being used by ESA spacecraft. We will do this in order to check the results of the on-board navigation and, if communication links permit it, to provide corrections that can be used by the spacecraft to improve its navigation accuracy. The second application that is of interest to us is to monitor the performance of the time and frequency standards installed in the ESA ground stations, by connecting them to our GPS receivers. The analysis of the characteristics of the GPS signal is also of high interest to us, because it allows us to predict the navigation performance of stand-alone users of the Standard Positioning Service (**SPS**).

THE CLOCKS OF THE GPS SATELLITES

The first thing that has to be considered is the feasibility of the GPS satellite clock bias estimation with the observations provided by the IGS receivers. We use carrier phase and pseudo-range observations in L 1 and L2 with a sampling time of 30 seconds. All the receivers output the observations received at the same GPS epoch using their own realization of GPS time. This means that the transmission times will be different even if we suppose that the local realization of GPS time is perfect. The maximum difference will be of 0.019 seconds, for the case of a satellite that is simultaneously tracked by two receivers, one having the satellite in the zenith and the other having it just above the horizon. This means that if the change of the GPS clock bias was such that in milliseconds the bias values were significantly different, clock biases, even at the common observation epochs, could not be estimated. As we know, this is not the case. GPS orbit estimation algorithms assume that the variations in clock bias do not have this high a frequency.

Another consideration is the validity of clock bias values, estimated every 30 seconds, between the observed epochs. To analyze this we tracked the GPS signal using one receiver at ESOC doing 2 second sampling. We obtained the clock bias at the **first** observation time and computed the residuals for a period of one hour using the same clock bias. The results are shown in Figure 1. The satellite for this example is **PRN#** 26 and the observations were taken on the 5 of March, 1993. In the right graph the observations that would have been taken with

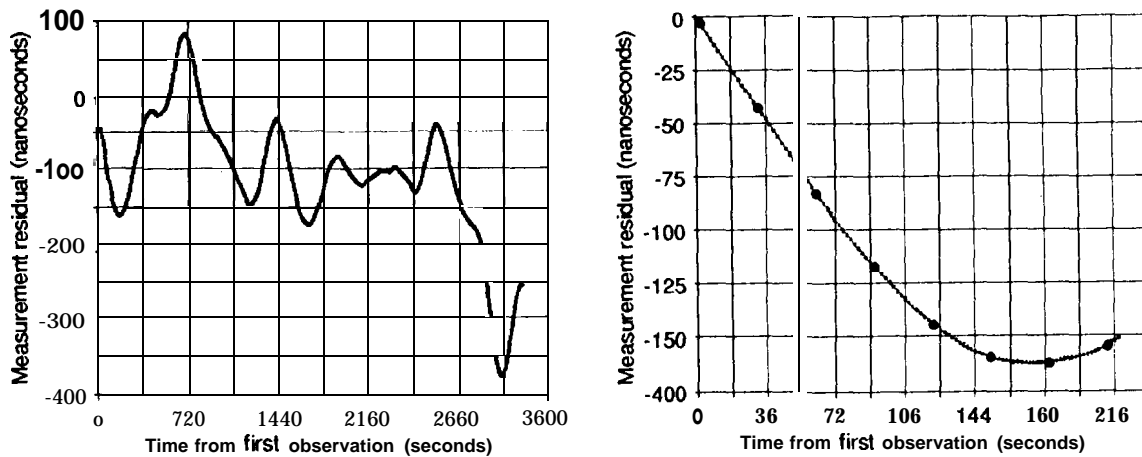


Fig. 1. Example of ionospheric-free carrier phase residuals.

30 second sampling are also plotted. Similar results were obtained for other satellites, It is clear that with 30 or 60 second sampling we can reconstitute the clock bias within the sampling interval by polynomial interpolation.

An interesting exercise is to obtain the clock biases and drifts of those satellites that are not performing clock dithering. This allows us to estimate the quality of the frequency standards installed in the GPS satellites. Our results show that they have an **Allan** standard deviation for 30 seconds sampling of 1 to 3 picosecond per second, as should be expected from Cesium and Rubidium standards. This means that the noise of the frequency standard will produce an error in the clock bias of about 0.06 nanoseconds after 30 seconds. This is the highest precision that we could possibly obtain for clock bias interpolation, even with exact estimates at the sampling times and without clock dithering.

The average values for some hours of the clock biases estimated for different satellites show an agreement of about 5 nanoseconds with the values obtained from the navigation message. The clock dithering implemented as part of the Selective Availability does not have a significant average effect over some hours for most of the satellites. The agreement in average clock drift over some hours is **in** the order of 5 **picoseconds/second**, except for satellites that are not performing SA, for which the agreement is in the order of 0.1 **picoseconds/second**. The effect of SA is to introduce frequency changes that have an Allan standard deviation of about 250 picoseconds/second for 30 second sampling.

THE GPS RECEIVERS

The data that ESOC is using for IGS analysis is obtained with Rogue, MiniRogue and TurboRogue receivers. Most of these receivers are connected to atomic frequency standards, some of them even to Hydrogen Masers.

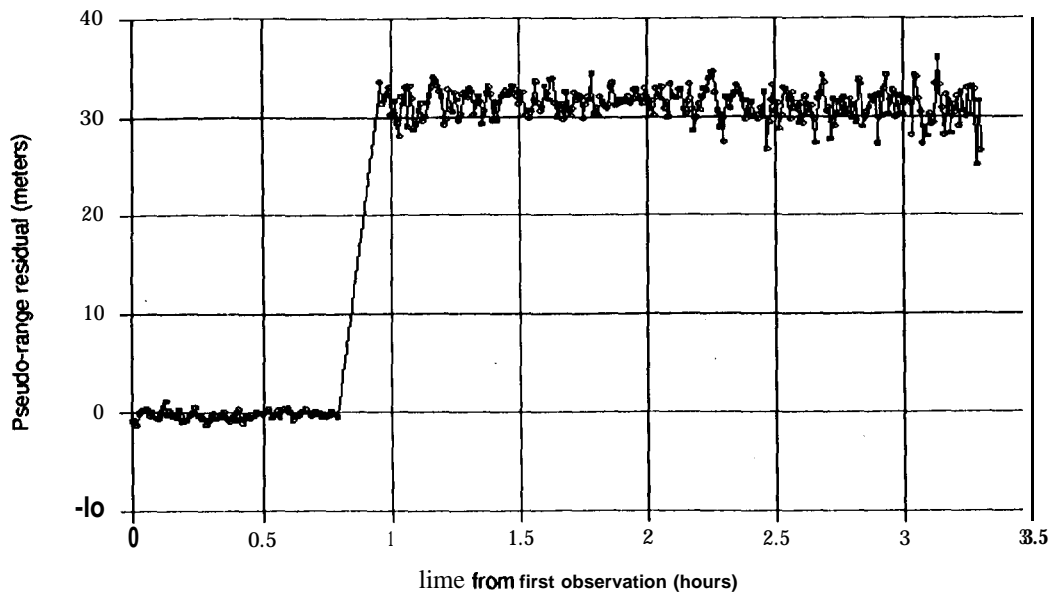


Fig. 2. Example of pseudo-range AS bias.

These receivers produce pseudo-range and phase observable in L1 and L2, even when Anti Spoofing (AS) is activated. The noise of these measurements is in the order of 1 mm for phase observations and 10 to 50 cm for pseudo-range observations. The accuracy of the phase observation is then of about 0.003 nanoseconds for the clock bias and, with 30 second sampling, of 0.1 picoseconds/second for clock drift. With the phase observable we can estimate the noise of the GPS satellite frequency standards, but they can not resolve the noise of the Hydrogen maser standards, because for the Hydrogen masers the clock drift variation is in the order of 0.007 picoseconds/second (Allan standard deviation for 30 second sampling). This means that a Hydrogen maser can be used as a reference for GPS clock drift estimation.

An important problem for the clock bias estimation is the existence of AS-tracking pseudo-range biases for Rogue and MiniRogue receivers. An example of the transition from non AS to AS tracking is shown in Figure 2. It shows the pseudo-range residuals of PRN# 24 for the KOKB receiver on the 3 of September, 1993. These AS biases can be as high as 60 meters and they need to be known in order to estimate clock biases. The AS biases seem to be very constant with time, but they complicate the realization of the receiver clock. If the receiver also tracks some satellites not in AS mode, then we can estimate the value of the biases supposing that the bias for those satellites not tracked in AS mode is zero. If that is not the case, then the absolute value of the AS biases, and of the receiver clock bias, can not be determined. Table 1 shows the average estimates for the AS biases for some of the stations of the IGS network. Two values are shown for some sites and they should correspond to receiver changes in those sites. For TROM the biases are PRN# dependent and they go from -14 m for PRN# 24 to 54 m for PRN# 22.

Table 1. Average pseudo-range AS biases for 1995

IGS code	AS bias (m)	IGS code	AS bias (m)
fair	25.26	mets	17.72
gold	20.51	nyal	23.63 / 62.03
hart	18.70	pama	6.37
kergr	15,10/54.92	sant	28.75
kokb	21.67/61.27	taiw	-1.00
kosg	23.12	tidb	19.37
kour	2.06	trom	PRN# dependent
madr	23.34	wett	10.48
mate	28.88	yarl	18.96

An additional problem is the existence of pseudo range and phase drifts (time changing biases) for some TurboRogue receivers of the **IGS** network when they are performing AS tracking. This problem has been detected for YELL and could be present in other receivers. The only thing that can be done when this problem is detected is to reject all the observations from the receiver. Figure 3 shows an example for **PRN# 22** on the 5 of February, 1995.

CLOCK ESTIMATION ALGORITHM

ESOC uses a clock estimation algorithm that has been designed with the following characteristics in mind:

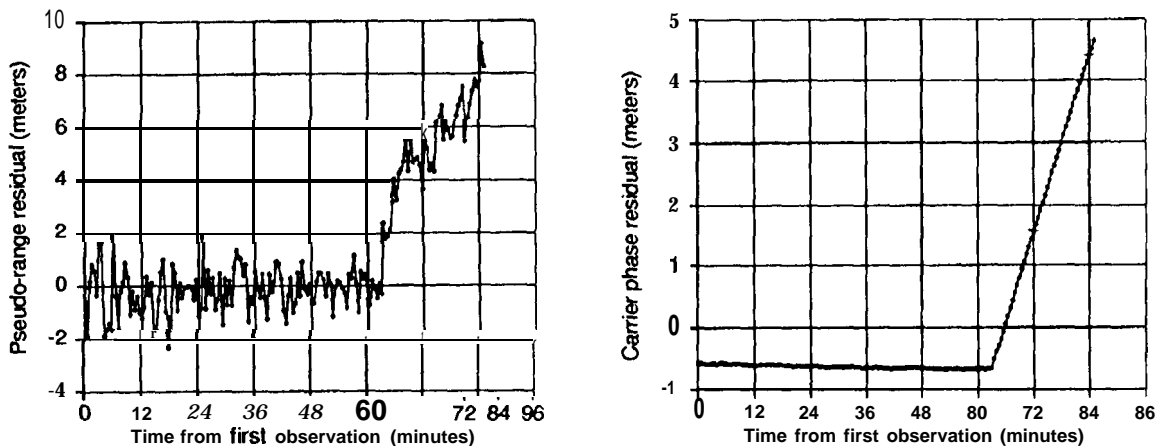


Fig. 3. Example of pseudo-range and phase drifts.

1. It shall be able to produce precise GPS satellite and receiver clock estimates. The user equivalent range error (**UERE**) created by errors in the clock bias estimation shall be of the same order as that created by errors in the estimation of the GPS satellite orbits, Actually the errors may in fact compensate for each other, reducing the total **UERE**.

2. It shall be able to process GPS data affected by Selective Availability or Anti Spoofing, minimizing or eliminating their effect as much as possible. The clock biases shall be estimated epoch by epoch to compensate for the variation produced by SA. AS pseudo-range biases have to be estimated in order to compensate for them. As these biases are receiver dependent, they shall not be considered fixed for any given site. These values shall be checked before every estimation.

3. It shall provide clock bias estimations that have the GPS system time as reference. This is difficult to realize because at any time the GPS time can only be resolved, because of SA, to a level of about 10 nanoseconds. This requirement was introduced to avoid the dependence on **only** one station, typically an Hydrogen maser, being used as time reference. Clock resets at this station will result in resets for the clock biases of all the satellites as well as jumps in the clock bias estimate of the user.

4. It shall provide clock biases to be used for precise point positioning. This means that the clock biases shall be estimated with a relatively high frequency. Right now we are obtaining clock biases every minute and this seems to be enough to obtain pseudo-range point positioning accuracies in the order of 1 meter for any epoch,

Description of the daily IGS data analysis at ESOC

The daily IGS data analysis at ESOC follows these steps:

1. Retrieval of RINEX observation files from up to 40 stations of the IGS network. The combined RINEX navigation file is also retrieved. These files are decompressed and archived.

2. Preprocessing. Double difference phase observable are generated every 6 minutes. Cycle slips are detected and flagged. Receiver clock biases are estimated for the observation times using pseudo-range observable and the satellite clock biases from the navigation message. The so obtained biases are fitted to a daily average bias and drift. Double difference pseudo range observable are generated for the estimation of AS biases.

3. Orbit determination. Orbits, Earth rotation parameters, double difference ambiguities, tropospheric parameters and station coordinates are estimated using the double difference phase observable with the program **BAHN**. **BAHN** is a batch least-squares estimator that can process not only GPS measurements, but all kind of commonly used satellite tracking measurements. Residuals for the double difference pseudo-ranges are obtained.

4. Estimation of AS biases. The double difference pseudo-range residuals are used to obtain average double difference pseudo range biases. From these, and supposing that the biases for satellites that are not tracked in AS mode are zero, individual **receiver/PRN#** AS biases are calculated. The values of the biases for every receiver are checked to assess whether they derive from the same **PRN#** independent value or not. The biases for those **receiver/PRN#** combinations that are observable are output to a file.

5. Precise clock bias estimation. The parameters obtained in the orbit determination, the AS biases, the clock biases from the navigation message and pseudo-range and phase observations are used to calculate clock biases every minute for **all** the observable satellites and receivers. The satellite clock biases are then corrected for periodic relativistic effect and output every 15 minutes to the SP3 format file. Values every minute are kept in a special format to be used in point positioning and time transfer studies.

Estimation of AS biases

These biases are estimated every day because they change when the receiver i's changed. It is not always possible to know beforehand which receivers have been changed on which days, so the biases have to be **re-estimated**. First **PRN#** dependent biases are obtained for all the receivers. Then these values are checked for every receiver to determine if they all represent the same **PRN#** independent value. If so, a **PRN#** independent value is then estimated, if not **PRN#** dependent values will be used. Currently only TROM has **PRN#** dependent AS biases. Biases are estimated for all the receivers and values for TurboRogue receivers are always around zero with actual values in the -0.3 to 0.3 m range. The biases are output to a file to be used in the clock bias estimation.

Our estimation of the AS biases has the following problems:

1. The values estimated are allowed to change from one day to the next, even without receiver change, in the order of 0.3 meters. If we could suppose that these values are constant our clock noise would be reduced.

2. A constant AS bias is calculated for the 24 hour period. If the receiver is changed in this interval, then the biases can not be calculated and all the observations from the receiver are rejected.

3. The information on which satellites are tracked in AS mode is lost in the generation of double differences. If the receiver changes from AS to non AS tracking mode, then the bias can not be calculated and the observations from the receiver can not be used.

4. There may be some combinations of double differences that make some of the biases unobservable. These combinations have then to be rejected and potentially valuable information is lost.

We are currently in the process of designing an improved AS bias estimation algorithm that can use the values estimated in previous days to increase the day to day consistency and that will have the information on which observations were made on AS mode so only those will be used to estimate the AS biases. Other observations will be used in order to provide a reference for the AS biases.

Precise clock bias estimation

We use GPSOBS, our GPS preprocessing program, to obtain the precise clock biases in post processing. The precise clock bias estimation algorithm is represented in Figure 4 and it has the following steps:

1. The measurement residuals for phase and pseudo-range are calculated using the orbits, station positions and tropospheric parameters obtained in the orbit determination. The phase observable are differentiated with time to obtain observations of the clock drift. By doing this the ambiguities are eliminated so they do not need to be estimated. Cycle slips can be detected as **outliers** in the clock drift estimation.

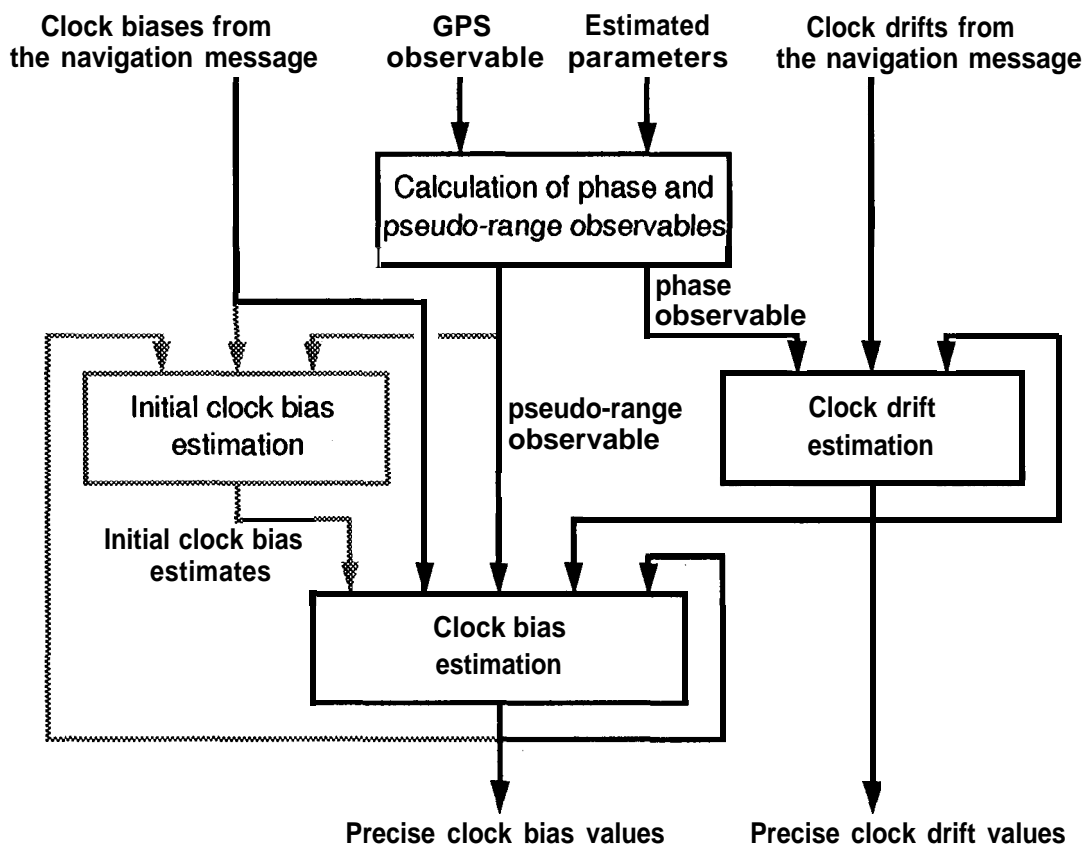


Fig. 4. ESOC's precise clock bias estimation process.

2. Clock biases for the first epoch are estimated, using least-squares, from the pseudo-range observable. For this the receiver clock biases of the previous estimation are used to constrain the solution in order to provide continuity. Navigation message clocks are used for the case when no receiver clock biases from a previous estimation are available. This estimator is also used to obtain new clock biases after clock resets or after periods without observations for a particular receiver or satellite.

3. The phase clock drift observable are used to estimate clock drifts. This is done with a **Kalman** filter. The changes in clock drift of the receivers connected to Hydrogen masers are constrained to provide a stable reference for the clock drift estimation. The satellite clock drifts of the navigation message are used as long term constraint of the clock drifts estimates. The estimation of clock drifts is done in batch for each interval in order to be able to detect cycle slips as **outliers**.

4. Pseudo range observable, clock drift estimates and the satellite clock biases from the navigation message are used in another **Kalman** filter to update the clock biases. The clock drift estimates constrain the short term evolution of the clock biases and the clock biases from the navigation message constrain the long term evolution of the biases. Pseudo-ranges are processed sequentially to save processing time.

Clock bias and clock drift estimates for all the receivers and satellites are produced every 60 seconds. The **Allan** standard variation for 60 second sampling is obtained for all the clock drifts in order to check whether the assumptions on the clock drift evolution are valid. Table 2 shows typical values for different types of clocks. Statistics on the pseudo-range residuals after clock bias estimation are also calculated. Typical rms of pseudo-range residuals are in the order of 0.5 m. If these residuals are unusually high for some station, then it may be needed to reprocess the data without this station,

Some changes are being considered in order to improve our estimation process. The most important is to change from sequential to batch processing of the pseudo-ranges in the clock bias estimation. We are processing pseudo-ranges sequentially to save CPU time, but in the near future, when our operational IGS analysis is performed in the workstation based system,

Table 2. Typical **Allan** standard deviation for 60 second sampling of clock **drift** estimates

Type of clock	ASD(60S) (pS/s)
Hydrogen masers	-0.3
Cesium or Rubidium receiver clocks	0.5-12
Internal receiver clock	250-450
GPS satellite not doing SA	0.8- 2.2
GPS satellite performing SA	-450

we will not be CPU time limited, The advantage of processing all the pseudo-ranges for one epoch together is that **outliers** can be identified. Another change is a reconsideration of the need for a initial clock bias estimator when clock biases values from the previous day are always available.

RESULTS

In order to check the quality of our satellite clock bias estimates we have performed **pseudo-range** point positioning using these values and the precise ESOC orbits. For day 120/95 we have calculated independently epoch by epoch every 30 seconds the position of four stations (**WETT**, **USUD**, **SANT** and **YAR1**). The distribution of the errors with respect to the **ITRF-93** position is shown in Figure 5. The typical horizontal rms is in the order of 0.6m and the

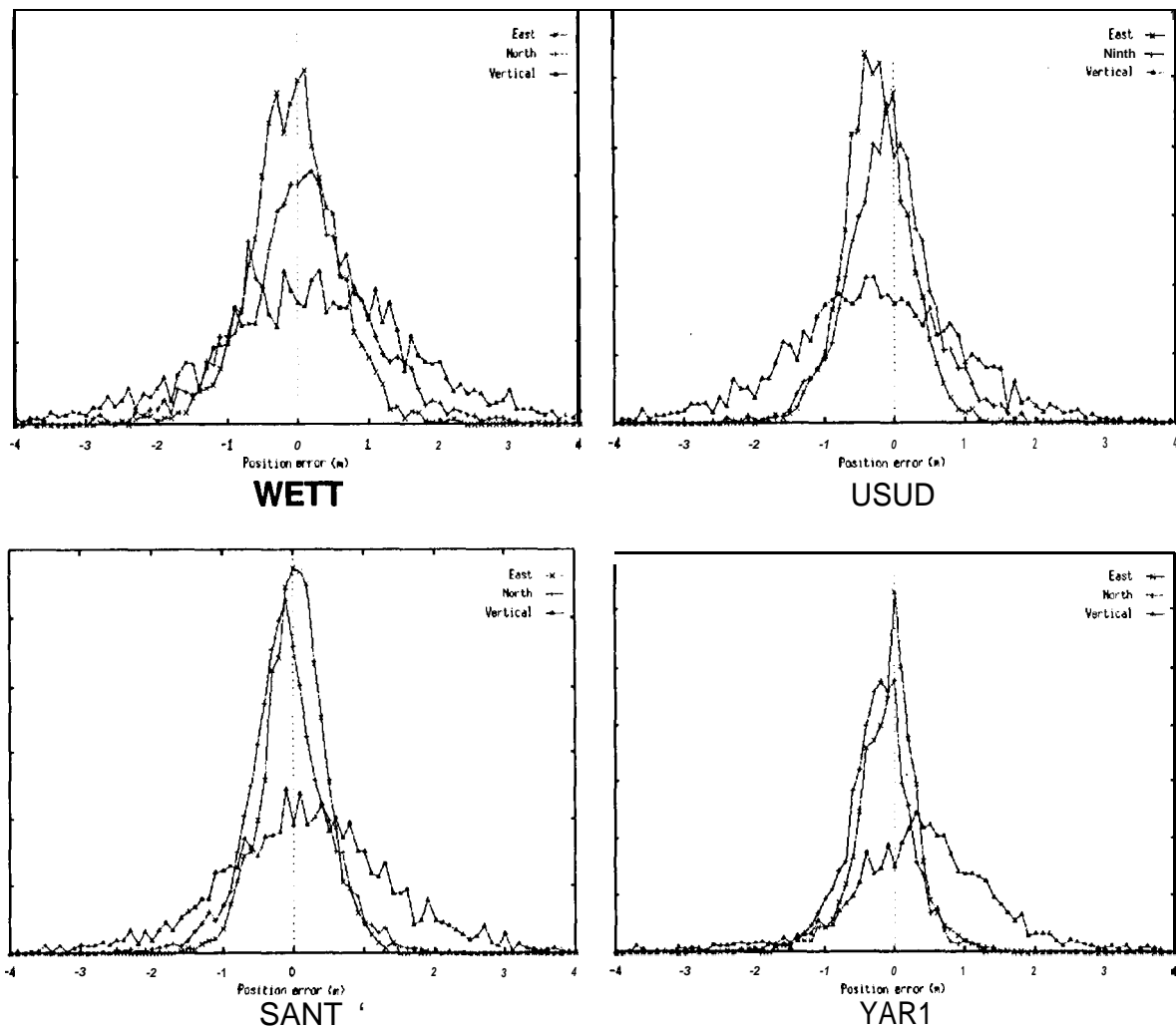


Fig. 5. Results of pseudo range point positioning with **ESOC's** orbits and clocks